Computer aided design and analysis of reaction-separation and separation-separation systems

Mitkowski, Piotr Tomasz; Gani, Rafiqul; Jonsson, Gunnar Eigil

Publication date:
2008

Document Version
Publisher's PDF, also known as Version of record

Computer aided design and analysis of reaction-separation and separation-separation systems

Ph. D. Thesis

Piotr Tomasz Mitkowski

15 May 2008

Computer Aided Process-Product Engineering Center
Department of Chemical and Biochemical Engineering
Technical University of Denmark

"A pessimist finds difficulty in every opportunity;
an optimist finds opportunity in every difficulty"

(Unknown)

Preface

This thesis is submitted as partial fulfilment of the requirements for the Ph.D. degree at Danmarks Tekniske Universitet (The Technical University of Denmark). The work has been carried out at the Computer Aided Process-Product Engineering Center (CAPEC) at Institut for Kemiteknik (Department of Chemical and Biochemical Engineering) from February 2005 to March 2008 under the main supervision of Prof. Rafiqul Gani and co-supervision of Prof. Gunnar Jonsson.

My sincerest thanks to my supervisors Professor Rafiqul Gani and Professor Gunnar Jonsson who have provided all possible help and guidance when and where required. A special thanks to my main supervisor Professor Rafiqul Gani for his patience and allowing me the freedom in research, which was a great help to me for completing this Ph-D project. Being in a very international and dynamic group such as CAPEC and numerous, travels which gave me an insight to the international research was an added bonus.

Many thanks to Professor Andrzej Górak and his group at Fluid Separation, Department of Biochemical and Chemical Engineering, University of Dortmund, especially Dr.-Ing. Peter Kreis and Dipl.-Ing. Carsten Buchaly for giving an opportunity to visit and do research with them. Special thanks to Professor Andrzej Górak for inspiration and hours of discussions.

I am obliged to Professor Michael Georgiadis for the opportunity to be involved in the very interesting, challenging and demanding Research Training (Marie Curie) Network-PRISM, under the 6th Framework Programme of the EU. The financial support from PRISM for this Ph.D.-thesis is very much appreciated.

I would like to thank all the CAPEC co-workers for technical and non-technical discussions during all these years. Many thanks to Jakob, Florin, Maurizio, Hassan, Ana, Agnieszka, Naweed and Oscar for endless coffee/tea and cake breaks, for remarkable Friday Evening Seminars, for being around and helping whenever it was needed. Thanks to PRISM-ers, Theodoros, Nuno, Teodora, Dragan, Bogdan and Oliver for sharing unforgettable time during various PRISM events around Europe and learning about different cultures. My special thanks to my officemate Vipasha Soni for limitless professional and personal discussions, correcting my English and dinners in the late working hours.

I want to express my gratitude to my parents for giving me a good education and teaching me that hard work is the key to success. Thanks also to them for being inexhaustible source of inspiration and trust.

Last but not the least, I want to express gratitude to my wife Iza, for her love, patience during countless and never ending phone calls and chats. Without Your support this work would never be completed.

Lyngby, May 2008

Piotr Tomasz Mitkowski

Abstract

This thesis describes the development and application of a general framework for design and analysis of integrated and hybrid chemical processes. Combination of at least two unit operations, based on different physical phenomena, is called a hybrid process since they jointly contribute to fulfil the process task. In principle, two types of hybrid processes are considered in this thesis: reaction-separation where, for example, the combination of batch reaction and membrane-based separation is considered, and separation-separation where, for example coupling of distillation with pervaporation is considered. An important issue in the design of hybrid chemical processes is the interdependency of the combined processes.

Generally, design of hybrid chemical process involves an iterative, trial and error experiment-based procedure where the experience of process designer plays an important role. Since experiments are usually time consuming and expensive, the search space of the potential designs needs to be significantly limited. Therefore, applying a computer-aided and model-based framework can significantly help in searching the domain of potential process designs and significantly narrow down the search space, where further optimization and experimental efforts can be concentrated on.

The key factors for the design of hybrid chemical process are the identification of process boundaries (for example azeotropes, miscibility gap), selection of feasible process combinations (for example to overcome azeotrope, is it better to combine distillation with pervaporation or with ultrafiltration?) and the dependency of the performance between constituent processes (for example how distillation should be combined with pervaporation?). Therefore, using the framework consisting of the three stages, (1) step-by-step methodology for design and analysis of hybrid chemical processes, (2) implementation, and (3) validation, it is possible to design the hybrid chemical process effectively. At all the stages various computer-aided tools and methods, some of which have been developed in this PhD-project, have been used.

The identification of process boundaries is performed in a conventional way, by performing analysis of pure component properties and mixture analysis. The driving force approach is used to compare various separation techniques and to select the feasible combination of the processes. The derivative of the driving force with respect to composition of the key compound (FD_x) is used to identify the "bottleneck" of the separation technique. For instance, the occurrence of a local minimum of the derivative of the *FD* indicates an inefficient separation technique. Therefore, a combination of this inefficient separation technique with another separation technique having a larger absolute FD_x in the "bottleneck", will lead to a hybrid chemical process which is more efficient than any of the constituent separation techniques separately. For the purpose of simulation and evaluation of the designed hybrid chemical process, specific models are generated from a generic model. The generic model describes the superstructure of two integrated processes, which under certain combination results in a hybrid process configuration.

The application of the developed model-based framework has been illustrated through five case studies involving reaction, distillation and membrane-based separation processes. The first case study deals with separation of a binary mixture of acetic acid and water. In this case two hybrid process designs consisting of distillation and pervaporation are proposed. This is followed by case study investigating the use of hybrid processing schemes to enhance production of modified phosphatidylcholine. Modified phosphatidylcholine is obtained in interesterification reaction of original phosphatidylcholine and oleic acid. The last three case studies deal with esterification reactions catalysed by the enzyme (esterification of cetyl oleate) or by ionic-exchange catalysts (esterification of ethyl lactate and n-propyl propionate). In all case studies involving reaction, hybrid process configurations consisting of reactors and pervaporations integrated at different levels, are proposed. It is important to point out that one of the hybrid chemical process designs has been verified experimentally. It was done for batch reactor combined with pervaporation to improve product yield in synthesis of n-propyl propionate.

It should also be noted that the framework is capable to be applied to other chemical and biochemical process design problems where integration of reaction-separation and separation-separation processes is looked for. It is not limited to only the five case studies discussed in this thesis. The framework is only limited by the availability of the property data of compounds, separation and reaction models.

Resume på Dansk

Denne afhandling omhandler udviklingen og anvendelse af en generel metode for design og analyse af integrerede og hybride kemiske processer. En hybrid proces er defineret som en proces hvor to eller flere enhedsoperationer, baseret på forskellige fysiske principper, kombineres for at udfører en overordnet operation. To typer af hybride processer er behandlet i denne afhandling: Reaktion/separation processer hvor f. eks. kombinationen af en batch reaktor og membran separation er benyttet. Separation/separation processer hvor f. eks. kombinationen af destillation og pervaporation er benyttet. Et vigtigt element i design af hybride kemiske processer er interaktionen mellem de kombinerede enhedsoperationer.

Design af hybride systemer indbefatter generelt en iterativ og *trail and error* eksperiment baseret procedure hvor erfaring og proces kendskab er helt centralt. Eftersom eksperimentelt arbejde typisk er meget tids- og resursekrævende er det nødvendigt, at begrænse operations området af potentielle design betragteligt. Denne begrænsning taler for at anvende en model- og computerbaseret metode til at bestemme mulige design. Simulering kan yderligere bidrage til at afsøge domainet af mulige design for, at begrænse området af interessante design og derved begrænse det efterfølgende eksperimentelle arbejde og optimeringen.

De centrale elementer i design af hybride processer er identifikationen af proces begrænsninger, f. eks. azeotrope eller flerfase bladninger. Udvælgelse af mulige design kombination, f. eks. for at eliminere effekten af en azeotrop, er kombinationen af destillation og pervaporation eller destillation og ultrafiltrering bedst? Undersøgelse af indvirkningen af de enkelte enhedsoperationer på den resulterende ydelse, det vil f.eks. sige hvordan skal destillation og pervaporation processerne kombineres. Den præsenterede metode består derfor af følgende tre dele: (1) trin for trin metode for design og analyse af hybride kemiske processer, (2) implementering og (3) validering. Denne metode muliggøre et effektivt design af hybride kemiske processer. I alle tre trin benyttes computer simulerings værktøjer som er blevet udviklet som del af dette Ph.d. arbejde.

Identifikation of procesbegrænsninger udføres på klassisk vis ved analyse af egenskaber for rene komponenter og analyse af bladninger. For at sammenligne mulige separations tekniker og udvælge mulige kombinationer of enhedsoperationer benyttes *driving force* analyse. Dennes afledte med hensyn til koncentrationen af nøgle komponenten (FD_x) benyttes til at identificere ”flaske halsen” for en separations teknik. F. eks. et lokalt minimum for den afledte af *FD* indikere ineffektiv separation. Kombinationen af en ineffektiv separations teknik med en teknik der har en større værdi for FD_x i ”flaske halsen” giver en hybrid kemisk proces, som vil have bedre separations egenskaber end de separate enhedsoperationer hver for sig. For at kunne simulere og evaluere den hybride kemiske proces er specifikke modeller udledt af en generisk model. Den generiske model beskriver en superstruktur for to integrerede processer for hvilken specielle kombinationer resultere i en konfiguration med en hybrid proces.

Anvendelsen af den udviklede modelbaserede metode er vist ved hjælp af fem illustrative eksempler. De involvere reaktion, destillation og membranbaseret separation. Det første eksempel viser separation af en binær blanding af vand og eddikesyre. Der argumenteres for en hybride proces bestående af destillation og pervaporation. Det andet eksempel undersøger anvendelsen af en hybrid proces til at forbedre inter-esterfikations reaktionen for phosphatidylcloline. De sidste tre eksempler omhandler enzymatisk esterfikation af cetyl oleate og esterfikation af ethyl lactate og n-propyl propionate med en ionbytter katalysator. I alle eksempler der involvere reaktion, er et design af den hybride proces bestående af reaktorer og pervaporation integreret på forskellige niveauer forslået. Eksemplet med den hybride proces bestående af batch reaktion og membran separation af n-propyl propionate er blevet verificeret eksperimentelt som væsentlig del af dette arbejde.

Det skal bemærkes, at den modelbaserede metoden er generel anvendelig til andre typer af kemiske eller biokemiske processer hvor integration af reaktion/separation og separation/separation indgår. Metoden er ikke begrænset til de fem eksampler, der indgår i denne tese. Metoden er begrænset til problemer hvor modeller for reaktion og separation haves, samt data for de fysiske egenskaber for all indbefattede kemikalier.

Contents

List of Tables

List of Figures

1. Introduction

"The first step to knowledge is to know that we are ignorant"

(Socrates, 470-399 B.C.)

In recent years many activities in the area of chemical process design have involved the design and analysis of reaction-separation and separation-separation systems which could be labelled as 'hybrid processes'. Within the context of this thesis, the term *hybrid process* refers to the combination of at least two chemical processes that are different in nature. In this work, the term *integrated chemical process* is the synonym of the *hybrid chemical process*. The term *design* refers to the generation of a preliminary design of chemical and biochemical processes.

Hybrid chemical processes can be found in chemical and biochemical manufacturing, in processes when: (1) reaction is equilibrium or kinetically controlled; (2) separation is limited because of phase behaviour, existence of azeotropes and/or tangent pinch; and (3) compounds to be separated are heat sensitive.

Membrane reactors have been successfully used when reaction is equilibrium or kinetically controlled (Whu et al., 1999; Parulekar, 2007) because on-site removal of product(s) enhances the product yield and suppresses undesired side reaction(s). Reactive distillation has been used in case of equilibrium controlled reactions such as esterification of methyl *tert*-butyl ether (Matouq et al., 1994; Schmidt-Traub & Górak, 2006). The combination of two separation processes into a hybrid process consisting of distillation and pervaporation has been used to separate ethanol-water mixtures (Mulder, 2003) and isopropanol-ethanol-water mixture (Lipnizki et al., 1999). The high-end hybrid combination of reactive distillation and pervaporation has been studied recently for the production of n-propyl propionate by Buchaly et al. (2007).

Most of the published works on hybrid chemical processes provide an overview of the application of hybrid processes and applicability of the specific hybrid process configurations but they do not provide general rules for process selection, which can be combined into the integrated processes. Moreover, design of a hybrid chemical process employs trial and error experimental procedure, for that reason, design of such processes is time consuming and expensive. Therefore, there is a need for development of the computer-aided and model-based framework which would save valuable resources and speed up the design of hybrid process.

The design of an integrated process is a task which can be addressed to some extend by different methods known from process synthesis: (1) knowledge or heuristic

rule-based methods, (2) optimization-based methods, and (3) hybrid approach which employ physical insights (Schmidt-Traub & Górak, 2006; d'Anterroches, 2005).

A knowledge based method employs a set of rules based on a combination of experience, insights and available knowledge and data. User of such method needs to closely interact because rules can not be applied to all kinds of situations and they might be in contradiction to each other.

Optimisation-based methods rely on the mathematical representation of the problem and subsequent use of the optimization technique to solve the problem. The advantage of these methods is handling the design problems with a rigorous analysis in terms of interactions between structural elements of the flowsheet and costs. However, process alternatives are limited to the processes considered in the superstructure a priori.

Hybrid approach combines physical insights of knowledge-based methods to decompose the design problem into a collection of mathematical problems. Hybrid approach consists of several steps after which user has to follow. In hybrid approach solutions of mathematical problems provide input information to the subsequent steps of the hybrid approach and finally lead to the identification of a final design. Note that this approach does not contain rules which might be in contradiction to each other as knowledge based method.

The method proposed in this PhD-thesis belongs to the hybrid approach. The objective was to develop a computer-aided and model-based framework which could ease the work of the process engineer designing hybrid processes. The developed framework for hybrid process design and analysis consists of three stages: (1) Hybrid process design and analysis; (2) Implementation; and (3) Validation. The first stage consists of five main steps. In the step 1a (Separation task and reaction data analysis) the mixture which needs to be separated with or without occurrence of the reaction is analysed. Main roles in the mixture analysis play pure compound properties, thermodynamic models used for the phase equilibria calculations and, when reaction takes place, kinetic model of the reaction used for reaction analysis. In this step process constraint like maximum operating temperature when using catalyst, existence of azeotropes, reaction conditions with respect to temperature, pressure and reactant ratio are identified. In the following step 1b (Need of solvent) the influence of a solvent on the investigated mixtures is considered. The goal of the process design is defined in step 2 (Determine process demands) in terms of product purity, conversion of reaction, processing time, etc. Also, in this step the type of the operation need to be selected, it can be either continues or semi-batch, or batch operation. In step 3 (Selection of separation technique), based on available models describing separation techniques and/or their experimental data, separation techniques are compared based on the driving force approach. Therefore, feasible hybrid process configurations are identified. In step 4 (State process conditions) the specific hybrid process model is generated for the most promising hybrid process configuration form a generic hybrid process model. The generic model describes the superstructure of the hybrid process. The specific hybrid process configuration is tested by means of the

process simulation and finally operational conditions are stated. In stage 2 the proposed hybrid process design in the last step of stage 1 can be implemented as lab-scale or pilot plant. Therefore, carefully selected experiments and their results are used to verify the hybrid process design in stage 3. Note that when experimental data of the proposed design are available in the literature there is no need to do the second stage of the framework, since available data can be used for validation of the design. It is important to point out that all stages interact with each other since experimental data can discover behaviour which has not been known when design decisions where taken, therefore review of taken decisions is needed. At all of the stages various computer-aided tools are used to assist user in the design and analysis of the hybrid process. Mainly computer-aided tools from the ICAS package have been used. The idea behind the developed framework is not that the process design and analysis can be done in a completely automatic manner. Rather, the framework will assist engineer in the steps of the problem analysis, generation and screening among alternatives, so that only feasible and the most promising design candidate is set for the final experimental evaluation.

The PhD-thesis is organized into five chapters including this chapter (Introduction). The following chapter (chapter 2) gives an overview of the theoretical background and state-of-the-art related to the analysis and design of reactive and separation processes. In this chapter, classification of reactive and separation processes is given, with emphasis on the membrane-based separation found in chemical and biochemical practise. Also, this overview includes a discussion about models used to describe membrane-based separation processes, which is reported along with property models that are also needed. A significant part of chapter 2 is dedicated to the review of methods and strategies for process design and process synthesis. Chapter 3 provides the full picture of the developed framework for design and analysis of hybrid processes (e.g. reaction-separation and separation-separation processes). The framework is presented in details along with presentation of used computer-aided tools. In this chapter the developed MemData-membrane database is presented. The developed framework has been applied in several design problems, which are presented in chapter 4. Case studies highlight application of the developed framework to various design problems from chemical and biochemical manufacturing. First case study deals with separation of binary mixture of water and acetic acid. The following case studies deals with: esterification reaction of cetyl oleate, interesterification of phosphatidylcholine, synthesis of ethyl lactate and production of n-propyl propionate. In the last case study, production of n-propyl propionate, the hybrid process membrane assisted batch reaction was verified experimentally. All related models and additional information to the presented case studies are provided in the Appendix 4. Finally chapter 5 presents conclusions and directions for future developments of this work.

2. Theoretical background

"Yes, we have to divide up our time like that, between our politics and our equations. But to me our equations are far more important, for politics are only a matter of present concern. A mathematical equation stands forever."

(Albert Einstein)

2.1. Introduction

Almost all industrial chemical processes transform a set of raw materials into useful product(s). Raw materials are usually subjected to several separation processes to obtain compounds which are used in the following reactive processes as reactants. Reactive processes transform reactants into products and usually proceed in a reactor or a network of reactors. Sometimes the final product is obtained directly from the reactive process. However, most often the post reaction mixture is subjected to separation processes which are recovering and purifying the transformed product(s). The simplified flowsheet of any chemical process is presented in Figure 2.1.

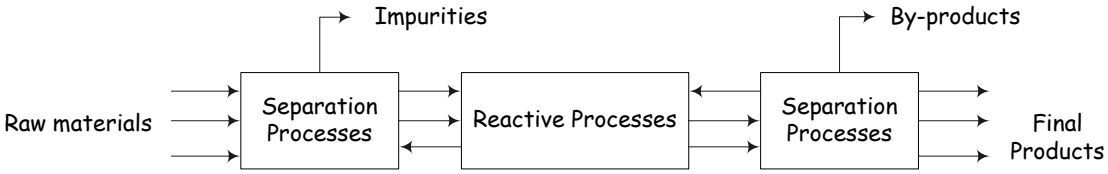

Figure 2.1: Simplified representation of chemical process (based on Burghardt & Bartelmus, 2001)

2.2. Hybrid processes

Equilibrium or kinetically controlled reactions are common in chemical and biochemical manufacturing. This type of reaction is usually characterized by low product yield or low selectivity towards the desired product, when parallel reactions occur. On-site removal of product(s) enhances the yield, suppresses undesired side reaction(s) and therefore leads to reduced processing times of batch operations. The combination of separation and reaction in an integrated unit can save economic and operational resources leading to a more sustainable process.

The products of the biochemical reactions in biochemical manufacturing are usually

heat sensitive. Therefore, in order to avoid thermal degradation the separation technique should operate at temperatures lower than the degradation temperature of the compounds. One option could be membrane-based separation processes where the separation proceeds because of the selectivity imparted by the membrane, based on either the difference in size or the chemical potential of the molecules. Also, membrane separation techniques enjoy advantages such as low operational costs, high selectivity, modular design and lower environmental impact.

Membrane separation techniques like pervaporation and nanofiltration have been extensively studied (Whu et al., 1999; Ferreira et al., 2002; Scarpello et al., 2002). Nanofiltration is emerging as an option in separation of molecules with molecular weight (M_w) ranging from 500 – 2000 g/mol from dilute solutions. Now the membranes which are resistant to degradation by organic solvent are also commercially available. These membranes are fairly reasonable option when the separation is based on size. For example Whu et al., (1999) studied two organic reactions where desired product produced in the first reaction has M_w around 600 g/mol and by-product M_w 50 g/mol. Reactants M_w were varied between 200-400 g/mol. The by-product was reacting with reactant leading to undesired product. Whu et al., (1999) combined reactor with membrane-based separation (nanofiltration) for selective removal of by-products (M_w 50 g/mol) leading to significant increases of process productivity (e.g. high conversion to desired products).

The advantage of membrane techniques, especially vapour permeation and pervaporation combined with reactive distillation has been utilized in synthesis of methyl *tert*-butyl ether (Matouq et al., 1994; Schmidt-Traub & Górak, 2006) and production of n-propyl propionate (Buchaly et al., 2007) giving very promising results. In these processes, researchers achieved high conversion of reactants and obtained outlet streams (distillate and bottom product) which can be easily separated to obtain final high purity product while unreacted reactants are recycled. Membrane-based separation techniques uniquely offer selective separation of components from mixtures by enhancing not only conversion of reactants to products but also a desired separation by breaking azeotropes like isopropanol/water (Sanz & Gmehling, 2006).

Coupling of two processes, either reaction with separation or two different separation processes is called a hybrid process. The two processes influence the performance of each other and the optimisation of the design must take into account this interdependency. Moreover, a true hybrid process circumvents the technical limitations (generally thermodynamic) that apply to at least one of the component unit operations. This definition was given by Lipnizki et al. (1999) who divided hybrid processes into two types S (separation) and R (reaction). The type S includes two hybrid configurations:

(1) S1: an interlinked inter-dependent combination (Figure 2.2A),

(2) S2: a combination of two consecutive processes achieving split that neither could be achieved alone (Figure 2.2B).

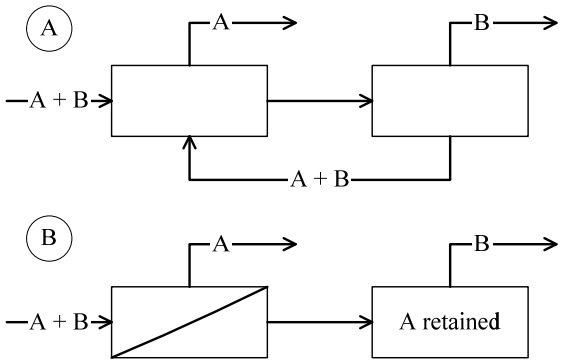

Figure 2.2: Hybrid separation processes; A) type S1 (with recycle), B) type S2 (no recycle) (Lipnizki et al., 1999)

Note that type S2 refers to the hybrid processes in which as the first process is a membrane-based separation followed by another non-membrane separation. Such processes can be found in the waste water and biotechnology applications. An example of such a hybrid process was given by Ray et al. (1986) for the wastewater treatment on the space-station where the reverse osmosis unit was followed by various sorption beds. The reverse osmosis unit recover 95% of water and sorption beds are used to remove all classes of remaining contaminants found in permeate of membrane unit.

The hybrid processes including reaction and membrane-based separation unit have been divided into two types:

(1) R1: the separation process removes the product (Figure 2.3A)

(2) R2: the separation process removes the by-product (Figure 2.3A)

It is important to point out, that integration of reactor and membrane-based separation into one unit as shown in Figure 2.3B is also possible but in this case very specific conditions need to be fulfilled with respect to resident time and rate of component(s) removal.

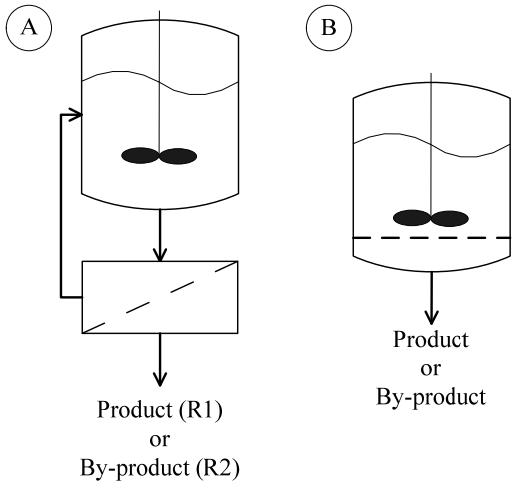

Figure 2.3: Hybrid process layouts, A) type R1 and R2 (Lipnizki et. al., 1999), B) internal membrane unit

2.3. Separation and reactive processes

In this section, first an overview about separation processes is given followed by a review of reactive processes with main focus on solvent-based reactive processes.

2.3.1. Separation processes

A separation process is used to separate a given feed mixture of chemicals into two or more compositionally-distinct products (mixtures). The classification of separation processes can be based on the employed chemical, or mechanical, or physical phenomena. Depending on the inlet stream characteristics, which may include solids, or liquid or gas/vapour, or a mixture of these phases, different separation processes can be employed to separate the stream into product streams. An overview of various mechanical and physical separation processes depending on what kind of stream needs to be separated is given in Figure 2.4. This figure does not contain separations which are based on the chemical phenomena. Such separations involve formation of a chemical bond, for example between compound and mass separation agent like in chemisorption, which is opposed to Van der Waals forces which cause physisorption. Many of the listed separation processes in Figure 2.4 require mass separation agents (MSA) such as solvents (solvent-based processes: extractive distillation, absorption, extraction), membrane (all membrane-based separation), adsorbent (adsorption), and absorbent (absorption). In the following sections solvent-based separation processes and membrane-based separation processes are discussed.

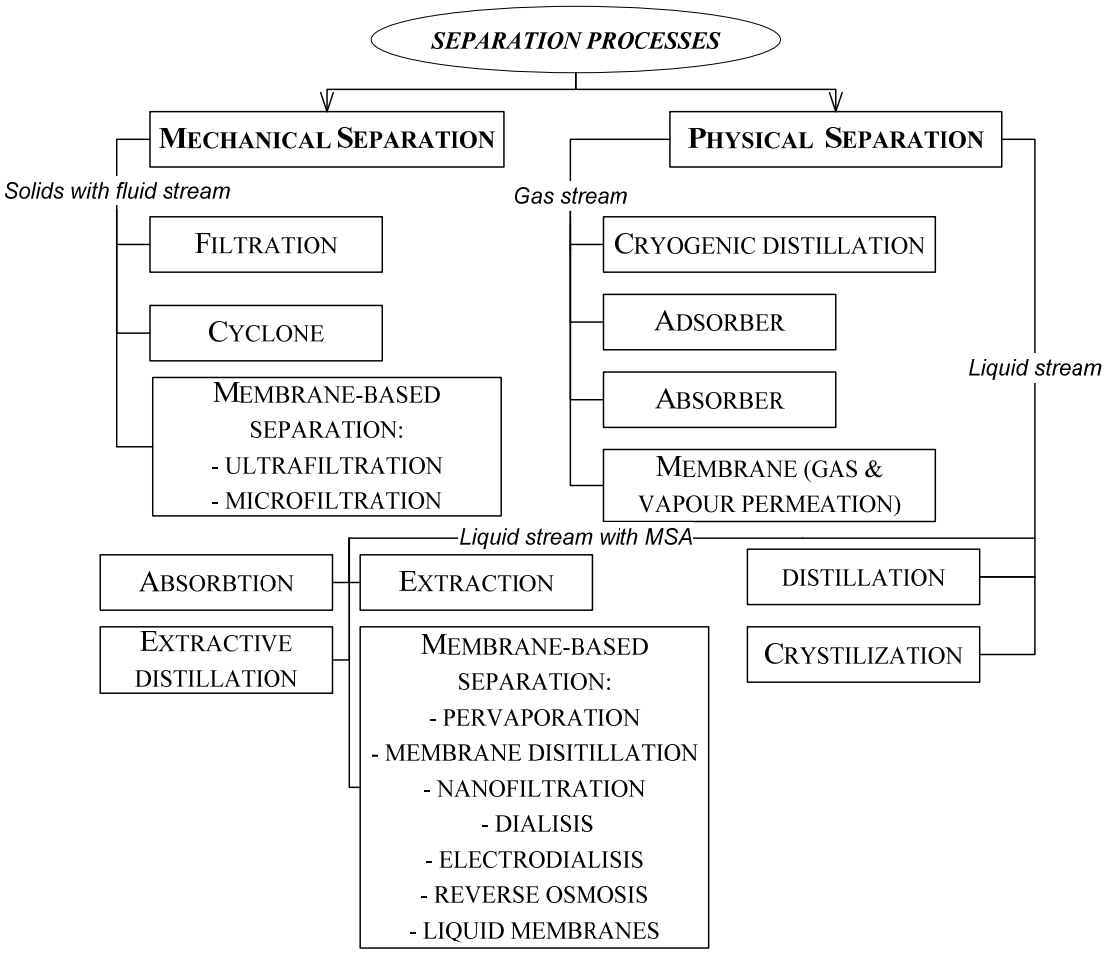

Figure 2.4: Classification of separation processes depending on the feed characteristic

2.3.2. Solvent-based separation processes

Solvent-based separation processes are employed when a mixture that needs to be separated consists of compounds having low relative volatilities or non-volatile compounds (solids). In this work solvent is defined as a compound which is liquid in the pure state and dissolves with other compound solute(s) of the solution. The solute might be a solid, gas or a liquid. Usually, concentration of the solvent in the separating mixture is larger than solute(s). Liquid-liquid extraction, extractive distillation, azeotropic distillation and absorption are some of the well-known solvent-based separation processes in chemical industry.

Liquid-liquid extraction is a method to separate compounds based on their relative solubilities in two different immiscible liquids. In that separation addition of solvent creates two immiscible liquid phases. Liquid-liquid extraction is the commonly used separation technique for separation of phenol from aqueous solutions.

Extractive distillation is used to separate azeotropes and other mixtures that have key components with a relative volatility below about 1.1 over an appreciable range of

concentration. The components in the feed must have different affinities for the solvent, which causes an increase in the relative volatility of the key components, to the extent that separation becomes feasible and economical. The solvent should not form an azeotrope with any components in the feed (Seader & Henley, 1998).

Two kinds of *azeotropic distillation* are distinguished: *heterogeneous azeotropic distillation* and *homogenous azeotropic distillation*. Heterogeneous azeotropic distillation is a method in which minimum-boiling azeotrope is formed by the entrainer. The azeotrope splits into two liquid phases in the overhead condensing system. One liquid phase is sent back to the column as a reflux, while the other liquid phase is sent to another separation step or is a product. The well known example is dehydration of ethanol by benzene (Seader & Henley, 1998). Homogeneous azeotropic distillation refers to a method of separating a mixture by adding an entrainer (solvent) that forms a homogeneous minimum- or maximum-boiling azeotrope with one or more feed components. The entrainer is added near the top of the column, to the feed, or near the bottom of the column, depending upon whether the azeotrope is removed from the top or bottom.

Absorption is referred to the process where a gas mixture is contacted with a liquid to selectively dissolve one or more components by mass transfer from the gas to the liquid (Seader & Henley, 1998). The liquid phase consists mainly of one solvent or mixture of solvents.

In all these solvent-based separation processes the key issue is the selection of the appropriate solvent which will enable efficient separation. Solvent selection is directly related to the specific solvent-based separation and the pure component properties of solvent like solubility parameter, boiling and melting points, as well as a phase split of the mixture.

Harper (2002) presented the computer-aided molecular design (CAMD) method to design compounds (solvent(s)) of specific physical and chemical properties using a 3-step iterative procedure:

- Pre-design step – computer-aided steps for problem formulation,
- Design step – compound identification,
- Post-design step – result analysis.

Following the description given by Harper and Gani (2000), the formulation of the design specifications is performed in a computer aided pre-design step where the problem is identified and the design goals (desired compound types and properties) are formulated in order to provide input to the applied method of solution for compound identification. The employed CAMD solution method is a hybrid of generate and test type where all feasible molecules are generated from a set of building blocks and subsequently tested against the design specifications. In order to avoid the so called combinatorial explosion problem, the multi-level approach of Harper et al. (1999) is employed where, through successive steps of generation and screening against the design criteria, the level of molecular detail is increased only on

the most promising candidates. In the post-design step the results from the solution procedure are analyzed with respect to properties and behaviour that could not be part of the design considerations. Examples of such properties and behaviour are price, availability, legislative restrictions and process wide performance. This step involves using other prediction methods, database sources, engineering insight, and if possible, simulation in order to get an overview of the suitability and capability of the designed compound(s) for the particular purpose.

2.3.3. Reactive processes

A chemical reaction is a process that always results in the interconversion of chemical substances (Muller, 1994). Chemical reactions are usually characterized by a chemical change, and they yield in one or more products which are, in general, different from the reactants. Chemical reactions encompass changes that strictly involve the motion of electrons in the formation and breakage of chemical bonds. The chemical reactions are symbolically represented by a chemical equation. The coefficients next to the symbols and formula of entities in a chemical equation are the absolute values of the stoichiometric numbers. Detectable chemical reactions normally involve of molecular entities but it is often conceptually convenient to use the term also for changes involving single molecular entities (i.e. "microscopic chemical events").

Chemical reactions can be classified depending on the phase in which reaction takes place. Therefore, chemical reaction can proceeds in homogenous phase, e.g. liquid, gas, or heterogeneous phase, like on liquid-solid, gas-solid, gas-liquid and liquid-liquid interfaces. Reactive processes can be also divided into two groups: solvent free and solvent-based reactive processes depending on absence or presence of the solvent. The solvent-based reactive processes are described in the following section 2.2.3.

2.3.4. Solvent-based reactive processes

Many reactions are carried on in a liquid phase with use of solvents, especially in pharmaceutical and agrochemical industries (Kolár et al., 2005). In general two kinds of liquid phase reactions can be distinguished with respect to their nature: aqueous and organic. The reacting compounds are placed in a one particular solvent or in a solvent mixture because solvent(s):

- bring reactants together; it creates a *reaction medium*,
- dissolve a solute and bring to another reactant(s); solvent is a *solubilisation agent,*
- deliver compounds in solution to their point of use in the required amounts; solvent acts as a *carrier*,
- supply heat for endothermic reactions; solvent is a *supplier*,
- remove surplus of heat in exothermic reactions,

- indirectly influence the reaction by removing one or more products on-site; solvent create a second phase, solvent is a *separation agent.*

The properties of solvent which has significant influence on the reaction set-up can be expressed by: solvent reactivity, chemical equilibrium constant for specific reaction in a solvent, boiling point, melting point, vapour pressure, liquid phase stability (for reactants and products), Hildebrand solubility parameter, activities, environmental, health and safety (EHS) properties, association, polymerization, oligomerisation, selectivity, viscosity, polarity and heat of vaporization. This list does not include all properties which have influence on solvent-reactive systems but gives an overview of complexity of the solvent selection problem.

The key issue in the design of solvent-based processes is a selection of a solvent or a mixture of solvents which will satisfy not only the process requirements but also numerous environmental, health and safety requirements. Several researchers provided numerous methodologies facilitating solvent selection for reactive system (Folić et al., 2004; Gani et al., 2005; Curzons & Constable, 1999). A short overview about some of them is given below.

Gani et al. (2005) presented a method for solvent selection for organic reaction which takes into account chemical and environmental requirements. The objective of this methodology is to find the solvents that can promote the reaction (in terms of yield, reaction mass and heat efficiency) and rank solvents according a particular evaluating system. The first necessary step before starting the solvent selection algorithm presented in Figure 2.5 is to evaluate if, for the considered reaction system, a solvent is necessary. The solution method applied by the methodology consists of retrieving or generating reaction data (the minimum data needed to solve the problem) at step 1 and based on these, allocates values to a set of reaction-indices (R) (step 2). In the next step, using a combination of rules (based on industrial practice and physical insights) and estimated solvent properties, values are allocated to a set of reaction-solvent property indices (RS). In the next step, these generated RS values for each solvent are converted to their corresponding score-values (S). The solvents that have the highest scores and do not have more than one lowest score are listed as feasible and selected for further detailed study (for example experimental verification) in step 5.

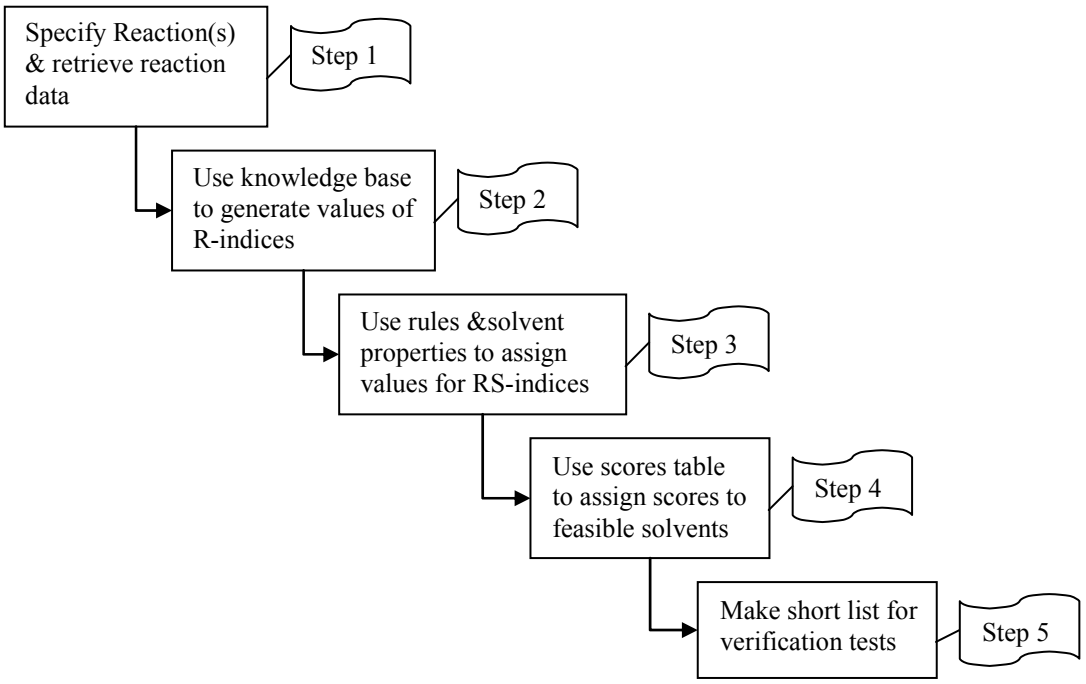

Figure 2.5: The main steps of solvent selection methodology proposed by Gani et al. (2005)

An interesting approach was proposed by Folić et al. (2004) using a multi-parameter solvatochromic equation, which correlates empirical solvatochromic parameters and Hildebrand solubility parameter with the logarithm of the reaction rate constant. The objective of this approach is to find candidate solvents which give high values of the reaction rate constant. This approach involves at first step generation of solvatochromic linear equation for reaction rate data of studied reaction in known solvents followed by the formulation and solution of an optimal computer-aided molecular design problem (*CAMD*) in which the reaction rate under given condition is maximized. The final step provides a way to verify the solutions obtained and it results in a final ranking of solvents which can be used as reaction media for the reaction studied. Verification can be done by performing experiments to test the best solvents generated. The methodology is limited to one step-reactions.

Another approach of solvent selection has been presented by Sheldon et al. (2006) using a quantum mechanical continuum solvation model. This model is based on a quantum mechanical representation of the solute, a continuum solvation model based on several bulk solvent properties and group contribution methods for the prediction of these properties. An optimization-based molecular design problem is formulated with the simple objective of minimizing the free energy of solvation. The resulting problem is a nonconvex mixed-integer nonlinear program with mixed-integer algebraic constraints. The outer-approximation algorithm is implemented to solve this optimization problem, using a combination of analytical and numerical gradients.

For toxicological reasons, drug manufacturers are required to reduce the number of

solvents employed in the pharmaceutical processes. There is also a need to replace certain classes of solvents by solvents with a lower toxic potential. Moreover, replacement of solvents can increase the process productivity. Solvent selection for synthetic pharmaceuticals is complicated because the molecules are multifunctional, polarisable and can form specific interactions with the solvent. The problems of solvent selection in this area have been discussed by Gani et al. (2005) and by Kolár et al. (2005). Synthetic pharmaceuticals are usually produced in a series of batch reactions via intermediates steps. Each synthetic step is typically followed by separations using usually extraction or crystallization. Most of pharmaceutical products are solids and the key requirements for the product quality are the purity, yield, crystal form and morphology. Particularly severe problems that may limit usability of some synthetic routes are insufficient reaction yields and excessive formation of by-products and related isomers in certain steps. The solvent may sometimes be a critical parameter in the synthetic process and its appropriate selection may enhance the reaction yield and determine the product quality, e.g. structure of crystals.

Kolár et al. (2005) proposed to study the thermodynamics of pharmaceutical products by first focusing on small to medium sized aromatic and heterocyclic molecules. They proposed a general procedure for studying interactions of pharmaceutical products with solvents involving the following four main steps:

- systematization of existing drugs into pharmacological categories,
- identification of common core fragments and functional groups in each category,
- systematic variation of the core fragments by the inclusion of mono- and bifunctional substituents,
- study of the solubility of the mono- and bifunctional derivatives in a series of solvents of varying polarity and hydrogen bonding tendency.

Kolár et al. (2005) consider solubilisation as the main function of the solvent in pharmaceutical manufacturing. However, Kolár et al. (2005) pointed out, the selectivity, reaction rate and yield of the synthesis can be significantly affected by the presence of the solvent. Direct solubility data in different solvents are available in some databases like the CAPEC Database (Nielsen et al., 2001). In practice, the selection of solvents is mostly guided by experience and experimental testing.

2.3.5. Phase and reaction equilibrium: Reactive flash

The computation of simultaneous chemical and physical equilibrium plays an important role in the prediction of the limits for conversion and separation of reactive and separation processes. Several computational approaches of simultaneous chemical and physical equilibrium calculations have been proposed by many researchers, for example Smith and Missen (1982), Michelsen (1989), Alejski and Duprat (1996), McDonald and Floudas (1995), and Ung and Doherty (1995). These

approaches can be divided into two groups: the stoichiometric approach which is based on the solution of a set of nonlinear algebraic equations involving expressions for apparent equilibrium constants and material balance equations (for example Smith and Missen, 1982), and the approach which minimises the thermodynamic function that defines the conditions of chemical and physical equilibrium. Algorithms for simultaneous calculation of chemical and physical equilibrium have been proposed by Michelsen (1989), McDonald and Floudas (1995), Ung and Doherty (1995). All these algorithms solve the model equations written in terms of component compositions of the coexisting phases. In other words, conditions for chemical and physical equilibrium are satisfied through component compositions. The second approach does not require experimental data of apparent equilibrium constant and the solution provide information about equilibrium composition for the given initial component composition and conditions of a mixture.

Michelsen (1995) proposed, for calculation of reactive phase equilibrium, the use of the chemical model concept where any appropriate physical model yielding the chemical potentials are incorporated into an element-based model (called the chemical model). The solution of the chemical model equations together with the condition of equilibrium provides the element phase compositions for the reactive system. Chemical element is an invariant fragment of the reactants present in the mixture. The rank of the formula matrix gives information about independent chemical elements and independent chemical reactions; additionally it gives the minimum number of molecular decompositions into atoms or fragments in which any chemical reaction system can be written.

In this section a short review on the second approach, as developed by Pérez-Cisneros et al. (1997) is given. When the Gibbs energy function is used to describe the thermodynamic system, the condition for thermodynamic equilibrium of a closed system is defined as the state for which the total Gibbs free energy attain its minimum with respect to all possible changes at the given T and P. This is formulated mathematically as:

$$\min G\left(\underline{n}\right) = \sum_{\beta=1}^{NP} \sum_{k=1}^{NC} n_k^{\beta} \mu_k^{\beta}\left(T, P, \underline{n}\right) \tag{2.1}$$

$$s.t. \quad \sum_{\beta=1}^{NP} \sum_{k=1}^{NC} A_{jk} n_k^{\beta} - b_k = 0, \quad k = 1,2,...,M;\ \beta = 1,2,...,NP \tag{2.2}$$

where $G\left(\underline{n}\right)$ is the total Gibbs free energy of a system containing NC species and NP phases, n_k^{β} is the number of moles of species k in phase β and μ_k^{β} is the chemical potential of species k in phase β.

The Lagrange multiplier formulation results in the following set of equation:

$$\mu_i - \sum_{\beta=1}^{NP} \sum_{k=1}^{M} A_{kj} \lambda_j^{\beta} = 0 \tag{2.3}$$

$$\sum_{\beta=1}^{NP}\sum_{k=1}^{NC} A_{kj} n_k^{\beta} - b_k = 0 \tag{2.4}$$

Pérez-Cisneros et al. (1997) applied the chemical element concept with combination of ideal solution chemical equilibrium procedure for simultaneous chemical and physical equilibrium computation. The two-phase reactive flash operation can be modelled through equations which represent component mole balance:

$$\theta^V \sum_{k=1}^{NC} A_{jk} y_k + \theta^L \sum_{k=1}^{NC} A_{jk} x_k - b_{jk} = 0, \quad j = 1,2,...,M \tag{2.5}$$

and the corresponding constraint equations:

$$\sum_{k=1}^{NC} y_k - 1 = 0 \tag{2.6}$$

$$\sum_{k=1}^{NC} x_k - 1 = 0 \tag{2.7}$$

where A_{jk} are invariant elements of the formula matrix (k - component, j - chemical element), b_{jk} are the elemental compositions, θ^V is mole phase fraction of vapour phase, θ^L is mole phase fraction of liquid phase.

The conditions of chemical and physical equilibrium (2.8) have to be satisfied.

$$\mu_k^V = \mu_k^L \tag{2.8}$$

However, the chemical potential (μ_k) is composition dependent and in case of a two phase system (vapour/liquid) is given by relations (2.9) and (2.10) for vapour phase and liquid phase respectively.

$$\frac{\mu_k^V}{RT} = \ln y_k + \ln \phi_k^V + \ln P + \frac{\mu_k^0}{RT} \tag{2.9}$$

$$\frac{\mu_k^L}{RT} = \ln x_k + \ln \gamma_k^L + \ln P_k^{sat} + \frac{\mu_k^0}{RT} \tag{2.10}$$

where μ_k^0 is the standard state chemical potential. Employing the Lagrange multiplier formulation of minimization problem (2.3), the conditions of chemical and physical equilibrium (2.8), Eqs. (2.9) and (2.10) are rewritten:

$$y_i = \exp\left(\sum_{j=1}^{M} \frac{\lambda_j}{RT} A_{jk} - \frac{\mu_k^0}{RT} - \ln \phi_k - \ln P \right) \tag{2.11}$$

$$x_i = \exp\left(\sum_{j=1}^{M} \frac{\lambda_j}{RT} A_{jk} - \frac{\mu_k^0}{RT} - \ln \gamma_k - \ln P_k^{sat} \right) \tag{2.12}$$

By substituting Eqs. (2.11-2.12) into Eqs. (2.5-2.7) the following set of *M+2*

equations is obtained:

$$\theta^V \sum_{k=1}^{NC} A_{jk} y_k\left(\lambda_j\right) + \theta^L \sum_{k=1}^{NC} A_{jk} x_k\left(\lambda_j\right) - b_{jk} = 0, \quad j = 1,2,...,M \tag{2.13}$$

$$\sum_{k=1}^{NC} y_k\left(\lambda_j\right) - 1 = 0 \tag{2.14}$$

$$\sum_{k=1}^{NC} x_k\left(\lambda_j\right) - 1 = 0 \tag{2.15}$$

Described above set of equations (2.13-2.15) results in $M+2$ equations with $M+2$ unknown variables: θ^V, θ^L and λ_j (where $j = 1,2,...,M$). In practise, vapour phase fugacity coefficients (ϕ_k) and liquid phase activity coefficients (γ_k) are composition dependent. Therefore, in the solution of Eqs. (2.13-2.15) an outer loop is required for updating the activity and fugacity coefficients. This idea has been used for reactive flash calculations and it is described in details in section 6.1 Appendix 1: Reactive flash calculation (see page 177).

2.4. Membrane-based separation processes

Membrane-based separation processes have wide industrial applications that include many existing and emerging applications in chemical, fine chemical, petrochemical, biochemical, petrochemical, water treatment, medical, food, dairy, beverage and paper industry. More and more membrane-based separation processes are replacing conventional separation processes like distillation, absorption because of advantages over conventional processes, which are listed below (Ho & Sirkar, 1992; Mulder, 2003; Baker,2004):

- membrane-based separation processes are often more capital and energy efficient compared to conventional separation processes,
- membrane modules and systems are usually compact and modular which makes easy to scale-up and implementation within processes,
- membrane technology is environmentally benign and in general is a clean technology,
- membrane processes usually operate on low pressures,
- Usually, membrane processes do not require complex operational strategies.

The chemical and mechanical stability as well as the change of the separation characteristics (e.g. component fluxes) over the long operation time are the main drawbacks of using novel membranes in the chemical industry. Due to stated advantages and the falling cost of membrane-based separation technologies in the recent years, there has been a huge acceptance of these technologies (Frost & Sullivan, 2006). Continued focus on membrane development has led to innovations of novel membranes and improvements of membrane-based separation processes.

A general membrane-based separation process is represented schematically on the diagram shown in Figure 2.6. A feed mixture coming to a membrane separation unit is separated into two streams, retentate and permeate. The membrane can be considered as a permeselctive barrier or interface between two phases. Separation is achieved because the membrane has the ability to transport at least one component from the feed mixture more readily than other component(s). This occurs through various mechanisms. In general, the driving force in membrane-based separation processes is characterized by difference in chemical potential, concentration, pressure, temperature or electrical field.

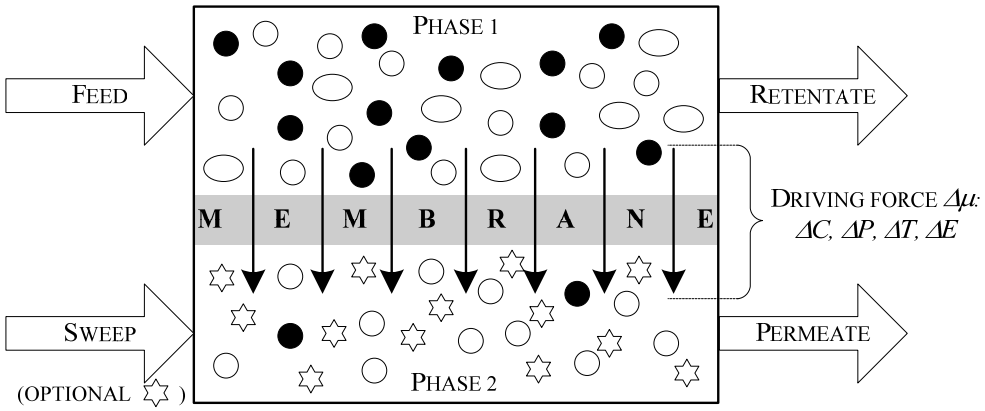

Figure 2.6: General concept of membrane-based separation

The membranes can be categorised into several groups based on the origin of the membrane (i.e. synthetic and biological), material (e.g. liquid, solid, organic or inorganic), morphology (e.g. porous, unporous), way of membrane production (phase inversion, casting, extrusion, etc.) and their application in process separation schemes. This classification of membranes is presented in Figure 2.7.

The membrane-based separation process can be divided into three classes: (1) gas separation, (2) liquid separation without phase change and (3) liquid separation with phase change. The examples of membrane-based separation processes are highlighted in Figure 2.8.

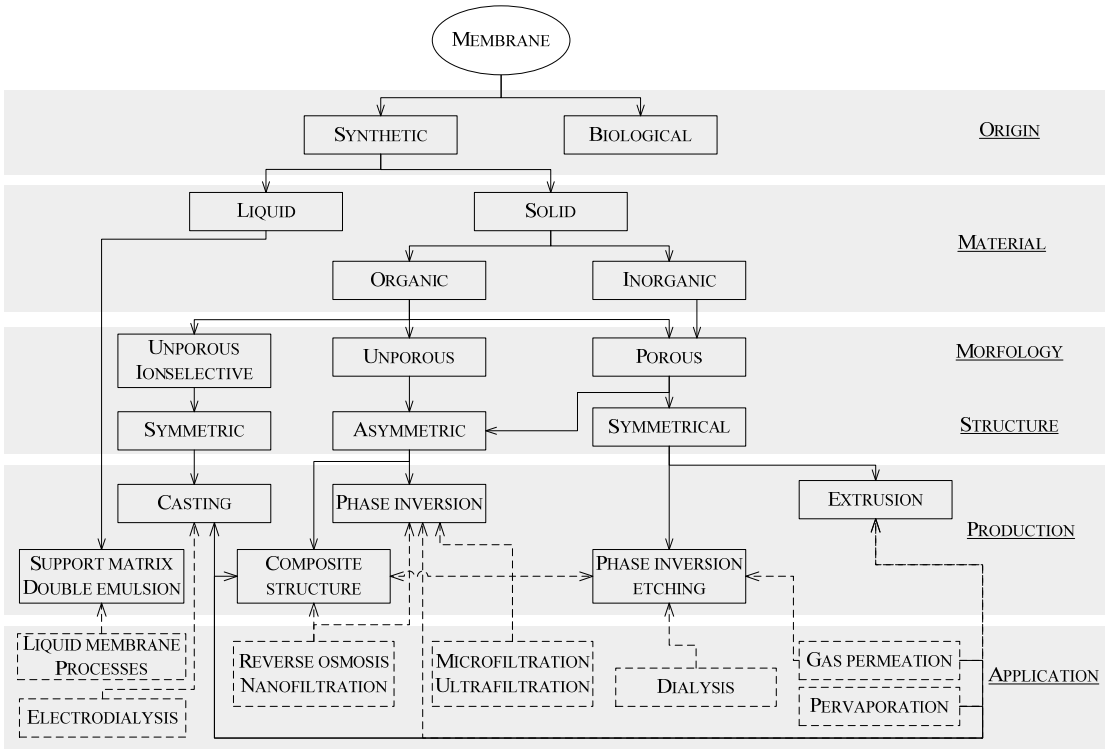

Figure 2.7: Classification of membranes and their application

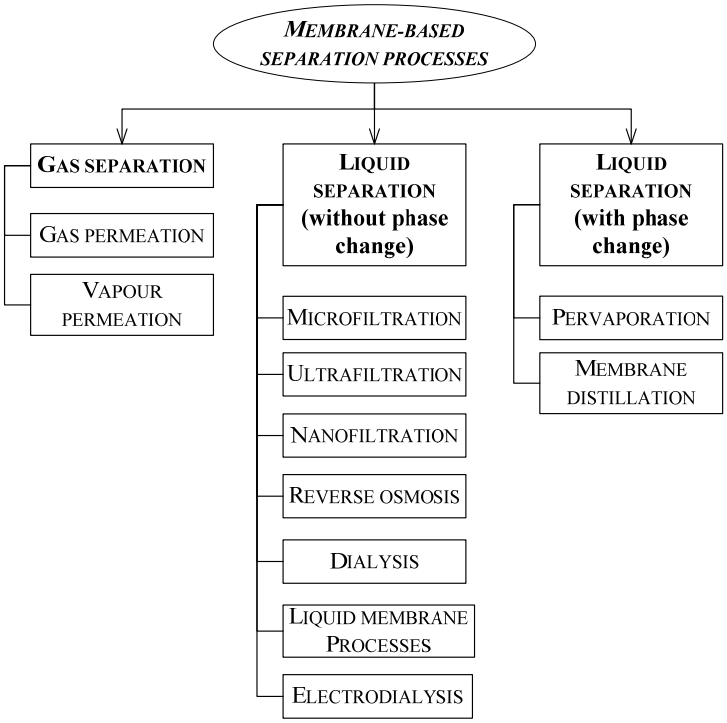

Figure 2.8: Classification of membrane-based separation processes depending on separated phases

Application of pressure driven membrane separation techniques depends on the size of separated molecules. This group consists of such processes as microfiltration, ultrafiltration, nanofiltration and reverse osmosis. The list of these processes along with their application range is given in Table 2.1. Other techniques use differences between molecules in terms of charge (electrodialysis), vapour pressure (membrane distillation) and affinity (gas separation, vapour permeation and pervaporation) (Mulder, 2003). The basic feature for gas separation, vapour permeation and pervaporation is the use of a nonporous membrane. The difference in permeability of components may differ significantly depending on whether they are permeating through an elastomeric or glassy polymer. This difference arises from large differences in segmental motion which is very restricted in the glassy state comparing to the elastomeric state. Another reason of this difference in permeability of components in elastomeric and glassy material is due to presence of a large free volume. The presence of polymer crystallites can further reduce the mobility. A factor that enhances segmental mobility in general, is the presence of low molecular size penetrants. Increasing concentrations of penetrants (either liquid or gas) inside the polymeric membrane leads to an increase in the chain mobility and consequently to an increase in permeability. The concentration of penetrants inside the polymeric membrane is determined mainly by the affinity between the penetrants and the polymer and the concentration (or activity) of the penetrants in the feed. When liquid interact with polymeric membrane the solubility of penetrants in the membrane may results in enhanced chain mobility. In membrane technology the interaction of liquid with polymeric membrane is described by the degree of swelling. Degree of swelling of the membrane is defined as the weight fraction of penetrants inside the membrane relative to the weight fraction of dry polymer (Mulder, 2003). The swelling of the membrane makes membrane more “open”; therefore, compounds can more easily diffuse through the membrane. Mulder (2003) demonstrated that the mobility of the polymer chains increases with increasing swelling. This happen when the diffusivity is comparable to diffusion in a liquid and a corresponding value of diffusion coefficient around 9-10 m^2/s. Thus swelling is a very important factor in assessment of transport through nonporous membrane.

Table 2.1: Ranges of membrane processes application

Membrane process	Range of separated molecules [nm]		Driving force
	Max	Min	
Microfiltration	10 000	100	ΔP
Ultrafiltration	200	1	ΔP
Nanofiltration	5	0.5	ΔP
Dialysis	5	0.5	ΔP
Reverse osmosis	1	0.15	ΔP

2.4.1. Pervaporation

Pervaporation is a separation process, which is based on the selective transport through a dense membrane combined with a phase change of the permeating components from liquid to vapour. Pervaporation is well established as a potential alternative for the dehydration of organic mixtures (Lipnizki et al., 1999; Lipnizki & Trägårdh, 2001; Kang et al., 2004; Sanz & Gmehling, 2006) and for recovery of organic compounds from water (Ohshima et al., 2005; Panek & Konieczny, 2006). Recently, the separations of organic-organic mixtures were investigated by Cai et al. (2003) and Marx et al. (2005). Modelling of transport phenomena in pervaporation plays an important role in understanding of the pervaporation process and therefore it helps in development of successful applications of pervaporation in chemical and biochemical industry. Pervaporation models are classified into four groups:

(1) theoretical models (e.g. model based on Maxwell-Stefan theory),

(2) semi-empirical / phenomological models (e.g. solution-diffusion model, model after Meyer-Blumenroth),

(3) empirical models (e.g. correlations between apparent permeability and concentration of component (Benedict et al., 2003),

(4) short-cut models (Q_i-models (Buchaly et al., 2007)).

Theoretical models usually are used for membrane development where a high analytical depth with regards to the trans-membrane mass transfer is required (Heintz & Stephan, 1994). Semi-empirical and empirical models are widely used in module and process design (Lipnizki et al., 2002) to have reasonable representation of all effects influencing the overall mass transfer in pervaporation. Short-cut models are used mainly in process design and analysis (Rautenbach, 1996; Benedict et al., 2006; Buchaly et al., 2007). In the following sections only some models belonging to the second, third and fourth group presented above are discussed in details, namely

solution-diffusion model, model after Meyer-Blumenroth, empirical models and short-cut models. These models are selected for further discussion since they are used in this work.

2.4.1.1. Solution-diffusion model

The solution-diffusion model describes the mass transport through a dense membrane in three steps:

- sorption of the permeating compounds into the polymer,
- diffusion through the polymer along the gradient of the chemical potential,
- desorption at the permeate side.

The schematic overview of typical profiles through the membrane is given in Figure 2.9. It is important to point out that the concentration profile in the membrane depends on the swelling of the membrane. Because of swelling, the permeant concentration inside the polymer will increase and diffusion coefficient will also increase under such circumstances (Mulder, 2003).

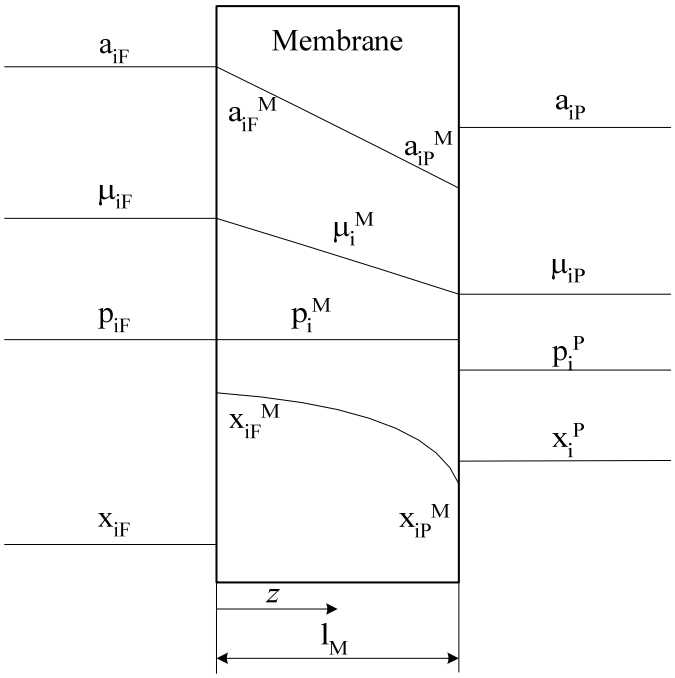

Figure 2.9: Gradients through the selective layer of a pervaporation membrane (Lipnizki & Trägårdh, 2001)

Lipnizki and Trägårdh (2001) presented derivation of the general equation for the flux in solution-diffusion model based on two starting points:

(1) Nernst's equation (Eq. 2.16) is introduced in general diffusion equation (Eq. 2.17)

$$D_i^T = R \cdot T \cdot b_{M,i} \tag{2.16}$$

$$J_i = -C_i(z) b_{M,i} \frac{d\mu_i}{dz} \tag{2.17}$$

By extending the diffusion equation the following formulation of flux J_i is obtained:

$$J_i(z) = -C_i(z) \cdot \frac{D_i^T(z)}{R \cdot T} \cdot \frac{d\mu_i}{dz} \tag{2.18}$$

(2) Fick's First Law

$$J_i(z) = -\dot{D}_i(z) \cdot \frac{dC_i(z)}{dz} \tag{2.19}$$

Based on the approach developed by Fels and Huang (1970) the thermodynamic diffusion coefficient (D_i^T) and Fickian diffusion coefficient ($\dot{D}_i$) are related by the volume fraction (Φ_i) of the solute i in the membrane and its activity a_i (see Eq. (2.20)).

$$D_i^T = \frac{\dot{D}_i}{1-\Phi_i} \cdot \frac{d\ln\Phi_i}{d\ln a_i} \tag{2.20}$$

Finally both approaches lead to the following equation for component flux in pervaporation:

$$J_i = \frac{\dot{D}_{M,i} C_{M,i}}{a_{M,i}} \frac{1}{l_M}\left(a_i^F - a_i^P\right) \tag{2.21}$$

Where $\dot{D}_{M,i}$ is a Fickian diffusion coefficient of component i through membrane, $C_{M,i}$ is a concentration of component i in membrane, l_M is a thickness of membrane, $a_{M,i}$, a_i^F and a_i^P represent activities of component i in membrane, feed and permeate side respectively.

In order to significantly reduce the experimental effort on determining component diffusion coefficients through the membrane, component concentration ($C_{M,i}$) and its activity ($a_{M,i}$) in the membrane a phenomenological permeability, P_i, is introduced which can be determined for specific system by simple pervaporation experiments:

$$P_i = \frac{\dot{D}_{M,i} C_{M,i}}{a_{M,i}} \tag{2.22}$$

Therefore, component flux expressed by eq. (2.21) simplifies to:

$$J_i = \frac{P_i}{l_M}\left(a_i^F - a_i^P\right) \tag{2.23}$$

Where phenomenological permeability depends on temperature:

$$P_i\left(T^F\right) = P_i^0\left(T^0\right)\cdot\exp\left[-\frac{E_i}{R}\left(\frac{1}{T^0}-\frac{1}{T^F}\right)\right] \tag{2.24}$$

The solution-diffusion model has been used for the testing and comparison of membranes, when the coupling of fluxes can be neglected, that is, when permeating components are present in a low concentration in the feed. Since the model includes the influence of all important process parameters the solution-diffusion model seems to be particularly suitable for the development and optimisation of the process using all types of polymeric membranes. However, use of this model in the simplified form (Eq. 2.23) for membrane development and optimization is limited comparing to model represented by Eq. (2.21) since all the fundamental variables ($\dot{D}_i$, $C_{M,i}$, $a_{M,i}$) are coupled into the single component permeability P_i variable.

2.4.1.2. Semi-empirical model after Meyer-Blumenroth

The semi-empirical Meyer-Blumenroth model in comparison to the solution diffusion model includes the effect of coupling of components present in the feed (Lipnizki & Trägårdh, 2001). The one-dimensional component flux through the membrane (J_i) is proportional to the driving force across the membrane which is expressed by the difference in pressure-based fugacity (f_i) instead of concentration-based activity in the original solution-diffusion model. Note, that both driving forces can be related through chemical potential. Therefore, the component flux can be written:

$$J_i = -C_i\,\frac{D_i^T}{f_i^0}\frac{1}{\gamma_{M,i}}\frac{df_i}{dz} \tag{2.25}$$

Assuming equilibrium at the interfaces of the membrane, the fugacities of the feed and permeate sides can be used as boundary conditions for the integration of Eq. (2.25). The integration of Eq. (2.25) for the flux of the component *i* across the membrane of thickness l_M results in following equation:

$$J_i = \frac{\bar{D}_i^T}{\bar{\gamma}_{M,i}}\left(\frac{f_i^F - f_i^P}{f_i^0}\right) \tag{2.26}$$

where

$$\bar{D}_i^T = \frac{C_{M,i}D_i^0}{l_M} \tag{2.27}$$

Due to the integration of Eq. (2.25) over the coordinate *z* the average activity coefficient ($\bar{\gamma}_{M,i}$) of component *i* in the membrane of thickness l_M and modified thermodynamic diffusion coefficient of component *i* across the membrane ($\bar{D}_i^T$) is introduced in Eq. (2.26). The component average activity coefficient across membrane is calculated according to Eq. (2.28). The local activity coefficient at the membrane and the local fugacities on the feed and permeate sides are related by

relationships expressed by Eqs. (2.29) and (2.30).

$$\overline{\gamma}_{M,i} = \sqrt{\gamma^F_{M,i}\gamma^P_{M,i}} \tag{2.28}$$

on the feed side:
$$\gamma^F_{M,i} = \exp\left(B^\circ_i \left(1 - \sum_{j=1}^{NC} B_{ij} \frac{f^F_i}{f^0_i} \right) \right) \tag{2.29}$$

on the permeate side:
$$\gamma^P_{M,i} = \exp\left(B^\circ_i \left(1 - \sum_{j=1}^{NC} B_{ij} \frac{f^P_{,i}}{f^0_i} \right) \right) \tag{2.30}$$

The temperature dependence of the modified thermodynamic diffusion coefficient is represented by an Arrhenius-type of equation:

$$\overline{D}^T_i\left(T^F\right) = \overline{D}^T_i\left(T^0\right) \cdot \exp\left[-\frac{E_i}{R}\left(\frac{1}{T^0} - \frac{1}{T^F} \right) \right] \tag{2.31}$$

This semi-empirical model (Eqs. 2.26, 2.28-2.31) with purely empirical coupling coefficients has no physical meaning. However, it improves predictions when coupling effect influence the component transfer through the dense membrane. But, when coupling does not occur it increases complexity of the model without significant improvement of prediction.

Comparing equations (2.22) and (2.23) with (2.26) and (2.27) the relation between the semi-empirical model by Meyer-Blumenroth and the solution diffusion model is demonstrated by eq. (2.32). Note that phenomological permeability P_i in Eq. (2.23) is equivalent to the modified thermodynamic diffusion coefficient $\overline{D}^T_i$ in Eq. (2.26).

$$\frac{P_i}{l_M} = \frac{D_{M,i}C_{M,i}}{a_{M,i}} = \frac{\overline{D}^T_i}{l_M} = \frac{C_{M,i}D^0_i}{\left(l_M\right)^2}\overline{\gamma}_{M,i} \tag{2.32}$$

2.4.1.3. Empirical models

The empirical model for trans-membrane mass transfer can be seen as a so-called "*black box*". In "*black box*" model no physico-chemical relations are considered as one presented in solution-diffusion model and model after Meyer-Blumenroth. The aim of this approaches it to obtain a good mathematical description of the mass transport by interpolation of the experimental measurement. An example of such a model is given by Lipnizki & Trägårdh (2001) which is derived under the following assumptions:

(1) the effect of temperature on the permeability is described by an Arrhenius-type equation,

(2) on the permeate side free permeate flow is assumed,

(3) the permeate pressure is assumed to be constant during experiments.

Therefore, the flux through the membrane, J_i, with temperature dependency is:

$$J_i = f\left(x_{iF}, T_F, p_p\right) \cdot \exp\left[-\frac{E_i}{R}\left(\frac{1}{T^\circ} - \frac{1}{T_F}\right)\right] \tag{2.33}$$

The required activation energy, E_i, in eq. (2.33) can be estimated by two measurements under the same conditions, i.e. permeate pressure, feed concentration and hydrodynamic conditions are kept constant but temperature change. Such a model offers a good foundation for interpolation of pervaporation data and consists of small number of parameters to estimate.

2.4.1.4. Short-cut models

The short-cut models relate component flux J_i to permeability Q_i and the driving force ΔDF of the process (see Eq. 2.34). In pervaporation the driving force is expressed in terms of the difference in chemical potential between the feed and the permeate side (Lipnizki & Trägårdh, 2001). The driving force can be also expressed in terms of difference in fugacities, partial pressures and activities (Kreis, 2005).

$$J_i = Q_i \Delta DF = Q_i \Delta \mu_i \tag{2.34}$$

In the short-cut approach Q_i is usually (see Eq. 2.36) assumed constant. Many researchers (Sommer & Melin, 2005) use the Arrhenius-type temperature dependency of permeance:

$$Q_i = Q_i^0 \exp\left[-\frac{E_i}{R}\left(\frac{1}{T^0} - \frac{1}{T}\right)\right] \tag{2.35}$$

Some researchers use engineering empirical correlations of permeance in dependency of component compositions (Buchaly et al., 2007):

$$Q_i = Q_i^0 w_i^F \tag{2.36}$$

In section 2.4.1 several models have been reviewed. The term which is standing next to the driving force represents permeance, therefore in each of the model presented in sections 2.4.1.1, 2.4.1.2, 2.4.1.4 the permeance term has been isolated and a summary of various expressions of permeance is given in Table 2.2. Selection of the pervaporation model depends on available experimental information and the specific pervaporation process being modelled. In most conceptual designs, the short-cut model and experimental correlations have been successfully applied (Rautenbach, 1996). More detailed models such as Meyer-Blumenroth and solution-diffusion models are used in detailed studies of pervaporation processes and module designs.

Table 2.2: Experimental and semi-experimental correlations of permeance

Mass transport model	Permeance	Notice
Short-Cut-Model (SC)	Q_i^0	Constant permeability
Arrhenius (AR)	$Q_i^0 \cdot \exp\left(-\frac{E_i}{R}\left(\frac{1}{T^0}-\frac{1}{T}\right)\right)$	Temperature dependence permeability
Empirical correlation (EC) in short-cut model	$Q_i^0 w_i^F$	Weight fraction dependency
Meyer-Blumenroth (MB)	$\frac{\dot{D}_i^T}{\tilde{\gamma}_i}$	Dependence of fugacity
Sorption/Diffusion (SD)	$\frac{\dot{D}_{M,i} C_{M,i}}{a_{M,i}} \frac{1}{l_M}$	Dependence of activity

2.5. Property models

In chemical process design and analysis a wide range of physical and thermodynamic properties are needed to obtain valuable solutions of process simulations and process optimizations. These properties includes pure component properties such as boiling and melting temperatures and temperature dependent like density, viscosity, vapour pressure enthalpy of vaporization, heat capacity, etc. and therefore adequate correlation and models to calculate them are required. In modelling and design of many chemical processes a prediction of the phase behaviour of chemical system is crucial. Therefore, adequate thermodynamic models to describe the properties of mixtures are required. In this section a short overview of the used property models is presented.

2.5.1. Pure component properties

Many pure component property data are gathered in various databases (the CAPEC database, DIPPR, etc.). However, it is not always possible to find such properties like boiling and melting temperatures, vapour pressure, enthalpy of vaporization, etc. for some components. In such cases, where properties are missing, the need for using efficient and reliable methods for the estimation of properties of organic compounds from their molecular structure are essential for the analysis and design of chemical and biochemical processes. The group contribution (GC) methods are very helpful in such cases. The basic GC methods consist of contributions for the first-order functional groups. These groups are used as building blocks to describe molecular

structures of compound. The summation of the contribution of each group times the number of occurrence of the functional group in the molecule is the prediction for that property. For any property GC model can be written as (Van Krevelen., 1990):

$$f(X) = \sum_i N_i C_i \tag{2.37}$$

where *f(X)* is a property function for the property *X* to be estimated, N_i is number of times the group C_i appears in the molecule and N_i is the contribution of the group C_i to the property function *f(X)*. The contribution of each functional group in the molecule is usually obtained through regression over a data set of chemical compounds and their corresponding experimentally measured values for property *X*.

Marrero and Gani (2001) presented a group contribution method where the molecular structure of a compound is considered to be a collection of three types of groups: first-order groups, second-order groups and third-order groups. The first-order groups are intended to describe a wide variety of organic compounds, while the role of the second and third order groups is to provide more structural information about molecular fragments of compounds whose description is insufficient through the first-order groups. The proposed property-estimation model in this case has the form of the following equation:

$$f(X) = \sum_i N_i C_i + w\sum_j M_j D_j + z\sum_k O_k E_k \tag{2.38}$$

where, C_i is the contribution of the first-order group of type *i* that occurs N_i times, D_j the contribution of the second-order group of type *j* that occurs M_j times and E_k the contribution of the third-order group of type *k* that has O_k occurrences in a compound. Program called ICAS-ProPred (Marrero and Gani, 2001) has been used in this work whenever pure component properties were missing. The ICAS-ProPred uses different group contribution methods to predict the properties of various organic compounds.

2.5.2. Activity coefficient models

The synthesis and design of separation and reactive processes requires a reliable knowledge of the phase behaviour of the mixture to be separated and/or reacted, where phase equilibria is expressed in terms of Gibbs free energy (*G*), chemical potential (μ), fugacities (f) or activities (γ). The condition for thermodynamic equilibrium of a closed system consisting of *N* phases and *NC* component is defined as the state for which the total Gibbs free energy attains its minimum with respect to all possible change at given *T* and *P*. This also implies that chemical potential of a particular species $\mu_i^{(N)}$ in multicomponent system is identical in all phases at physical equilibrium:

$$\mu_i^{(1)} = \mu_i^{(2)} = \ldots \mu_i^{(N)} \tag{2.39}$$

Chemical potential can not be expressed as an absolute quantity, and the numerical

values of chemical potential are difficult to relate to more easily understood physical quantities. The chemical potential approaches infinite negative values as pressure approaches zero. For these reasons, the chemical potential is not favoured for phase equilibria calculations; instead, fugacity (f_i) is employed as a surrogate (Seader & Henley, 1998). The partial fugacity of species i in a mixture are defined in terms of chemical potential by:

$$\overline{f}_i = C \exp\left(\frac{\mu_i}{RT}\right) \tag{2.40}$$

where C is a temperature dependent constant. Because of the close relationship between fugacity and pressure, the fugacity coefficient is defined as:

$$\overline{\phi}_{iV} \equiv \frac{\overline{f}_{iV}}{y_i P} \tag{2.41}$$

$$\overline{\phi}_{iL} \equiv \frac{\overline{f}_{iL}}{x_i P} \tag{2.42}$$

When as ideal gas behaviour is approached, $\overline{\phi}_{iV} \to 1$ and $\overline{\phi}_{iL} \to P_i^{sat} / P$.

The ratio of partial fugacity of a component to its fugacity is defined as activity. If the standard state is selected as the pure species at the same pressure and phase condition as the mixture, then

$$a_i \equiv \frac{\overline{f}_i}{f_i^o} \tag{2.43}$$

Activity coefficient based on mole fraction is defined by Eq. (2.44). The activity coefficient indicates how much activity departures from a mole fraction when solution is non-ideal. When solution is ideal activity coefficients are equal to one.

$$\gamma_{iL} \equiv \frac{a_{iL}}{x_i} \tag{2.44}$$

Deviations from ideal solution behaviour are conveniently accounted for in terms of the excess properties of the solution. The excess Gibbs free energy is related to the activity coefficients by the equation:

$$G^E\left(T,P,n\right) = RT\sum_{i=1}^{NC} n_i \ln \gamma_i \tag{2.45}$$

Activity coefficients are usually calculated from models of the excess properties that are functions of temperature and composition only. In chemical engineering practise for the phase equilibria calculations of multicomponent non-electrolyte systems, G^E-models or equations of state can be applied to calculate activity and fugacity coefficients of components. However, for many multicomponent mixtures

experimental phase equilibria data are often missing. In such cases group contribution methods such as UNIFAC (Fredenslund et al., 1977) can be successfully applied to predict the activity coefficient of compounds.

2.5.2.1. UNIFAC

The Universal quasichemical Functional Group Activity Coefficients (UNIFAC) model is a method for the predication of non-electrolyte activity in liquid phase of mixtures. To use this method, no experimental data is required for the particular mixture of interest. In addition to the temperature and composition of the system, it is necessary only to know the molecular structure of every component in the mixture and the necessary group parameters (Fredenslund et al., 1977). A drawback of this method is a need for group-interaction parameters.

The advantage of a GC method is that it enables systematic interpolation and extrapolation of data simultaneously for many chemically related mixtures. Most important, it provides a reasonable method for predicting activity coefficients of components in the mixtures where no mixture data are available (Fredenslund et al., 1977). For such mixtures it is not necessary to measure the intermolecular interactions because these can be calculated whenever the appropriate group-interaction parameters are known.

During the last decades several modifications of the UNIFAC model presented by Fredenslund et al. (1977) have been proposed. All UNIFAC methods (Larsen et. al., 1987; Gmehling et al., 1993) have the same basis, the activity coefficient is a sum of combinatorial (γ_i^c) and residual (γ_i^r) parts:

$$\ln \gamma_i = \ln \gamma_i^c + \ln \gamma_i^r \tag{2.46}$$

A combinatorial contribution to the activity coefficients is essentially due to differences in size and shape of the molecules, while a residual contribution is essentially due to energetic interactions (Fredenslund et al., 1975). UNIFAC methods require description of each chemical molecule in terms of constituent groups which contributes to the overall activity coefficient. Each of the group is described by two parameters: volume parameter (R_k) and surface area parameter (Q_k). These parameters are measures of molecular van der Waals volumes and molecular surface areas, (V_k) and (A_k) respectively, given by Bondi (1968).

$$R_k = \frac{V_k}{15.17}; \quad Q_k = \frac{A_k}{2.5 \times 10^9} \tag{2.47}$$

In the residual part, the interaction between each group present in the system is taken into account. These interactions depend on temperature of the mixture. Gmehling et al. (1993) comparing to Larsen et al. (1987) defined differently the modified volume fraction parameter and included the relative van der Waals surface area of component *i* and surface area fraction of component *i* in mixture. Moreover, the temperature

dependency of interaction parameters is represented differently in both models. The main differences are summarized in Table 2.3 while the detailed analysis along with lists of all the equations and variables for Modified UNIFAC (Lyngby) and Modified UNIFAC (Dortmund) are given in Appendix 6.2.1 and 6.2.2 respectively.

Table 2.3: The main differences between Modified UNIFAC (Lyngby) and Modified UNIFAC (Dortmund)

	Mod. UNIFAC (Lyngby)	Mod. UNIFAC (Dortmund)
Temperature dependence of the interaction parameters for *i-j* interactions	$a_{k,d} = a_{k,d,1} + a_{k,d,2}\left(T - T_0\right) + a_{k,d,3}\left(T \ln \frac{T_0}{T} + T - T_0\right)$	$a_{k,d} = a_{k,d,1} + b_{k,d}T + c_{k,d}T^2$
Combinatorial part	$\ln \gamma_i^c = \ln\left(\frac{\omega_i}{x_i}\right) + 1 - \frac{\omega_i}{x_i}$	$\ln \gamma_i^c = 1 - \upsilon_{P,i} + \ln\left(\upsilon_{P,i}\right) - 5q_i\left(1 - \frac{\upsilon_{I,i}}{\psi_i} + \ln\left(\frac{\upsilon_{I,i}}{\psi_i}\right)\right)$
Modified volume fraction of component *i* in mixture	$\omega_i = \frac{x_i \left(r_i\right)^{\frac{2}{3}}}{\sum_{p=1}^{NC} x_p \left(r_p\right)^{\frac{2}{3}}}$	$\upsilon_{P,i} = \frac{\left(r_i\right)^{\frac{3}{4}}}{\sum_{j=1}^{NC} x_j \left(r_j\right)^{\frac{3}{4}}}$

2.6. Process synthesis

The process synthesis and design problem is described by Hostrup (2002) as:

Given the feed and product specifications in the process, determine a flowsheet including the required tasks, appropriate equipments and solvents needed (see Figure 2.10). The flowsheet must be capable of converting input (feed streams) to output (product streams). Furthermore, determine the design of the equipments in the flowsheet and the appropriate conditions of operation. Finally, the identified solution must be analysed for verification.

d'Anterroches (2005) grouped all methods used in solving the synthesis problems into the three main classes: (1) methods that employ heuristics and/or knowledge based, (2) methods that employ mathematical and optimization techniques and (3) hybrid methods combining two previous approaches into one method.

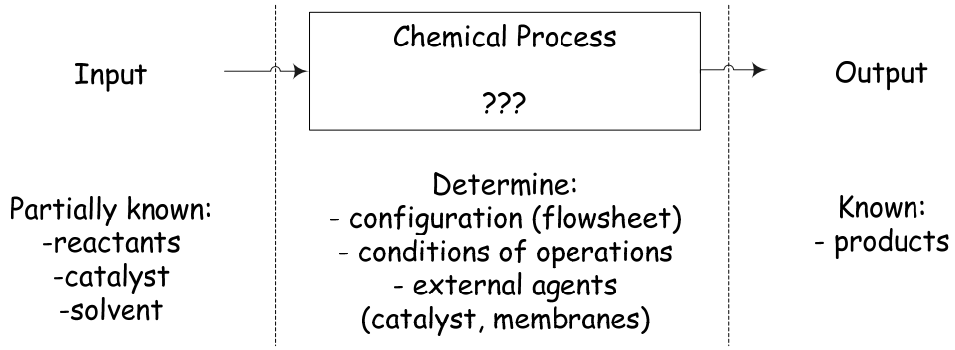

Figure 2.10: Definition of problem synthesis and design problem (adapted from Hostrup, 2002)

2.6.1. Heuristics or knowledge based methods

A heuristics or knowledge based method employs a set of rules based on a combination of experience, insights and available knowledge and data. These methods rely on a set of heuristic rules in the form of "remove the most plentiful component first" and "perform the least complicated separation task first". Jaskland (1996) has shown that some of these rules may be contradictory. What to do, if two previous statements are true for the same component, in other words, if separation of the most plentiful component is the most difficult? Therefore, the rules need careful consideration by the user before application as the context in which they can be applied is not necessarily fully defined.

The hierarchical decomposition technique proposed by Douglas (1988) where heuristic rules are applied at different design levels to generate the flowsheet alternatives breaks the synthesis problem into five discrete hierarchal decision levels:

(1) Batch versus continuous.

(2) Input–output structure of the flowsheet.

(3) Recycle structure and reactor considerations.

(4) Separation system synthesis.

(5) Heat exchange network.

This method utilizes heuristics, short-cut design procedures, and physical insights to develop an initial base-case design. The approach is motivated by Douglas's claim that only 1% of all designs are ever implemented in practice, and thus this screening procedure avoids detailed evaluation of most alternatives. Drawback of such a method is that due to the sequential nature of the flowsheet synthesis, interactions among the design variables at the various decision levels may not be properly accounted for, as it is necessary to solve for them simultaneously.

d'Anterroches (2005) summarized that these methods tried to mimic the human approach in solving the problems, where the human tends to access already available

knowledge by searching for relevant information from which useful knowledge is extracted and adapted to solve the current problem.

2.6.2. Optimisation-based methods

The optimization of process synthesis problem can be stated as follows: for a given process superstructure (e.g. described mathematically) find the best solutions to this process within constraints. The best solution is quantified by means of the objective function. A superstructure includes all possible interconnected unit operations in a possible flowsheet. Decision variable (describing presence of the unit operation) and structural parameters (like size of reactor, number of plates in distillation column, membrane area) are included in the mathematical formulation of the problem. This kind of problem formulation leads to mixed-integer linear programming (MILP) and mixed-integer nonlinear programming (MINLP) problems. Solution of these problems (MILP and MINLP) requires efficient numerical solvers and a good knowledge of the mathematical programming techniques. Nowadays more and more research is going on application of stochastic and evolutionary algorithms such as genetic algorithms and meta-heuristic Tabu Search (Lin & Miller, 2004).

The main features of optimisation-based methods are the mathematical representations of the problem and subsequent use of suitable optimization techniques. With optimisation-based methods rigorous analysis of the investment cost, operational cost and interactions between structural elements of the flowsheet is done. However, Li and Krasławski (2004) pointed out three main disadvantages of these methods: (1) lack of the ability to automatically generate a flowsheet superstructure, (2) the optimality of the solution can only be guaranteed with respect to the alternatives that have been considered in the superstructure a priori, and (3) need for a huge computational effort.

2.6.3. Hybrid methods

Hybrid methods use the physical insights of knowledge-based methods to narrow the search space, and decomposes the synthesis problem into a collection of related but smaller mathematical problems. It is usually done in a step-by-step procedure in which solution of one problem provides input information to the subsequent steps where other smaller mathematical problems are solved. Finally, such a procedure leads to an estimate of one or more feasible process flowsheets. The final step of hybrid methods is a rigorous simulation for verification of proposed process flowsheet.

2.6.3.1. Method based on thermodynamic insights

Jaksland (1996) developed a methodology for separation process synthesis and design which employs physicochemical properties and their relationships to separation techniques. Using this methodology, separation tasks are selected and sequenced, therefore, corresponding separation techniques are identified with estimates of

conditions of operations. In that way a physically feasible flowsheet is designed. The advantage of this method is that relationships between properties, process synthesis, process design and product design have been indentified and exploited in a systematic manner to solve a range of problems related to synthesis and design of separation processes.

The methodology consists of two communicating levels with increasing degree of complexity for the higher level. The problem solution starts from level one and proceeds to the next higher level. However, it is possible to return to the lower level if a specific solution path rejected earlier becomes a feasible option. The methodology assumes that a knowledge base consisting of information on pure component properties, separation techniques, etc., is available together with methods for prediction of pure component properties (not covered by the knowledge base) and mixture properties.

The first level consists of 6 steps: mixture analysis (generates information on type of mixture, phase identity at the specified condition, presence of azeotropes, presence of mutual solubilities, etc.), computation of a binary ratio matrix (represents the property differences between all binary pairs of components in terms of property ratios), separation process identification (determines the feasible separation techniques for each binary pair of components taking into account the binary ratio matrix and a matrix of allowable values for the property values), screening of alternatives (reduces the number of feasible alternatives to at least one per binary pair), initial estimates of split factors (determines estimates for split factors so that mass balance calculations can be made) and choice of the first separation task (determines the binary pair which splits the multicomponent mixture into two).

In level 2, pure component properties and mixture properties are considered to simultaneously order and select the separation tasks and separation techniques, select compounds or mixtures for mass separation agent (MSA) based processes and determine improved, compared to level 1 values, estimates for conditions of operation and separation efficiency. The steps in level 2 therefore involve identification of separation tasks (verification of the choice of separation tasks from level 1 by considering the property values in addition to the property ratio values), MSA selection (selection of MSA for identified separation techniques which require them), screening of alternatives (further screening of separation techniques per separation task), ordering and selection of separation tasks (generation of a flowsheet with alternatives for each separation task) and determination of conditions of operation.

2.6.3.2. Driving force based synthesis and design

The driving force is defined as the difference in composition of a key component between two co-existing phases. Based on definition of driving force, Bek-Pedersen and Gani (2004) developed a framework for synthesis and design of separation schemes. That framework comprises methods for sequencing of distillation columns and the generation of hybrid separation schemes. The driving force approach employs

thermodynamic insights and fundamentals of separation theory, in terms of the causes of separation. With use of this approach it is possible to identify feasible distillation sequences and also to identify other separation techniques (different than distillation).

This method of using the concept of driving force leads to optimum or near optimum solutions in terms of energy consumption while allowing the visualisation and comparison of different separation tasks/techniques in driving force diagrams. The important feature of this concept is that driving force is inversely proportional to the energy consumed to create it. Therefore, a process using the maximum available driving force will be using the minimum energy needed to run the operation. The developed framework has been successfully used not only to the design and synthesis problems but also to retrofit and controllability/operability issues.

2.6.3.3. Process flowsheet generation and design through a group contribution approach

In case of group contribution approach for molecular property prediction, the building blocks are molecular groups, whereas for process flowsheet synthesis the building blocks can be unit operations like distillation column with their associated driving forces, mass and heat exchange modules. d'Anterroches in 2005 presented the framework for Computer Aided Flowsheet Design (CAFD) which uses the group contribution approach and consists of eight main steps:

(1) Definition of the process synthesis problem. User defined available materials and desired products.

(2) Analysis of the process synthesis problem. Using physical insights and knowledge based methods a set of feasible process operations are defined.

(3) Selection of the process groups matching with synthesis problem. The process groups are matched between appropriate process tasks selected in the analysis and the mixture involved in the problem.

(4) Synthesis and test of the flowsheet structure alternatives. Based on the developed connectivity rules, the process groups are combined into the flowsheet alternatives.

(5) Ranking of the generated alternatives and selection of the most promising alternatives. Based on flowsheet property model, the performance of the alternatives are predicted and compared.

(6) Design of the selected flowsheet structure alternatives. It is achieved by applying a reverse simulation approach to determine the design parameters of the unit operations from specifications inherited from underlining process groups.

(7) Post analysis of the designed alternatives. Issues related to heat integration and environmental impacts are considered.

(8) The final flowsheet is verified through rigorous simulation and/or plant data.

With the CAFD framework it is possible to generate the process alternatives for given problem specification (e.g. defined in terms of available raw materials and desired products). This framework has two main advantages, (1) it is applicable to a large range of problems (e.g. includes various process operations like distillation column, solvent-based separation, fixed conversion reactor and many more), and (2) does not need to employ rigorous models at each decision step (rigorous models are used in the final step). The drawback of this framework is that adding a new process group requires an extension of the process flowsheet model and secondly, that the generated flowsheet alternatives are implicitly providing the superstructure of the all possible combination. The generation of all the alternatives for a 15 component separation using only distillation column leads to 2674440 feasible alternatives (d'Anterroches, 2005).

3. General framework for design and analysis of hybrid and integrated processes

"We can't solve problems by using the same kind of thinking we used when we created them."

(Albert Einstein)

3.1. Introduction

Design of a hybrid process, which is in general a combination of different interlinked unit operations, need to take into account their interdependency in terms of process conditions like temperature, pressure and/or compositions to determine the optimal configuration. In this case, through qualitative and quantitative analyses of models describing each of the constituent process (like pervaporation, vapour permeation, nanofiltration, distillation, and reactor) at different modelling depths can lead to the efficient identification of the optimal hybrid process design. Through a model-based computer-aided methodology it is therefore possible to identify reliable and feasible design alternatives, saving thereby valuable experimental resources, which could than be used only for implementation and verification of the design. In the following section and subsections, a motivating example is presented, followed by problem formulation and a detailed description of the general framework for hybrid process design and analysis.

3.1.1. Motivating example

The motivation for this work is highlighted through an example given by Whu et al., (1999) where conversion of diketone (compound *A*) to a hydroxyester (compound *C*) using an alkoxide (compound *B*) in organic solvent is explored. The objective is to produce compound *C* via the following reversible reaction:

$$A + B \underset{k_{-1}}{\overset{k_1}{\rightleftharpoons}} C + D \tag{3.1}$$

It is assumed that the by-product *D* consumes reactant *A* to produce an undesired product *E* according to the irreversible reaction:

$$A + D \xrightarrow{k_2} E \tag{3.2}$$

Three compounds *A*, *C* and *E* were assumed to be large molecules with molecular weights in the range of 400-600 g/mol, whereas compounds *B* and *D* are much smaller, their molecular weights were assumed to be in the range of 50-100 g/mol. Both reactions (Eqs. (3.1-3.2)) were assumed to take place in a solvent of low molecular weight which was totally miscible with all five components. Toluene has been used as a solvent.

Whu et al. (1999) came up with design of a semi-batch process where continuous stirred tank reactor is coupled with a nanofiltration (NF) membrane unit (see Figure 3.1). They studied the influence of various process parameters like different component selectivities and fluxes through the nanofiltration membrane and altered addition of reactants.

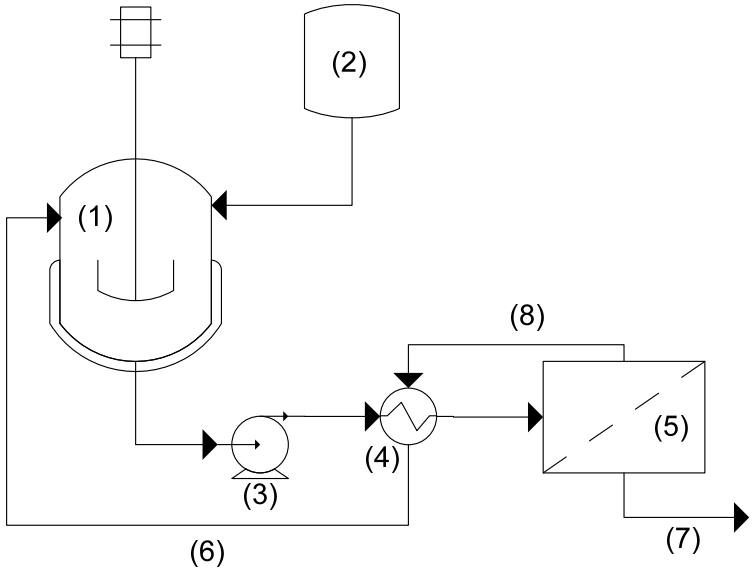

Figure 3.1: Schematic representation of the coupling of a semi-batch reactor with a nanofiltration membrane unit: (1) reactor vessel (jacketed), (2) drum containing solution of reactant *B*, (3) pump, (4) heat exchanger, (5) NF membrane unit, (6) transfer lines, (7)permeate, (8) retentate (adapted from Whu et al., 1999)

The component mass balance around the semi-batch reactor with nanofiltration membrane unit is written as follow:

$$\frac{dn_i}{dt} = L_v C_{id} - J_i A_m + V \sum_{j=1}^{2} v_{ij} \left(r_{A,j} \right) \tag{3.3}$$

Where $L_v C_{id}$ represents the addition of the compound, $J_i A_m$ stand for component removal from the system. The reaction rate for the reversible reaction (see Eq. (3.1)) is given by Eq. (3.4) while for the irreversible (see Eq. (3.2)) by Eq. (3.5).

$$r_{A,1} = k_1 \left(C_A C_B - \frac{1}{K_{eq}} C_C C_D \right) \tag{3.4}$$

$$r_{A,2} = k_1 C_A C_D \tag{3.5}$$

The performance of the nanofiltration process is defined by the component flux:

$$J_i = C_i J_s \left(1 - R_i\right) \tag{3.6}$$

where J_s is total flux.

The compound rejection (R_i) is defined as the ratio between the difference of the concentration of compound *i* in feed to membrane separation unit ($C_{f,i}$) and the concentration of compound *i* in permeate ($C_{p,i}$) to the feed concentration ($C_{f,i}$) (see Eq. (3.7)).

$$R_i = \frac{C_{f,i} - C_{p,i}}{C_{f,i}} \tag{3.7}$$

The measure of the process performance has been defined in terms of process yield which is a ratio between numbers of moles of reaction product (product *C* or by-product *E*) and the initial number of moles of limiting component *A*.

Several scenarios are presented: two batch reactors (Batch-1, Batch-2), semi-batch reactor (Semi-batch-3)) and six hybrid processes (CNF0 – CNF5) for which all parameters are presented in Table 3.1. Scenarios Batch-1, Batch-2, Semi-batch-3 and CNF1-CNF2 were reproduced after Whu et al., (1999) since the rest (CNF3-CNF4) were added for purpose of further analyses of hybrid operation. Even with enormous process time (1600 h) the process yield is much smaller compared to semi-batch or hybrid processes. Semi-batch reactor operation gives high conversion but it is finished with 3 times higher volume, which could be not acceptable in reality (restriction to the volume of reactor). For hybrid processes it is significantly important that with variation of rejection factor R_B and R_D, the process yield changes not more than 3% (see Table 3.1, CNF1-CNF4).

Table 3.1: Parameters for conceptual hybrid process modelling

Parameter	Batch-1	Batch-2	Semi-batch-3	CNF0	CNF1	CNF2	CNF3	CNF4
C_{A0} [mol/dm^3]	0.04	0.04	0.04	0.04	0.04	0.04	0.04	0.04
C_{B0} [mol/dm^3]	0.04	0.04	0.04	0.04	0.04	0.04	0.04	0.04
V_0 [dm^3]	2	2	2	2	2	2	2	2
L_v [dm^3/s]	-	-	0.0001	0.0001	0.0001	0.0001	0.0001	0.0001
J_S[dm^3/s*m^2]	-	-	-	0.005	0.005	0.005	0.005	0.005
C_{Bd}[mol/dm^3]	-	-	2.5	2.5	2.5	2.5	2.5	2.5
R_A [-]	-	-	-	1	1	1	1	1
R_B [-]	-	-	-	0	0.5	0	0.25	0
R_C [-]	-	-	-	1	1	1	1	1
R_D [-]	-	-	-	0	0	0.5	0	0.25
R_E [-]	-	-	-	1	1	1	1	1
t [h]	16	1600	16	16	16	16	16	16
V [dm^3]	2	2	7.75	2	2	2	2	2
Yield A => C	0.102	0.509	0.903	0.924	0.935	0.911	0.924	0.918
Yield A => E	0.040	0.487	0.060	0.069	0.064	0.082	0.069	0.075

From this study it is clear that such combination of reactor and nanofiltration gives promising results in overcoming equilibrium and kinetically controlled reaction. However, there are couple of questions which rose during analysis of this problem:

- Is there a better process configuration?
- Is there a better separation technique than nanofiltration?
- Is there any other feasible membrane?
- Is it worthy to start combined operations only in the beginning of the reaction?

If not, when should it start?

- Is it possible to integrate these two unit operations into one unit?

Besides the particular questions listed above, some more general questions also come up:

- Which compounds should be removed to promote conversion to desired product?
- How to design processes which will enhance production of desired product?
- How to select the separation technique(s)?
- How to select solvents which would promote the chemical reaction?
- How to select solvents which will promote reaction and still allowed efficient separation?
- Is there a systematic way to solve such a complex design problem which involves reaction, selection of separation technique(s) and selection of solvent(s)?
- What "knock-off" criteria with respect to the reaction phase, catalyst, residence time and operating temperature and pressure should be met in order to integrate reaction and separation zones into one unit?
- Is it possible to integrate two or even more separation techniques?

To some of these questions raised above it is possible to obtain answers using available methods (e.g. method for selection of solvents for promotion of organic reactions proposed by Gani et al., 2005; process configuration can be selected using optimization-based techniques if adequate superstructure of the process is provided). However, there is no method or framework which would guide the chemical engineer in the whole design and analysis of such complex problems of design of hybrid process schemes.

3.1.2. Problem formulation

From all the questions raised in the previous subsection (3.1.1), the focus of this work is on the development of a general framework for systemic design and analyses of hybrid processes. The framework will guide the user through a step-by-step procedure for analysis of the design problem, generation of feasible hybrid process configurations and testing of the proposed design. The objective of the framework is to provide answers to most of the questions raised in subsection 3.1.1 in a comprehensive way. The framework is constructed to deal with aqueous or organic systems and with reaction taking place in the liquid phase.

3.2. Framework for hybrid process design and analysis

As shown in Figure 3.2, the framework consists of three stages: (1) hybrid process design and analysis, (2) process implementation (including experimental setup) and (3) process-model validation.

3.2.1. Stage 1: Hybrid process design and analysis

For the first stage, a systematic model based methodology for process design and analysis of hybrid reaction-separation (R-S) and separation-separation (S-S) systems have been developed. This methodology consists of four main steps as highlighted in Figure 3.2, which also shows the data-flow and the computer-aided tools used. The steps of the methodology are described below.

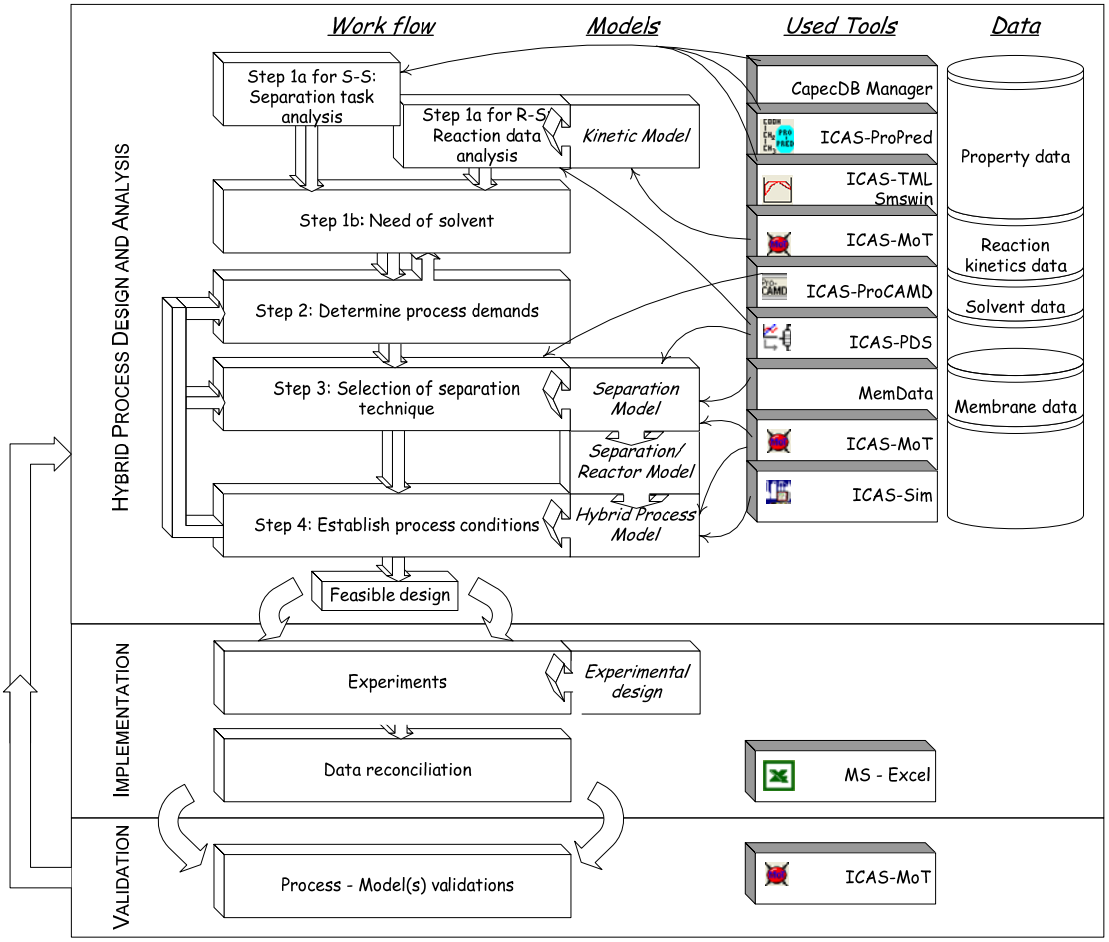

Figure 3.2: Framework with data flow and associated computer-aided tools

3.2.1.1. Step 1a: Separation task and reaction data analysis

The objective of this step is to gather available information about the given mixture which needs to be separated with or without the occurrence of reaction(s). The mixture is analysed in order to identify its physical boundaries, which defines operating conditions in terms of temperature, pressure and composition. The analysis is done in a 4-steps procedure.

1a.1. Identify mixture type

At first, the mixture is analyzed in terms of mixture type. Based on the information of compounds present in the mixture, a mixture is identified as ideal or non ideal (for example of type: polar, aqueous, electrolyte, polymer, etc.) and based on this, the appropriate thermodynamic model for prediction of phase equilibria is selected. It is done based on the knowledge-based system developed, by Gani and O'Connell (1989), for the selection of appropriate property models for calculations involving phase equilibria. For given compounds and the range of expected conditions, a list of feasible property models is generated. Note that selected property models are used in all subsequent steps, e.g., for phase equilibria and process simulations.

1a.2. Analysis based on pure component properties

An initial estimate of the system boundaries can be quickly established through an analysis of the pure component properties of the constituent chemicals. For example, knowledge of boiling points and melting points help establish the liquid phase region in terms of temperature at a specified pressure. A liquid phase is likely to exist at a temperature, which is higher than largest pure component melting point and lower than the lowest pure component boiling point. Information on mutual miscibility plays an important role in reactor and separation process design since occurrence of miscibility gap can change performance of reactor and separation significantly. If the compounds have widely different solubility parameters, the liquid phase may split into two phases. Presence of enzymes, active pharmaceutical ingredients or other speciality chemicals may require strict monitoring of temperature because of the possibility of decomposition or denaturation of them if the process temperature is too high. For example, denaturation of *Candida Antarctica* lipase is occurring at 80°C (Garcia et al., 2000), therefore reaction while using that lipase has to be kept below 80°C.

1a.3. System analysis based on mixture properties

This analysis is done at the level of binary mixtures because most phase equilibrium based separations occur due to differences in driving force between two adjacent compounds. VLE, LLE and SLE calculations are performed for indentified binary pairs to determine the existence of eutectic points and azeotropes because they will influence the downstream separation tasks. It is also important to collect VLE, LLE and SLE experimental data for as many binary pairs as possible so that the performance of the selected thermodynamic model can be verified. In this case, if data for ternary systems are also collected they will help to evaluate the predictive

power to the selected property model. If performance of the selected property models is not acceptable, the model parameters may need to be re-estimated or fine tuned.

1a.4. Reaction analysis

This sub-step is necessary only when reactions occur within the process. The phase boundaries in terms of temperature, pressure and composition help to establish the reactor condition of operation. For kinetically controlled reactions, a catalyst that makes the reaction feasible needs to be selected. It is also important to define the concentration range of reactants and products, because of product stability and downstream separation operations. For example, in the production of lactic acid, the concentration of lactic acid should not exceed concentration more than 20 w% because of the occurrence of dimerization reaction (Delgado et al., 2007).

Many reactions are equilibrium controlled, like the ester hydrolysis, etherifications, and esterification reaction, (which can be expressed symbolically by Eq. (3.8)), where the reaction rate can be modelled by Eq. (3.9) and the reaction equilibrium constant (K_{eq}) is defined by Eq. (3.10).

$$A + B \underset{k_{-1}}{\overset{k_1}{\rightleftarrows}} C + D \tag{3.8}$$

$$r = k_1 \left(C_A C_B - \frac{C_C C_D}{K_{eq}} \right) \tag{3.9}$$

$$K_{eq} = \frac{C_C^{(eq)} C_D^{(eq)}}{C_A^{(eq)} C_B^{(eq)}} \tag{3.10}$$

where k_1 is a reaction rate constant and C_A, C_B, C_C, C_A represents the concentration of compounds A, B, C, D respectively, superscript (eq) stands for concentration of compound at chemical equilibrium.

In this case, it is important to define the reactant ratio and determine the conditions at which the reacting system reaches chemical equilibrium. An initial ratio of reactants different from 1:1 is usually beneficial in equilibrium controlled reactions because it increases the conversion of the limiting reactant but when this ratio is too high, it can cause a significant increase of mass holdup and a decrease in the efficiency of the separation of products. The influence of the initial ratio of reactants is assessed by plotting initial ratio of reactant versus reaction conversion (when one reaction occurs) or process yield (when more than one reaction occurs). In that way a range of initial concentration of reactants can be defined.

In the absence of experimental data, the reaction composition at chemical equilibrium for a given initial composition, temperature and pressure can be computed by means of the reactive flash calculation procedure proposed by Pérez-Cisneros et al. (1997). If experimental data is available, the calculated values can be compared with experimental data.

3.2.1.2. Step 1b: Need of solvent

In this step, the influence of solvents in the reaction is considered in terms of whether a solvent is necessary or not. Generally, the use of an inert solvent might be considered if the reaction mass efficiency is smaller than 80 % (Gani et. al., 2005). The product yield can be increased through the use of an appropriate solvent. For example, solvents can be used to create a second phase with the product or precipitation of the product, or to dissolve the reactant(s). Also, when an undesired reaction occurs in the reaction system, a solvent can create another phase with the by-product. In non-reactive separation tasks, the solvent might be needed when the mixture to be separated has azeotropes, have low relative volatility among the mixture compounds or form eutectics. Three kinds of separation processes using solvent are considered in this work, namely: liquid-liquid extraction, extractive distillation and azeotropic distillation (discussed in section 2.3.2). If any of the pointed above cases is applicable to the analysed problem, the solvent selection is required in Step 3.

3.2.1.3. Step 2: Determine process demands

The objective of this step is to define the process demands based on the choice of the mode of operation - batch or continuous. This choice is made based on, among others, production rate and residence time. Also, process performance criteria are defined in terms of required product purity, reaction conversion, process yield and processing time (in case of a batch process), which are used in the next steps to evaluate the generated process operation scenarios.

3.2.1.4. Step 3: Selection of separation techniques

In this step the separation techniques to be combined with either another separation task or a reaction task for the hybrid scheme, is identified. The steps to follow are different when combining with a separation task than when combining with a reaction task. For hybrid non-reactive separation schemes, the following 5-step procedure is proposed:

S3.1. Generate and/or collect data of phase compositions for as many separation methods as desired or available.

S3.1.1. Distillation

At first check for the feasibility of application of distillation by first listing all compounds present in the system, then ordering them in terms of their normal boiling points and providing, as well, their relative volatilities, α_{ij}, for compound i with respect to reference compound j. Retrieve vapour liquid equilibrium data for each binary pair, if available. Note that in step 1a VLE analysis of the mixture has been performed and the corresponding data is already available.

S3.1.2. Solvent-based separation techniques

If step 1b pointed out the need for solvents (when a binary pair forms an azeotrope and both compounds need to be recovered in high purity), the three step method for solvent selection as given by Harper and Gani (2000), is employed to identify compounds capable of performing a separation task pointed out in step 1b (liquid-liquid extraction, azeotropic distillation and extractive distillation). This is achieved by generating compounds (solvents) matching a set of specifications with respect to compound type, physical and chemical properties. This method consists of three steps: a problem formulation step, a step for solution of problem through the computer-aided molecular design (CAMD) technique, and, an analysis step. In this way, for selected solvent(s) and separation techniques, such as liquid-liquid extraction and extractive distillation, the separation equilibrium data can be generated. This method is described below.

S3.1.2.1. Problem formulation

In order to identify compounds that are able to perform the needed tasks it is important that the desired properties match the types important for the intended use. The requirements for a compound can be expressed using a set of essential properties and desirable properties. Table 3.2 contains a set of pure compound and mixture properties important for specific separation techniques. The design goals for the solvent defined in 3.2.1.2 Step 1b: Need of solvent, has to be translated into desired compound types and properties. The quantitative formulation of desired properties is a very important step when solving CAMD problem, in the following sub-step, since the formulated constraints control the generation and screening algorithms used to solve the compound design problem.

Table 3.2: Pure component and mixture properties for solvent selection problem for three separation techniques. E: essential property, D: desired property. (Based on Harper, 2002)

Properties		Solvent properties					
		L-L extraction		Extractive distillation		Azeotropic distillation	
		E	D	E	D	E	D
Pure	Solubility parameter	*	*	*	*	*	*
	Surface tension		*				
	Viscosity		*				
	Boiling point	*		*		*	
	Melting point	*		*		*	
	Density					*	
	Vapour pressure			*			
	Enthalpy of vaporization				*		*
Mixture	Selectivity		*		*		*
	Solvent loss		*				*
	Solvent power		*		*		*
	Distribution coefficient		*		*		*
	Phase split	*		*		*	
	Azeotropes				*	*	
	Mixture viscosity		*				

S3.1.2.2. Solution of the solvent selection problem

The compound design problem is solved by employing CAMD method in which feasible molecules are generated and tested against the design specifications. In order to avoid the so-called combinatorial explosion problem, the multi-level approach of Harper et al. (1999) is employed where, through successive steps of generation and

screening against the design criteria, the level of molecular detail is increased only on the most promising candidates. At this step the software ICAS-ProCAMD is utilized (the software is described in more details in section 3.3.1, page 68).

S3.1.2.3. Solution analysis

In the post-design step the answers from the solution procedure are analyzed with respect to properties and behaviour that could not be part of the design considerations. Examples of such properties and behaviour are price, availability and legislative restrictions. Finally, the user selects the most promising solvents satisfying the design criteria defined in S3.1.2.1. In that way, additional separation methods like extractive distillation, liquid-liquid extraction can be found and corresponding equilibrium data are generated.

S3.1.3. Membrane-based separation techniques

Retrieve data from the membrane database or other adequate literature source for each binary pair in order to find if any membrane-based technique had been used to separate such mixture. Extract separation characteristics to obtain composition in the feed and permeate.

S3.2. Calculate and plot all driving forces on one plot for each identified separation methods from step S3.1.

The driving force, as defined by Bek-Pedersen and Gani (2004), is the difference in compositions of compound *i* in two co-existing phases and is described by Eq. (3.11).

$$FD_i = \left| x_i^1 - x_i^2 \right| \tag{3.11}$$

S3.3. Screen for feasible solutions

A feasible solution is characterized by having the driving force value higher than zero in the whole separation region. In other words, it does not have any separation boundary like azeotrope. If at least one of the driving force curves is feasible in the entire separation region, then combine it with other separation techniques which have larger driving force at least in some concentration range. If any of the driving force curves for individual separation techniques do not provide feasible solutions, e.g., it has separation boundary (like azeotrope) than combinations have to be generated which can overcome the separation boundary. For example, for separation of a binary mixture presented in Figure 3.3, any of separation techniques (distillation and pervaporation) can not achieve high purity streams because both techniques have their own limitation. However, combining distillation with pervaporation is feasible and produces the desired high purity ethanol product.

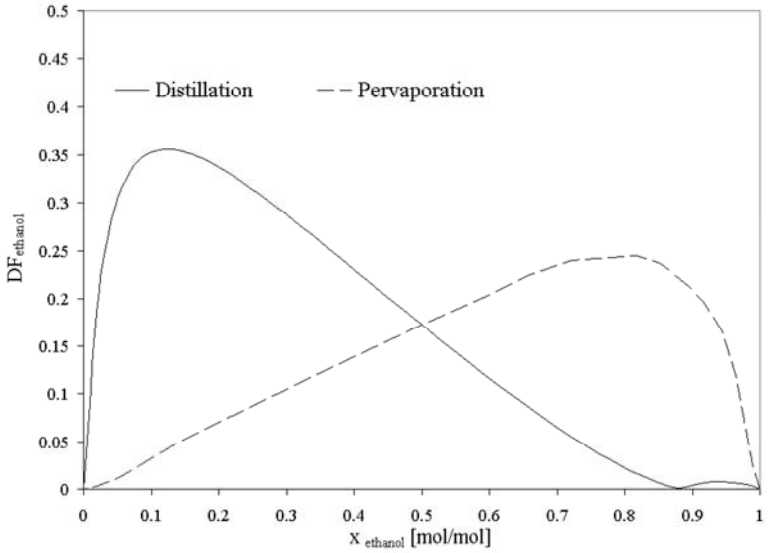

Figure 3.3: Driving force for feasible combination between distillation and pervaporation for separation of binary mixture of water and ethanol

The term bulk separation is used to indicate the separation operation when concentration of separated components in the feed is larger than 5 w%. Due to economical reasons, for bulk separations, the following separation techniques are favourable: flash operation, distillation, azeotropic distillation, extractive distillation, condensation, decanter, simple crystallisation and physical absorption (component composition in the parent mixture needs to be higher than 2%).

S3.4. Identify feasible combinations

Feasible combinations obtained in the previous step are analysed by the use of the derivative of driving force with respect to the key components, defined as:

$$FD_x = \frac{d\left(FD_i\right)}{dx_i} = \frac{\Delta\left(FD_i\right)}{\Delta x_i} \tag{3.12}$$

These derivatives identify the region where the individual separation technique is inefficient, indicated by the occurrence of a local minimum along the composition axis. However, since the objective is to design a process with the largest driving force, a *separation technique A* may be considered with a *separation technique B* if at the same composition, *separation technique B* has a larger absolute value for FD_x than *separation technique A* (Mitkowski et al., 2007). For example, consider the separation of a binary mixture of water and acetic acid. The derivative FD_x (see Figure 3.4) for distillation (bold line) has a local minimum around $x_{H2O} = 0.80$ and $x_{H2O} = 0.90$. The FD_x value for pervaporation showing (dashed line in Figure 3.4) for the same composition range has a larger absolute value. Therefore, it is beneficial to combine distillation with pervaporation into a hybrid scheme in such a way that pervaporation is used to separate the mixture from $x_{H2O} = 0.80$ to at least $x_{H2O} = 0.90$,

i.e., in the region where its driving force is greater than that of distillation.

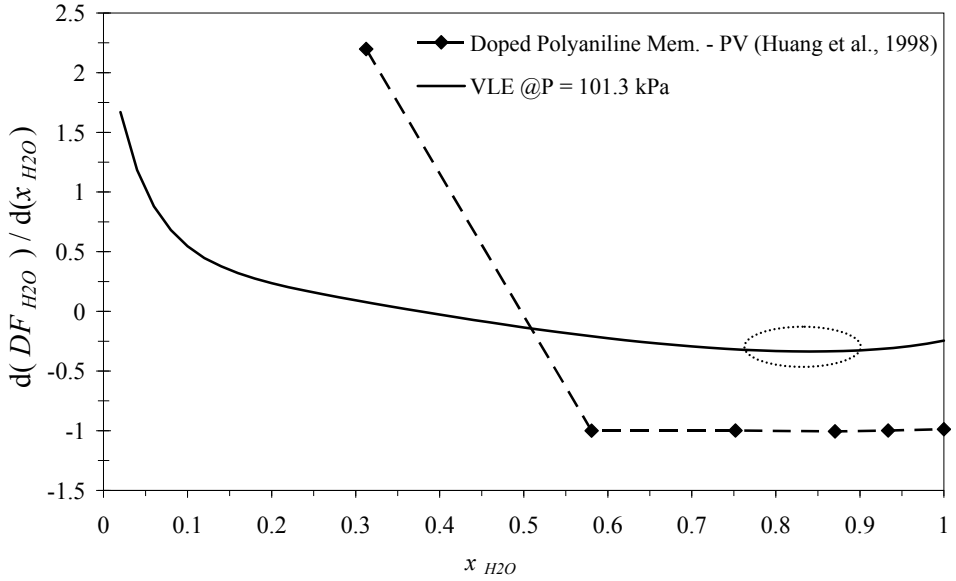

Figure 3.4: Derivative of driving force for water - acetic acid mixture

S3.5. Identify the solution with biggest driving force

If more than one feasible combination has been indentified in the previous step, than identify the solution with the greatest maximum driving force. Evaluate selected alternative in step 4 through process simulation for its performance.

For hybrid reaction-separation schemes, the following 5-step procedure is proposed. The objective here is to identify the compounds whose removal will enhance the reaction, and based on this, to select a suitable separation technique for the reaction effluent.

R3.1. Identify compound(s) to remove from reaction medium

Based on reaction kinetics and identified mixture boundaries in step 1, identify reaction products whose selective removal will increase the conversion of reaction.

- Despite the reaction being equilibrium or kinetically controlled, remove the most distinctive product from the reactive mixture. For example, in case of esterification reaction, water is the inorganic compound among other organic compounds. Therefore, it should be removed at first. Note that distinctive products can be also one which has significantly higher molecular weight because in that way ultrafiltration, microfiltration or other filtration techniques can be a good option.
- If analysis of the reaction mixture pointed out appearance of separation boundaries due to a product, than identify removal of that product to avoid the difficulties associated with separation boundaries. For example, consider that

reactive mixture contains four compounds (reactants: *A*, *B*; products: *C*, *D*), which form two binary azeotropes (*A* and *D*, *B* and *D*) and one ternary azeotrope (*A*, *C* and *D*). Therefore, removal of compound *D* will remove the problem with post separation of the reactive mixture. However, if products from the same reaction create two phases, within the reaction composition range, then creation of a phase that is richer in one of the products is preferred.

- In case of multireaction systems, identify compounds whose removal will slowdown and/or even eliminate unwanted reaction(s). For example, in motivating example (see section 3.1.1, page 37) absence of compound *D* will not allow the start of the second reaction (Eq. (3.2)).

R3.2. Feasibility of distillation

Check for feasibility of distillation to remove the product(s) from reaction mixture. List all components with their relative volatility, α_{ij}, and rank the compounds by normal boiling point. If the identified reaction product from the previous step R3.1 is in the top or bottom of the list then use of distillation is recommended for separation of the product from the reacting mixture.

R3.3. Feasibility of membrane-based separation

Retrieve data from the membrane database or other appropriate literature sources if information on a membrane-based separation technique(s) used to separate the same or similar mixture is available. Then, collect the separation characteristic data and for each membrane separation, list all compounds according to decreasing component flux, e.g. the component with the largest flux is in top of the list. Select that membrane for the compound which needs to be removed from the mixture (identified in step R3.1) is in the top of the list. If there is more than one membrane that satisfies this criteria, then compare their driving forces to identify the best alternative (select the one with the highest driving force).

If the most distinctive product has significantly higher molecular weight than other components present in the mixture, then consider the use of filtration techniques such as ultrafiltration, microfiltration or nanofiltration. In such a case, utilize information provided in Table 2.1 (page 21) to select the appropriate membrane-based separation technique.

R3.4. Solvent selection

Analyze possibility of adding a solvent to:

- create a second phase which would extract product(s) from reactants, or
- promote precipitation of a product, or
- decrease product activity and therefore move reaction equilibrium towards the product(s) in case of activity driven reaction.

At this sub-step (R3.4) the solvent selection methodology given by Gani et al. (2005)

is applied. The description of all steps of that methodology adapted here is given below.

R3.4.1. Generate the values of R-indices

Based on the data collected in step 1a, assign values to the reaction *R*-indices, using the reaction-solvent rules given below (R3.4.1.1.-R3.4.1.8). Also assign the reaction-solvent *RS*-indices. Following the reaction-solvent rules, calculate the reaction-solvent indices (*RS*). Consult the known solvent database and identify the set of solvents that satisfy the reaction-solvent properties within 10% (score 10), 20% (score 8), 30% (score 6), 40% (score 4), 50% (score 2). The score for values outside the 50% range is one.

R3.4.1.1. Solvent must be liquid at the reaction temperature

R_1 = specified reaction temperature

Remove solvents from the candidates list that are not likely to be a liquid at $R_1 \pm 20$ K, where R_1 is the specified reaction temperature. The melting point of the solvent must be lower, and the boiling point must be higher, than the reaction temperature. This rule is implemented as follows: retrieve the boiling point (T_b) and melting point (T_m) temperatures of each solvent and determine the average temperature $(T_b+T_m)/2 = T_S$. Based on the calculated value of T_S, assign the corresponding RS_1 values according to the following rules:

$RS_1 = 1$ if $T_S - R_1 = \pm 5$ K;

$RS_1 = 2$ if $T_S - R_1 = \pm 10$ K;

$RS_1 = 3$ if $T_S - R_1 = \pm 15$ K;

$RS_1 = 4$ if $T_S - R_1 = \pm 20$ K;

$RS_1 = 5$ if $T_S - R_1 = > \pm 20$ K

R3.4.1.2. Need for solvent as carrier

If one or more of the reactants are solids set $R_2 = 1$. Otherwise, set $R_2 = 0$.

If $R_2 = 1$, solvents are needed as carrier for the reactant in the liquid phase. Assign *RS* values for solvents according to the following rules:

$RS_2 = 1$ if solvents are totally miscible

$RS_2 = 2$ if solvents are highly soluble

$RS_2 = 3$ if solvents are soluble

$RS_2 = 4$ if solvents are slightly soluble

$RS_2 = 5$ if solvents are not soluble

R3.4.1.3. Need for solvents to remove reactants or products

If one or more of the products are solids set $R_3 = 1$. Otherwise, set $R_3 = 0$.

If R_3 = 1, solvents are needed to remove the product from the reacting phase. Assign *RS* values for solvents according to the following rules:

RS_3 = 1 if solvents are totally miscible

RS_3 = 2 if solvents are highly soluble

RS_3 = 3 if solvents are soluble

RS_3 = 4 if solvents are slightly soluble

RS_3 = 5 if solvents are not soluble

R3.4.1.4. Need for phase split

If phase split is necessary, set R_4 =1. Otherwise, set R_4 = 0.

If R_4 = 1, check for solvent partial solubility with respect to one of the compounds from the reacting system (reactant, product or carrier). If solvent is partially soluble, RS_4 = 1, 2, 3 or 4. Otherwise, RS_4 = 5. Assign RS_4 indices in similar way as RS_4.

R3.4.1.5. Matching of solubility parameters of solute and solvent

The solvent must have a solubility parameter value, which is within ±5% of the "key" reactant (if R_1 = 1) or product (if R_3 = 1). If R_1 = 1 or R_3 = 1, then R_5 = 1. Otherwise, R_5 = 0.

If R_5 = 1, retrieve the solubility parameter (SP) values for the feasible solvents and assign the RS_5 values according to the following rules:

RS_5 = 1, if SPS = SP ±5%

RS_5 = 2, if SPS = SP ±10%

RS_5 = 3, if SPS = SP ±15%

RS_5 = 4, if SPS = SP ±20%

RS_5 = 5, if SPS > SP ±20%

R3.4.1.6. Neutrality of solvents

If R_1 = 1 or R_3 = 1, set R_6 = 1 if the solvent must be neutral to all compounds present in the reacting system. Otherwise, set R_6 = 0.

If R_6 = 1, check for the solvent pKa value for the feasible solvents and assign RS_6 values based on the following rules:

RS_6 = 1, if pKa > 3

RS_6 = 2, if 2 < pKa <3

RS_6 = 3, if 1 <pKa <2

RS_6 = 4, if 0 <pKa < 1

RS_6 = 5, if pKa < 0

R3.4.1.7. Association/dissociation properties of solvents

If the solvent must not associate or dissociate, set $R_7 = 1$. Otherwise, set $R_7 = 0$.

If $R_7 = 1$, check for the solvent molecule type data (solvents table) for the feasible solvents and assign RS_7 values based on the following rules:

$RS_7 = 1$, if solvent is non-polar

$RS_7 = 2$ or 3, if solvent is polar non-associating

$RS_7 = 4$, if solvent is associating

$RS_7 = 5$, if solvent is ionic

R3.4.1.8. Environmental, health and safety (EHS) property constraints

If EHS properties are to be used as constraints, set $R_8 = 1$. Otherwise, set $R_8 = 0$. Since there are a number of EHS properties, each R_8 and its corresponding RS_8 index has a second subscript to identify the specific EHS property (see Table 3.3). For example, R_{81} corresponds to log P and R_{82} corresponds to LC50 and so on.

If $R_8 = 1$, the set goal values for log P, LC50, etc. and retrieve the solvent values for the corresponding properties and assign the RS_8 values according to the following rules:

$RS_8 = 1$, if $\theta_S = \theta \pm 5\%$

$RS_8 = 2$, if $\theta_S = \theta \pm 10\%$

$RS_8 = 3$, if $\theta_S = \theta \pm 15\%$

$RS_8 = 4$, if $\theta_S = \theta \pm 20\%$

$RS_8 = 5$, if $\theta_S > \theta \pm 20\%$

Where, θ is the goal value of a specific EHS property θ_S is the corresponding solvent property.

R3.4.2. Assign scores to solvent candidates

Create a list of feasible solvents that satisfy all the selection criteria. The scores (on a scale of 1 (worst) to 10 (best)) are assigned from the calculated values of *RS* indices, using the scale shown in Table 3.4. Any solvent having one or more scores of 1 for any solvent index is rejected as infeasible or unsuitable.

R3.4.3. Final solvent selection

As the best possible solvent select the one with the best (highest) score.

Table 3.3: Properties used to addressing the environmental, health and safety consideration (adapted from Harper, 2002)

Properties		Environmental concern		
		Health	Safety	Environment
Implicit	Toxicity	*		*
	Biological persistence			*
	Chemical stability		*	
	Reactivity	*	*	
Explicit	Biodegradability		*	
	Vapour pressure	*	*	*
	LogP	*		*
	Water solubility			*
	Flash point		*	
	Biological oxygen demand			*
	Vapour density	*	*	
	Evaporation rate	*	*	
	LD50	*		*
	Ozone depletion potential			*

Table 3.4: Scores table (adapted from Gani et al., 2005)

Variable	Value				
RS	1	2	3	4	5
Score (S_i)	10	8	6	4	1

R3.5. Separation technique selection

Compare all separation techniques obtained in steps R3.2-R3.4, calculate the driving

force between products, plot on the same figure and identify the separation technique, which offers the largest driving force to assure effective separation of product from reacting mixture.

Some recommendations of the feasible combinations of process schemes either for separation-separation or reaction-separation problems are given in Table 3.5.

Table 3.5. Candidate processes for hybrid operation schemes

Process barrier	Hybrid scheme	Other process scheme
Homogeneous azeotrope	Distillation and membrane	Extractive separation Pressure swing distillation Pressure distillation
Heterogeneous azeotrope	Distillation and membrane	Azeotropic distillation Liquid-liquid extraction Distillation and decanter
Low relative volatility	Distillation and membrane	Extractive separation
Eutectic point	Crystallization and distillation/extraction (MSA required)	-
Removal of undesired compound(s)	Distillation/extraction and external agent* Membrane-based separations	-
Reaction equilibrium	Reactor and distillation (reactive distillation) Reactor and membrane (membrane reactor) Reactor and extraction Reactor and distillation with membrane	-

* External agent might be adsorbent or membrane

3.2.1.5. Step 4: Establish process conditions

In this step, for the separation techniques identified in step 3 and from a superstructure of hybrid schemes (see Figure 3.5), different process scenarios are generated and evaluated using the performance criteria specified in step 2. The superstructure (see Figure 3.5) for hybrid processes consists of two processes, *Process 1* and *Process 2*, which are interconnected by four connectors, namely $\xi^{1\alpha}$, $\xi^{1\beta}$, $\xi^{2\alpha}$ and $\xi^{2\beta}$. Note that *Process 1* and *Process 2* are selected in step 3 and in this step only the specific hybrid process model is generated from hybrid process superstructure by setting up the appropriate decision variables, what is discussed latter on in this section. Specific hybrid process model is used to simulate hybrid process and assess influence of different operational conditions such as temperature, pressure, concentration of compounds, etc. In superstructure presented on Figure 3.5, each constituent process is allowed to a maximum of two outlet and three inlet streams. Each constituent process corresponds to the single separation or reaction process where inlet streams are separated into maximum two product streams. Each stream on Figure 3.5 represents the component molar flow rate.

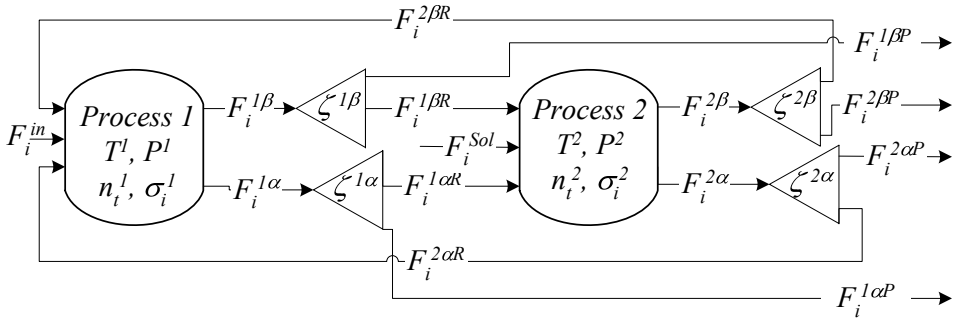

Figure 3.5: Hybrid process superstructure

A simple generic model for any hybrid process represented by the superstructure (Figure 3.5) has been developed. The model consists of mass and energy balance equations and connection equations. Depending on batch or continuous operation modes, (selected in step 2, section 3.2.1.3, page 45), dynamic or steady state models are generated for each process operation scenarios. Dynamic model is used always when batch or semi-batch processes are considered, or when any change in any of the inlet or outlet streams change in time, namely $F_i^{1in} = f(t) \vee F_i^{2in} = f(t) \vee F_i^{1\alpha} = f(t) \vee F_i^{1\beta} = f(t) \vee F_i^{1\alpha} = f(t) \vee F_i^{2\beta} = f(t)$, or non isothermal process occurs, or heat addition or heat removal is required. If steady state process model is selected, the left hand side of Eqs. (3.13-3.14) is set to zero.

Mass balance for compound *i* :

$$\left[\frac{\partial n_i}{\partial t}\right]=\left[\xi^1\xi^{1in}F_i^{1in}\right]+\left[\xi^2\xi^{2in}F_i^{2in}\right]-\left[\xi^1\xi^{1\alpha}F_i^{1\alpha P}\right]-\left[\xi^1\xi^{1\beta}F_i^{1\beta P}\right]-\left[\xi^2\xi^{2\alpha}F_i^{2\alpha P}\right]$$
$$-\left[\xi^2\xi^{2\beta}F_i^{2\beta P}\right]+\left[\xi^R\left(\xi^{(homog)}\sum_{k=1}^{NKR}\nu_{i,k}^{1\alpha}r_k^{1\alpha(homog)}+\xi^{(heterog)}\sum_{h=1}^{NKRh}\nu_{i,h}^{1\alpha}r_h^{1\alpha(heterog)}\right)\right] \tag{3.13}$$

Energy balance:

$$\left[\frac{\partial H}{\partial t}\right]=\left[\xi^1\xi^{1in}\sum_{i=1}^{NC}F_i^{1in}h_i^{1in}\right]+\left[\xi^2\xi^{2in}\sum_{i=1}^{NC}F_i^{2in}h_i^{2in}\right]-\left[\xi^1\xi^{1\alpha}\sum_{i=1}^{NC}F_i^{1\alpha P}h_i^{1\alpha P}\right]$$
$$-\left[\xi^1\xi^{1\beta}\sum_{i=1}^{NC}F_i^{1\beta P}h_i^{1\beta P}\right]-\left[\xi^2\xi^{2\alpha}\sum_{i=1}^{NC}F_i^{2\alpha P}h_i^{2\alpha P}\right]-\left[\xi^2\xi^{2\beta}\sum_{i=1}^{NC}F_i^{2\beta P}h_i^{2\beta P}\right]+\left[Q_1\right]+\left[Q_2\right] \tag{3.14}$$

The existence of the *Process 1* and *Process 2* is described by decision variables ξ^1 and ξ^2. The outlet streams from *Process 1* are defined in terms of molar fraction $x_i^{1\alpha}$, $x_i^{1\beta}$ and outlet total molar flow rates $F_{TOT}^{1\alpha}$, $F_{TOT}^{1\beta}$ (defined by the designer).

$$F_i^{1\alpha}=a\xi^1x_i^{1\alpha}F_{TOT}^{1\alpha} \tag{3.15}$$

$$F_i^{1\beta}=a\xi^1\xi^\beta x_i^{1\beta}F_{TOT}^{1\beta} \tag{3.16}$$

ξ^β defines existence of a second phase (β) in the *Process 1*. The component composition in *Process 1* depends on the separation factors $\sigma_i^{1\alpha}$ and $\sigma_i^{1\beta}$.

$$x_i^{1\alpha}=\frac{\sigma_i^{1\alpha}n_i}{\sum_{i=1}^{NC}\sigma_i^{1\alpha}n_i} \tag{3.17}$$

$$x_i^{1\beta}=\frac{\sigma_i^{1\beta}n_i}{\sum_{i=1}^{NC}\sigma_i^{1\beta}n_i} \tag{3.18}$$

From mass balance around *Process 2*, the outlet streams $F_i^{2\alpha}$ and $F_i^{2\beta}$ are defined by the component separation factors $\sigma_i^{2\alpha}$, $\sigma_i^{2\beta}$ and inlet component flow rates F_i^{2in}, $F_i^{1\beta R}$ and $F_i^{1\alpha R}$.

$$F_i^{2\alpha}=\sigma_i^{2\alpha}\xi^2\left(\xi^{2in}F_i^{2in}+F_i^{1\beta R}+F_i^{1\alpha R}\right) \tag{3.19}$$

$$F_i^{2\beta}=\sigma_i^{2\beta}\xi^2\left(\xi^{2in}F_i^{2in}+F_i^{1\beta R}+F_i^{1\alpha R}\right) \tag{3.20}$$

Existence of streams F_i^{1in} and F_i^{2in} is defined by binary decision variables ξ^{1in} and ξ^{2in}, which can either be 0 or 1. Other streams are defined by decision variables $\xi^{1\alpha}$, $\xi^{1\beta}$, $\xi^{2\alpha}$ and $\xi^{2\beta}$ which can vary between 0 and 1, and expressed as follows:

compound flow rate of bottom product from *Process 1*: $F_i^{1\alpha P} = \xi^{1\alpha} F_i^{1\alpha}$ (3.21)

compound flow rate of top product from *Process 1*: $F_i^{1\beta P} = \xi^{1\beta} F_i^{1\beta}$ (3.22)

compound flow rate of bottom recycle from *Process 1*: $F_i^{1\alpha R} = \left(1-\xi^{1\alpha}\right) F_i^{1\alpha}$ (3.23)

compound flow rate of top recycle from *Process 1*: $F_i^{1\beta R} = \left(1-\xi^{1\beta}\right) F_i^{1\beta}$ (3.24)

compound flow rate of bottom product from *Process 2*: $F_i^{2\alpha P} = \xi^{2\alpha} F_i^{2\alpha}$ (3.25)

compound flow rate of top product from *Process 2*: $F_i^{2\beta P} = \xi^{2\beta} F_i^{2\beta}$ (3.26)

compound flow rate of bottom recycle from *Process 2*: $F_i^{2\alpha R} = \left(1-\xi^{2\alpha}\right) F_i^{2\alpha}$ (3.27)

compound flow rate of top recycle from *Process 2*: $F_i^{2\beta R} = \left(1-\xi^{2\beta}\right) F_i^{2\beta}$ (3.28)

In cases where minimum concentration of compound(s) in *Process 1* is necessary to start *Process 2* additional binary variable *a* is defined (see Eq. 3.29) which depends on switching time (t_{switch}).

$$a = if\ (t \geq t_{switch})\ than\ (1)\ else\ (0) \tag{3.29}$$

The reaction rate of homogeneous reaction ($r_k^{1\alpha(homog)}$) in general can be expressed by the following law of mass action:

$$r_k^{1\alpha(homog)} = k_p^{(homog)} V^{1\alpha} \prod_{i=1}^{NRK} \left(a_i^{1\alpha}\right)^{\upsilon_{i,k}^{1\alpha}} \tag{3.30}$$

When heterogeneous catalyst is used the reaction rate is expressed in many cases in the form of pseudo homogeneous reaction kinetics:

$$r_h^{1\alpha(heterog)} = k_p^{(heterog)} m_{cat} L \prod_{i=1}^{NRKh} \left(a_i^{1\alpha}\right)^{\upsilon_{i,h}^{1\alpha}} \tag{3.31}$$

The component activity $a_i^{1\alpha}$ is defined by Eq. (3.32).

$$a_i^{1\alpha} = x_i^{1\alpha} \gamma_i^{1\alpha} \tag{3.32}$$

The enthalpies of each inlet stream (F_i^{1in}, F_i^{2in}) and outlet stream ($F_i^{1\alpha P}$, $F_i^{1\beta P}$, $F_i^{2\alpha P}$, $F_i^{2\beta P}$) from the hybrid process scheme can be calculated according to Eq. (3.33):

$$\begin{aligned} h_i^j &= \int_{T_0}^{T_j} C_{p_i} dT + \zeta^j \Delta H_{vap,i}^j \\ &= \left| A_i \cdot T + \frac{B_i \cdot T^2}{2} + \frac{C_i \cdot T^3}{3} + \frac{D_i \cdot T^4}{4} + \frac{E_i \cdot T^5}{5} \right|_{T_0}^{T_j} + \zeta^j \Delta H_{vap,i}^j \end{aligned} \tag{3.33}$$

This simple model consists of $23 \cdot NC + NRK + NRKh + 2$ equations summarized in Table 3.7 with $35 \cdot NC + NRK \cdot NC + 2 \cdot NRK + NRKh \cdot NC + 2 \cdot NRKh + 35$ variables which are listed in Table 3.6, where, *NC* is the number of components, *NKR* and *NKRh* is the number of independent homogeneous and heterogeneous reactions which occur only in phase (α). The degree of freedom is therefore equal to $12 \cdot NC + NRK \cdot NC + NRK + NRKh \cdot NC + NRKh + 33$ (see Table 3.6 for list of these variables). In order to solve the above model for any hybrid process it is necessary to specify the following variables: 2 decision variable ξ^1 and ξ^2 representing existence of the *Process 1* and *Process 2*, 6 decision variables related to the connections between the two processes and external inlets ($\xi^{1\alpha}$, $\xi^{1\beta}$, $\xi^{2\alpha}$, $\xi^{2\beta}$, ξ^{1in}, ξ^{2in}), $2 \cdot NC$ inlet streams (F_i^{1in} and F_i^{2in}), 2 total flow rates of streams from *Process 1* ($F_{TOT}^{1\alpha}$, $F_{TOT}^{1\beta}$), 4 *NC* component separation factors in *Process 1* and *Process 2* ($\sigma_i^{1\alpha}$, $\sigma_i^{1\beta}$, $\sigma_i^{2\alpha}$, $\sigma_i^{2\beta}$), 1 occurrence of reaction(s) (ξ^R), 1 existence of second phase in *Process 1* (ξ^β), 6 if stream is in the vapour phase (ζ^j). When reaction(s) take place ($\xi^R = 1$) and either homogenous or heterogeneous reaction occurs, 2 decision variables $\xi^{(homog)}$ and $\xi^{(heterog)}$ are need to be specified. For each kind of reaction the *NRK* and/or *NRKh* corresponding to the reaction rate constants ($k_{p,k}^{(homog)}$, $k_{p,k}^{(heterog)}$) along with $NRK \cdot NC$ and/or $NRKh \cdot NC$ stoichiometric coefficients ($\upsilon_{i,k}^{1\alpha(homog)}$, $\upsilon_{i,k}^{1\alpha(heterog)}$), 1 reaction volume ($V^{1\alpha}$), 1 mass of catalyst ($m_{CAT}$) and 1 concentration of active sides (*L*) need to be specified. Additionally, the time when hybrid operation starts (t_{switch}) has to be specified. Moreover, when computing the energy balance relations for $6 \cdot$temperatures (T^j) of each inlet and outlet stream from hybrid scheme needs to be provided, along with $5 \cdot NC$ parameters of liquid heat capacity of each component (A_i, B_i, C_i, D_i, E_i) and 1 reference temperature (T_0). The *NC* heat of vaporization ($\Delta H_{vap,i}^j$) is added to the enthalpy of liquid at (T^j). Moreover, the addition of heat to the *Process 1* and *Process 2* need be specified by setting Q_1 and Q_2. If derived model is a dynamic model all necessary $NC+1$ initial conditions needs to be provided (n_i, H). Since the reaction kinetics are expressed in terms of activity, the *NC* activity coefficients need to be calculated by the external subroutine according to adequate thermodynamic model such as UNIFAC, UNIQUAC, etc. (model for $\gamma_i^{1\alpha}$ - *NC* equations)

Table 3.6: List of variables in general hybrid process model (*NC*: number of components, *NRK*: number of independent homogeneous reactions, *NRKh*: number of independent heterogeneous reactions)

Differential variables		Number
Molar hold-up in hybrid process	n_i	NC
Enthalpy hold-up	H	1
Algebraic variables (unknowns)		**Number**
Outlet streams of *Process 1* and *Process 2*	$F_i^{1\alpha}$, $F_i^{1\beta}$, $F_i^{2\alpha}$, $F_i^{2\beta}$	$4 \cdot NC$
Product streams	$F_i^{1\alpha P}$, $F_i^{1\beta P}$, $F_i^{2\alpha P}$, $F_i^{2\beta P}$	$4 \cdot NC$
Recycled streams	$F_i^{1\alpha R}$, $F_i^{1\beta R}$, $F_i^{2\alpha R}$, $F_i^{2\beta R}$	$4 \cdot NC$
Reaction rate (homogeneous)	$r_k^{1\alpha(homog)}$	NRK
Reaction rate (heterogeneous)	$r_k^{1\alpha(heterog)}$	$NRKh$
Molar fraction	$x_i^{1\alpha}, x_i^{1\beta}$	$2 \cdot NC$
Component activity	$a_i^{1\alpha}$	NC
Other variable	a	1
Enthalpies of inlet and outlet streams	h_i^{1in}, h_i^{2in}, $h_i^{1\alpha P}$, $h_i^{1\beta P}$, $h_i^{2\alpha P}$, $h_i^{2\beta P}$	$6 \cdot NC$
Algebraic variables (unknowns) calculated by subroutine		**Number**
Activity coefficient of compound	$\gamma_i^{1\alpha}$	NC
Decision variables (specified)		**Number**
Existence of *Process 1* and *Process 2*	ξ^1, ξ^2	2
Existence of outlet streams from *Process 1* and *Process 2*	$\xi^{1\alpha}$, $\xi^{1\beta}$, $\xi^{2\alpha}$, $\xi^{2\beta}$	4

Continuation of Table 3.6		
Existence of inlet streams	ξ^{1in} , ξ^{2in}	2
Existence of reaction	ξ^{R}	1
Decision variables (specified)		Number
Type of reaction	$\xi^{(homog)}$, $\xi^{(heterog)}$	2
Existence of second phase	ξ^{β}	1
Switching time	t_{switch}	1
Phase of the stream (liquid or vapour)	ζ^{j}	6
Parameters (specified)		Number
Inlet streams of *Process 1* and *Process 2*	F_i^{1in}, F_i^{2in}	$2 \cdot NC$
Total flow rates of outlet stream from Process 1	$F_{TOT}^{1\alpha}$, $F_{TOT}^{1\beta}$	2
Reaction volume	$V^{1\alpha}$	1
Mass of catalyst	m_{CAT}	1
Concentration of active sides	L	1
Separation factors	$\sigma_i^{1\alpha}$, $\sigma_i^{1\beta}$, $\sigma_i^{2\alpha}$, $\sigma_i^{2\beta}$	$4 \cdot NC$
Temperature in hybrid process	T^{j}	6
Energy added	Q_1 , Q_2	2
Known variables (specified)		Number
Stoichiometric coefficients (homogeneous)	$\upsilon_{i,k}^{1\alpha}$	$NRK \cdot NC$
Reaction rate constants(homogeneous)	$k_{p,k}^{(homog)}$	NRK

Continuation of Table 3.6		
Stoichiometric coefficients (heterogeneous)	$\upsilon_{i,h}^{1\alpha}$	$NRKh \cdot NC$
Reaction rate constants (heterogeneous)	$k_{p,k}^{(heterog)}$	$NRKh$
Known variables		Number
Heat of vaporization	$\Delta H_{vap,i}$	NC
Liquid heat capacity	A_i , B_i , C_i , D_i , E_i	$5 \cdot NC$
Reference temperature	T_0	1
Unknown variables:	$22 \cdot NC + NRK + NRKh + 1$	
Differential variables:	$NC + 1$	
Specified variables:	$12 \cdot NC + NRK \cdot NC + NRK + NRKh \cdot NC + NRKh + 33$	
All variables in model Eq. (3.13 - 3.33):	$35 \cdot NC + NRK \cdot NC + 2 \cdot NRK + NRKh \cdot NC + 2 \cdot NRKh + 35$	

Table 3.7: List of equations present in the general hybrid process model (*NC*: number of components, *NRK*: number of independent homogeneous reactions, *NRKh*: number of independent heterogeneous reactions)

	Equations	Number of equations
Mass balance (ODEs)	(3.13)	*NC*
Energy balance (ODEs)	(3.14)	1
Outlet streams from *Process 1* and *Process 2*	(3.15-3.16, 3.19-3.20)	$4 \cdot NC$
Molar composition	(3.17-3.18)	$2 \cdot NC$
Relations between streams	(3.21-3.28)	$8 \cdot NC$
t_{switch} condition	(3.29)	1
Reaction kinetics (homog.)	(3.30)	*NRK*
Reaction kinetics (heterog.)	(3.31)	*NRKh*
Components activity	(3.32) plus model for $\gamma_i^{1\alpha}$	$2 \cdot NC$
Components enthalpy	(3.33)	$6 \cdot NC$
Total number of ordinary differential equations (ODEs): $NC + 1$		
Total number of algebraic equations: $22 \cdot NC + NRK + NRKh + 1$		
Total number of equations: $23 \cdot NC + NRK + NRKh + 2$		

Any hybrid process model is obtained from the above generic model by specifying all decision variables (see Table 3.6), substituting in the model equations (Eqs. 3.13 - 3.33) which reduces some of the terms in balance equations and equations corresponding to Eq. (3.15-3.33). Therefore, a generated hybrid model will contain less equations unless new constitutive models are added (for example for properties of the membrane, chemicals, etc.). However, the generated model includes separation factors which need to be set or defined as separate models in a different scale. Examples of such models are provided in this section and in the case studies. First, the derivation of a specific hybrid process model is illustrated by the following example. Let us assume that during the analysis of the problem in previous steps reactor, where homogeneous reaction takes place, is selected as *Process 1* and membrane-based separation is chosen for *Process 2*. Moreover, retentate is recycled

to reactor and hybrid process is operated in the batch mode. Therefore decision variables are defined as follows: $\xi^{1}=1$, $\xi^{2}=1$, $\xi^{1in}=0$, $\xi^{2in}=0$, $\xi^{1\alpha}=0$, $\xi^{1\beta}=0$, $\xi^{2\alpha}=1$, $\xi^{2\beta}=0$, $\xi^{R}=1$, $\xi^{R\beta}=0$, $\xi^{(homog)}=1$, $\xi^{(heterog)}=0$, $t_{switch}=0$ and consider only the dynamic mass balance. Substituting decision variables to the model equations (Eq. 3.13 - 3.33) and rearranging them, yields in the following model:

$$\left[\frac{\partial n_i}{\partial t}\right]=-\left[\sigma_i^{2\alpha}x_i^{1\alpha}F_{TOT}^{1\alpha}\right]+\left[\sum_{k=1}^{NKR}\nu_{i,k}^{1\alpha}r_k^{1\alpha(homog)}\right] \tag{3.34}$$

with

$$x_i^{1\alpha}=\frac{n_i}{\sum_{i=1}^{NC}n_i} \tag{3.35}$$

$$a_i^{1\alpha}=x_i^{1\alpha}\gamma_i^{1\alpha} \tag{3.36}$$

$$r_k^{1\alpha(homog)}=k_p^{(homog)}V^{1\alpha}\prod_{i=1}^{NRK}\left(a_i^{1\alpha}\right)^{\upsilon_{i,k}^{1\alpha}} \tag{3.37}$$

In order to solve that model only $\sigma_i^{2\alpha}$, $\nu_{i,k}^{1\alpha(homog)}$, $F_{TOT}^{1\alpha}$ and $k_{p,k}^{(homog)}$ need to be specified while initial conditions for n_i needs to be provided. Note, that when $t_{switch}=0$ than a is equal to 1 (at the beginning of the operation). The derived model represents the configuration presented in Figure 3.6. The model has been obtained by replacing and rearranging variables through the following algebraic equations:

$$F_i^{1\alpha}=x_i^{1\alpha}F_{TOT}^{1\alpha} \tag{3.38}$$

$$F_i^{2\alpha}=\sigma_i^{2\alpha}x_i^{1\alpha}F_{TOT}^{1\alpha} \tag{3.39}$$

$$F_i^{2\beta}=\sigma_i^{2\beta}x_i^{1\alpha}F_{TOT}^{1\alpha} \tag{3.40}$$

$$F_i^{1\alpha R}=F_i^{1\alpha} \tag{3.41}$$

$$F_i^{1\beta R}=F_i^{1\beta} \tag{3.42}$$

$$F_i^{2\alpha P}=F_i^{2\alpha} \tag{3.43}$$

$$F_i^{2\beta R}=F_i^{2\beta} \tag{3.44}$$

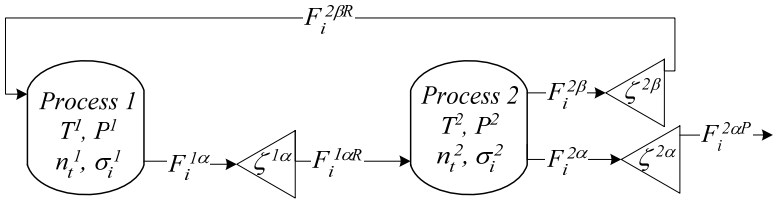

Figure 3.6: Example of generated hybrid scheme, separation (*Process 2*) assisting reaction (*Process 1*)

Advantage of such a reformulated model is simplicity to investigate the performance of different hybrid schemes rapidly and efficiently. Using the superstructure of the hybrid scheme with the generic model and the specific details of the process design problem, the specific hybrid R-S or S-S process can therefore be generated and tested. Note, that product from one operational scenario can be considered as the feed to the next subsequent process operational scenario and therefore lead to the design of a network. If a candidate hybrid scheme does not fulfil the criteria defined in step 2, then decisions taken in step 3 and/or step 1 need to be reviewed.

Note that in the above generic model the component separation factors ($\sigma_i^{1\alpha}$, $\sigma_i^{1\beta}$, $\sigma_i^{2\alpha}$, $\sigma_i^{2\beta}$) are specified as constant values. However in some cases, especially when separation factors depend on the feed composition, temperature and/or pressure of operation, such as in pervaporation (where transmembrane component fluxes depend on the differences between activities in the feed and permeate sides of the membrane) models will be needed to calculate them. The component separation factor is defined as the ratio between inlet and outlet component flow rate from the process (Eq. 3.45).

$$\sigma_i = \frac{F_i^{out}}{F_i^{in}} \tag{3.45}$$

Knowing the process component inlet flow rate the component outlet flow rate can be easily computed. For example, when pervaporation is selected as *Process 2* the process inlet is:

$$F_i^{in} = F_i^{2in} + F_i^{1\beta R} + F_i^{1\alpha R} \tag{3.46}$$

Therefore, for given inlet flow rate, the outlet component flow rate can be calculated using another models, and return to the hybrid process model value of component separation factor (σ_i). In such case the component flux (J_i) is related to the component and membrane specific permeance (Q_i) and the driving force between the feed and permeate (ΔDF), which is expressed by Eq. (3.47). The driving force in general is expressed as the difference in chemical potential between the feed and the permeate side (Lipnizki & Trägårdh, 2001).

$$J_i = Q_i \cdot \Delta DF = Q_i \cdot \Delta\mu_i \tag{3.47}$$

Permeance can be expressed as the constant permeability (short-cut model) or by the one of the other permeance models summarized in the Table 2.2.

When a 2-phase flash separation is considered as *Process 2* the separation factor can be obtained by solving the 2-phase flash model equations, as shown below. Write the overall mass balance equation (Eq. 3.48), component composition in phase 2α (Eq. 3.49) and the component composition in the second phase 2β (Eq. 3.50).

$$F_{TOT}^{2\alpha} = F_{TOT}^{in} - F_{TOT}^{2\beta} \tag{3.48}$$

$$0 = x_i^{2\alpha} - \frac{z_i F_{TOT}^{in}}{\left(K_i F_{TOT}^{2\beta} - F_{TOT}^{in} - F_{TOT}^{2\beta}\right)} \tag{3.49}$$

$$0 = x_i^{2\beta} - K_i x_i^{2\alpha} \tag{3.50}$$

The condition of phase equilibrium is satisfied when, Eq. (3.51) is satisfied.

$$0 = \sum_{i=1}^{NC} x_i^{2\beta} - \sum_{i=1}^{NC} x_i^{2\alpha} \tag{3.51}$$

Where, the *K*-values are calculated according to Eq. (3.52), which requires values of component fugacity coefficients in coexisting phases (assuming a 2-phase vapour-liquid system where an equation of state will be used to predict the fugacities). Fugacities can be calculated using an appropriate property model, such as the SRK-EOS (Soave, 1972).

$$K_i = \frac{\phi_i^{2\beta}}{\phi_i^{2\alpha}} \tag{3.52}$$

The inlet composition z_i is defined by Eq. (3.53).

$$z_i = \frac{F_i^{in}}{F_{TOT}^{in}} \tag{3.53}$$

$$F_{TOT}^{in} = \sum_{i=1}^{NC} F_i^{in} \tag{3.54}$$

Finally the component molar outlet flow rates are obtained (Eq. 3.55-3.56) and the separation factors can be computed according Eq. (3.45).

$$F_i^{2\alpha} = x_i^{2\alpha} F_{TOT}^{2\alpha} \tag{3.55}$$

$$F_i^{2\beta} = x_i^{2\beta} F_{TOT}^{2\beta} \tag{3.56}$$

Such 2-phase flash model consists of 5*NC*+3 equations (3.48-3.51, 3.53-3.56). All model variables 7*NC*+3 can be classified as follows: (1) 3*NC*+2 algebraic variables: (F_{TOT}^{in}, $F_{TOT}^{2\alpha}$, $F_i^{2\alpha}$, $F_i^{2\beta}$, z_i), (2) 2*NC* parameters (F_i^{in}, K_i) and (3) 2*NC*+1 implicit unknown variables ($x_i^{2\beta}, x_i^{2\alpha}, F_{TOT}^{2\beta}$), not counting the fugacity coefficients and their models (see Eq. (3.52)). This means that for given 2*NC* parameters (F_i^{in}, K_i) inlet composition (z_i) and total inlet flow rate (F_{TOT}^{in}) are calculated using Eqs. (3.53-3.54), therefore 2*NC*+1 algebraic equations (3.49-3.51) are solved for 2*NC*+1 unknown variables ($F_{TOT}^{2\beta}$, $x_i^{2\beta}$, $x_i^{2\alpha}$). Therefore all other variables ($F_{TOT}^{2\alpha}$, $F_i^{2\alpha}$, $F_i^{2\beta}$) can be calculated using Eqs. (3.48, 3.55, 3.56).

It is important to realize that in same cases, for some hybrid process configurations, it is possible to eliminate the separation factor by simple substitution which will be presented later on in the case study.

3.2.2. Stage 2: Implementation

This stage is needed if the hybrid schemes from stage 1 need to be verified by experiment. In this case, an experimental set-up needs to be built using the design data from stage 1. Note, however, that if and when experimental data are available it is not necessary to perform experiments. Experiments need to be carefully planned in order to verify not only the hybrid schemes as such but also constitutive models like the reaction kinetic, component flux through the membrane and phase equilibria. The quality of the experimental data needs to be checked by evaluating all experimental errors and formulating an adequate experimental data reconciliation problem. By data reconciliation problem it is meant here that obtained measurements should satisfy process constraint like component mass.

3.2.3. Stage 3: Validation

In this stage a final validation of the proposed design is made by comparing model based simulation results with experimental data if available (or collected in stage 2). If experimental results do not reflect the prediction of the proposed design, the adjustment of parameters used might be needed. Based on newly estimated model parameters, the revision of the decisions taken when following the framework have to be made in order to obtain an improved design. The ultimate objective is to identify the hybrid scheme that best satisfies the process demands set in step 2.

3.3. Computer-aided tools in the Framework

3.3.1. Integrated Computer-Aided System for designing, analysing and simulating chemical processes: ICAS

In the proposed framework various computer-aided tools are used, which are part of the Integrated Computer-Aided System (ICAS). A list of the tools used at different steps of the framework is given in Table 3.8. In the first step of the methodology the CAPEC Database Manager (Nielsen et. al., 2001) is used to retrieve the necessary pure component data. To predict the missing pure component properties of the chemicals, ICAS-ProPred (Marrero and Gani, 2001) is used. For calculations of VLE, LLE and multiphase flash, SMSwin (Gani, 2001) and ICAS-TML (Nielsen and Gani, 2001) are used. ICAS-TML is also used for identifying adequate thermodynamic model for given mixtures and also for estimation of thermodynamic model parameters based on user-supplied experimental data. The thermodynamic models library includes a wide range of Equation of State models (EoS) and Excess Gibbs energy models (GE). For reactive flash calculations, the element-based approach (Pérez-Cisneros et al., 1997) available in ICAS-PDS is used. In step 3 thermodynamic models and various databases are used in order to provide data to generate the necessary driving force plots. In ICAS it is possible to generate VLE, LLE data and to plot the corresponding driving force diagrams. The separation characteristics data for membrane-based techniques are retrieved from the membrane database MemData.

The user specific models are introduced in ICAS-MoT which is a modelling environment for model analysis and solution (Sales & Gani, 2003). Process simulation and optimization is performed in ICAS-Sim (Gani, 2001). More details of already developed computer-aided tools are given in the following subsections 3.3.1.1-3.3.1.7 and of the developed MemData database is given in next section 3.3.2.

Table 3.8. Computer-aided tools used in the framework

Name of tool	Purpose	Used in	Reference
CAPEC DB Manager	Retrieval of pure component properties and mixture properties	Step 1a	(Nielsen et al., 2001)
ICAS-ProPred	Prediction of pure component properties based on various group contribution methods.	Step 1a	(Marrero and Gani, R., 2001)
ICAS-TML	VLE, LLE calculations. Estimation of thermodynamic model parameters.	Step 1a	(Nielsen and Gani, 2001)
ICAS utility toolbox	VLE, LLE and SLE diagrams. Separation efficiency diagrams.	Step 1a Step 3	(Gani, 2001)
SMSWin	VLE, LLE and SLE calculations.	Step 1a	(Gani, 2001)
ICAS-MoT	Solution and analysis of user defined model.	Step 1a, 3 and 4 Stage 3	(Sales & Gani, 2003)
ICAS-ProCAMD	Computer-aided tool for molecular and mixture design; used for solvents design.	Step 3	(Gani, 2001)
ICAS-PDS	Reactive flash calculation. Design and synthesis of distillation based separation schemes.	Step 1a Step 3	(Gani, 2001)
MemData	Search of membrane-based separation used for mixture separation.	Step 3	-
ICAS-Sim	Process simulation and optimization.	Step 4	(Gani, 2001)

3.3.1.1. The CAPEC database

The methodology for process design and analysis of hybrid processes requires information related to the properties of the compounds of a given system. Therefore, use of a database for properties of chemicals is essential. The CAPEC database (Nielsen et al., 2001) includes collected and screened experimental data of pure component properties for approximately 13200 pure compounds, mixture data and solubility data from the open literature. A very important feature of the CAPEC database is that it allows the user to add new compounds along with their experimental property data in user defined databases. Unless otherwise stated, all properties of compounds used in this thesis were retrieved from the CAPEC database.

3.3.1.2. ICAS-ProPred: Property prediction toolbox

When a specific compound either does not exist in the CAPEC database or experimental data is not available, a computational tool for the prediction of pure compound properties is required. In such cases, it is necessary to predict properties of these compounds before they can be added to the database and used in the solution of a given problem.

ICAS-ProPred is a tool integrated into ICAS directly for property prediction of pure component properties. ICAS-ProPred is an interactive program, where via a graphical interface the user can build a molecule by connecting fragments of molecules such as CH2, CH3, OH, etc, into feasible molecules. Presently the program can predict properties using the Marrero and Gani (2001), Constantinou and Gani (1994), Joback and Reid (1987), Wilson (1996), Polymer CI – MG and Polymer Van Krevelen group contribution methods (Satyanarayana & Gani, 2007). ICAS-ProPred was used in this work to calculate properties of the compound only in the case when they could not be found in the available databases or other sources did not contain the needed property.

3.3.1.3. ICAS-TML: thermodynamic model library

ICA-TML is used for three purposes. Firstly, for advising which thermodynamic model should be used in process simulations for given the composition ranges of compounds present in the mixture and the condition ranges (e.g. range of temperature and pressure). This implementation is based on the methodology presented by Gani and O'Connell (1989). Secondly, with ICAS-TML it is possible to obtain mixture properties like bubble and dew points, calculate multiphase flash, etc. Last but not the least, when the selected thermodynamic model exhibits unsatisfactory deviations from experimental data, it is possible to estimate with ICAS-TML the thermodynamic model parameters. In this work ICAS-TML has been used for two purposes: (1) for selection of the thermodynamic model, and (2) for optimizing the parameters of selected thermodynamic model based on available experimental data.

3.3.1.4. Utility toolbox in ICAS

A number of "utility" calculations are available in the "property" window of ICAS. An essential need for the developed methodology is the calculation of separation efficiency curves (driving force) and phase diagrams (solid-liquid, liquid-liquid, vapour-liquid equilibrium diagrams). ICAS utility toolbox is used in this thesis at step 1a and step 3 of the methodology where the analysis of the mixture is done and for generation of driving force diagrams based on VLE data.

3.3.1.5. ICAS-PDS: Process Design Studio

The Process Design Studio is used in this thesis to design the distillation columns. The special feature of the tool is the analysis of the feasibility of achieving a specified distillate or bottom product composition from a specific feed, by manipulating the reflux ratio. In the distillation design part of PDS, given the identity of the mixture compounds, the thermodynamic model, the desired product compositions and reflux, the program returns the number of stages and the feed stage location. Moreover, ICAS-PDS can also be used to compute binary and ternary azeotropes, phase diagrams, distillation boundaries and residue curves. In this way, it can be used for preliminary analysis of a mixture to be separated by distillation. Moreover, in this thesis, ICAS-PDS has been used to compute simultaneous chemical and physical equilibrium (reactive flash) for given component compositions, temperature, pressure and chemical elements (identified according to the method proposed by Pérez-Cisneros et al. (1997)).

3.3.1.6. ICAS-ProCAMD: Computer Aided Molecular Design

ICAS-ProCAMD is based on the multi-level computer-aided molecular design technique developed by Harper and Gani (2000). It can be used for various types of molecular as well as the mixture design problems. Each problem is defined in terms of six main categories, represented by a page in the problem setup menu. The six categories are: (1) general problem control, (2) non temperature dependent properties, (3) temperature dependent properties, (4) mixture properties, (5) azeotrope/miscibility calculations and (6) biodegradation calculations. The generated molecules can be listed and ordered according different target (desired) properties and highlighted if they are present in the CAPEC database. In this thesis ICAS-ProCAMD has been used only when selection of solvent was required in the step 3 of the methodology.

3.3.1.7. ICAS-MoT: Modelling Test Bed

A computer-aided modelling tool ICAS-MoT assists the model developer in the modelling process, reducing the overall time consumed. With ICAS-MoT it is possible, for example, to develop mathematical models of bio- and chemical processes, for steady state and dynamic simulations, static and dynamic process optimisation studies and for model (dynamic and steady state model) identification.

Moreover, with this modelling tool it is possible to generate process models which are not currently available in the process simulator. In the developed hybrid methodology of this thesis, ICAS-MoT has been used extensively to develop various process and property models.

3.3.2. MemData: Membrane database

In step 3 of the hybrid methodology (see section 3.2.1.4, p. 45) a separation technique needs to be selected. Membrane-based separation techniques emerge as good options, especially when separation boundaries (like azeotrope) or selective removal of component from a reactive mixture are necessary. Usually, the membrane-based separation is selected by researchers and/or engineers mainly based on their experience. There is very little information available on prediction of component permabilities, especially in multicomponent mixtures. Therefore, extensive literature survey is required to identify the promising membrane-based separation technique along with appropriate membrane and process conditions. Therefore, to facilitate the search, a membrane database, MemData, has been created by collecting the available data. The data in MemData is classified into different categories and a search engine helps to find the necessary data, if available in the database.

The objective of the membrane database, MemData, is to deliver reliable information about existing membrane-based separation used to separate the given mixture. The process designer can use the database as a supportive tool in the design of membrane-based separation process (e.g. selection of feasible membrane, operational range in terms of component concentrations, temperature, pressure, etc.). The designer is interacting with MemData using predefined queries. The concept of MemData is highlighted in Figure 3.7.

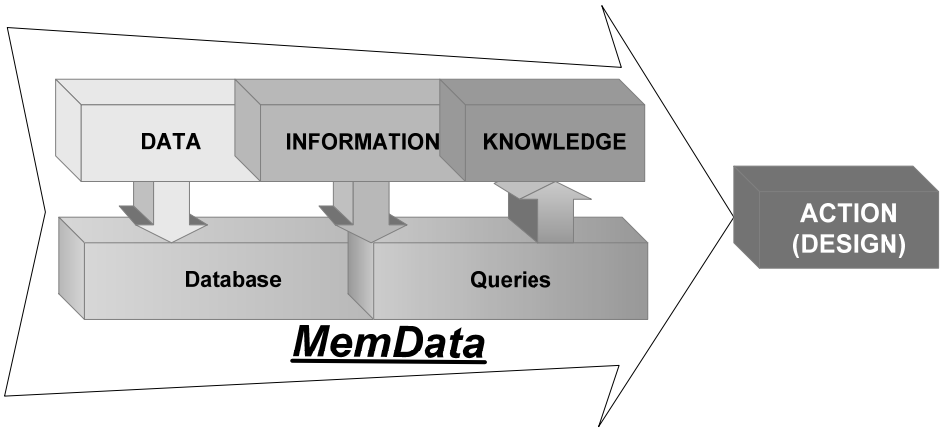

Figure 3.7: Concept of membrane database: MemData

In the following subsections, first available databases are described (subsection 3.3.2.1, page 73) followed by needs and structure of the new membrane database (subsection 3.3.2.2, page 75) and the implementation as a software tool (subsection 3.3.2.3, page 79).

3.3.2.1. Existing membrane databases

A search through the internet could identify the following membrane databases: (1) Catalogue Membrane Technology provided by Dechema, (2) MBR-database provided by MBR-Network. Besides these two membrane databases, reference to a third database developed by Günther & Hapke, (1996) could be found. This project was however, suspended a few years ago and database is therefore no longer available.

The Catalogue Membrane Technology is provided by Dechema, Subject Division: Membrane Technology (http://www.dechema.de/membrankatalog.html). This database aims at giving a comprehensive survey on research and development of membrane processes as well as on suppliers of membranes and membrane-based modules in Germany, Austria and Switzerland. Data can be retrieved in terms of institutions, researchers, research topics, techniques, processes and application fields. The database does not provide information about separation characteristics or any other operation related data (e.g. temperature, pressure). The Catalogue Membrane Technology is based on the membrane catalogue of Institut für Verfahrenstechnik (IVT) at Rheinisch-Westfälische Technische Hochschule (RWTH) Aachen and a list collected by Dr. Paul from GKSS-Forschungszentrum Geesthacht GmbH in 2001. Since than, most of the institutions have updated their entries.

The MBR-database is handled by the MBR-Network and is dedicated to membrane bioreactor (MBR) used in wastewater treatment (e.g. municipal, industrial and maritime sewage). The MBR-database is available in internet (http://www.mbr-network.eu/mbr-database/index.php). The database provides information about producers of membrane bioreactor systems, possible scale of the application (e.g. municipal, household MBR, etc.) but no information about membrane characteristics is available.

It is important to point out that the Polymer handbook (Brandrupet al., 1999) also provides information about permeability, diffusivity and solubility of pure components (mainly gases) through polymeric membranes.

Günther and Hapke (1996) from Technical University of Hamburg-Harburg developed a database dedicated to the specialists in the field of membrane separation processes. The objective of their database was to help the specialist in selecting modules in advance of pilot scale and detailed engineering studies. Their database consisted of three main parts that are related to each other:

(1) basic information about the membrane module with the data provided by the manufacturer,

(2) calculation part to compute the performance of the modules under self defined conditions (this option is available only for reverse osmosis),

(3) extended data related to the application and performance (including experimental separation characteristic of the membrane) of the membrane-based module.

Günther and Hapke (1996) included in their database four kinds of membrane-based separation processes: reverse osmosis, nanofiltration, ultrafiltration and microfiltration. They pointed out that the objective of the database was to assist engineers and specialists in the design of membrane-based separation processes but not to replace them. Without any knowledge about design of membrane-based separation processes the use of the database was not going to be effective. It is because, the database is not an expert system and the relationship between module selection, feed analysis, operating conditions and feed pre-treatment are not considered; this part has to be done by engineer. The structure of the database reported by Günther and Hapke (1996) is shown in Figure 3.8.

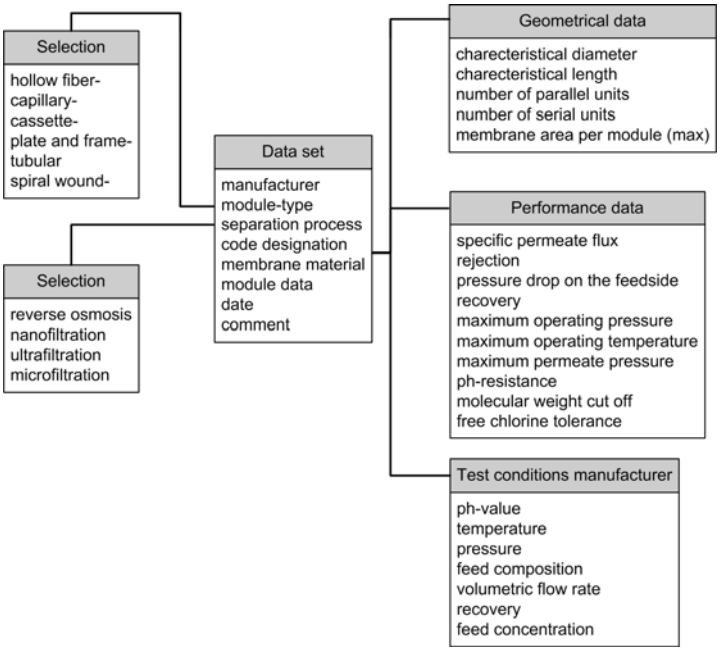

Figure 3.8: Structure of module database by Günther and Hapke (1996)

A summary of the all existing databases related to the membrane-based separation processes is given in Table 3.9. It is clear that from the point of view of the design engineer the most valuable is the module database (Günther & Hapke, 1996) which can provide extensive information about 4 types membrane-based separation processes. Other two databases provide only list of producers that design engineers can contact with respect to their specific applications.

Table 3.9 Summary of data reported in the existing membrane databases

Database	Producers	Separation characteristic	Operational conditions	Information modules	Membrane processes
Catalogue Membrane Technology	Available	NA	NA	NA	*
MBR-database	Available	NA	NA-	NA	membrane bioreactors**
Module database of Günther and Hapke (1996)	Available	Available	Available	Available	reverse osmosis nanofiltration ultrafiltration microfiltratio n

* The database consists of the list of companies which are providing their service with respect to all kind of membrane-based separation; ** utilize microfiltration or ultrafiltration

3.3.2.2. Structure of the MemData database

In general, the structure of the new database reflects the structure of the different types of information stored in it. The membrane database provides information needed by the process designer in order to evaluate the possibility of the separation of a given mixture using membrane-based separation techniques. Therefore, the user of the database should have an access to all important data describing the membrane-based separation techniques such as type of process, separation conditions, composition of separated mixture, membrane details, component permeability, component flux, literature references from which data were obtained and many more. All these information are collected from open sources and stored in the MemData while the reference files are placed in the reference folder (see Figure 3.9).

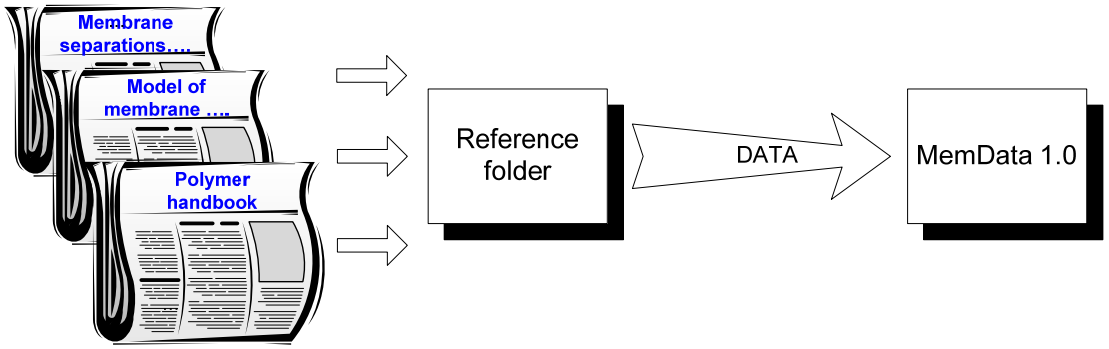

Figure 3.9: Relation between database and sources

Relations between data in the database are established by using the entity-relationship model. It is used widely in software engineering to produce a type of conceptual data model of a system. An entity represents a discrete object in the model. The entity-relationship model of the MemData is shown in Figure 3.10. The entities are represented by oval-shaped figures and rhombuses provide information about relationships between the connected entities.

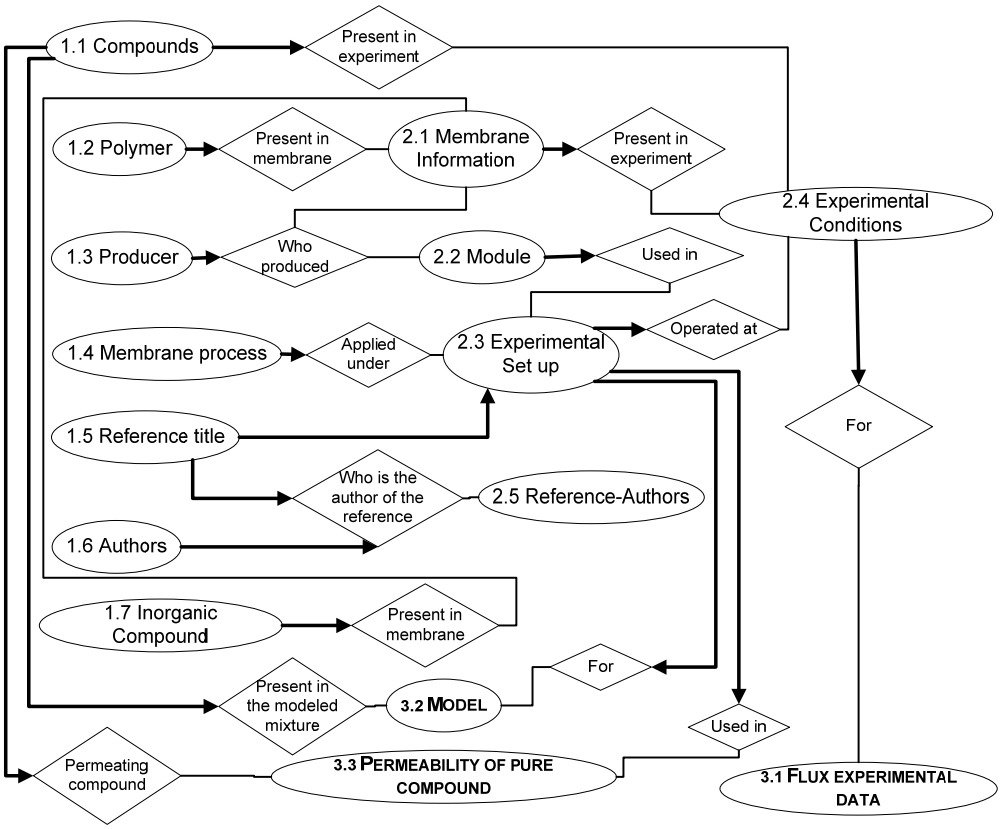

Figure 3.10: General structure of knowledge database MemData. Entity-relationship model

In MemData, four kinds of entities are distinguished: (1) fundamental entity, (2) collection entity, (3) end entity, and (4) sub-entity.

Fundamental entity is an entity which provides the initial information to other entities. Fundamental entity has outgoing relation of type one-to-many to other entities. For example, record from entity 1.4 (Membrane process) can be connected to many records in the collection entity 2.3 (Experimental set up) which means that the same kind of membrane process (e.g. pervaporation) has been applied in different experimental configurations. In the MemData, 7 fundamental entities are distinguished: 1.1 (Compounds), 1.2 (Polymer), 1.3 (Producer), 1.4 (Membrane process), 1.5 (Reference title), 1.6 (Authors) and 1.7 (Inorganic compound).

Collection entity: beside new information, it collects information from fundamental entities and passes then to the end entities. Collection entity has incoming and outgoing relations of type many-to-one to fundamental entities and one-to-many end entities. Collection entities in the MemData are: 2.1 (Membrane information), 2.2 (Module), 2.3 (Experimental set up), 2.4 (Experimental conditions) and 2.5 (Reference-author).

End entity: stores final information and have connection with fundamental and collection entities. End entities in the MemData are: 3.1 (Flux experimental data), 3.2 (Model), and 3.3 (Permeability of pure compound).

An entity contains attributes which describes each record. In other word, attribute describes entity. For example, the entity 1.1 (Compound) represents class of chemical compounds, each chemical compound is a record which has a CAS number and component name as attribute. The detailed list of all entities and attributes is given in Appendix 6.3 (page 187).

Besides component permabilities (or fluxes), data of inlet and outlet streams, are stored in the MemData, for several related properties that influence the component permeability through a membrane and the operation conditions. A short description of the properties included in the MemData is given below. It is important to point out that all units follow SI-units, if otherwise it is stated clearly.

Glass transition temperature indicates change in the polymer structure from the glassy state to the rubbery state. Between glass transition temperature and melting temperature, the free volume of the polymer increases, and has a significant influence on the associated permeability values.

Density of polymer when it increases, the permeability decreases; the higher the *crystalinity* the higher is the density; the higher crystalinity, the permeability is lower. Polymer density depends also on the draw ratio.

Draw ratio is the ratio between the length of the deformed specimen and the length of the initial undeformed specimen.

Thickness of the polymer film in principle does not affect the permeability coefficient, the diffusion coefficient and the solubility coefficient. In practise, different values may be obtained from films of variable thickness, which in turn may be due to

differences in drawing, orientation and crystalinity.

Porosity (ε), pore size (r), tortuosity (τ) are used for calculating the hydraulic permeability (L_p) in Hagen-Poiseuile equation (Mulder, 2003):

$$L_p = \frac{\varepsilon \cdot r^2}{8 \cdot \eta \cdot \tau} \tag{3.57}$$

Permeability is defined as the transmission of molecules through polymer films and depends on composition of investigated mixture (Brandrup et al., 1999). The permeability coefficient is defined as:

$$P = \frac{\left(quantity\ of\ \ permeant\right) \cdot \left(film\ thinckenss\right)}{\left(area\right) \cdot \left(time\right) \cdot \left(pressure\ drop\ across\ the\ film\right)} \tag{3.58}$$

The permeation of molecules through polymer film is governed by two steps; dissolution of penetrant in the polymer (solubility (S)) and diffusion (D) of dissolved permeant and is expressed by Eq.(3.59).

$$P = D \cdot S \tag{3.59}$$

The temperature dependence of the permeability coefficient P, the diffusion coefficient D and the solubility coefficient S is represented as:

$$P = P_0 \cdot \exp\left(\frac{-E_P}{RT}\right) \tag{3.60}$$

$$D = D_0 \cdot \exp\left(\frac{-E_D}{RT}\right) \tag{3.61}$$

$$S = S_0 \cdot \exp\left(\frac{-E_S}{RT}\right) \tag{3.62}$$

Component flux is defined as quantity of component permeating through membrane area in time:

$$J = \frac{\left(quantity\ of\ \ permeant\right)}{\left(area\right) \cdot \left(time\right)} \tag{3.63}$$

Since flux J does not include either the pressure of the permeant nor the thickness of the polymer in its dimension, it is necessary to know either the pressure or the concentration of the permeant in the feed and the thickness of the polymer under the conditions of measurement.

In literature various models and correlations describing membrane-based separations are found. The option to provide the parameters to most command experimental and semi-experimental permeability models is also included in the MemData. The list of included correlations is given in Table 3.10. Moreover, there is an option to provide another correlation and link to file with ready-to-use models for example in ICAS-MoT file.

Table 3.10: Experimental and semi-experimental correlations of permeability included in MemData

Mass transport model	Permeability	Model parameters (input in the MemData)
Short-Cut-Model (SC) with Arrhenius (AR)	$Q_i^0 \cdot \exp\left(-\frac{E_i}{R}\left(\frac{1}{T^0}-\frac{1}{T}\right)\right)$	Q_i^0, E_i, T^0, $R = 8.3144\left[J/mol/K\right]$
Meyer-Blumenroth (MB)	See equations (2.28-2.30, 2.31)	$\bar{D}_i^T\left(T^0\right)$, E_i, T^0, B_i°, B_{ij}, $R = 8.3144\left[J/mol/K\right]$
Solution-Diffusion (SD)	$\frac{P_i^0}{l_M} \cdot \exp\left(-\frac{E_i}{R}\left(\frac{1}{T^0}-\frac{1}{T}\right)\right)$	P_i^0, l_M, E_i, T^0, $R = 8.3144\left[J/mol/K\right]$

3.3.2.3. The MemData implementation

The entity-relationship model is translated into a software where each entity is represented by a table since attributes are the columns in a table. Records are placed in the rows of the table. The MemData is implemented according to the *divide and conquer* rule which in the development of the database means: divide all entities and their attributes into tables in such a way that duplication of information is avoided. However, each record has to be still uniquely identifiable.

Microsoft Access was selected as the most suitable environment for the database development since it is possible to create single user applications with user friendly interface. Moreover, Microsoft Access offers a unique possibility to link Visual Basic for Applications (VBA) language with Sequential Query Language (SQL) to enhance the operations on the database. In this way, the user can easily interact with the database and transfer data between applications in Microsoft Office package, e.g. Excel were further calculation or other representation can be done.

All the entities presented in the entity-relationship model (Figure 3.10) are translated by means of introducing tables in Microsoft Access. The unique identification of records in the tables is assured by the attribute id.NameOfEntity which is type of the auto-number with additional property of the primary key. Type auto-number assigns the next number of the record automatically. Records in the table are sorted in ascending manner according attribute with the primary key. The open data structure of the database is assured by introducing the component unique CAS number. In this

way MemData can communicate with other property databases such as CAPEC Database.

The relations between all entities and the end entity, namely, 3.1 (Flux experimental data), 3.2 (Model), and 3.3 (Permeability of pure compound), are highlighted in Figures 3.11-3.14, respectively. The list of all entities and attributes is given in Appendix 6.3 (page 187).

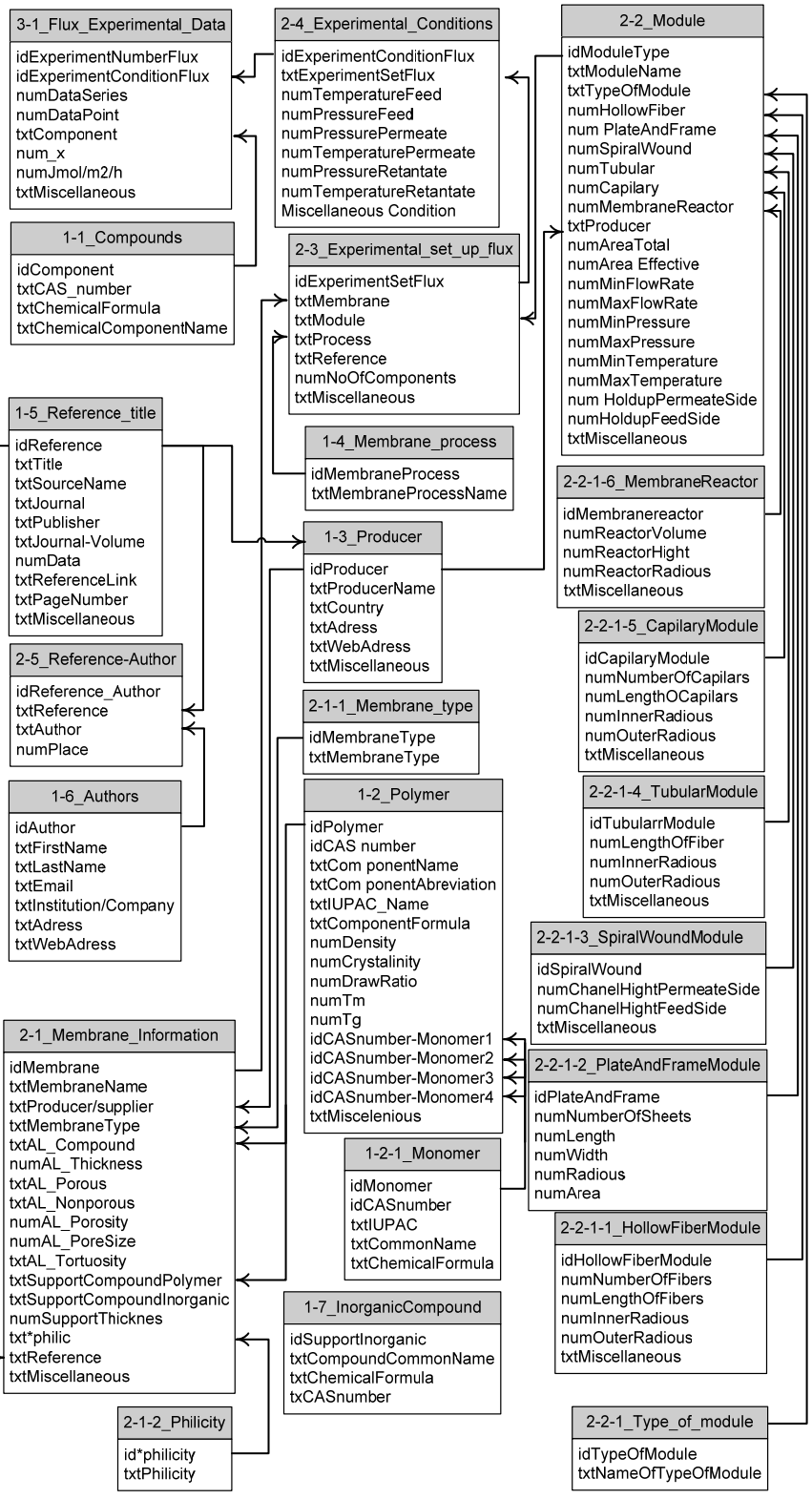

Figure 3.11: Relation map for component flux data

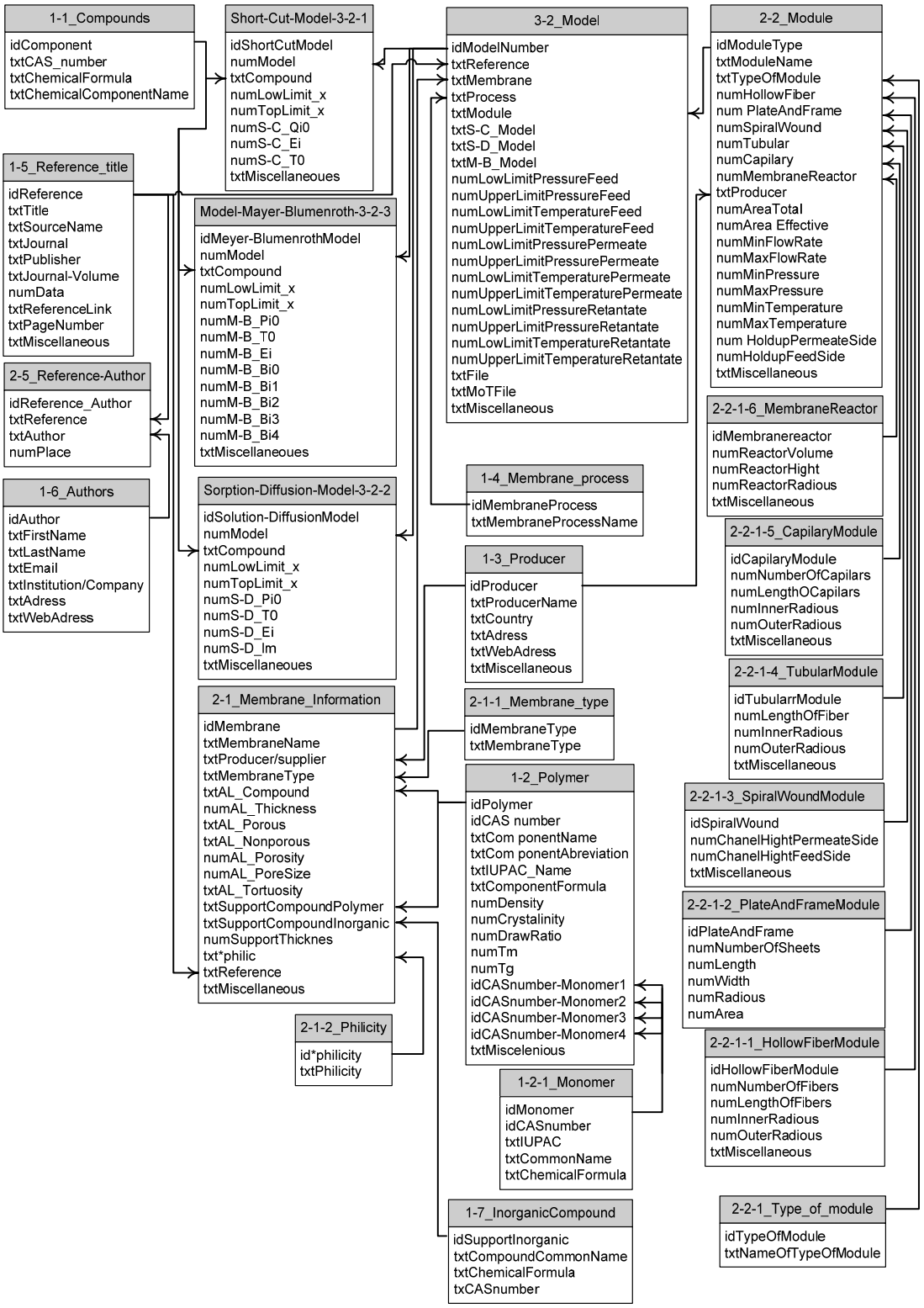

Figure 3.12: Relation map for models

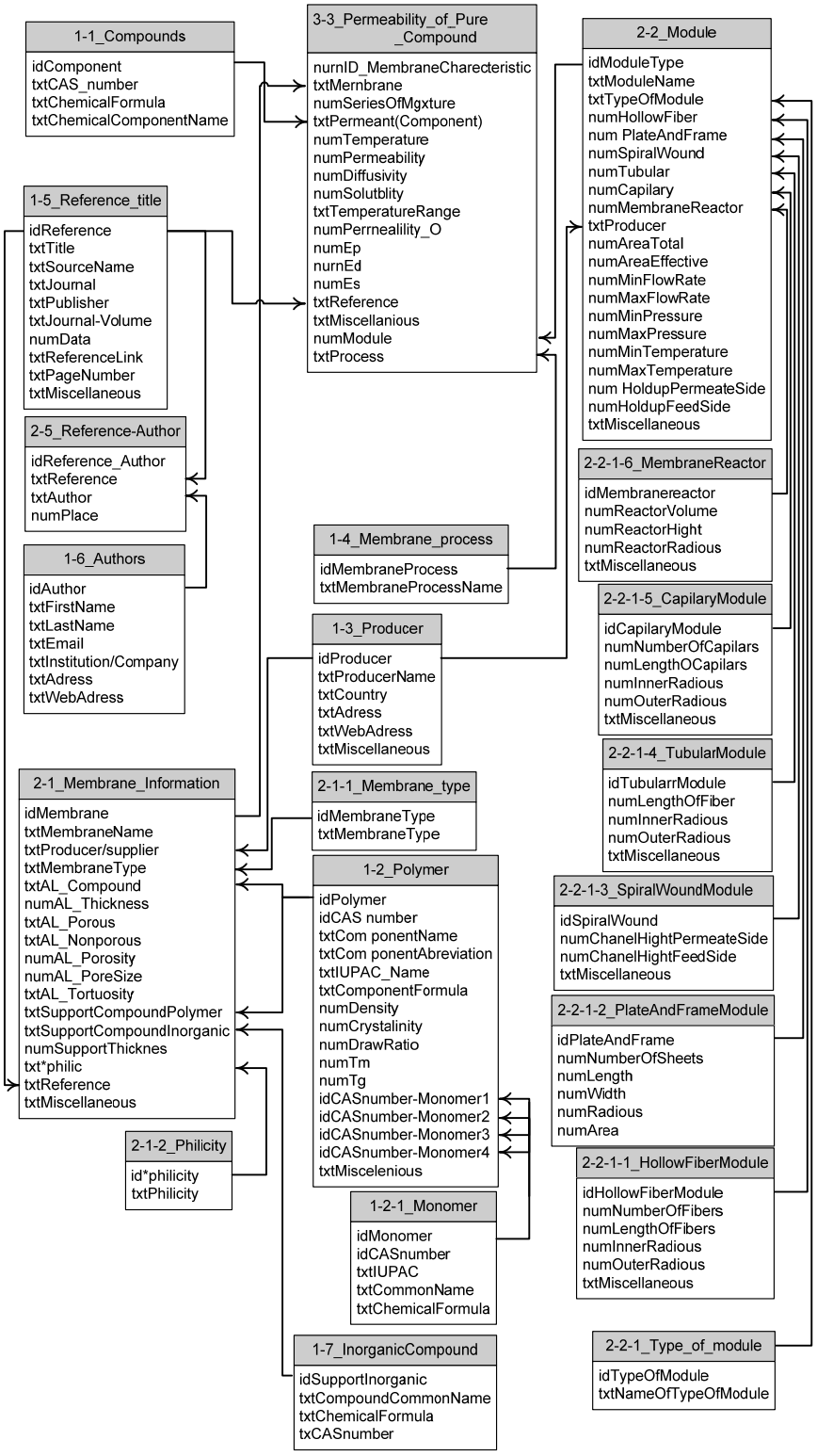

Figure 3.13: Relation map for pure component permeability, diffusivity and solubility data

The database is questioned through query objects. In order to save time a user friendly interface was developed and the database can be queried for available data as well as to introduce new data. The user is interacting at first with main window of the MemData presented on Figure 3.14 from which several options can be selected like (1) view the list of chemical components, (2) add or edit data, (3) search database and (4) view the statistics of the MemData. The database can be searched in order to find experimental flux results and/or pure component permeability through various membranes and their temperature dependencies as well as for model and their associated parameters for a given mixture.

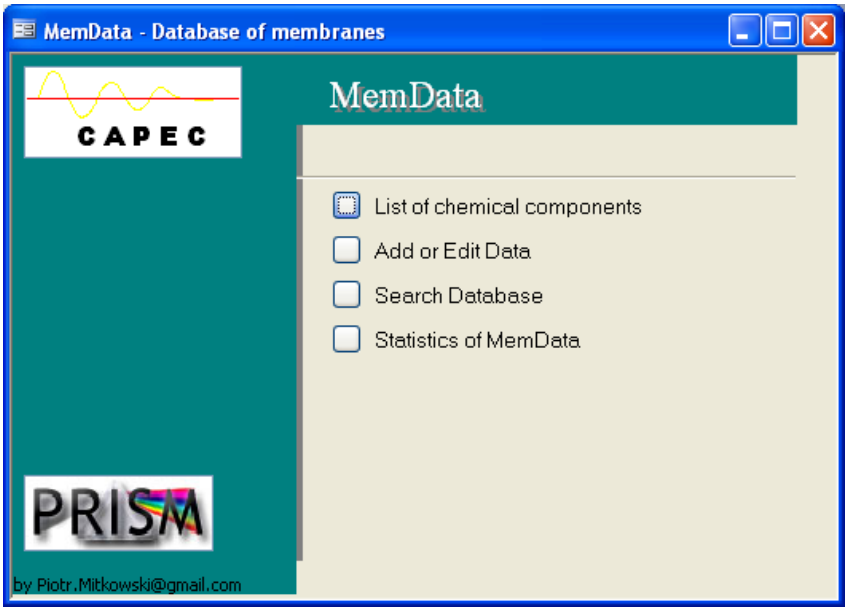

Figure 3.14: Main window of MemData

Table 3.11: MemData in numbers

	Total number of entries
Number of membranes	277
Number of references	17
Number of experimental points	112
Number of pure component permeability data points	1123
Number of models and correlations	4

4. Case studies

"All models are wrong but some models are useful"

(George E.P. Box)

4.1. Introduction

This chapter is divided into two main sections Separation-Separation systems and Reaction-Separation systems to reflect two different kinds of processes included in the consideration of the developed framework. The first case study presents the application of the methodology to the separation-separation system. The four case studies that follow, deal with reaction-separation systems. The first stage of the framework was applied in all of the five case studies. All identified designs have been verified by means of the process simulations. It is important to point out that the whole framework, which includes also experimental verification of the identified design, was applied to the last case study, the synthesis of n-propyl propionate. In each case study the workflow along with dataflow and the tools used are highlighted through figures reflecting the first stage of the framework. All mathematical models used in this chapter are presented in detail in the Appendix 6.4.

4.2. Separation-Separation systems

4.2.1. Separation of binary mixture of water and acetic acid

The key technology in producing a purified terephtalic acid (PTA) involves a separation step to attain the high purity product required for polyester manufacturing. Several processes have been developed to produce PTA and all of them use acetic acid (HAc) as a solvent to remove water, which is the main by-product (Zhou, 2005). In industry the exothermic oxidation reaction of p-xylene to terephtalic acid takes place in the continuously fed reactor with air, p-xylene, catalyst and solvent. Once the oxidation reaction is completed, two moles of water are formed per mole of p-xylene reacted. For this study it is assumed that solvent for reaction was already selected and recycle of pure solvent (HAc) is expected in order to increase profitability of the process. Since in this case study the reaction is fixed, the steps related to reaction in the framework are omitted (see Figure 4.1).

4.2.1.1. Step 1a: Separation task analysis

The workflow and used tools in this step are highlighted on Figure 4.1.

1a.1. Identify mixture type

Mixture contains two compounds: water and acetic acid. According to the mixture classification rule (Gani & O'Connell, 1989), the mixture is classified as non-ideal and aqueous type. Therefore, the two model approach is selected for phase equilibria calculations with the Modified UNIFAC Lyngby model for the liquid phase and the SRK equation of state for the vapour phase.

1a.2. Analysis based on pure component properties

Constituent components of the mixture are in the liquid state between 289.81 K and 373.15 K at the standard pressure of 1 atm. Significant differences in the solubility parameters indicate possibility of the existence of a miscibility gap (see Table 4.1).

Table 4.1: Pure component properties of water and acetic acid

Compound	T_m [K]	T_b [K]	*Sol. Par* [MPa$^{0.5}$]
acetic acid	289.81	391.05	19.0078
water	273.15	373.15	47.8127

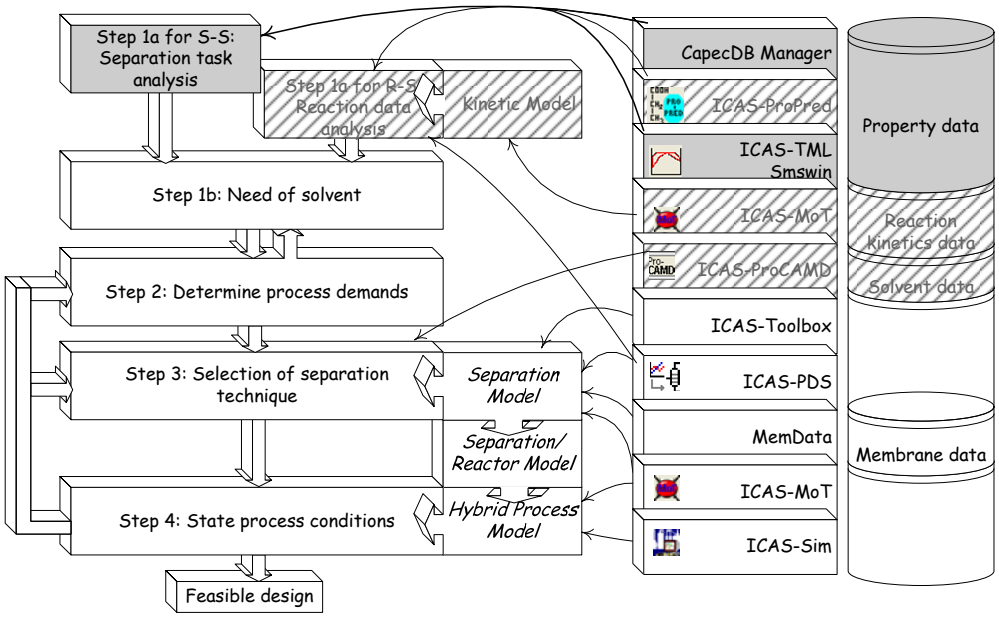

Figure 4.1: Step 1 in the case study of separation of water–acetic acid mixture

1a.3. System analysis based on mixture properties

The experimental VLE data found in literature (Gmehling et al., 1977) were fitted to the Modified UNIFAC (Lyngby) model (Larsen et al., 1987) using ICAS-TML. The regressed parameters are given in Table 4.2 and Table 4.3. Group representations of the molecules present in the mixture are given in Table 4.4. The VLE diagram of binary mixture of water and acetic acid does not show any azeotrope but a tangent pinch on the pure water is observed (see highlighted section of Figure 4.2). Even though there is a significant difference in the solubility parameters of water and acetic acid, the mixture was reported as fully miscible (Colombo et al., 1999).

Table 4.2: Estimated parameters for Modified UNIFAC (Lyngby)

	CH2	H2O	COOH
		A_{ij}	
CH2	0	9686.305	1085.252
H2O	3759.772	0	334.4505
COOH	3676.853	2159.947	0
		B_{ij}	
CH2	0	-42.9044	-42.4595
H2O	-126.404	0	-30.2669
COOH	-132.343	-32.7982	0
		C_{ij}	
CH2	0	-14.416	-95.1047
H2O	4.605278	0	-50.0667
COOH	-12.0356	-114.68	0

Table 4.3: R_i and Q_i for Modified UNIFAC (Lyngby)

	R_i	Q_i
H2O	0.92	1.4
CH3	0.9011	0.848
COOH	1.3013	1.224

Table 4.4: Representation of compounds in terms of Modified UNIFAC (Lyngby) groups

	Representation	Sub group	Main group
Water	1	'H2O'	'H2O'
Acetic Acid	1	'CH3'	'CH2'
	1	'COOH'	'COOH'

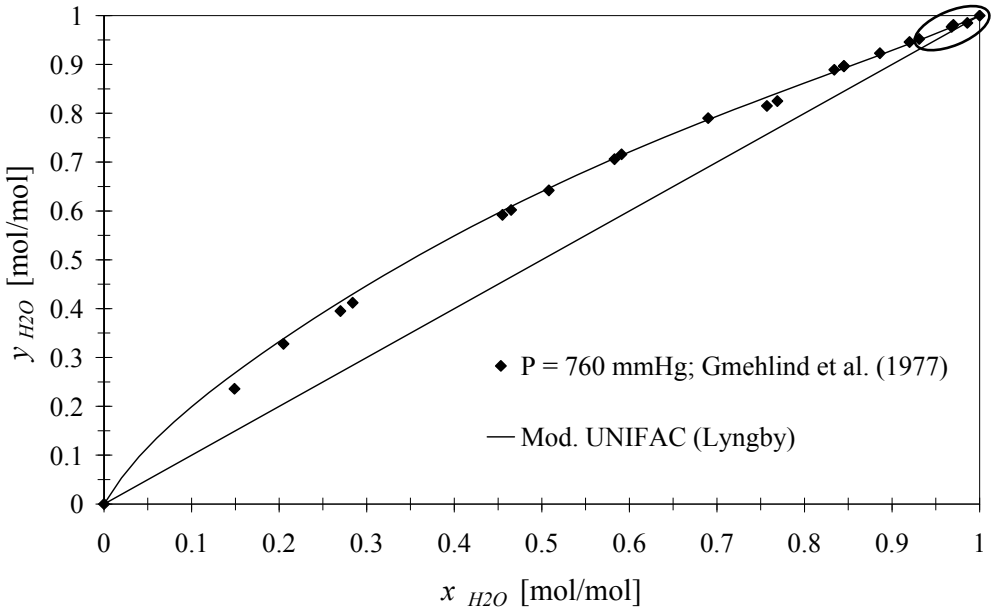

Figure 4.2: VLE diagram of the binary mixture of water and acetic acid at 1 atm.

4.2.1.2. Step 1b: Need of solvent

Addition of solvent is advantageous to break the azeotrope. Even though the investigated mixture does not have any azeotrope, the possibility of introducing a solvent can be one option to overcome difficult separation region around the tangent pinch. In such a region an extractive distillation might be considered. However, other separation techniques than solvent-based separation should be considered at first to avoid addition of other compounds to the system.

4.2.1.3. Step 2: Determine process demands

The equimolar mixture of H_2O and HAc needs to be separated into two streams with a purity of 99.5 mol% for each of the compounds. The feed flow rate is 100 kmol/h, at 300 K and 1 atm. A continuous separation process is investigated, because of a continuous feed.

4.2.1.4. Step 3: Selection of separation techniques

S3.1. Generate and/or collect data of phase compositions for as many separation methods as desired or available.

S3.1.1. Distillation

Water is a more volatile component than acetic acid. Distillation is a feasible separation technique in the whole concentration range since the relative volatility of

binary mixture is higher than 1.05 (see Figure 4.3). The data to calculate the relative volatility has been obtained in ICAS-Utility toolbox (see Figure 4.4).

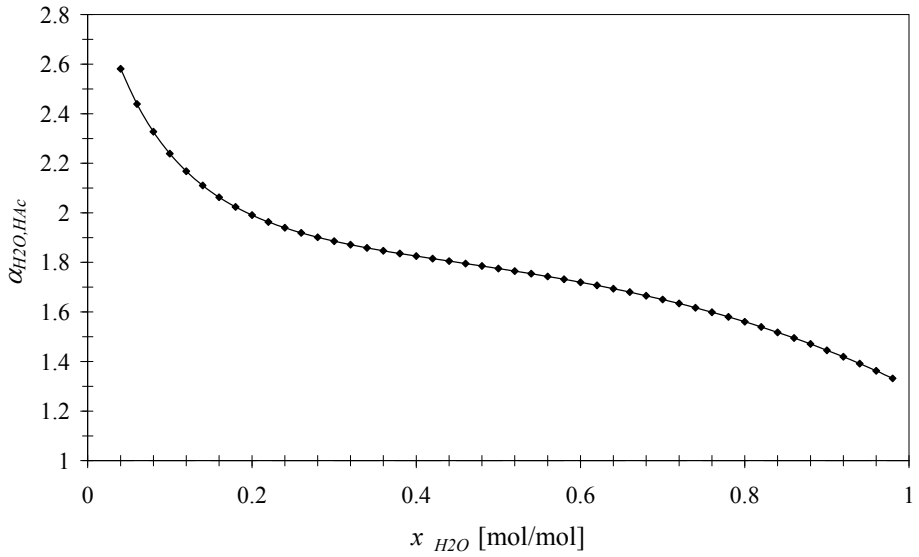

Figure 4.3: Relative volatility between water and acetic acid at atmospheric pressure

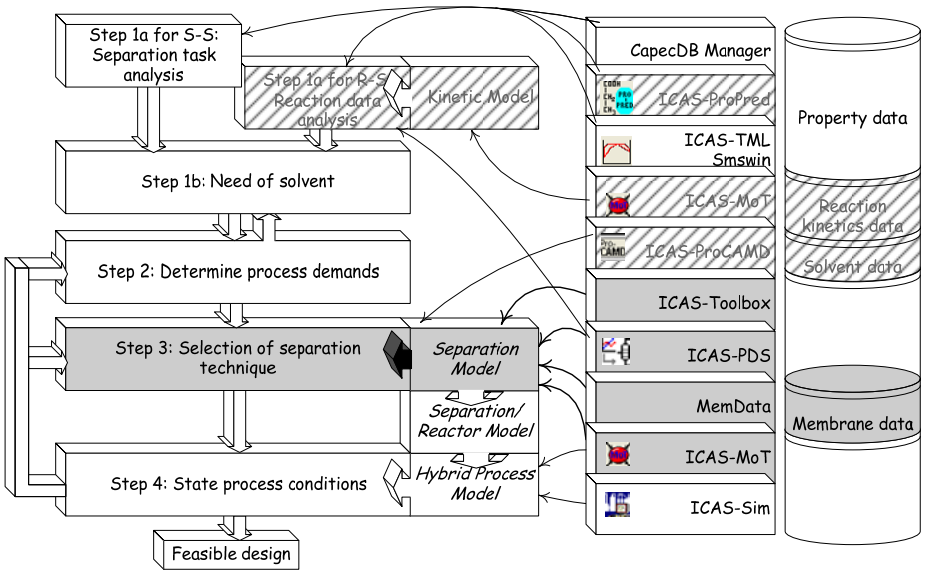

Figure 4.4: Step 3 in the case study of separation of water–acetic acid mixture

S3.1.2. Solvent-based separation techniques

Following the analysis given in the Step 1b the design of solvent separation technique is skipped.

S3.1.3. Membrane-based separation techniques

Several authors have reported the possibility of dehydration of organic mixtures using pervaporation and vapour permeation (Mulder, 2003; Koszorz et al., 2004; Sanz & Gmehling, 2006). Zhou (2005) studied commercially available polyimide Matrimid ® membrane to remove selectively water from binary mixture of water and acetic acid in pervaporation process. Huang et al. (1998) reported polyaniline membrane as stable and very selective for the separation of aqueous mixtures of carboxylic acid (acetic acid, formic acid and propionic acid).

S3.2. Calculate and plot all driving forces on one plot for each identified separation methods from step S3.1.

The driving force curves for vapour liquid equilibria at different pressures (53.3 kPa, 101.3 kPa and 273.7 kPa) have been presented in Figure 4.5 together with pervaporation experimental data for doped and undoped polyaniline membrane retrieved from the MemData. As it can be seen from the Figure 4.5, the influence of pressure on the driving force of distillation is small. Pervaporation data exhibits significantly higher driving force (*FD*) than distillation irrespective of which polyaniline membrane is compared. Doped polyaniline membrane gave the highest *FD* among all the separation methods in water concentration from $x_{H2O} = 0.35$ to $x_{H2O} = 1$.

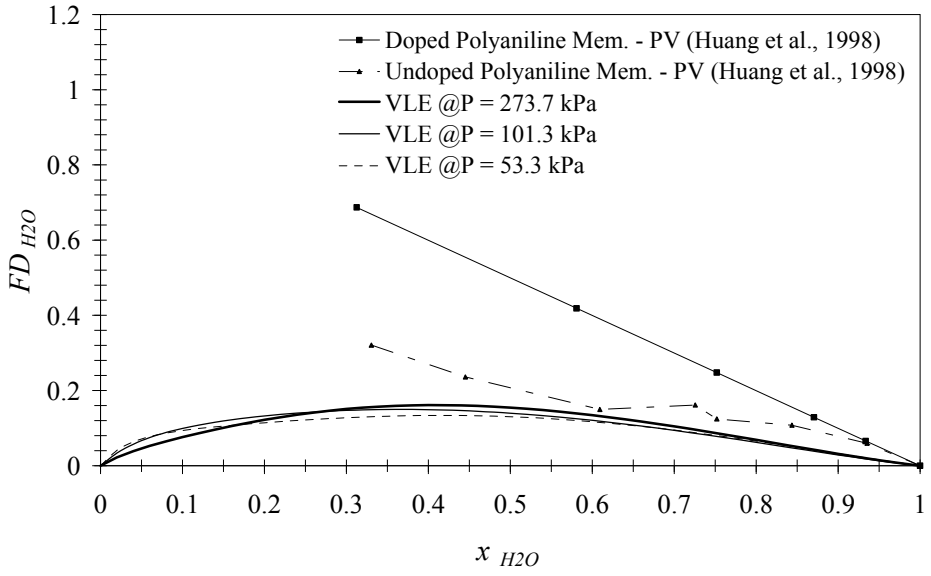

Figure 4.5: Driving force diagram for separation water-acetic acid mixture

S3.3. Screen for feasible solution

Distillation is feasible in the whole concentration range and pervaporation is feasible in concentration range from $x_{H2O} = 0.35$ to $x_{H2O} = 1$ since data for only that region was available (see Figure 4.5).

S3.4. Identify feasible combinations

From the point of view of driving force feasibility, the best hybrid process combines distillation at normal pressure (101.3 kPa) followed by pervaporation using the doped polyaniline membrane (see Figure 4.5).

S3.5. Identify the solution with biggest driving force

Since it is well known that distillation is more economic for bulk processes than the membrane-based separation techniques, the distillation is selected as a first separation step and the membrane as process which will enrich distillate to the required level. Therefore pervaporation is used where distillation is less effective, in other words, when the derivative of *FD* (see Figure 4.6) for distillation (bold line) has a local minimum and it has smaller absolute value than pervaporation. According to Figure 4.6, pervaporation is able to show its superiority over distillation between 0.77 – 0.90 of x_{H2O}. In other words, distillation has its bottleneck between x_{H2O} 0.77 – 0.90. In this region, the change of *FD* is very small (Figure 4.6). At this step two possible configurations of processes are pointed out: distillation followed by pervaporation (DFP) and distillation with side pervaporation (DSP). The objective of these two configurations is to overcome the local minimum of the driving force of distillation. In both configurations the bottom products of the distillation achieves 0.995 molar fraction of acetic acid. However, in the first configuration (DFP) distillate achieves $x_{H2O} = 0.77$ and than pervaporation is used to enrich distillate from $x_{H2O} = 0.77$ to the required $x_{H2O} = 0.995$ (see bold line on Figure 4.7). The retentate from pervaporation is recycled to the distillation column. In the second configuration DSP the distillate achieves 0.995 molar fraction of water and pervaporation is used as a side separation, to enhance the distillation in the bottleneck of distillation in region 0.77 – 0.90 of x_{H2O}. Feed to pervaporation withdrawn from distillation column contains $x_{H2O} = 0.77$ and permeate achieves $x_{H2O} = 0.90$. Derivative of driving force for the DSP operation is presented by bold line on Figure 4.8.

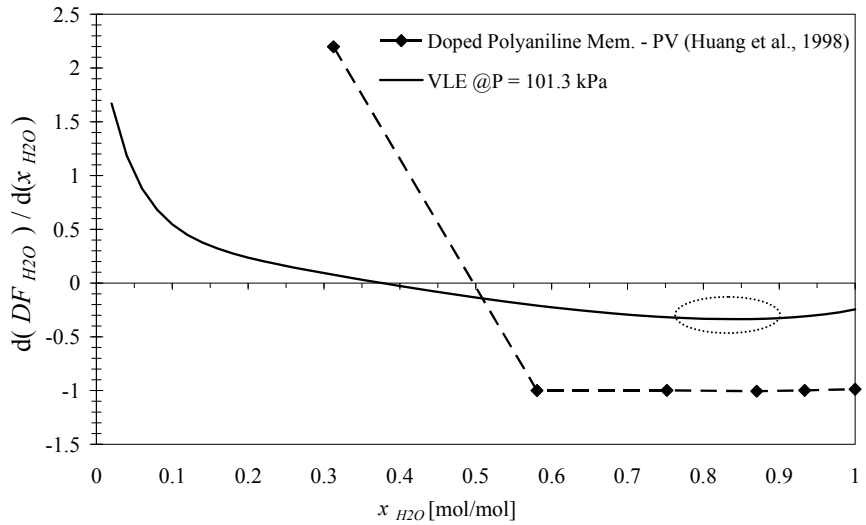

Figure 4.6: Derivative of driving force

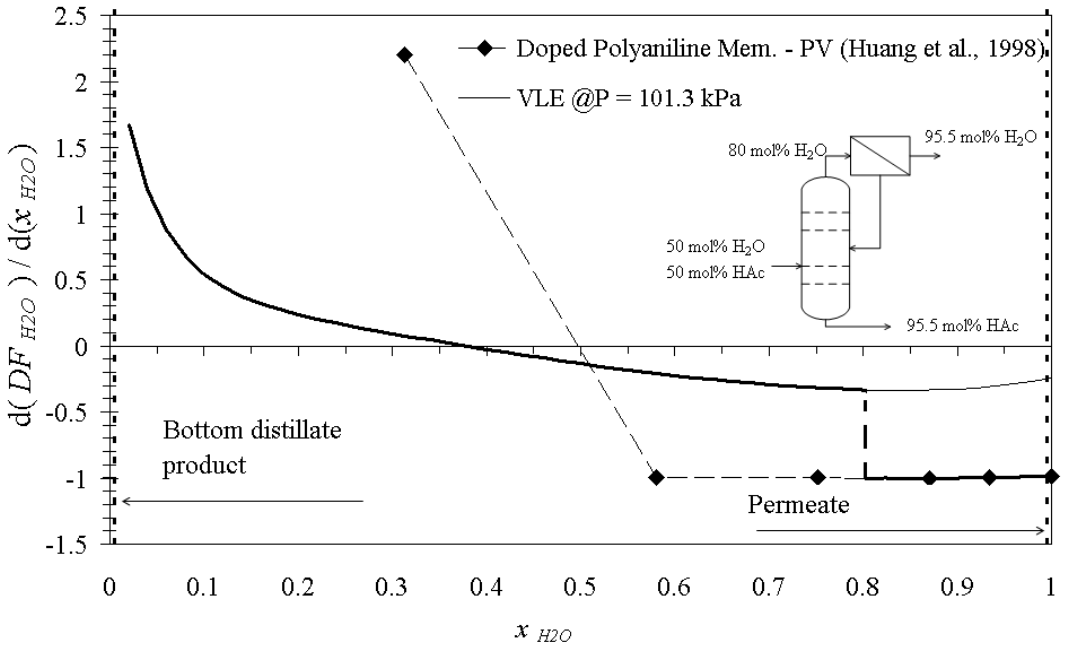

Figure 4.7: First process configuration: distillation followed by membrane-based separation (pervaporation)

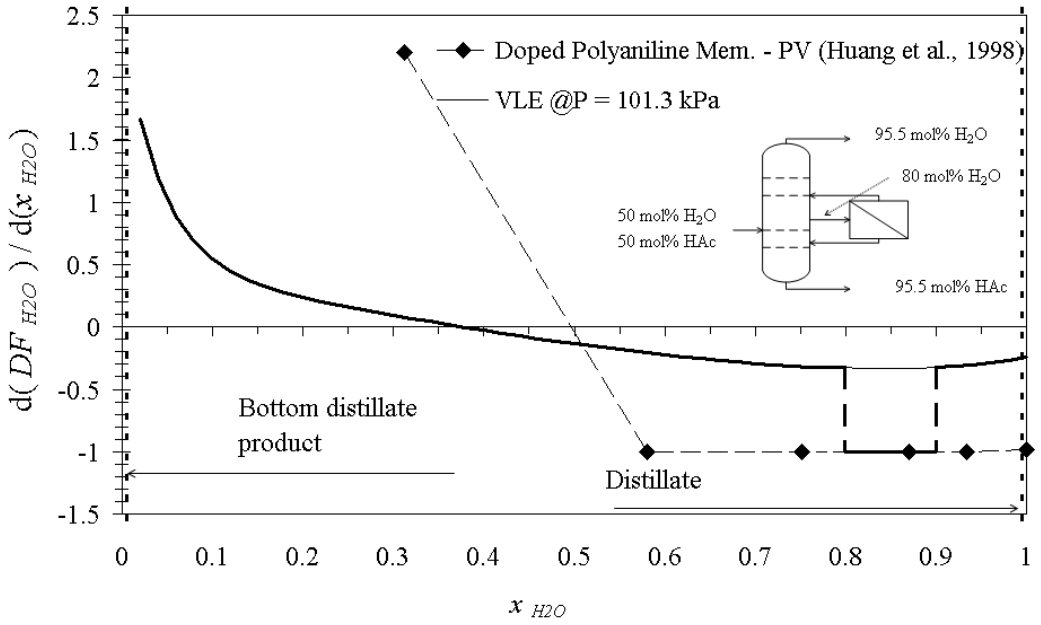

Figure 4.8: Second process configuration: distillation with side membrane-based separation (pervaporation)

4.2.1.5. Step 4: Establish process conditions

At first the configuration with distillation followed by pervaporation is considered. Therefore the specific steady state model is derived from the generic model presented in section 3.2.1.5 (page 57). The decision variables have following values $\xi^{1}=1$, $\xi^{2}=1$, $\xi^{1in}=1$, $\xi^{2in}=0$, $\xi^{1\alpha}=1$, $\xi^{1\beta}=1$, $\xi^{2\alpha}=0$, $\xi^{2\beta}=1$, $\xi^{R}=0$, $\xi^{\beta}=1$, $\xi^{homog}=0$, $\xi^{heterog}=0$, $a=1$ and specific process configuration is shown in Figure 4.9. Retentate from pervaporation (stream $F_i^{2\alpha R}$) is recycled to the distillation.

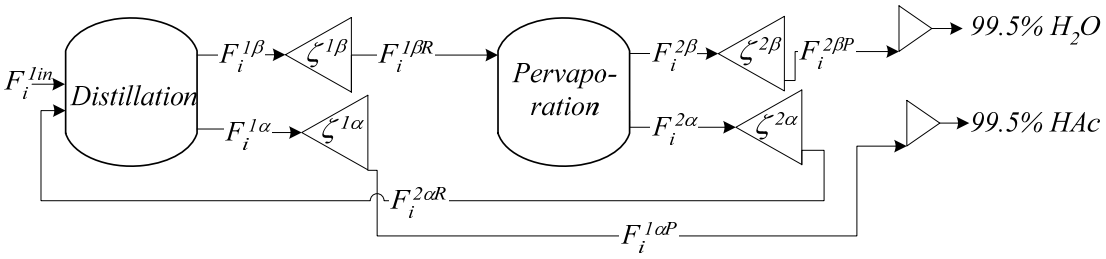

Figure 4.9: From hybrid process superstructure to the specific process configuration: distillation followed by pervaporation

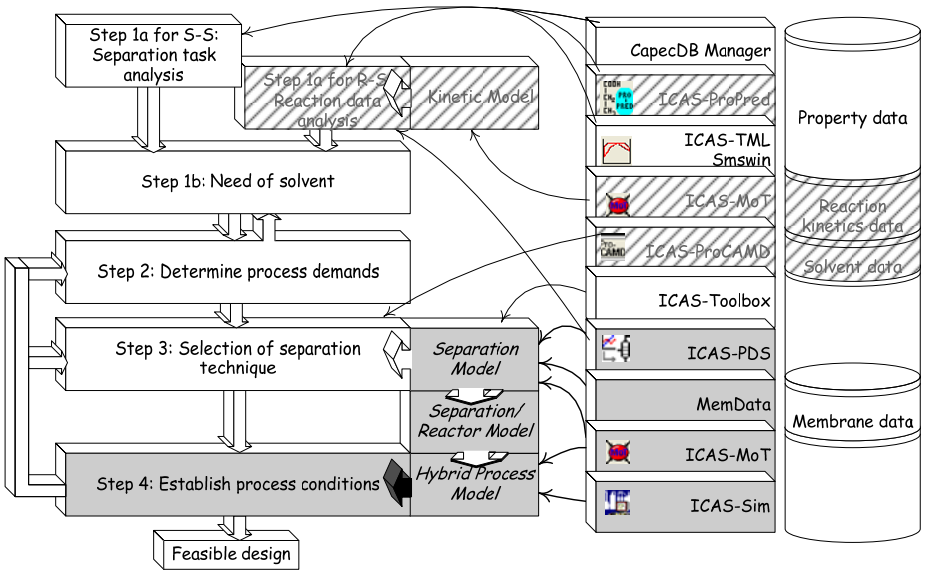

Figure 4.10: Step 4 in the case study of separation of water–acetic acid mixture

The overall component mass balance of the hybrid system DFP is:

$$0 = F_i - F_i^{(1\alpha P)} - F_i^{(2\beta P)} \tag{4.1}$$

The calculations of retentate component flow rate $F_i^{(2\alpha R)}$ is accomplished by defining the membrane separation factor α, pervaporation module cut θ and mass balance equations around the pervaporation module:

$$\alpha = \frac{F_i^{(2\beta P)}\left(1 - F_i^{(1\beta)}\right)}{F_i^{(1\beta)}\left(1 - F_i^{(2\beta P)}\right)} \tag{4.2}$$

$$\theta = \frac{F_i^{(2\beta P)}}{F_i^{(1\beta)}} \tag{4.3}$$

$$0 = F_i^{(1\beta)} - F_i^{(2\beta P)} - F_i^{(2\alpha R)} \tag{4.4}$$

The first configuration (DFP) consists of the distillation whose bottom product contains 99.5 mol% of HAc, top product 80 mol% of H_2O and membrane module whose permeate product contains 99.5 mol% of H_2O (see Figure 4.7).

In the second configuration (DSP) product streams from the distillation column reach required purities, e.g. distillate 99.5 mol% water and bottom product 99.5 mol% acetic acid. Membrane module is used to separate the draw stream from stage of the distillation column at which liquid phase has 80 mol% of water and recycle permeate (90 mol% of water) and retentate to the column (see Figure 4.8.). In this case, derivation of the specific process configuration utilizes possibility of using the hybrid process superstructure to derive each of submodel balance equation. The DSP configuration consists of five submodels describing balance equations around five balance volumes restricted by dashed line on Figure 4.11. The distillation column has been divided into 5 sections, called *Process* 1 – 5. *Process 1* represents the first tray of the distillation column from which distillate is obtained. *Process 3* represents the tray from which liquid stream is withdrawn to *Pervaporation* module. Permeate is fed to *Process 2* and retentate is fed to *Process 4*. *Process 2* and *Process 4* represent the sections of distillation column above and below the tray from which liquid stream is withdrawn to *Pervaporation*. *Process 5* represents the last tray of distillation column from which 99.5 mol% acetic acid is obtained. For each balance volume the superstructure of hybrid process has been used to derive the specific model equations. All submodels are described by equations (4.5-4.9) along with required decision variables. Note that all variables related to the occurrence of reaction ($\xi^R, \xi^{homog}, \xi^{heterog}$) are set to 0.

Process 1: $\xi^1 = 1, \xi^2 = 0, \xi^{1in} = 1, \xi^{2in} = 0, \ \xi^{1\alpha} = 1, \xi^{1\beta} = 1, \xi^{2\alpha} = 0, \xi^{2\beta} = 0, \xi^{\beta} = 1$

$$0 = F_i^{1in}(P1) - F_i^{1\alpha P}(P1) - F_i^{1\beta P}(P1) \tag{4.5}$$

Process 2: $\xi^1 = 1, \xi^2 = 0, \xi^{1in} = 1, \xi^{2in} = 0, \ \xi^{1\alpha} = 1, \xi^{1\beta} = 1, \xi^{2\alpha} = 0, \xi^{2\beta} = 0,$

$$0 = F_i^{1in}(P2) - F_i^{1\alpha P}(P2) - F_i^{1\beta P}(P2) \tag{4.6}$$

Process 3 + Pervaporation: $\xi^{1in} = 1, \xi^{2in} = 0, \ \xi^{1\alpha} = (0,1), \xi^{1\beta} = 1, \xi^{2\alpha} = 1, \xi^{2\beta} = 1, \xi^{\beta} = 1$

$$\begin{aligned} 0 = {} & F_i^{1in}(P3) - x^{1a} F_i^{1aP}(P3) - F_i^{1bP}(P3) \\ & - F_i^{2aP}(P3) - F_i^{2bP}(P3) \end{aligned} \tag{4.7}$$

Process 4: $\xi^{1}=1,\xi^{2}=0,\xi^{1in}=1,\xi^{2in}=0,\ \xi^{1\alpha}=1,\xi^{1\beta}=1,\xi^{2\alpha}=0,\xi^{2\beta}=0,\ \xi^{\beta}=1$

$$0=F_i^{1in}\left(P4\right)-F_i^{1aP}\left(P4\right)-F_i^{1bP}\left(P4\right) \tag{4.8}$$

Process 5: $\xi^{1}=1,\xi^{2}=0,\xi^{1in}=1,\xi^{2in}=0,\ \xi^{1\alpha}=1,\xi^{1\beta}=1,\xi^{2\alpha}=0,\xi^{2\beta}=0,\ \xi^{\beta}=1$

$$0=F_i^{1in}\left(P5\right)-F_i^{1aP}\left(P5\right)-F_i^{1bP}\left(P5\right) \tag{4.9}$$

P1, *P2*, *P3*, *P4* and *P5* stands for variables associated with *Process 1*, *Process 2*, *Process 3*, *Process 4* and *Process 5*. All submodels are related to each other by equations (4.10-4.15). Variables $\xi^{in}\left(P2\right)$, $\xi^{in}\left(F\right)$ and $\xi^{in}\left(P3\right)$ (binary variables $\left\{0,1\right\}$) represent where the fresh feed is directed.

$$0=F_i^{1in}\left(P1\right)-F_i^{1\beta P}\left(P2\right) \tag{4.10}$$

$$0=F_i^{1in}\left(P2\right)-F_i^{2\beta P}\left(P3\right)-F_i^{1\beta P}\left(P3\right)-\xi^{in}\left(P2\right)F_i^{1in} \tag{4.11}$$

$$0=F_i^{1in}\left(P3\right)-F_i^{1aR}\left(P2\right)-F_i^{1bP}\left(P4\right)-x^{in}\left(P3\right)F_i^{1in} \tag{4.12}$$

$$0=F_i^{1in}\left(P4\right)-x^{1a}F_i^{1aP}\left(P3\right)-F_i^{2aP}\left(P3\right)-F_i^{1bP}\left(P5\right)-x^{in}\left(P4\right)F_i^{1in} \tag{4.13}$$

$$0=F_i^{1in}\left(P5\right)-F_i^{1aP}\left(P4\right) \tag{4.14}$$

$$\xi^{in}\left(P2\right)+\xi^{in}\left(P3\right)+\xi^{in}\left(P4\right)=1 \tag{4.15}$$

Simplifying equations (4.5-4.15) lead to overall mass balance for DSP configurations:

$$0=F_i^{in}-F_i^{1\alpha P}\left(P1\right)-F_i^{2\beta P}\left(P5\right) \tag{4.16}$$

Note that the membrane separation factor α and membrane module cut θ for DSP configuration are represented by Eqs. 4.17-4.18.

$$\alpha=\frac{F_i^{(2\beta P)}\left(1-F_i^{(1\alpha R)}\left(P3\right)\right)}{F_i^{(1\alpha R)}\left(P3\right)\left(1-F_i^{(2\beta P)}\right)} \tag{4.17}$$

$$\theta=\frac{F_i^{(2\beta P)}}{F_i^{(1\alpha R)}\left(P3\right)} \tag{4.18}$$

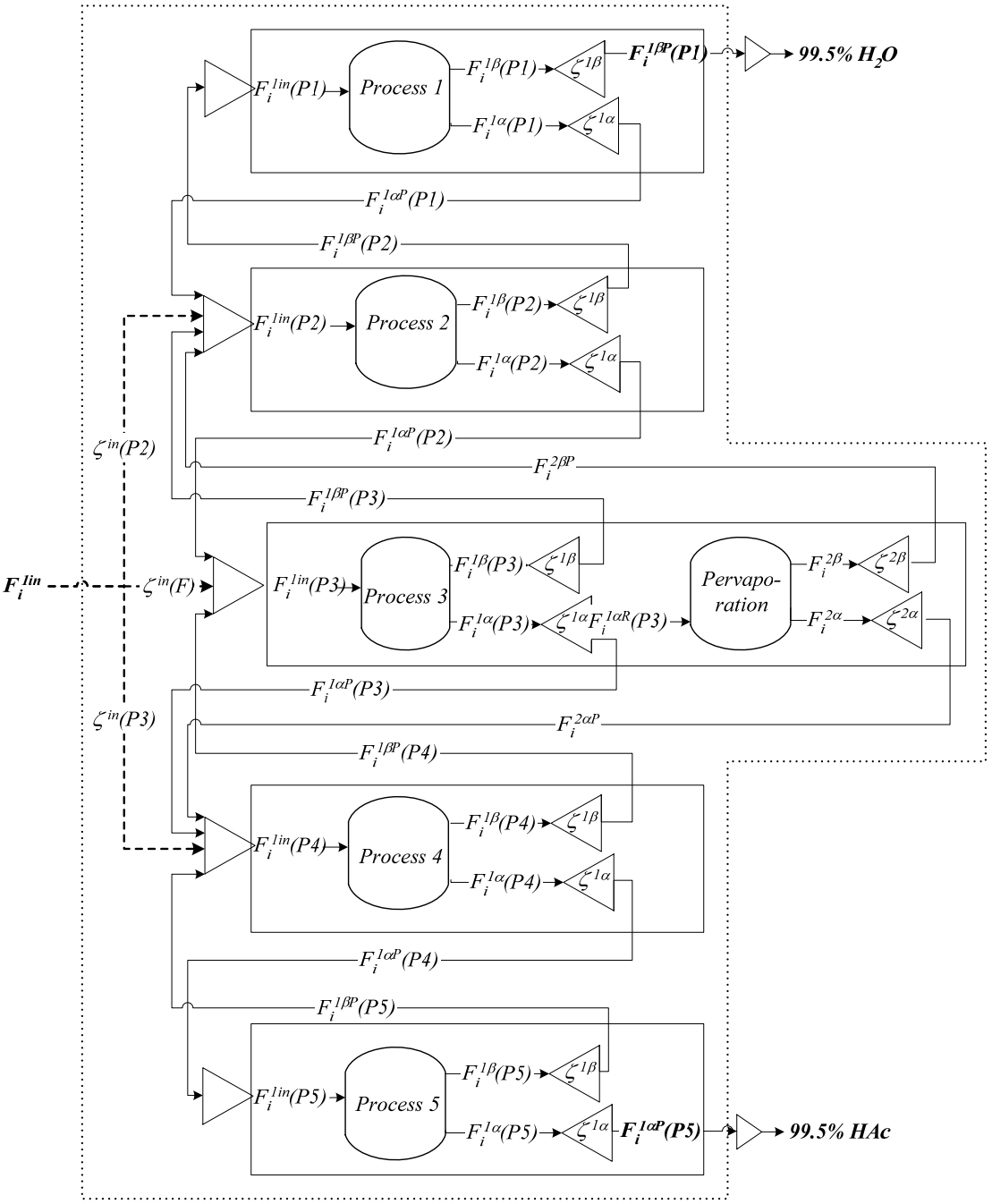

Figure 4.11: From hybrid process superstructure to specific process configuration: distillation side pervaporation (DSP)

Both specific hybrid separation systems generated above have been implemented and simulated in ICAS-Sim where the distillation columns have been designed through the driving force approach in ICAS-PDS. The model for a simple pervaporation model (short-cut model) has been developed in ICAS-MoT and successfully used in

simulations.

Distillation column in the first configuration is designed to obtain a bottom product with 99.5 mol% of acetic acid and distillate reaches 80 mol% of water. Permeate in the membrane process achieved the desired concentration of water. In the second configuration, the distillation column was designed to achieve the desired concentrations by itself. Afterwards the pervaporation module was added. In this case, the feed to the pervaporation is withdrawn from the distillation column from the tray on which liquid phase contains 80 mol% of water. Permeate contains 90 mol% of water. Permeate and retentate are recycled to the trays with similar compositions.

Various characteristics of the membrane unit (e.g. module cut and selectivity) have been tested for the two design alternatives. It is important to realize that since the feed stream to the membrane module and permeate are fixed, the selectivity of the membrane module is also fixed.

The design alternatives are compared with a base case design (the single distillation column) in terms of the heat duty of distillation. The membrane process is assumed isothermal. For each column the heat duty was optimized to give the minimum value. Results are presented in Figure 4.12 and Figure 4.13, the design details are given in Table 4.5 and Table 4.6. In general the first configuration gives the better performance but the drawback is the requirement of highly selective membrane module ($\alpha = 50$). However, even for the low selective membrane modules ($\alpha = 2.25$) the second design alternatives will give improvement in comparison to the base case. It is important to observe that in the investigated separation task there is a rather small influence of the cut values (θ). The feasible membrane which fulfils the requirement of high selectivity is doped polyaniline membrane (Huang, 1998). Note that in these calculations the heat requirement of the membrane unit has not been included but these calculations give an estimate of heat consumption at which the membrane-based separation would be preferable to the distillation.

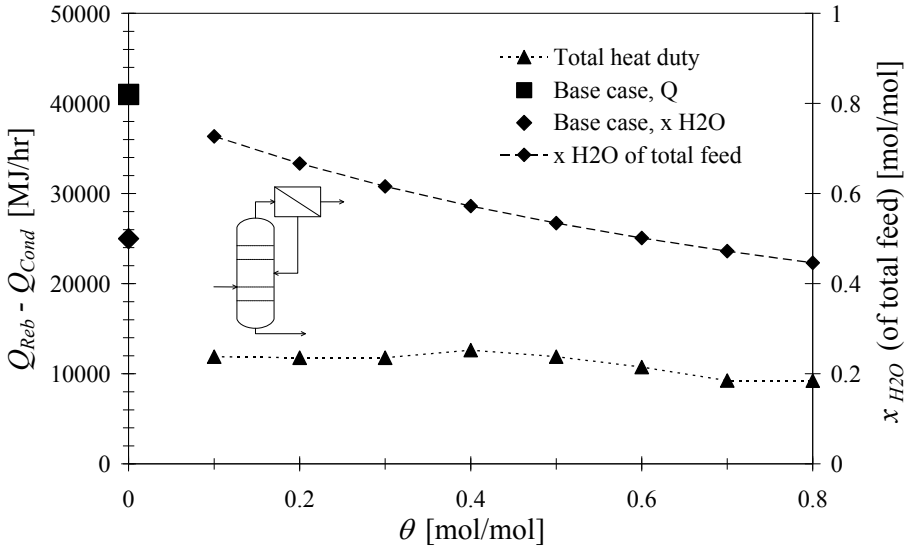

Figure 4.12: Minimized heat duties for DFP configuration

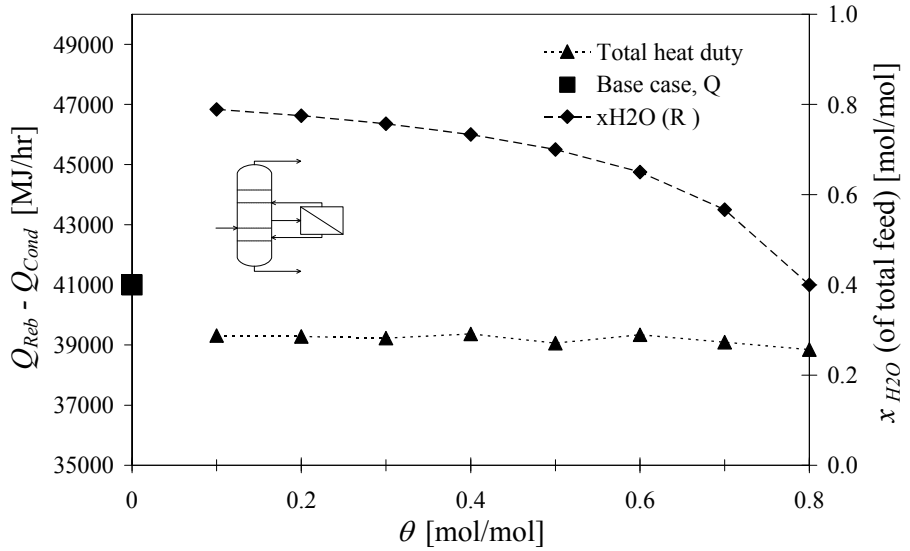

Figure 4.13: Minimized heat duties for the DSP configuration

Table 4.5. Process parameters and heat requirements for DFP configuration

	Base case	DFP1	DFP2	DFP3	DFP4	DFP5	DFP6	DFP7	DFP8
No of stages	51	20	20	20	20	20	20	20	20
Q [MJ/h]	40998	11899	11781	11778	12620	11900	10739	9246	9227
θ	0	0.1	0.2	0.3	0.4	0.5	0.6	0.7	0.8
α	50	50	50	50	50	50	50	50	50
x_{H2O} Retentate	-	0.777	0.750	0.715	0.669	0.603	0.505	0.342	0.016

Table 4.6. Process parameters and heat duties for DSP configuration

	Base case	DSP1	DSP2	DSP3	DSP4	DSP5	DSP6	DSP7	DSP8
No of stages	51	51	51	51	51	51	51	51	51
Q [MJ/h]	40998	39315	39285	39227	39369	39062	39340	39091	38849
θ	0	0.1	0.2	0.3	0.4	0.5	0.6	0.7	0.8
α	2.25	2.25	2.25	2.25	2.25	2.25	2.25	2.25	2.25
x_{H2O} Retentate	-	0.789	0.775	0.757	0.733	0.700	0.650	0.567	0.400
x_{H2O} Permeate	-	0.9	0.9	0.9	0.9	0.9	0.9	0.9	0.9
FM*	-	17	17	16	16	16	16	16	16

*FM-number of the stage from which liquid is drawn out and feed to the membrane.

4.3. Reaction-Separation systems

4.3.1. Synthesis of cetyl-oleate

This case study deals with an enzymatic esterification of cetyl-oleate ester. This ester is a sperm whale oil analogue and it has important applications in the cosmetics, lubricants, food and pharmaceutical industries (Garcia et al., 2000; Salis et al., 2003).

4.3.1.1. Step 1a: Reaction data analysis

1a.1 Identify mixture type

Cetyl-oleate is synthesized in the esterification reaction from cetyl alcohol (1-hexadecanol) and oleic acid where water is a by-product. Reactive mixture is of

aqueous type since water is a by-product of that reaction. To model vapour-liquid equilibrium, the Modified UNIFAC Lyngby has been used for the calculation of the activity coefficients in the liquid phase and the SRK equation of state has been used to calculate the vapour phase fugacity coefficients of the compounds present in this quaternary mixture.

1a.2 Analysis based on pure component properties

All compounds are liquid between melting temperature of cetyl oleate and boiling temperature of water (e.g. 322.35 K and 373.15 K). Values of solubility parameters indicate that compounds might not be miscible with each other. Boiling and melting temperature and solubility parameter for all compounds present in the mixture are given in Table 4.7. It is important to point out that properties of cetyl oleate have been obtained using Marrero-Gani group contribution method in ICAS-ProPred. Other tools used at the step 1a are depicted on Figure 4.14.

Table 4.7: Pure component properties of cetyl alcohol, oleic acid, cetyl oleate and water

Compound	T_m [K]	T_b [K]	*Sol. Par* [MPa$^{0.5}$]
Cetyl alcohol (Al)	322.35	597.23	18.8752
Oleic acid (Ac)	286.53	633.00	18.3985
Cetyl oleate (Es)	310.15 (Place & Roby, 1986)	726.17	18.7216
Water (W)	273.15	373.15	47.8127

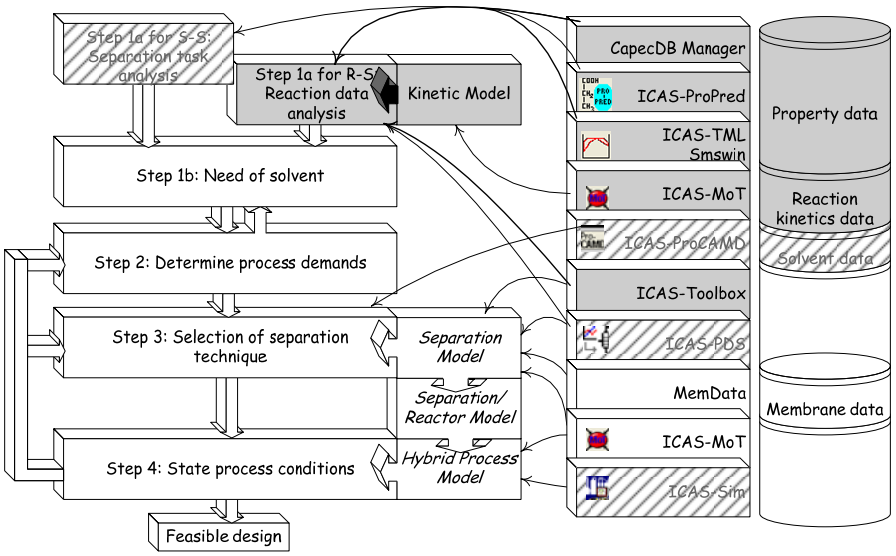

Figure 4.14: Workflow and used tools at the step 1a in the case study of synthesis of cetyl-oleate

1a.3. System analysis based on mixture properties

The total number of binary pairs to analyse in terms of the phase behaviour in this quaternary mixture is 6 and number of ternary mixture is 4. All these binary pairs and ternary mixtures have been analyzed through the utility toolbox in ICAS and through SMSWin. One homogenous azeotrope has been found between cetyl alcohol and oleic acid and one heterogeneous azeotrope between oleic acid and water. However experimental data reflecting phase equilibria between any binary or ternary pairs of compounds present in this mixture have not been found in the open literature.

Table 4.8. List of azeotropes present in analysed mixture

Composition	Type of azeotrope	x [mol/mol]				T [K]
		Water	Cetyl alcohol	Oleic acid	Cetyl oleate	
Cetyl alcohol – oleic acid	Homogeneous	-	0.2867	0.7133	-	366.71 @ 101.32 kPa
Oleic acid-water	Heterogeneous	0.9829	-	0.0171	-	371.95 @ 101.32 kPa
Oleic acid-water	Heterogeneous	0.9868	-	0.0132	-	352.15 @ 47 kPa
Cetyl alcohol – oleic acid	Homogeneous	-	0.1744	0.8256	-	332.59 @ 47 kPa

1a.4. Reaction analysis

The esterification of cetyl alcohol with oleic acid is carried out over Novozym 435 (commercially available *Canadia anatarctica* immobilized lipase on acrylic resin) in the liquid phase. The reaction kinetic model published by Garcia et al. (2000) considers competitive inhibition between reactants and products. The overall reaction can be represented as follows:

$$C_{16}H_{33}OH + C_{17}H_{33}COOH \xrightleftharpoons{Novozym\,435} C_{34}H_{66}O_2 + H_2O \qquad (4.19)$$

Operational window for this reaction with respect to temperature is between 322.3 K (melting point of 1-hexadecanol) and 353 K (temperature of denaturation of lipase). In subsequent simulations, the reaction temperature is set to 348.15 K since in engineering practise reaction would be operated few degrees below temperature of denaturation of lipase. Reaction is limited by the stability of the enzyme, which depends on the activity of water in the mixture. Adlercreutz et al., (2003) found that Novozym 435 lose its activity below water activity of 0.11. Reaction rate expression, presented along with batch reaction model in details in Appendix 4, section 6.4.1.1 (page 193), depends on the amount of the enzyme in the mixture. How fast the reaction is reaching conversion in a batch reactor operation depends on temperature at which reaction is progressing and amount of enzyme added to the mixture. To assets influence of the addition of catalyst on the batch reaction several simulations of batch reactor have been performed and results are depicted in Figure 4.15. In all batch reaction simulations the equimolar mixture of reactants (oleic acid and cetyl alcohol) has been used. In this case, significant decrease of a batch reaction time is observed for increasing weight percentage of enzyme from 5 w% to 25 w%. Increase above 25 w% of the added enzyme reduces the batch reaction time only by couple of minutes to reach the same conversion (see Figure 4.15).

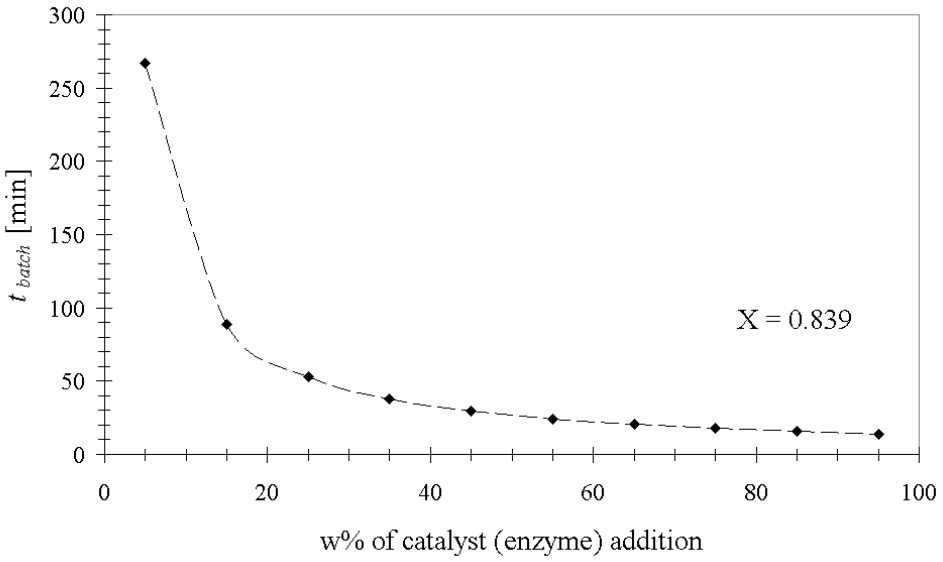

Figure 4.15: Influence of amount of the added catalyst (enzyme) on the batch reaction time to reach molar conversion of 0.839. Initial reactants molar ratio 1:1, T = 348.15 K, P = 1 atm.

4.3.1.2. Step 1b: Need of solvent

Since reported kinetic data were obtained in a solvent free system with reasonable conversion (at atmospheric pressure conversion is 0.84 according Garcia et. al., 2000), it is assumed that a solvent is not required.

4.3.1.3. Step 2: Determine process demands

The objective is to increase the productivity of the batch process within the operation time of 5 h. Commercially available cetyl oleate is of 98 w% purity and traces of oleic acid and cetyl alcohol are acceptable, therefore process design which would obtain such final product is looked for.

4.3.1.4. Step 3: Selection of separation techniques

Since the reaction is kinetically controlled the addition of the reactant in excess will increase the conversion of the limiting reactant, whereas, removal of the product(s) will push the reaction rate towards the product(s) and simultaneously increases the overall conversion. At this step various computer-aided tools are used which are presented along with the whole methodology used in the stage 1 in Figure 4.16.

R3.1. Identify compound(s) to remove from reaction medium

The most distinctive compound in the investigated quaternary mixture in terms of solubility and a boiling temperature is water (see Table 4.7). All other compounds are

organic with almost the same solubility parameter. Therefore water is selected as the compound which is the most favourable to remove.

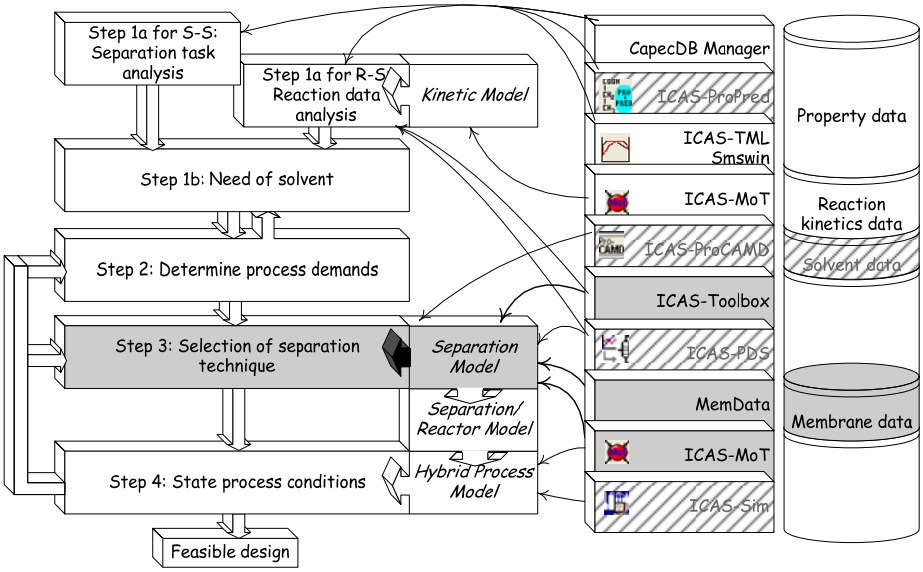

Figure 4.16: Step 3 in the case study of synthesis of cetyl-oleate

R3.2. Feasibility of distillation

Since this reaction system is limited with respect to the denaturation temperature of Novozym 435, distillation under reduced pressure (e.g. below atmospheric pressure) is considered. The bubble point pressure of the compound (water) with the lowest boiling temperature at operating reaction temperature of 348.15 K is 38.56 kPa. The relative volatilities of compounds present in the feed mixture are given in Table 4.9. The composition of the feed to the flash calculation is equivalent to the composition of post reaction mixture with the initial molar ratio of reactants 1:1 (cetyl alcohol and oleic acid). It is clear that by carrying out the reaction under reduced pressure, only water will be removed as vapour from the reactive system.

R3.3. Feasibility of membrane-based separation

Pervaporation (PV) is selected as the membrane-based separation technique because of the possibility of introducing hydrophilic membranes that would allow only water to permeate. Several authors (Mulder, (2003); Sanz & Gmehling, (2006); Zhou (2005); Buchaly et al., (2007)) had reported PV membranes to dehydrate organic mixtures with selectivity close to 1, even for very small water concentrations. Koszorz et al. (2004) used PV to enhance enzymatic esterification reaction between oleic-acid and i-amyl alcohol.

R3.4. Solvent selection

Due to reasoning presented in step 1b (see section 4.3.1.2 on page 103) addition of a solvent is not considered.

R3.5. Separation technique selection

Two separation techniques, pervaporation and distillation, are compared using the driving force approach for binary mixture of the most volatile compounds, namely cetyl alcohol and water. As can be observed through Figure 4.17 distillation and pervaporation have almost the same driving force (*FD*) in the whole separation region. However, pervaporation has *FD* bigger than distillation; therefore, the pervaporation is selected for further investigation. Pervaporation data used for calculating *FD* has been used after the component flux model given by Koszorz et al., (2004).

Table 4.9. Relative volatility of components in the post reaction mixture computed at 38.56 kPa and 348.15 K.

Compound		$\alpha_{i,water}$
Water (T_b = 373.15 K)		1
Cetyl alcohol (T_b = 597.23 K)		$8 \cdot 10^7$
Oleic acid (T_b = 633 K)		0
Cetyl oleate (T_b =726.17 K)		0
Feed composition to the flash calculation	Water [mol/mol]	0.42
	Cetyl oleate [mol/mol]	0.42
	Oleic acid [mol/mol]	0.08
	Cetyl alcohol [mol/mol]	0.08

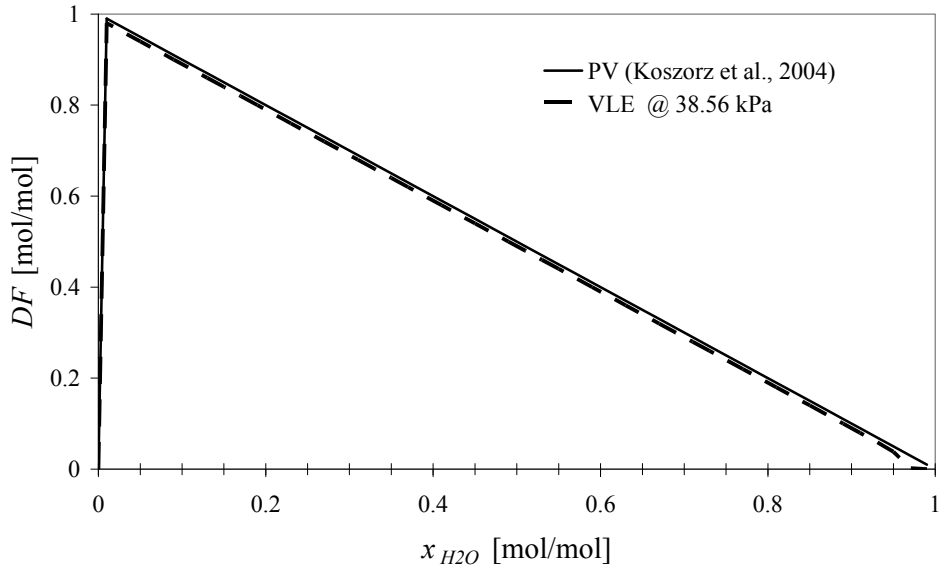

Figure 4.17: Driving force diagram for binary mixtures of water and cetyl alcohol

4.3.1.5. Step 4: Establish process conditions

Two operational alternatives are compared in this section: batch reaction operation and semi-batch hybrid reaction separation operation (membrane assisted batch reaction) since batch production is considered. In semi-batch hybrid operation reactor and PV can be combined together in one unit since feed to PV unit does not need to be preheated (T_R = 348.15K). Both set-ups are investigated under assumptions that:

(1) reactor is well mixed,

(2) activity of enzyme does not change during operation, and

(3) water activity in the mixture can not be lower than a_{H2O} = 0.11.

From the superstructure of hybrid process (Figure 3.5, page 57) the specific hybrid process scheme is generated where the *Process 1* is reactor where the enzymatic esterification of cetyl oleate takes place and *Process 2* is pervaporation where mixture is dehydrated (see Figure 4.18). Defining the decision variables as follow $\xi^1 = 1$, $\xi^2 = 1$, $\xi^{1in} = 0$, $\xi^{2in} = 0$, $\xi^R = 1$, $\xi^\beta = 0$, $\xi^{homog} = 0$, $\xi^{heterog} = 1$, $\xi^{1\alpha} = 0$, $\xi^{1\beta} = 0$, $\xi^{2\alpha} = 1$, $\xi^{2\beta} = 0$ lead to the specific model described by Eq. 4.20. With respect to membrane-based separation, the water flux depends on the molar fraction of water in the mixture (Eq. 4.21) (Koszorz et al., 2004) and fluxes for all other components present in the system are neglected.

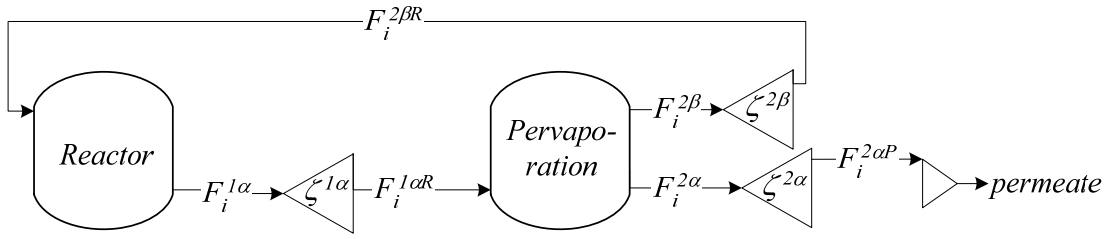

Figure 4.18: From superstructure to the specific hybrid process scheme (membrane assisted batch reaction)

The component mass balance for the hybrid process scheme shown on Figure 4.18 is described by Eq. (4.20).

$$\frac{dn_i}{dt} = a \cdot b \cdot \left(-J_i A_m\right) + \nu_i r^{1\alpha(heterog)} \tag{4.20}$$

$$J_w = P_w x_w \tag{4.21}$$

Where *a* and *b* reflect either the hybrid operation is carried on or not, more precisely *a* stands for the decision variable related to the switching time (see Eq. 3.29) and *b* related to the condition that the activity of water in the reacting mixture can not dropped below 0.11; J_w stand for flux of water through the membrane, P_w is proportional factor. Reaction rate $r^{1\alpha(heterog)}$ is described by the reversible Michaelis-Menten kinetics type. Detailed model derivation and analysis are provided in Appendix 6.4.1 (page 193). All the scenarios of membrane assisted batch reaction are compared in terms of conversion which is defined as ratio of moles of desired product (cetyl-oleate) to initial amount of reactant, ($X = N_{Eters}/N^0_{Acid}$). The hybrid process model consists of 4 ordinary differential equations, 51 algebraic equations with 122 variables, plus the equations for the constitutive model (Modified UNIFAC (Lyngby)). The model is solved and analyzed through ICAS-MoT. Other tools used at this step are highlighted on Figure 4.19.

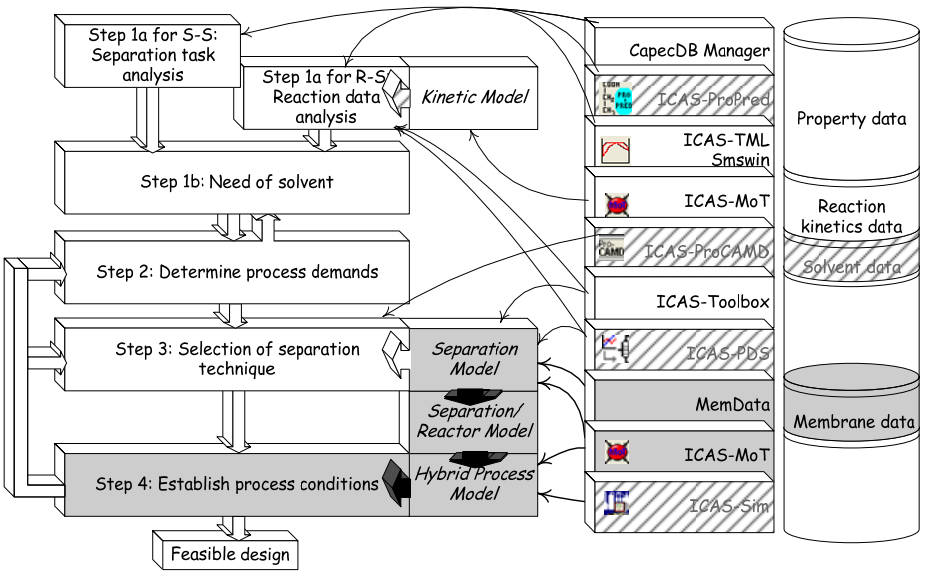

Figure 4.19: Step 4 in the case study of synthesis of cetyl-oleate

With the generated specific hybrid process model, five scenarios of membrane assisted batch reaction (with five different membrane areas) have been investigated in terms of process yield and superiority of the hybrid process over batch reaction. All simulations have been performed with the same initial conditions with respect to reactor: C_{Al}=1.58 mol/dm^3, C_{Ac}=1.58 mol/dm^3, C_{Es}= 0 mol/dm^3, C_W= 0.005 mol/dm^3 and V= 6 dm^3. Performance of the hybrid system is strongly dependent on the membrane area (A_m) and component fluxes (J_i). The conversion-time behaviour is shown on Figure 4.20 while design variables and conversion at t_{end} are given in Table 4.10.

Table 4.10 Process parameters and process conversions. 5 w% of Novozym 435.

	Batch	RCPV1	RCPV2	RCPV3	RCPV4	RCPV4	RCPV5
A_m [m^2]	-	0.0036	0.0144	0.0288	0.0432	0.0144	0.0576
t_{end} [min]	300	300	300	300	300	900	300
X [mol/mol]	0.841	0.872	0.917	0.927	0.929	0.967	0.930

For membrane assisted batch reaction operations carried out for 5 h, conversion is improved from 0.84 (batch) to 0.927 (RCPV3) by removing water from the system using a reasonable design for a PV-unit (A_m = 0.0288 m^2). However, in 15 h operation with RCPV4 it is possible to achieve conversion close to the limiting value. The limiting value of conversion is 0.988 and is represented by dashed line on Figure 4.20. What is important to observe is that the increase of A_m from 0.0288 m^2 to 0.0576 m^2 does not give significant improvement, both cases RCPV4 and RCPV5 reach conversion of 0.93 in t_{end} of 300 min.

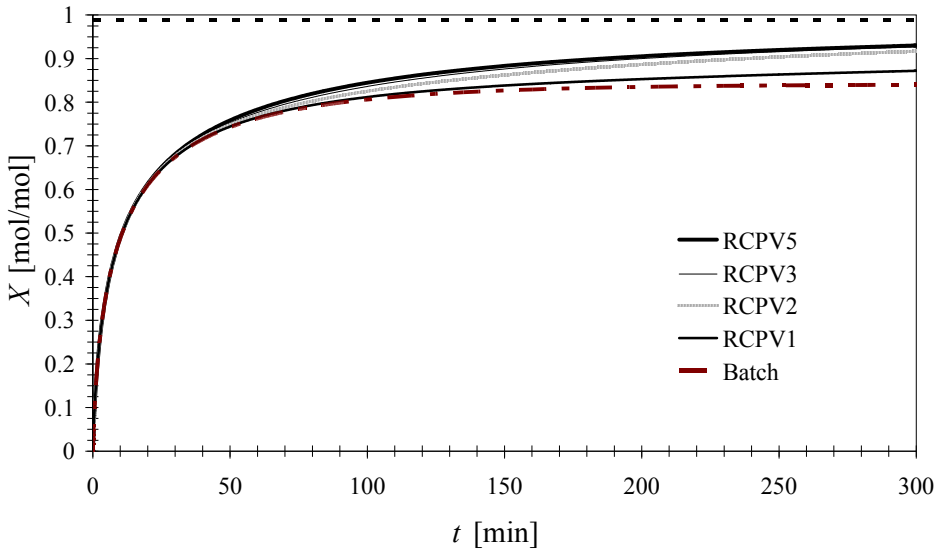

Figure 4.20: Comparison of hybrid process operations with batch reaction in terms of conversion

Another important issue in hybrid process operation, especially in the batch operation involving reaction and separation, is switching time (t_{switch}) from batch reaction to the hybrid reaction-separation operation. This process variable is used in the reaction-separation system in which compound which has to be removed is not present from the beginning of the operation. Another reason to use switching time is that when a separation technique can not tolerate high concentration of reactants such as acid. For example many polymeric membranes change their separation characteristics dramatically after contact with concentrated acids (Kreis, 2007). The influence of switching time on the enzymatic esterification (process scenario RCPV3) is presented in Figure 4.21. Switching from batch reaction operation to hybrid operation after two hours gives only a 1% decrease of conversion.

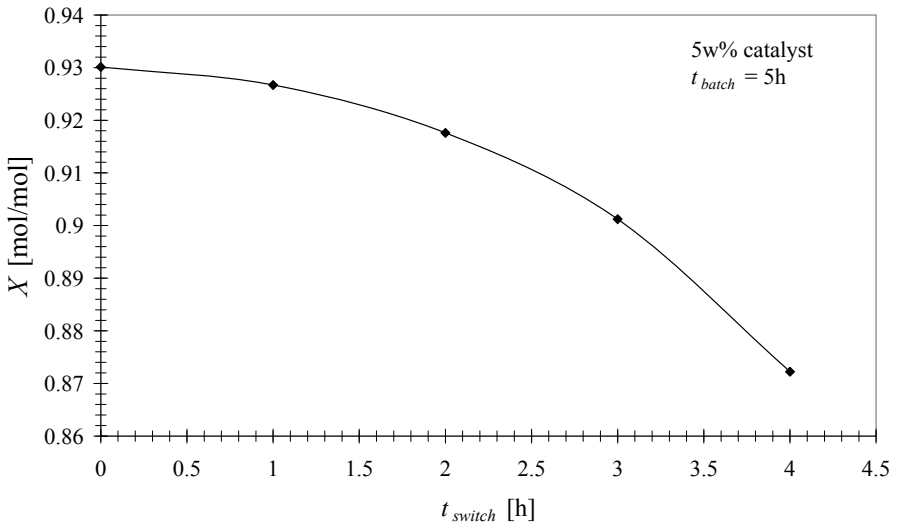

Figure 4.21: Influence of switching time from batch reaction operation to the hybrid operation on the conversion (X)

With initial conditions and with hybrid operation studied it is possible to achieve high purity ester (98 w%) as it is available commercially. This purity corresponds to the yield of $X = 0.983$. In Figure 4.22 different loading of catalyst is plotted versus operation time needed to achieve various yields. The batch time for operation RCPV5 to reach $X = 0.983$ is 33.5 h (not presented in the Figure 4.22). Increasing loading of enzyme to 25 w% reduces process time significantly to 5.5 h. Therefore for further studies the configuration RCPV5 with a loading of 35 w% of Novozym 435 is recommended. A feasible membrane that would meet this design is a commercially available polyvinyl alcohol membrane (PERVAP 1005, GFT).

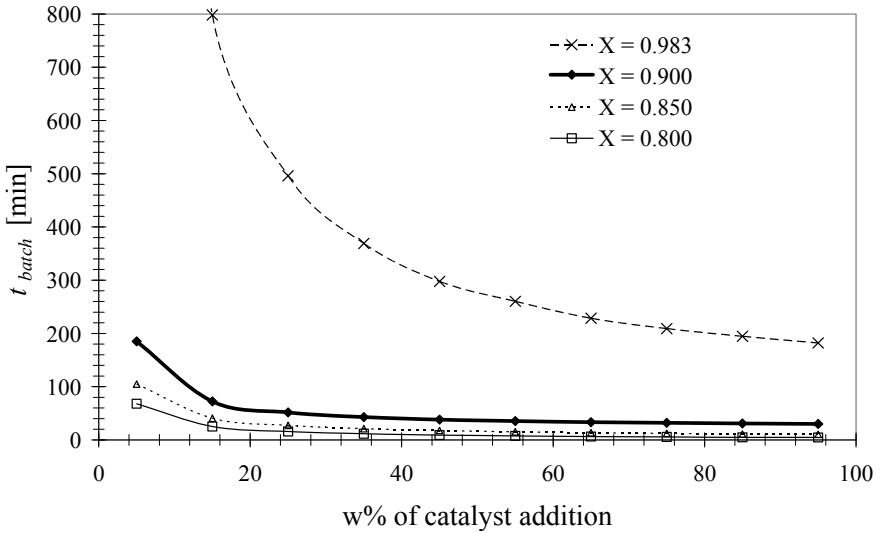

Figure 4.22:Influence of catalyst loading on process time of hybrid operation (RCPV5)

4.3.2. Enzymatic interesterification of phosphatidylcholine

Application of the framework is illustrated in this section through an enzymatic interesterification reaction. Interesterified fats are oils that have been chemically modified, for example turning soybean oil into interesterified soybean oil. Phospholipids have wide application in food, pharmaceutical and cosmetic products where they function as emulsifiers, stabilizers and antioxidants (Vikbjerg et al., 2005). The interest in production of structured phospholipids containing special fatty acids in one or both positions of glycerol chain has increased continuously. Replacement of existing fatty acid in original phospholipid with desired acids might improve physical, chemical or even nutritional and medical properties and functions. This case study was inspired by Ph.D. - student Anders Vikbjerg from BioCentrum-DTU. The objective was to understand how to carry out an enzymatic interesterification of phosphatidylcholine.

Interesterified fats can be obtained in two ways. One way is to get the required phosphatidylcholine from lysophosphatidylcholine with the use of enzyme phospholiphase A_2. This reaction is occurring with excess of fatty acid which is required in *sn*-2 position of phosphatidylcholine. The second way is to carry out the reaction between phosphatidylcholine with excess of a free fatty acid which is substituted in *sn*-2 position (with the same enzyme) to obtain required phosphatidylcholine. In this case study the second way is investigated.

Usually soybean phosphatidylcholine is used as an original substrate (reactant) in lipase-catalysed acyl exchange. The soybean phosphatidylcholine consists of several fatty acids substituted in *sn*-1 and *sn*-2 positions. Vikbjerg et al. (2005) reported distribution of six fatty acids in soybean phosphatidylcholine. It consists of C8:0, C16:0, C18:0, C18:1, C18:2 and C18:3 acids chains.

4.3.2.1. Step 1a: Reaction data analysis

Data used in this case study has been mainly obtained from Egger et al. (1997). It is assumed than phosphatidylcholine had in *sn*-1 and *sn*-2 positions palmitic acid (C16:0). Oleic acid was substituted in *sn*-2 position by phospholiphase A_2 (PA2). All the kinetic data has been obtained in water activity controlled environment (e.g. salt container) and in the toluene as solvent. The tools and type of data required at this step are depicted on Figure 4.23.

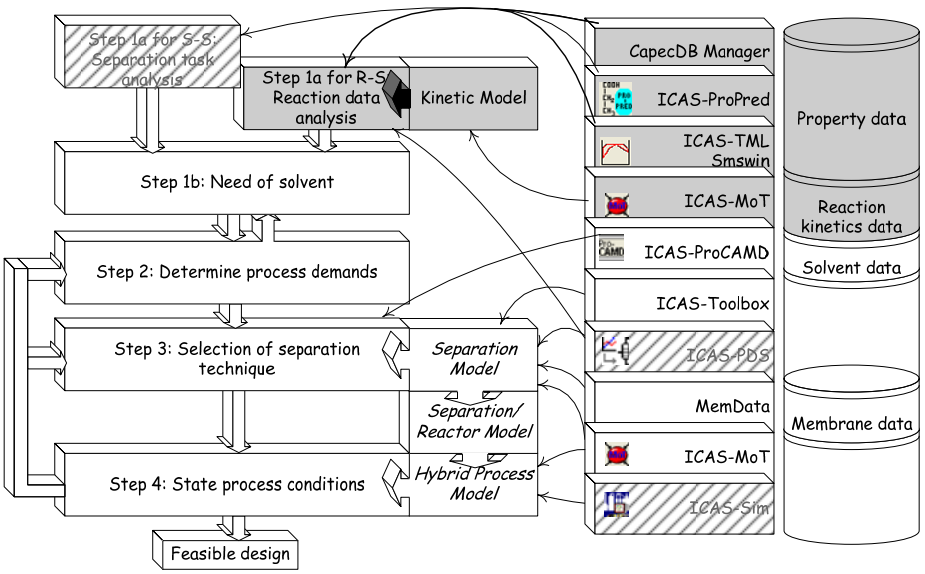

Figure 4.23: Workflow at step 1 in the case study of enzymatic interesterification of phosphatidylcholine

1a.1. Identify mixture type

The reacting mixture consists of 1,2-dihexadecanoyl-glycero-3-phosphocholine, water, 1-hexadecanoyl-glycero-3-phosphocholine, palmitic acid, oleic acid, 1-hexadeca-2-octadeca-9,12-dienoyl-glycero-2-phosphocholine and toluene. This mixture contains mainly organic compound and very small amount of water. For calculation of activity coefficient in liquid phase Modified UNIFAC (Lyngby) model is selected.

1a.2. Analysis based on pure component properties

The availability of pure component properties for the mixture to be analysed is very limited, especially with respect to phosphatidylcholine. Properties for water, oleic acid and toluene have been retrieved from the CAPEC database (Table 4.11). Properties for the rest of the compounds have been obtained from ACD/Chemsketch Freeware, software from Advanced Chemistry Development Inc. and are reported in Table 4.12. It is important to point out that in the concentration range of oleic acid from 400 to 800 mmol/dm^3, phosphatidylcholine and lysophosphatidylcholine from 5 to 30 mmol/dm^3 and water from 18 to 111 mmol/dm^3 all compounds dissolved in toluene at room temperature (25°C) (Egger et al., 1997). All forms of phosphatidylcholine have molecular (M_w) weight between 500 and 700 g/mol while M_w of palmitic acid and oleic acid is around 285 g/mol.

Table 4.11: Compound properties obtained from CAPEC database

Component	Molecular formula	M_w [g/mol]	T_m [K]	T_b [K]	*Sol. Par* [$MPa^{0.5}$]
Water (2)	H_2O	18.01	273.15	373.15	47.8127
Oleic acid (5)	$C_{18}H_{34}O_2$	282.46	286.53	633	18.3985
Toluene (0)	C_7H_8	92.14	178.18	383.78	18.3242

Table 4.12: Properties of compounds absent in CAPEC database

Component	Molecular formula	M_w [g/mol]	ρ [g/cm^3]	T_m [K]	T_b [K]
1,2-dihexadecanoyl-glycero-3-phosphocholine (1)	$C_{40}H_{80}NO_8P$	734.03	0.994	NA	NA
1-hexadecanoyl-glycero-3-phosphocholine (3)	$C_{24}H_{50}NO_7P$	495.63	1.058	NA	NA
Palmitic acid (4)	$C_{16}H_{32}O_2$	256.43	0.892	336.25[1]	612.15[1]
1-hexadeca-2-octadeca-9,12-dienoyl-glycero-2-phosphocholine (6)	$C_{42}H_{82}NO_8P$	760.07	0.993	NA	NA

[1]obtained from http://webbook.nist.gov

1a.3. System analysis based on mixture properties

Considering the mixture which Egger et al. (1999) have investigated, it can be assumed that the mixture contains mainly toluene, oleic acid and water with traces of other heavy compounds. In ternary mixture of toluene, oleic acid and water two heterogeneous azeotropes are predicted between toluene and water, and oleic acid and water.

Table 4.13. List of azeotropes present in the analysed mixture (Mod. UNIFAC (Lyngby) and SRK equation of state)

Composition	Type of azeotrope	Molar fraction			T [K] @ 101.32 kPa
		Water	Oleic acid	Toluene	
Toluene-water	Heterogeneous	0.5766	-	0.4234	346.75
Oleic acid-water	Heterogeneous	0.9829	0.0171	-	371.95

1a.4. Reaction analysis

At first hydrolysis of original (not modified) phosphatidylcholine (1,2-dihexadecanoyl-glycero-3-phosphocholine) to lysophosphatidylcholine (1-hexadecanoyl-glycero-3-phosphocholine) occurs according Eq. 4.22.

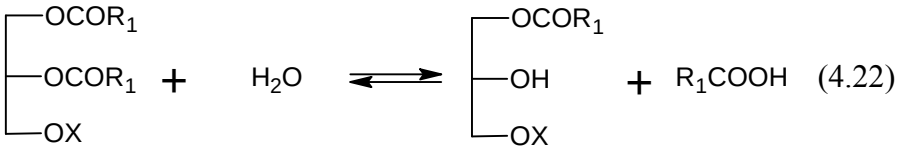

(4.22)

The second reaction is an esterification, synthesis reaction, (Eq. 4.23) of lysophosphatidylcholine to modified phosphatidylcholine (1-hexadeca-2-octadeca-9,12-dienoyl-glycero-2-phosphocholine) with fatty acid substituted in *sn*-2 position.

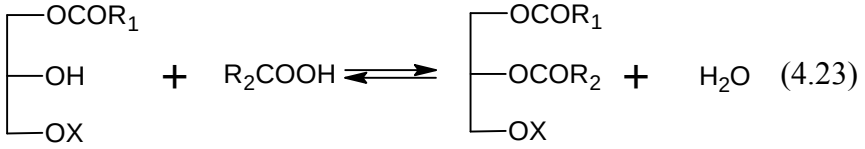

(4.23)

Two above reactions can be summarized into one acidolysis reaction (Eq. 4.24).

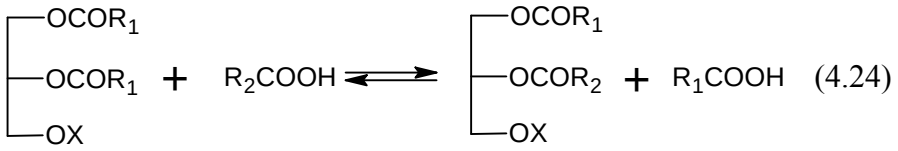

(4.24)

The group R_1 stands for acid radical of palmitic acid ($R_1 = C_{15}H_{31}$) and the group R_2 stands for acid radical of oleic acid ($R_2 = C_{17}H_{31}$), (see Figure 4.24). The group X stands for phospholipid group which is presented on Figure 4.25. The selective substitution in *sn*-2 position is possible when using phospholipase A_2 (PLA 2). It is important to point out that Mingarro et al. (1994) pointed decrease of activity of porcine pancreatic phospholipase (ppPLA2) above 333.15 K.

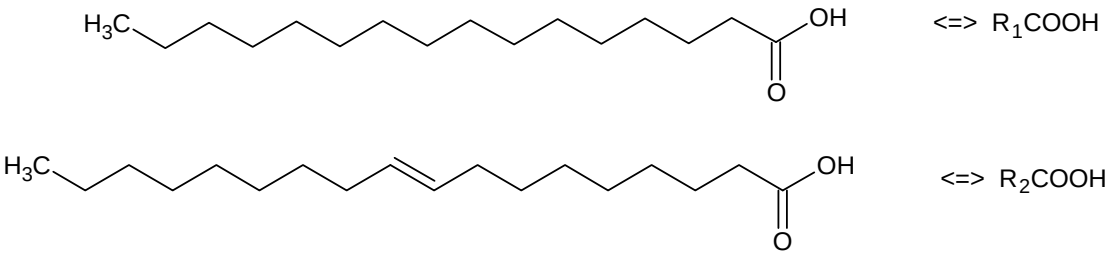

Figure 4.24: Structure of palmitic acid (R_1COOH) and oleic acid (R_2COOH)

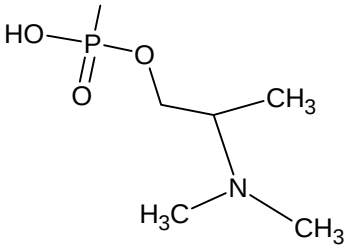

Figure 4.25: Polar phospholipid group (X)

Although, these reactions have been studied at temperatures equal to or higher than 323.15 K, all data used in this work has been obtained at ambient conditions. Egger et al., (1997) reported yields in various water activity conditions and substrate concentrations, which has been correlated and verified with the kinetic model. Comparison between experimental data and simulated are given in Appendix 6.4.2.1 (page 204) along with all model equations and model analysis of the batch reaction model.

4.3.2.2. Step 1b: Need of solvent

Reactions required solvent to reduce viscosity of reaction medium and to keep low water content but still sufficient amount required for enzyme stability (Egger et al., 1997; Adlercreutz et al., 2003). Additionally, solvent need to be inert to all reactants.

4.3.2.3. Step 2: Determine process demands

Reaction, which is kinetically controlled, has a low product yield (yield = 25 mol% for m_{enz} = 50 mg, n_1 = 0 mmol, n_2 = 46.0 mmol, n_3 = 10.0 mmol, n_4 = 0 mmol, n_5 = 800 mmol, n_6 = 0.00 mmol, n_7 = 8185 mmol). The objective is to increase the process productivity in 12 h batch operation. The process yield is defined here as the ratio between modified phosphatidylcholine to original phosphatidylcholine.

4.3.2.4. Step 3: Selection of separation techniques

At this step several computer-aided tools from ICAS are used, namely

ICAS-ProCAMD, ICAS-Utility toolbox, ICAS-MoT and membrane database (see Figure 4.26).

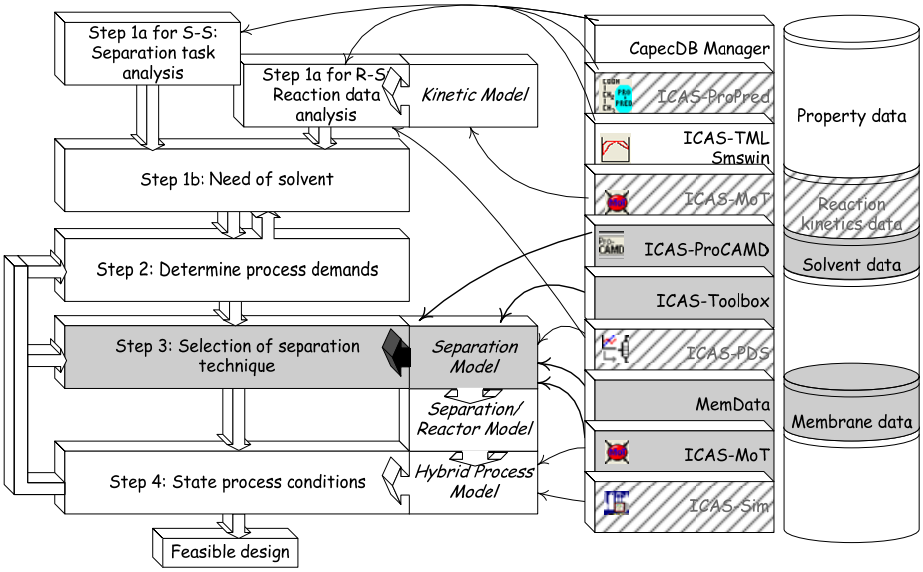

Figure 4.26: Step 3 in the case study of enzymatic interesterification of phosphatidylcholine

R3.1. Identify compound(s) to remove from reaction medium

The most distinctive component in the mixture is water. Besides, as stated earlier, water creates two azeotropes (see Table 4.13). It is important to point out that in the first reaction (Eq. 4.22) water is consumed while in the second reaction (Eq. 4.23) it is produced. Note that in the beginning of the interesterification the lysophosphatidylcholine is absent and the production of the modified phosphatidylcholine is not possible. Therefore, addition of the water is favourable in the beginning of the interesterification process to produce the lysophosphatidylcholine. However, removal of the initially provided water would increase the overall performance of the reaction system when the not modified phosphatidylcholine (1,2-dihexadecanoyl-glycero-3-phosphocholine) is transformed into lysophosphatidylcholine. Egger et al. (1997) and other authors (Mingarro et al., 1994; Adlercreutz et al., 2003) pointed that controlling of water content in the reaction medium has crucial effect on the overall process performance, although, the mixture can not be dehydrated completely because of the enzyme.

R3.2. Feasibility of distillation

Due to phosolipase A_2 it is not possible to work in temperature higher than 333.15 K, therefore, distillation is not feasible under normal pressure. The bubble point pressure of the compound (water) with the lowest boiling temperature at operating reaction temperature of 333.15 K is 20.07 kPa. The relative volatility of components in the post reaction mixture computed at 20 kPa and 333.15 K are reported in Table 4.14. At

these conditions oleic acid is not present in the vapour phase.

Table 4.14. Relative volatility of compounds in the post reaction mixture computed at 20.0 kPa and 333.15 K

Compound		$\alpha_{i,toluene}$
Water (T_b = 373.15 K)		96.4
Toluene (T_b = 383.78 K)		1
Oleic acid (T_b = 633 K)		-
Feed composition to flash	Water [mol/mol]	0.005
	Toluene [mol/mol]	0.91
	Oleic acid [mol/mol]	0.085

R3.3. Feasibility of membrane-based separation

As in the previous case study (section 4.3.1 Synthesis of cetyl-oleate, page 99) pervaporation (PV) is feasible as the membrane-based separation technique because of the possibility of introducing hydrophilic membranes that would allow only water to permeate through the membrane. It is important to point out that Kwon et al. (1994) successfully used pervaporation with the cellulose acetate membrane for selective removal of water from esterification reaction of oleic acid and n-butanol. As catalyst they used Lipozyme, *mucour miehei* lipase.

R3.4. Solvent selection

Egger et al. (1997) selected toluene as the solvent. In this section other likely solvents will be proposed. From section 4.3.2.2 (page 115) it is known that solvent is needed to reduce viscosity of reaction medium, bring all reactants together and to keep low water content but still sufficient amount required for enzyme stability. Reaction temperature is set to 298.15 K.

R3.4.1. Generate the values of R-indices

R3.4.1.1. Solvent must be liquid at the reaction temperature

Solvent must be liquid at reaction temperature R_1 = 298.15 K

R3.4.1.2. Need for solvent as carrier

One of reactants is a big molecules with molecular weight above 700 g/mol therefore R_2 = 1.

R3.4.1.3. Need for solvents to remove reactants or products

One of product is a big molecule with molecular weight above 700 g/mol therefore $R_3 = 1$.

R3.4.1.4. Need for phase split

Phase split is not necessary $R_4 = 0$.

R3.4.1.5. Matching of solubility parameters of solute and solvent

Since $R_3 = 1$ than $R_5 = 1$.

R3.4.1.6. Neutrality of solvents

Solvent must be neutral to all compounds and $R_3 = 1$, than $R_6 = 1$.

R3.4.1.7. Association/dissociation properties of solvents

Solvent does not have to associate or dissociate $R_7 = 0$.

R3.4.1.8. Environmental, health and safety (EHS) property constraints

Solvent should be EHS friendly so $R_8 = 1$.

Upper and lower bounds for solvent properties are defined as follows:

- Normal boiling point $T_b < 333.15$ K
- Normal melting point $T_m < 273.15$ K
- Solvent must be partially miscibility with water and miscible with oleic acid and phosphatidylcholine.
- Toxicity – log $LC_{50} < 4$
- Solvent must be allowed in food industry therefore non-aromatic and non-cyclic are generated (only acyclic component).
- Solvent must be neutral therefore alcohol, acid or ester are not allowed.

R3.4.2. Assign scores to solvent candidates

With all the criteria listed above and using ICAS-ProCAMD, 20 molecular structures have been generated. Six out of them are present in the CAPEC database and they are reported in Table 4.15. To the all generated solvents the scores has been assigned and reported in Table 4.16.

R3.4.3. Final solvent selection

Egger et al. (1997) used as a solvent toluene, other likely solvents worth considering for further studies are 2,2-dimethyl-3-ethylpentane and 2,2,3-trimethylbutane. All generated solvents along with assigned scores are reported in Table 4.17. It is important to point out that 2-methyl-3-ethylpentane, 2-methylheptane, n-octane, n-heptane and n-hexane are also possible solvents but they obtained worse score due

to the reaction temperature. However for further studies toluene is consider as the solvent since only reaction data for this solvent have been reported.

Table 4.15: Properties of solvent generated by ICAS-ProCAMD

No	Compound name	T_m [K]	T_b [K]	*Sol. Par.* [$MPa^{0.5}$]	$LogLC_{50}$	viscosity [cP] @ 298.15 K
1	2-methyl-3-ethylpentane	158.2	388.76	16.15	3.67	0.53
2	2-methylheptane	164.16	390.8	15.051	3.79	0.534
3	n-octane	216.38	398.83	15.4	3.91	0.538
4	2,2-dimethyl-3-ethylpentane	173.68	406.99	14.832	3.94	0.885
5	2,2,3,4-tetramethylpentane	152.06	406.18	14.928	3.82	0.879
6	2,4-dimethyl-3-ethylpentane	150.79	409.87	14.971	3.99	0.664
7	2,2-dimethylpentane	149.34	352.34	14.202	3.18	0.551
8	2,2,3-trimethylbutane	248.57	354.03	14.246	3.05	0.547
9	2,3-dimethylpentane	153.91	353.64	14.292	3.22	0.414
10	2-methylhexane	154.9	363.19	14.724	3.34	0.417
11	n-heptane	182.57	371.58	15.2	3.47	0.42
12	n-hexane	177.83	341.88	14.9	3.02	0.321

Table 4.16: List of feasible solvents with their RS values

No	Compound name	RS1	RS2	RS3	RS4	RS5	RS6	RS9
1	2-methyl-3-ethylpentane	4	1	1	1	1	1	1
2	2-methylheptane	4	1	1	1	1	1	1
3	n-octane	3	1	1	1	1	1	1
4	2,2-dimethyl-3-ethylpentane	1	1	1	1	1	1	1
5	2,2,3,4-tetramethylpentane	3	1	1	1	1	1	1
6	2,4-dimethyl-3-ethylpentane	3	1	1	1	1	1	1
7	2,2-dimethylpentane	5	1	1	1	1	1	1
8	2,2,3-trimethylbutane	2	1	1	2	1	1	1
9	2,3-dimethylpentane	5	1	1	1	1	1	1
10	2-methylhexane	5	1	1	1	1	1	1
11	n-heptane	4	1	1	1	1	1	1
12	n-hexane	4	1	1	1	1	1	1

Table 4.17: List of feasible solvents with their scores

No	Compound name	S1	S2	S3	S4	S5	S6	S9	Action
1	2-methyl-3-ethylpentane	4	10	10	10	10	10	10	Possible
2	2-methylheptane	4	10	10	10	10	10	10	Possible
3	n-octane	6	10	10	10	10	10	10	Possible
4	2,2-dimethyl-3-ethylpentane	10	10	10	10	10	10	10	Feasible
5	2,2,3,4-tetramethylpentane	6	10	10	10	10	10	10	Possible
6	2,4-dimethyl-3-ethylpentane	6	10	10	10	10	10	10	Possible
7	2,2-dimethylpentane	1	10	10	10	10	10	10	Rejected
8	2,2,3-trimethylbutane	8	10	10	8	10	10	10	Feasible
9	2,3-dimethylpentane	1	10	10	10	10	10	10	Rejected
10	2-methylhexane	1	10	10	10	10	10	10	Rejected
11	n-heptane	4	10	10	10	10	10	10	Possible
12	n-hexane	4	10	10	10	10	10	10	Possible

R3.5. Separation technique selection

Distillation and pervaporation have been compared using driving force diagram in the water concentration range from 0 to 0.02 mol/mol since this is the range in which reaction would preferably take place. It is clear that using pervaporation to dehydrate organic mixture like n-hexane or isopropanol is much better than distillation from driving force point of view (see Figure 4.27).

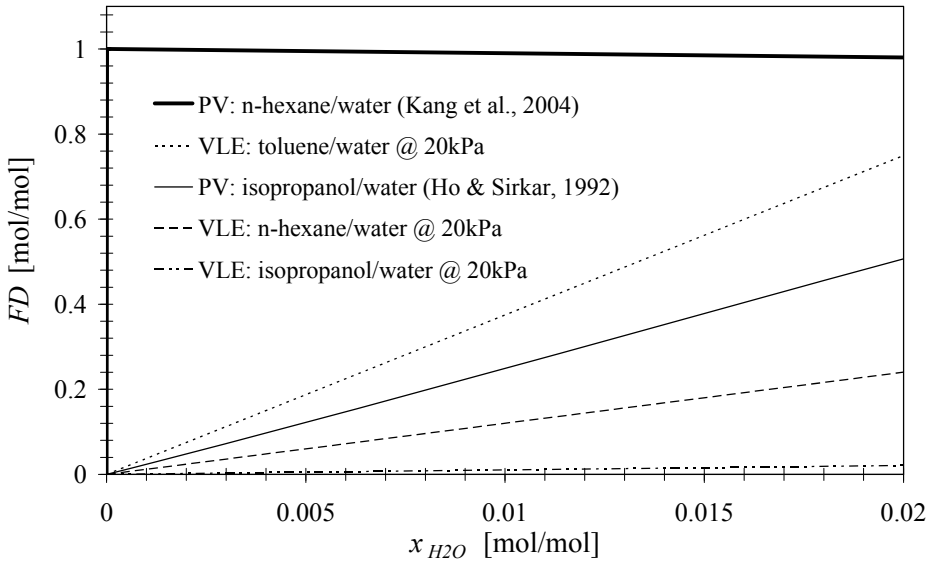

Figure 4.27: Driving force diagram for distillation and pervaporation (PV) for different binary mixtures

4.3.2.5. Step 4: Establish process conditions

Two operational alternatives are presented in this section: batch reaction operation and semi-batch hybrid operation (membrane assisted batch reaction) since a small production rate is considered. In this case reactor and pervaporation can be combined together into one unit since feed to PV unit does not need to be pre-heated (T_R = 298.15K). The initial condition for all the studied cases in terms of component concentration are the same as used by Egger et al. (1997). All simulations have been performed with the same initial conditions with respect to reactor: C_1 = 10mM, C_2 = 36.5 mM, C_5 = 800 mM and reactants volume V = 1 dm^3. 2 w% of enzyme was added to the mixture. Toluene was assumed as solvent. The workflow, dataflow and tools used in this step are presented on Figure 4.28.

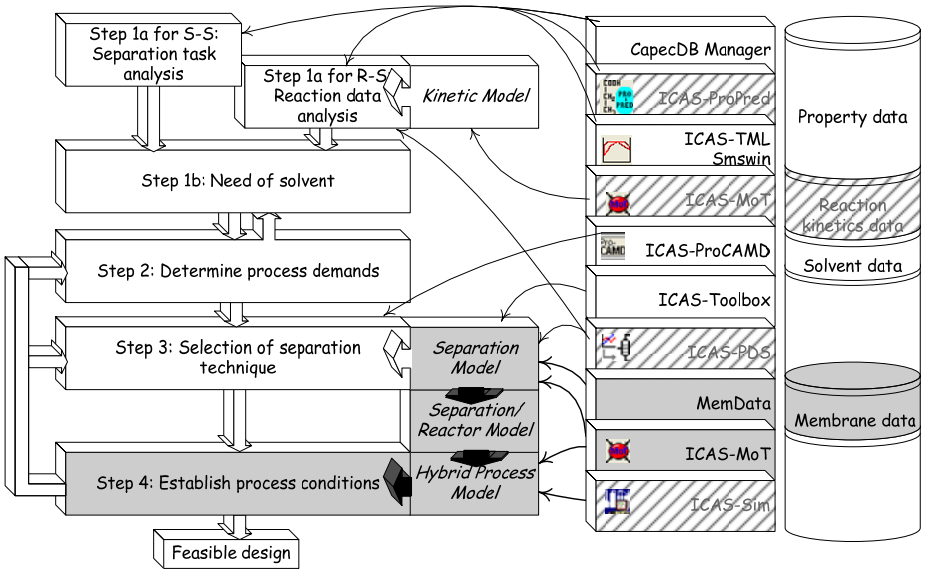

Figure 4.28: Step 4 in the case study of enzymatic interesterification of phosphatidylcholine

Both set-ups are investigated under assumptions that: (1) reactor is well mixed (2) activity of enzyme does not change during operation and (3) reaction is stopped when concentration of water drops below 3.32 mmol/dm^3.

From the superstructure of hybrid process (Figure 3.5, page 57) a specific hybrid process scheme is generated where the *Process 1* is a reactor and *Process 2* is pervaporation. Defining the decision variables as follow $\xi^{1}=1$, $\xi^{2}=1$, $\xi^{1in}=0$, $\xi^{2in}=0$, $\xi^{R}=1$, $\xi^{\beta}=0$, $\xi^{homog}=0$, $\xi^{heterog}=1$, $\xi^{1\alpha}=0$, $\xi^{1\beta}=0$, $\xi^{2\alpha}=1$, $\xi^{2\beta}=0$ lead to the specific model described by Eq. 4.25(see Figure 4.29). With respect to membrane, water flux is assumed constant J_2 = 0.5 mmol/h/m^2 and fluxes for all other components present in the system are neglected. Reaction kinetics is described by the reversible Michaelis-Menten kinetics type. Detailed model derivation and analysis is provided in Appendix 6.4.2.2 (page 210).

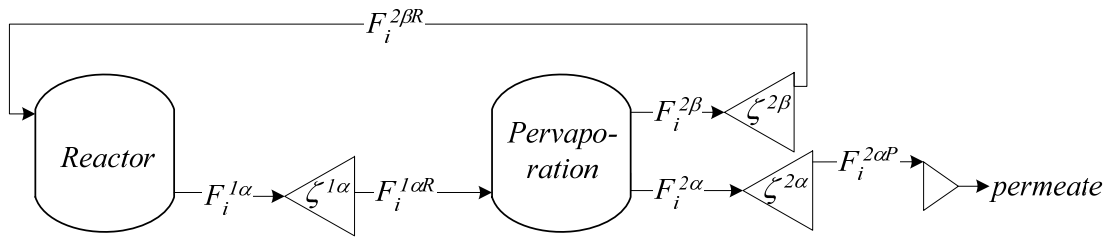

Figure 4.29: From superstructure to the specific hybrid process scheme (membrane assisted batch reaction)

$$\frac{dn_i}{dt} = a \cdot \left(-J_i\, A_m\right) + \nu_{1,i} r_1 + \nu_{2,i} r_2 \qquad (4.25)$$

Where a stands for the decision variable related to the switching time (see Eq. (3.29)), r_1 and r_2 describes the reaction rate of Eq. (4.22) and Eq. (4.23). Note that only mass balance is used because no heat effect was reported (Egger et al., 1997). Process yield is defined as ratio of moles of desired product (modified phosphatidylcholine) to initial moles of limiting reactant (original phosphatidylcholine).

Performance of the hybrid system strongly depends on the membrane area (A_m) and the component fluxes (J_i). For reactor coupled with pervaporation unit (RCPV), four cases with different values of factor $J_2 \cdot A_m$ (J_2 – water flux) have been studied. For process carried out in 20 h the process yield is improved from 0.25 (batch) to 0.57 (RCPV3) by removing water from the system using a possible design for a PV-unit (J_2 = 5 mmol/(m^2·h), A_m = 0.256 m^2). However, it is possible to reduce the process time to 10 h when total removal of water is equal to 2.56 mmol/h. Values for the different design variables for the five scenarios are given in Table 4.18 while the yield-time behaviour is shown in Figure 4.30.

Table 4.18: Process parameters and process yields. Switching time t_{switch} = 0

	Batch	RCPV1	RCPV2	RCPV3	RCPV4
$J_2 \cdot A_m$ [mmol/h]	-	0.32	0.64	1.28	2.56
t [h]	20.00	20.00	20.00	20.00	9.91
Yield [-]	0.25	0.30	0.37	0.57	0.60

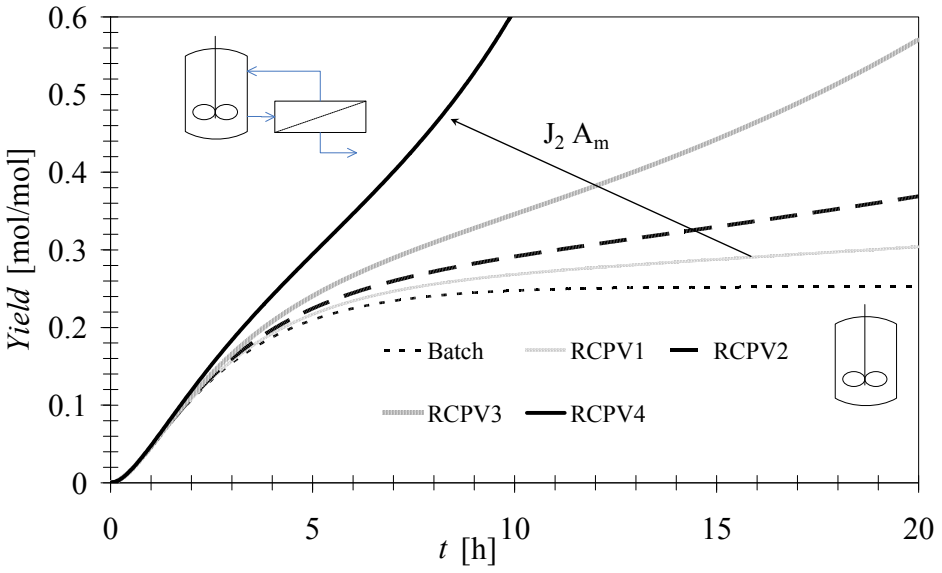

Figure 4.30: Comparison of hybrid process systems with batch in terms of process yield

Two different membranes polyvinyl alcohol and cellulose acetate membranes with various solvents have been investigated under the assumption that solvent does not change kinetic parameters and fluxes of other compounds than water can be neglected. To make easy comparison between membranes the same membrane area and time of starting hybrid separation (5 h) was used in all simulations. Data used for pervaporation unit was found in literature and result are summarised in Table 4.19 since yield-time behaviour is presented in Figure 4.31. For further experimental studies semi-batch reactor coupled with pervaporation is recommended with volume of 1 dm^3 and membrane area of 0.064 m^2. However, at first impact of hexane on reaction should be verified experimentally. If experiments would represent no change in kinetics, the recommended solvent is n-hexane with assisted cellulose acetate membrane.

Table 4.19: Various membranes versus different solvents. Switching time t_{switch} = 5 h

Possible membranes	Solvents	Yield [-]	t [h]
Poly(vinyl alcohol) (Sirkar and Ho, 1992)	isopropanol	0.26	20
Cellulose acetate (Kang et al., 2005)	n-hexane	0.5	20

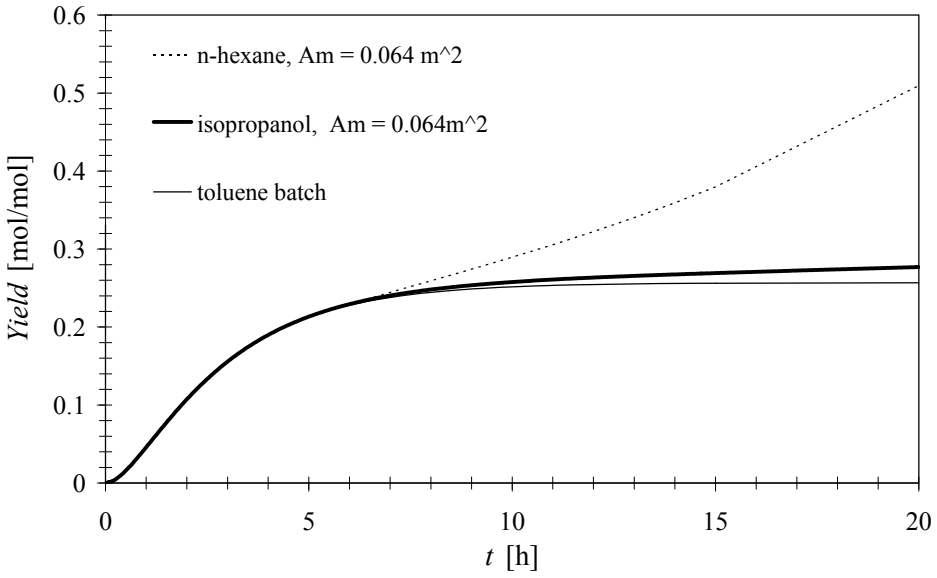

Figure 4.31: Comparison of hybrid process systems with various membranes and solvents

4.3.3. Synthesis of ethyl lactate

Lactic acid and their esters are used in the food industry for preservation and flavouring purposes, as well as in pharmaceutical and cosmetic industries as additives

and solvents (Delgado et al., 2007). Ethyl lactate has found industrial applications in specialty coatings, inks, cleaners and solvent which can dissolve cellulose and many resins. Ethyl lactate is considered biodegradable and can be used as a water-rinsable degreaser (Zhang et al., 2004). The odour of ethyl lactate is mild, buttery, and creamy, with hints of fruit and coconut.

4.3.3.1. Step 1a: Separation task and reaction data analysis

The workflow with type of data and used tools at first step in the case study of esterification of ethyl lactate is shown on Figure 4.32.

1a.1. Identify mixture type

The mixture consists of water and three organic compounds: lactic acid, ethanol and ethyl lactate. Based on the mixture classification rule by Gani and O'Connell (1989) the mixture in the reactive system is classified as non-ideal and aqueous type. This problem requires calculation of activity in the liquid phase and the UNIFAC (Original) is selected. The vapour phase is modelled with SRK equation of state.

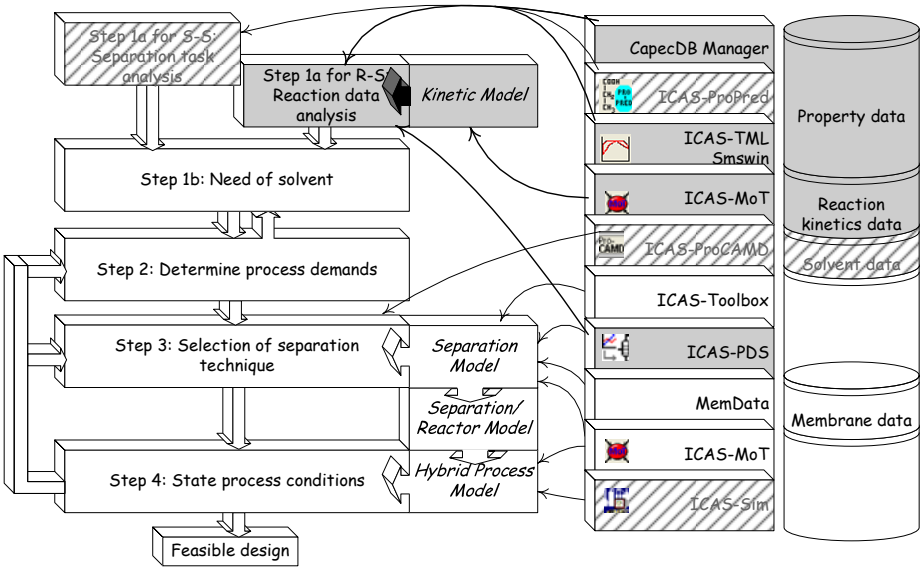

Figure 4.32: Work flow along with used tools at step 1 in the case study of esterification of ethyl lactate

1a.2. Analysis based on pure component properties

Compounds present in the investigated mixture are in the liquid state between 289.9 K (the largest melting point, which is lactic acid) and 351.44 K (the lowest boiling point which is ethanol). The organic compounds are likely to form a single liquid phase since their solubility parameters are similar. Presence of water, which has the solubility parameter almost 1.5 times higher than other compounds in the mixture, may create a second liquid phase (see Table 4.20).

Table 4.20. Properties of pure compounds (obtained from CAPEC Database)

Composition	T_m [K]	T_b [K] @ 1atm.	T_b [K] @ 2atm	*Sol. Par* [$MPa^{0.5}$]
Lactic acid (HL)	289.9	490.00	512.71	33.1095
Ethanol (EtOH)	159.05	351.44	370.18	26.1333
Ethyl lactate (EtL)	247.15	427.65	452.46	22.3818
Water (H_2O)	273.15	373.15	393.84	47.8127

1a.3. System analysis based on mixture properties

The compounds present in the mixture form the 6 binary pairs and 4 ternary mixtures which need to be analysed. The performed phase equilibrium calculations revealed the complex behaviour of the reaction mixture which is visualized through the data presented in the Table 4.21. It can be noted that water is present in all founded azeotropes.

Vu et al. (2006) reported existence of minimum boiling azeotrope in binary mixture of ethyl lactate and water which occurs between 5 and 7 mol% at isothermal conditions at temperature of 313 K and 333 K respectively. The representation in terms of the UNIFAC groups for all compounds and their parameters are summarized in the Appendix in section 6.4.3.3 (page 219), in Table 6.24 and Table 6.26.

Table 4.21. Reaction mixture analysis (SMSwin). UNIFAC (Original) and SRK.

Composition	Type of azeotrope	Molar fraction [%]				*T* [K] @ 1atm.
		HL	EtOH	EtL	H2O	
EtL – H2O	Heterogeneous	-	-	6.60	93.40	372.14
EtOH – H_2O	Homogeneous	-	89.25	-	10.75	351.46
EtOH – EtL – H_2O	Heterogeneous	-	18.21	4.32	77.47	367.52

1a.4. Reaction analysis

Ethyl lactate (lactic acid ethyl ester) is a monobasic ester formed from lactic acid and ethanol according Eq. 4.26.

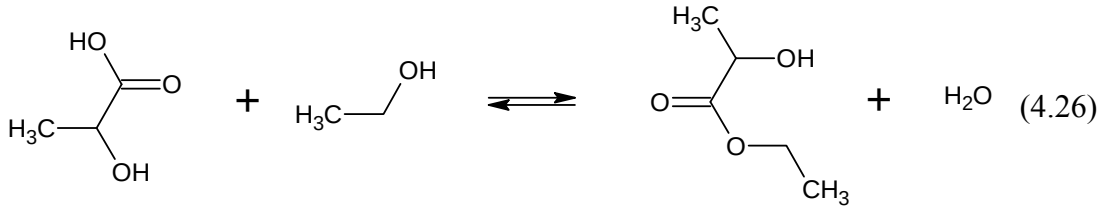

(4.26)

Lactic acid is commercially available in water solution with concentration varied between 20 w% and 97 w% (Acros, 2007). Low concentrated solutions of lactic acid are used during esterification reaction in order to avoid the presence of polylactic acid with high molecular weight. It is because of the two functional groups: acid and hydroxyl groups, due to which lactic acid can suffer intermolecular esterification and form polylactic acid. Dilute lactic acid solutions containing about 20 w% lactic acid correspond only to monomer lactic acid and water (Delgado et al., 2007). However, Parulekar (2007) and Yang et al., (2004) used 80 w% lactic acid solution in their studies of synthesis ethyl lactate.

Esterification reaction of lactic acid and ethanol is a reversible reaction. The conventional way to produce ethyl lactate is the esterification of lactic acid with ethanol catalyzed by sulphuric acid (Zhang et al., 2004). Several researchers has been investigated application of various catalysts like heterogeneous acidic ion-exchange resin, Amberlyst 15 with exchange capacity of 4.75 mequiv H^+/g of dry catalyst (Delgado et al., 2007), hetero-poly-acid supported on ion-exchange resins, Lewatit® S100 (Engin et al., 2003). Zhang et al. (2004) studied esterification of ethyl lactate over five different cation-exchange resins: Amberlyst 15, D001, D002, NKC and 002.

The homogenous reaction kinetics of esterification of lactic acid and ethanol is described by the rate expression in terms of the reactants concentration (Parulekar, 2007; Benedict et al., 2003):

$$r = k_1\left(C_0C_1 - \frac{1}{K_{eq}}C_2C_3\right);\ K_{eq} = \frac{C_2C_3}{C_0C_1} \tag{4.27}$$

where 0-lactic acid, 1-ethanol, 2-ethyl lactate, 3-water.

Since other researcher expressed reaction kinetics in terms of compound activities (Delgado et al., 2007):

$$r = k_1\left(a_0a_1 - \frac{1}{K_{eq}}a_2a_3\right);\ K_{eq} = \frac{a_2a_3}{a_0a_1} \tag{4.28}$$

In case of the heterogeneously catalyzed reaction the reaction kinetics are described by psedohomogeneous rate expression (similar to Eq. (4.28)) or by Langmuir -Hinshelwood mechanism (Delgado et al., 2007). The basic idea of the Langmuir -Hinshelwood mechanism is that all reactants are adsorbed on the catalyst surface before the chemical reaction takes place and in general it is described by Eq. (4.29).

$$r = \frac{k_1\left(a_0 a_1 - \frac{1}{K_{eq}} a_2 a_3\right)}{\left(1 + k_0 a_0 + k_1 a_1 + k_2 a_2 + k_3 a_3\right)^2} \tag{4.29}$$

However some researchers (Parulekar, 2007; Benedict et al., 2003) simplified the Eq. (4.29) to the form of Eq. (4.30). From the denominator on the right-hand side of Eq. (4.30) is evident that the adsorption of lactic acid is the rate determining step in the single-site mechanism and the reaction products, ethyl lactate and water, are absorbed insignificantly.

$$r = \frac{k_1\left(C_0 C_1 - \frac{1}{K_{eq}} C_2 C_3\right)}{C_1 + K_1 C_2 C_3} \tag{4.30}$$

In further considerations reaction rate expression described by Eq. (4.30) and reported by Parulekar (2007) for Amberlyst XN-1010 is used.

The only restriction in terms of initial concentration of reactants is related to the lactic acid, which should be delivered in the monomer form, therefore the highest concentration of lactic acid is fixed to 80 w% in the water solution. Therefore, it is concluded that only excess of ethanol is reasonable since water, which is the by-product of the reaction is delivered together with reactant (ethyl lactate). Since reaction occurs only in liquid phase the operating temperature needs to be below boiling temperature of the reactive mixture and also below boiling points of pure components. Operating temperature is fixed to 363.15 K and is identical to the one studied by Parulekar (2007).

The experimental concentration of compounds measured in the end of experiments published by Benedict et al. (2003) has been verified if they represent the chemical equilibrium using the reactive flash calculations in ICAS-PDS. The corresponding chemical element matrix for this esterification problem is reported in Table 4.22. The comparison between experimental data and calculation obtained in the reactive flash calculation is given in Table 4.23. The best agreement between calculation and experimental data was obtained when UNIFAC (Original) was used to calculate the activity coefficients. It is concluded here that the equilibrium constant reported by Benedict et al. (2003) represent well the reaction system.

Table 4.22. Chemical element matrix representing the synthesis of ethyl lactate from ethanol and lactic acid (Eq. (4.26))

	C_2H_5OH	$C_3H_4O_2$	H_2O
Ethanol	1	0	0
Ethyl lactate	1	1	0
Lactic acid	0	1	1
Water	0	0	1

Table 4.23. Comparison of experimental equilibrium data with reactive flash calculation at $T = 368.15$ K, $P = 2$ atm.

	x_i^{exp} (Benedict et al. 2003)	x_i - Reactive flash (Willson)	x_i - Reactive flash (UNIFAC)	$(x_i^{exp} - x_i(\text{UNIFAC}))^2$
Lactic acid	0.180885	0.225424	0.169961	0.000119
Ethanol	0.20589	0.248174	0.192711	0.000174
Ethyl lactate	0.158821	0.112973	0.168436	0.000092
Water	0.454404	0.413429	0.468892	0.00021

Process yield is defined as ratio between consumed and initial moles of lactic acid. The initial ratio of lactic acid and ethanol has influence on the process yield. The influence of higher ratios of reactants on the process yield is amplified because of the increasing ratio of ethanol to water (water is delivered with lactic acid). However, increase over 1:2 ratio does not give significant influence on the reaction yield (see Figure 4.33). Data shown on Figure 4.33 has been obtained in simulations of batch reaction using reaction kinetic expressed by Eq. (4.30). The batch reaction model is reported in the Appendix, section 6.4.3.1 (page 213).

Since the heterogeneously catalysed reaction is analysed here it is important to investigate the influence of catalyst addition. In general, if more catalyst is present in the batch reactor than faster the equilibrium is reached. The dependency of the addition of the catalyst on the batch time required to reach specific yield is reflected on Figure 4.34. On the same figure different initial reactant ratios and their batch time are depicted. It is important to point out that increase of catalyst loading to above

20 w% does not decrease significantly the operation time of the batch reaction, e.g. increase of catalyst loading from 20 w% to 30 w% decrease the operation time only by 3 minutes for initial reactant ratio 1:1 (reaching Yield=0.45).

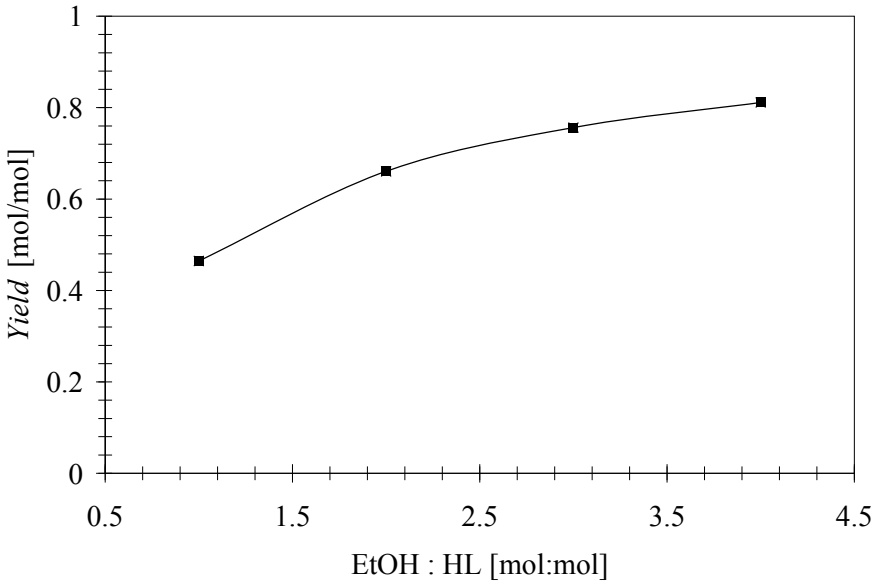

Figure 4.33: Influence of reactant ratio on the process yield

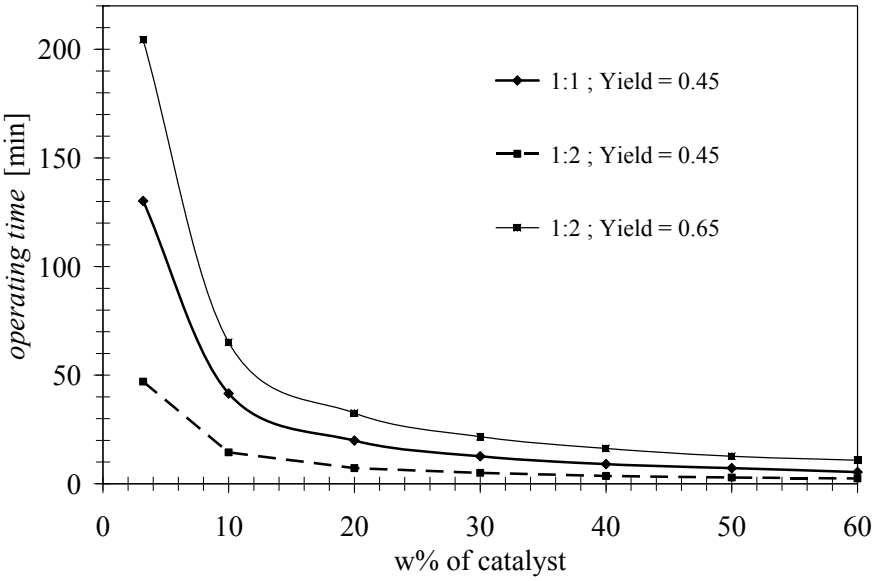

Figure 4.34: Influence of catalyst addition on the operation time of batch reaction

4.3.3.2. Step 1b: Need of solvent

In this study, the use of solvents has not been investigated since all reactants are

liquid and miscible in the operation window. However, addition of non-reactive solvents to create the second phase with water thereby decreasing water concentration in the organic-reactive mixture and moving reaction towards product is foreseen.

4.3.3.3. Step 2: Determine process demands

The batch process in which lactic acid and ethanol is converted to ethyl lactate with yield close to 1 is looked for. The operating time of batch process is set to 12 h but possibility of reducing this time is also anticipated.

4.3.3.4. Step 3: Selection of separation techniques

In this step the separation technique is selected. Various computer aided-tools are used at this step such as ICAS-Toolbox and membrane database MemData (see Figure 4.35).

R3.1. Identify compound(s) to remove from reaction medium

One option is to continuously remove the main product, ester. However in this case, it has to be kept in mind the possibility of formation of the heterogeneous azeotropes between alcohol, ester and water. Another option is to remove water (reaction by-product), the compound which is present in all azeotropes (see Table 4.21).

R3.2. Feasibility of distillation

The mixture of ethanol, lactic acid, ethyl lactate and water at chemical equilibrium has been used as a feed to the flash calculation. The list of compounds ranked according boiling point and corresponding relative volatilities is presented in Table 4.24. The by-product which was recommended to remove, water, is not on the top or bottom of that list, so use of simple distillation to enhance reaction is not possible. However, it is important to highlight the significant difference in relative volatilities between products, water and ethyl lactate, which point out possibility of use of reactive distillation to separate them.

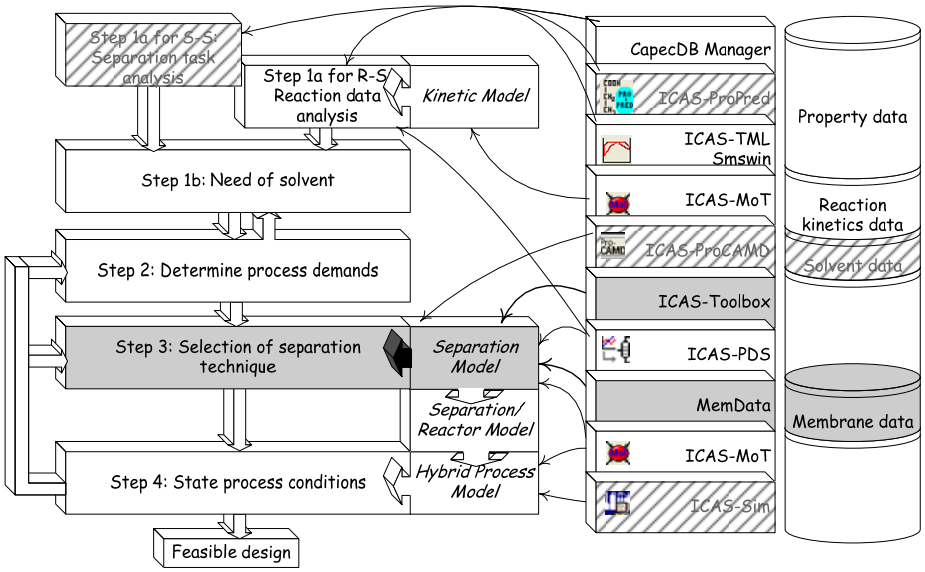

Figure 4.35: Work flow along with used tools at step 3 in the case study of esterification of ethyl lactate

Table 4.24. Relative volatility of compounds in the post reaction mixture computed at boiling point

Compound		$\alpha_{i,HL}$	$\alpha_{i,HL}$
Lactic acid (T_b = 490.00 K)		1	1
Ethyl lactate (T_b = 427.65 K)		46.63	85.85
Water (T_b = 373.15.25 K)		229.21	456.23
Ethanol (T_b = 351.44 K)		549.03	1128.82
Feed composition to flash	Lactic acid	0.17	0.17
	Ethanol	0.19	0.19
	Ethyl lactate	0.17	0.17
	Water	0.47	0.47
Flash condition	T [K]	387.72	367.13
	P [atm]	2	1

R3.3. Feasibility of membrane-based separation

Many membrane-based separation processes offer selective removal of a specific chemical, for example, pervaporation and vapour permeation are widely used for dehydration of organic mixtures (Koszorz et al., 2004, Van Baelen et al., 2005). Comparison of driving force curves for different membrane processes for separation of binary mixture of ethanol and water is presented on Figure 4.36. Benedict et al. (2006) reported using a pervaporation with GFT-1005 membrane to dehydrate a quaternary mixture of ethanol, lactic acid, ethyl lactate and water. Van Baelen et al. (2005) used Pervap 2201 from Sulzer to dehydrate binary mixtures of water and alcohol (e.g. water-methanol, water-ethanol and water-isopropanol). In their studies the mixture of water and ethanol gave the lowest flux through the pervaporation membrane. The selectivity of these membranes is close to one.

R3.4. Solvent selection

As it was already explained above (see section 4.3.2.2, page 115), addition of solvent is not investigated in this case study.

R3.5. Separation technique selection

All here reported membrane-based separation techniques have much higher driving force (*FD*) comparing to distillation in the low concentrations of water where the separation technique is going to be used. High selectivity towards water and relatively large driving force available for pervaporation comparing to distillation makes the pervaporation favourable candidate for the further investigation.

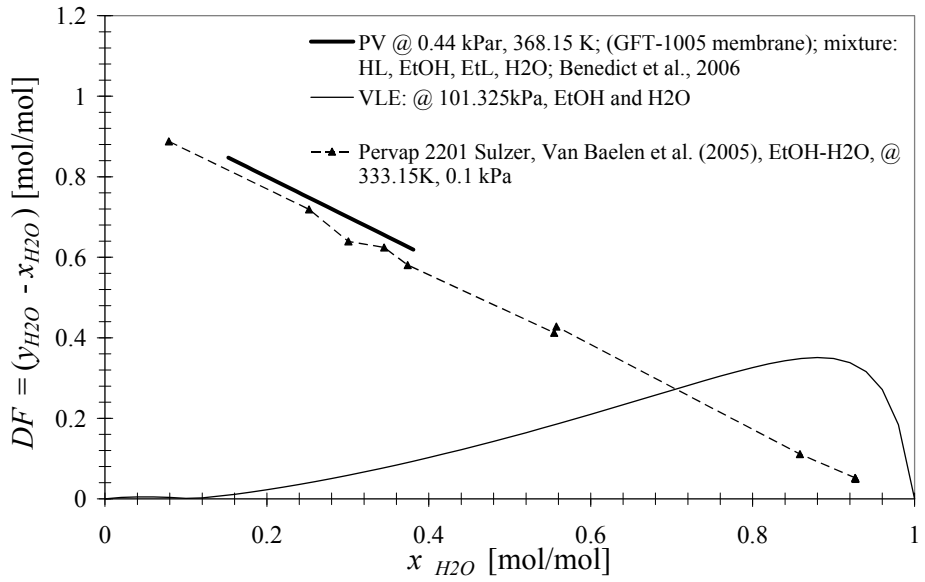

Figure 4.36 : Driving force diagrams for membrane-based separation of binary mixture ethanol (EtOH)-water. PV – pervaporation.

4.3.3.5. Step 4: Establish process conditions

In this step, the hybrid process scheme along with model is developed and process conditions are stated (see Figure 4.37). Based on the superstructure (see Figure 3.5, page 57) the specific configuration as shown in Figure 4.38, where *Process 1* is the reactor and *Process 2* is the pervaporation for selective removal of water, is obtained. Note that in order to utilize the Amberlyst XN-1010 catalyst, a liquid feed to the reaction zone is required.

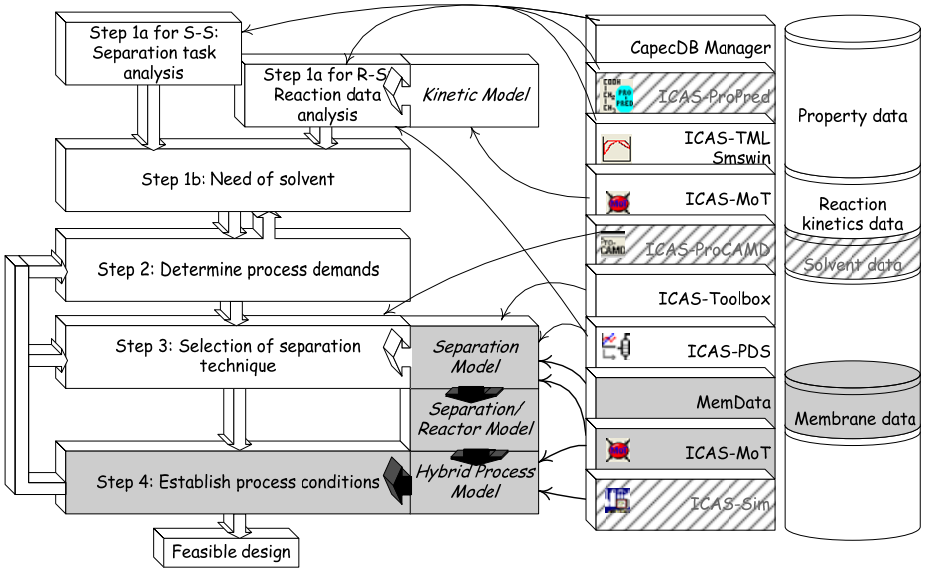

Figure 4.37: Work flow along with used tools at step 4 in the case study of esterification of ethyl lactate

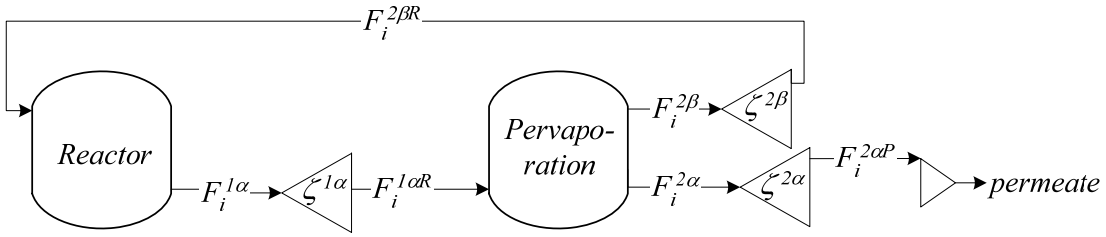

Figure 4.38: From superstructure to the specific hybrid process scheme (membrane assisted batch reaction)

From the general model (see section 3.2.1.5) the dynamic process model is generated based on the following assumptions:

- reaction occur only with the use of catalyst,
- reaction occur only in the liquid phase, and
- only water permeates through the membrane.

The generated dynamic process model for the process system represented in Figure 4.38 is as follows:

Mass balance:

$$\frac{dn_i}{dt} = -a \cdot J_i \, A_m + \nu_i \, r^{1\alpha(heterog)} \tag{4.31}$$

Constitutive equations:

$$r^{1\alpha(heterog)} = \frac{k_1 \left(C_0 C_1 - \frac{1}{K_{eq}} C_2 C_3 \right)}{C_1 + K_1 C_2 C_3} \frac{m_{CAT}}{1000} \tag{4.32}$$

Component flux is calculated using correlation reported by Benedict et al. (2006) for the quaternary mixture of lactic acid, ethanol, ethyl lactate and water. Membrane GFT-1005 has high selectivity; therefore it is assumed that only water permeates. Correlation given by Eq. (4.33) is valid for temperature of 368.15 K and pressure of permeate of 0.44 kPa.

$$J_3 = \alpha_3 C_3^{\beta_3} \frac{1000}{60 \cdot Mw_3} \tag{4.33}$$

$$J_i = 0 \quad i \in \{0,1,2\} \tag{4.34}$$

Detailed model derivation and analysis are reported in Appendix 6.4.3.2 (page 216).

The model used here has been validated with results reported by Benedict et al. (2003) and Parulekar (2007). The comparison of experimental yield and reaction volume defined by Eq. (4.35) with simulation results are presented on Figure 4.39 and Figure 4.40 respectively.

$$v = \frac{V_0 - V_{permeate}}{V_0} \tag{4.35}$$

where V_0 – initial volume of a semi-batch reactor, $V_{permeate}$ –volume of permeate

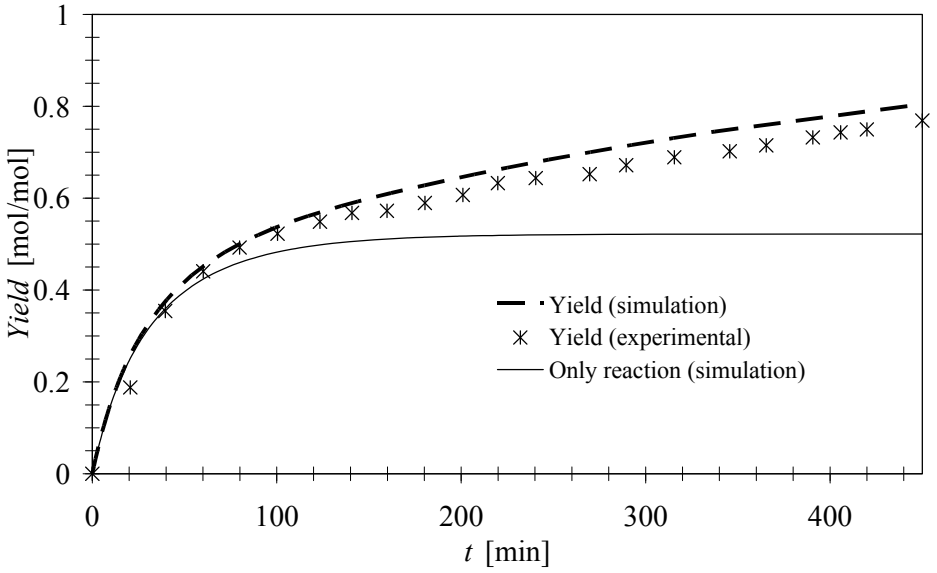

Figure 4.39: Comparison of experimental data yield published by Benedict et al. (2003) with simulation result

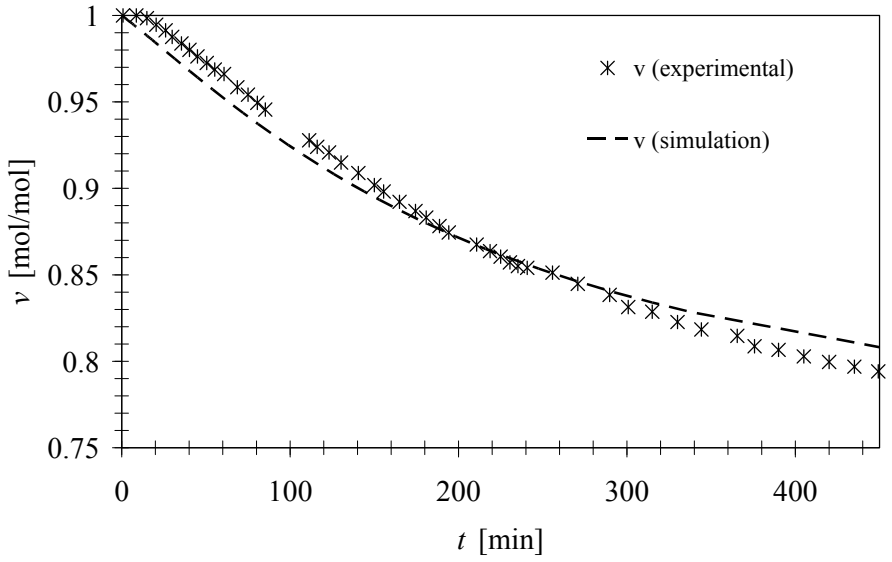

Figure 4.40: Comparison of experimental yield with simulation result

Since a high conversion of lactic acid is desirable, the introduction of excess of ethanol will shift the reaction towards higher ester concentrations. When the batch reactor is combined with the pervaporation unit it is important to observe the influence of the amount of catalyst as well as the switching time (t_{switch}) from the batch reaction operation into the hybrid operation (membrane assisted batch reaction). Since in this case component which has to be removed, water, is present in the reaction mixture from the beginning the switching time is not studied, the separation

is started since the beginning of the reaction.

Increase of molar ratio of lactic acid and ethanol leads to higher value of the process yield. With the same initial molar ratio of reactants the process yield increases with increase of the membrane area which is easily observed on the figures representing change of the process yield during the operation time (see Figure 4.41, Figure 4.42 and Figure 4.43). The initial conditions for all these simulations are reported in Table 4.25. It is important to point out that three configurations achieved almost full conversion. The process yield close to one was obtained for membrane assisted batch reaction for initial molar ratio of 1 : 1.2 and membrane area (A_m) 0.08 m^2 and for ratio 1 : 2 and A_m = 0.04 m^2 and A_m = 0.08 m^2.

Table 4.25: Initial conditions for different reactant ratios

Ratio	1:1	1:1.2	1:2
n_{HL} [mol]	11.52	11.52	11.52
n_{EtOH} [mol]	11.52	13.86	23.04
n_{EtL} [mol]	0.00	0.00	0.00
n_{H2O} [mol]	14.40	14.40	14.40
T [K]	363.15	363.15	363.15
m_{cat} [g]	58.49 (3.2 w%)	61.94 (3.2 w%)	75.47 (3.2 w%)

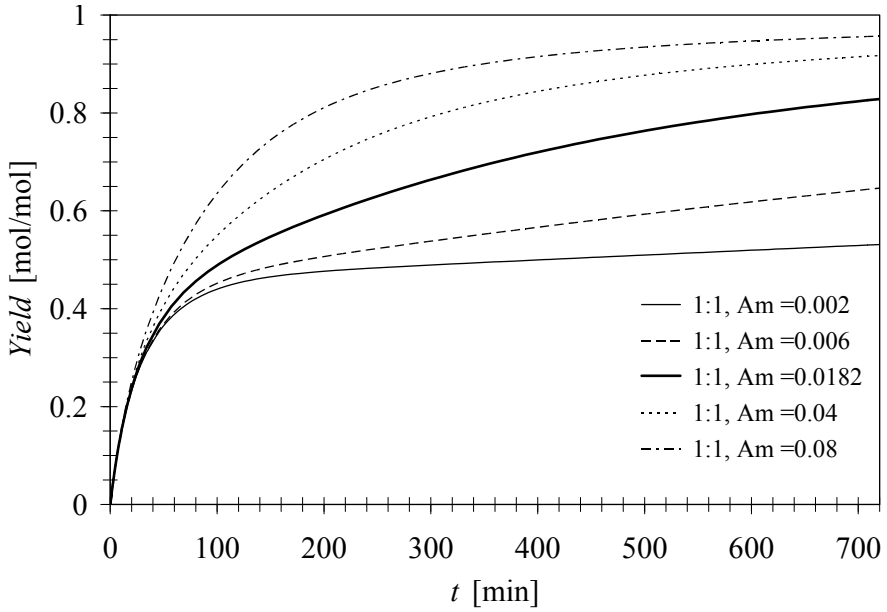

Figure 4.41: Process yield of membrane assisted batch reaction. Initial molar ratio 1:1, 3.2w% of catalyst (more details about initial conditions see Table 4.25)

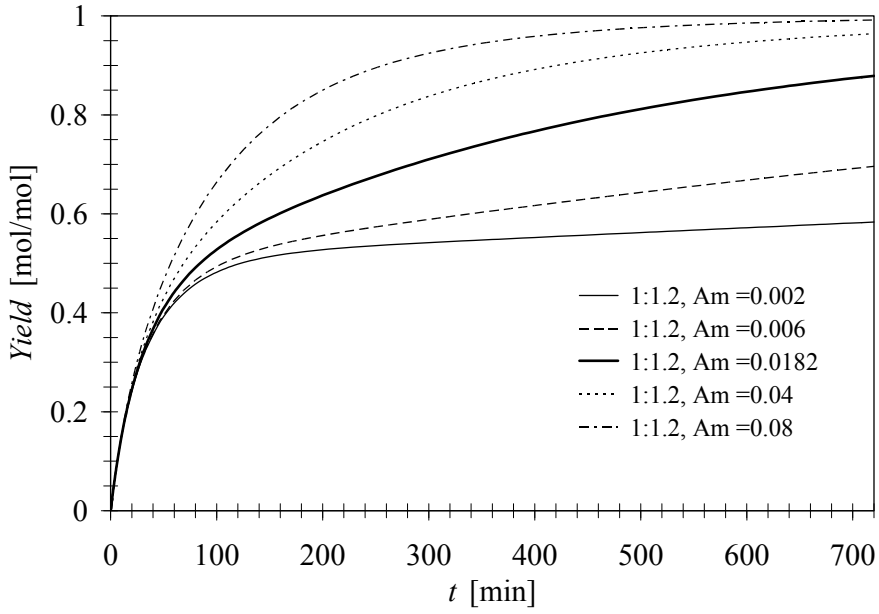

Figure 4.42: Process yield of membrane assisted batch reaction. Initial molar ration 1:1.2 (more details about initial conditions see Table 4.25)

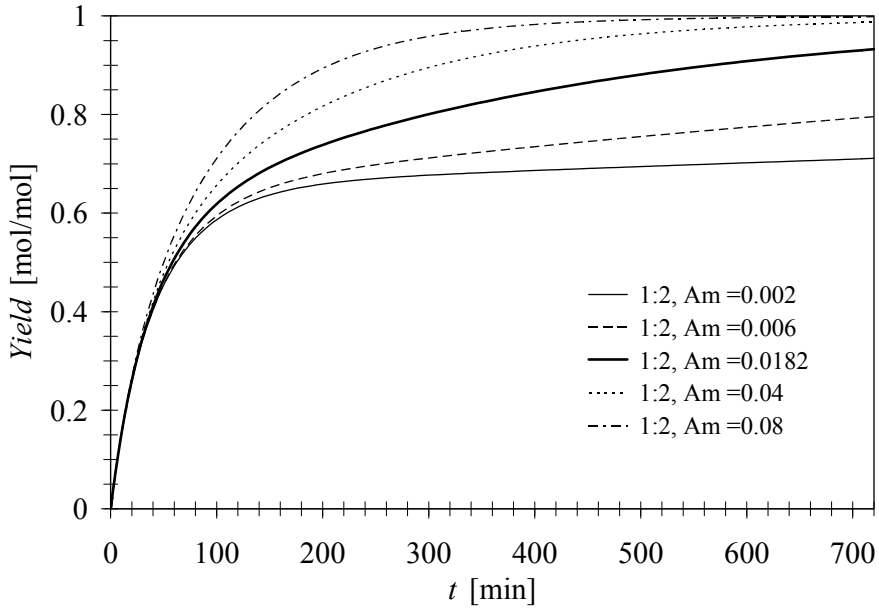

Figure 4.43: Process yield of membrane assisted batch reaction. Initial molar ration 1:2 (more details about initial conditions see Table 4.25)

Let us introduce a concept of a perfect membrane. Perfect membrane (PM) is a membrane which totally and instantly removes only one compound form the feed. The perfect membrane towards water was also studied here and yield trajectories are presented on Figure 4.44. It is important to note that for the perfect membrane the

process yield equal to 1 is achieved much faster comparing to the cases when the GFT-1001 membrane were used. However, when the perfect membrane is considered, for the higher reactant ratio the time to achieve yield = 1 decreases, e.g. for reactant ratio 1:1 membrane assisted batch reaction needs 170 min to reach Yield = 1 since for reactant ratio 1:2 needs 300 min. It is because of increased of ethanol concentration which is in the denominator of the reaction kinetic expression (Eq. (4.32)).

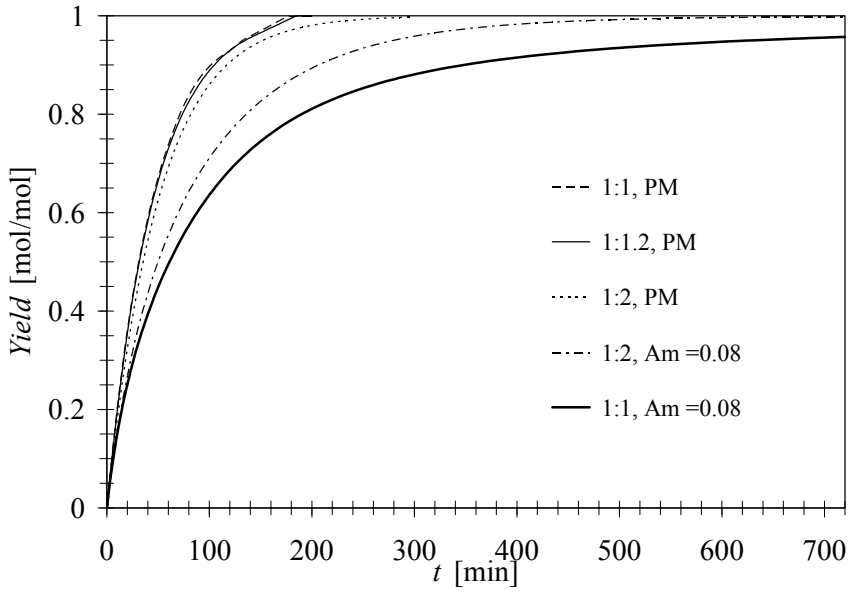

Figure 4.44: Comparison between perfect membrane (PF) and GFT-1001 membrane

Influence of catalyst addition on the membrane assisted batch reaction is not that significant than comparing with the batch reaction alone. Difference in the process yield between membrane assisted batch reaction with catalyst loading 3.2 w% and 20 w% is not higher than 3 % (see Table 4.26).

From this case study it is clear that it is beneficial to start membrane assisted batch reaction with water present in the mixture with molar ratio 1:1 with catalyst loading of 3.2 w%, to have as big as possible membrane (recommended 0.08 m^2 for GFT-1001 membrane) and operate at 363.15 K. Note that the operation time is reduced to 170 min.

Table 4.26: Influence of the catalyst addition on the membrane assisted batch reaction (T=363.15 K)

A_m [m^2]	0.002	0.006	0.0182	0.04	0.08	PM
Molar ratio	1:1	1:1	1:1	1:1	1:1	1:1
Yield @ 3.2 w% (@720min)	0.53	0.65	0.83	0.92	0.96	1.00
Yield @ 20 w% (@720min)	0.54	0.66	0.84	0.93	0.96	1.00
Difference	0.01	0.01	0.01	0.01	0.01	0.00
Yield @ 3.2 w% (@360min)	0.49	0.55	0.70	0.82	0.90	1.00
Yield @ 20 w% (@360min)	0.50	0.57	0.72	0.85	0.92	1.00
Difference	0.01	0.01	0.02	0.03	0.02	0.00
Molar ratio	1:1.2	1:1.2	1:1.2	1:1.2	1:1.2	1:1.2
Yield @ 3.2 w% (@720min)	0.58	0.70	0.88	0.96	0.99	1.00
Yield @ 20 w% (@720min)	0.59	0.71	0.89	0.97	1.00	1.00
Difference	0.01	0.01	0.01	0.01	0.00	0.00
Yield @ 3.2 w% (@360min)	0.55	0.60	0.74	0.87	0.95	1.00
Yield @ 20 w% (@360min)	0.55	0.62	0.77	0.90	0.97	1.00
Difference	0.01	0.01	0.03	0.03	0.03	0.00
Molar ratio	1:2	1:2	1:2	1:2	1:2	1:2
Yield @ 3.2 w% (@720min)	0.71	0.80	0.93	0.99	1.00	1.00
Yield @ 20 w% (@720min)	0.72	0.81	0.94	0.99	1.00	1.00
Difference	0.01	0.01	0.01	0.00	0.00	0.00
Yield @ 3.2 w% (@360min)	0.68	0.72	0.83	0.92	0.97	1.00
Yield @ 20 w% (@360min)	0.69	0.74	0.85	0.95	0.99	1.00
Difference	0.01	0.01	0.03	0.03	0.02	0.00

4.3.4. Synthesis of n-propyl-propionate

The framework for hybrid process design/analysis has been tested by generating and verifying hybrid scheme for synthesis of n-propyl-propionate from 1-propanol and propionic acid. N-propyl propionate is used as paint thinner, food additive and essence for perfumes by giving an apple-like, fruity taste. This ester is commercially available from Dow Chemical Company with a minimum purity of 99.5 wt% (The Dow Chemical Company, 2006).

4.3.4.1. Stage 1: Hybrid process design and analysis

4.3.4.1.1. Step 1a: Separation task and reaction data analysis

The reaction data related to synthesis of n-propyl propionate is analysed in this step. The work-flow along with the tools used in this step are highlighted in Figure 4.45, where, shaded boxes indicate the tools used, the white boxes indicate the tools needed for this problem but not for this step and the lined boxes indicate the steps/tools not needed for this problem.

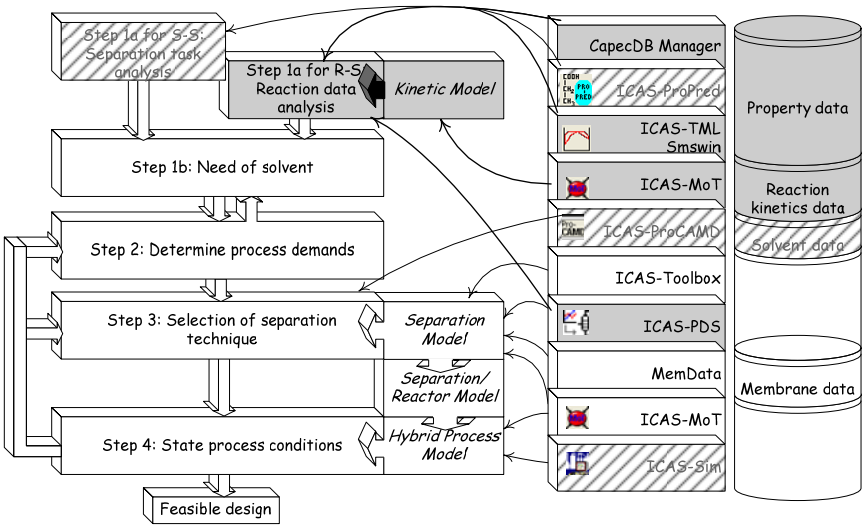

Figure 4.45: Work flow along with used tools at step 1 in the case study of synthesis of n-propyl propionate

1a.1. Identify mixture type

The reaction system consists of water and three organic chemicals, 1-propanol, propionic acid and n-propyl propionate. According to the mixture classification rule (Gani & O'Connell, 1989) the mixture in the reactive system is classified as non-ideal and aqueous type. Therefore for phase equilibria calculations involving this mixture, the Modified UNIFAC (Lyngby) (Larsen et al., 1987) is selected for calculations of activities in the liquid phase. The vapour phase is modelled with SRK equation of state (Soave, 1972).

1a.2. Analysis based on pure component properties

Since the largest melting temperature is 273.15 K and the lowest boiling temperature is 370.35 K, the mixture can be assumed to be in the liquid state at 1 atm for temperature between 273.15-370.35 K. Since the solubility parameter of water is almost two times higher than that of other compounds in the reacting mixture, formation of a second liquid phase is very likely (see Table 4.27).

Table 4.27. Boiling points, melting points and solubility parameters of pure compounds

Compound	T_b [K] @ 1atm.	T_m [K]	*Sol. Par.* [$MPa^{0.5}$]
1-propanol	370.35	146.95	24.4518
water	373.15	273.15	47.8127
n-propyl propionate	395.65	197.25	17.5677
propionic acid	414.25	252.45	19.4116

1a.3. System analysis based on mixture properties

The total number of binary pairs that needs to be analysed with respect to their boiling points is 6. The results of phase equilibrium calculations given in Table 4.28, show the presence of three binary azeotropes. Also, the presence of a ternary azeotrope was identified.

Table 4.28. List of azeotropes present in analysed mixture. In calculation the Modified UNIFAC (Lyngby) (Larsen et al., 1987) has been used in SMS Win (SMS Windows 2.0). POH: 1-propanol, PAc: propionic acid, ProPro: n-propyl propionate.

Composition	Type of azeotrope	Molar fraction [%]				T [K] @ 1atm.
		POH	H_2O	ProPro	ProAc	
POH – H_2O – ProPro	Heterogeneous	24.50	57.82	17.68	-	359.46
ProPro – H_2O	Heterogeneous	-	68.63	31.37	-	363.14
H_2O – ProAc	Homogeneous	-	93.34	-	6.666	372.69
H_2O – POH	Heterogeneous	57.26	42.74	-	-	361.88

1a.4. Reaction analysis

The esterification of 1-propanol with propionic acid to n-propyl propionate and water is represented by the Eq. (4.36).

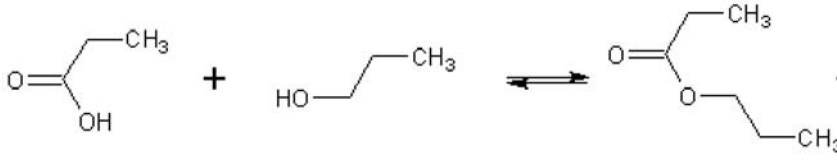

(4.36)

The reaction kinetics of this heterogeneous esterification reaction has been studied by Duarte et al. (2006) at a pressure of 5 atm and temperatures ranging from 363.15 K to 383.15 K. The reaction takes place only in the liquid phase in the presence of a heterogeneous catalyst Amberlyst 46, which is an acidic ion-exchange resin and can withstand a maximum temperature of 393.15 K. The use of this very selective catalyst eliminates other competing etherification reactions to form di-n-propyl ether and dehydration of propanol to propene. The chemical equilibrium of this reaction is expressed in terms of component activities (Duarte et al., 2006):

$$K_{eq} = \frac{a_{ProPro} \cdot a_{H2O}}{a_{PAc} \cdot a_{POH}} \tag{4.37}$$

To be sure that experimental data and equilibrium constant (K_{eq}) reported by Duarte et al. (2006) represent the chemical equilibrium the reactive flash calculation has been performed. Initial reactor compositions reported by Duarte et al. (2006) at various temperatures and pressure of 5 atm were used as input for calculations of the reactive flash operations (performed with ICAS-PDS). Only three chemical elements were needed by the element-based method of Pérez-Cisneros et al. (1997) since only one independent reaction was considered (see Table 4.29). The differences in the measured component concentration (x_i^{exp}) reported by Duarte et al. (2006) and those obtained by reactive flash calculations (x_i^{RF}) in this work are very small (see the last column of Table 4.30). This confirms that all experiments reached chemical equilibrium. Therefore, reaction parameters (K_{eq} and reaction rate parameter) given by Duarte et al. (2006) describe this reaction system very well. Moreover, the assumption that only esterification reaction takes place, when Amberlyst 46 is used as catalyst, is also correct.

Table 4.29. Chemical element matrix used in reactive flash calculation

Chemical elements / Components	C_3H_8O	C_3H_4	H_2O
1-propanol	1	0	0
propionic acid	0	1	1
n-propyl propionate	1	1	0
Water	0	0	1

Table 4.30. Experimental equilibrium compositions data versus composition obtained in reactive flash calculation. P = 5 atm. POH: 1-propanol, PAc: propionic acid, ProPro: n-propyl propionate.

No of exp		1	2	3	4	5	6	7	8
T [K]		383	383	373	373	373	373	363	363
Experimental equilibrium data (Duarte et al., 2006)	x_{POH}^{exp}	0.1797	0.4054	0.1908	0.191	0.1823	0.4018	0.4098	0.1826
	x_{PAc}^{exp}	0.1641	0.0609	0.1785	0.1838	0.1727	0.0671	0.0699	0.1718
	x_{ProPro}^{exp}	0.3281	0.2668	0.3153	0.3126	0.3225	0.2655	0.2602	0.3228
	x_{H2O}^{exp}	0.3281	0.2668	0.3153	0.3126	0.3225	0.2655	0.2602	0.3228
Reactive flash (UNIFAC (Fredenslund et al., 1977) and SRK)	x_{POH}^{exp}	0.1943	0.4109	0.1912	0.1885	0.1898	0.4026	0.4057	0.189
	x_{PAc}^{exp}	0.1787	0.0664	0.1789	0.1813	0.1802	0.0679	0.0658	0.1782
	x_{ProPro}^{exp}	0.3135	0.2613	0.3149	0.3151	0.3155	0.2647	0.2643	0.3164
	x_{H2O}^{exp}	0.3135	0.2613	0.3149	0.3151	0.3145	0.2647	0.2643	0.3164
$\sum(x_i^{exp} - x_i^{RF})^2$		$8.57 \cdot 10^{-4}$	$1.21 \cdot 10^{-4}$	$7.03 \cdot 10^{-7}$	$2.42 \cdot 10^{-5}$	$2.24 \cdot 10^{-4}$	$2.43 \cdot 10^{-6}$	$6.67 \cdot 10^{-5}$	$1.64 \cdot 10^{-4}$

Based on the reactive flash calculation performed at a wide range of temperature (350-415 K) at atmospheric pressure, the phase fraction diagram was plotted in Figure 4.46. The reactant ratio in all these calculations was 1:1 (1-propanol : propionic acid). The two phase region is between 363.4 K and 376.7 K.

The maximum temperature at which only liquid is present is 363.4 K, therefore, this temperature is considered as the maximum operating temperature.

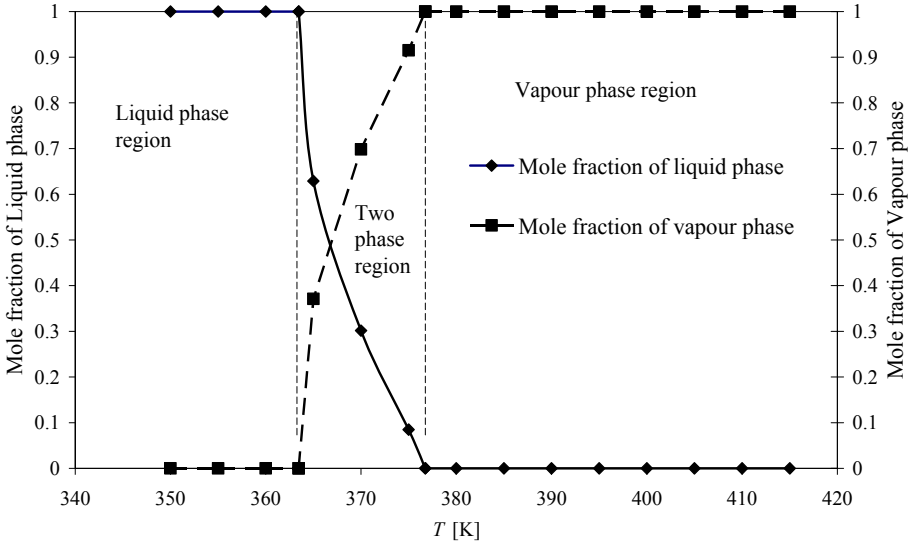

Figure 4.46: Phase fraction distribution at $P = 1$ atm. Obtained in reactive flash calculation for substrate ratio 1:1.

Simulations of the batch operation of the reactor were performed to determine the relationship between the product yield and feed ratios of 1-propanol to propionic acid. The results, plotted in Figure 4.47, indicate that process yield increases with increase of the molar ratio. However, the increase of molar ratio above 3 does not give significant increase in the yield, therefore, a range for this design variable between 2 and 3 is recommended.

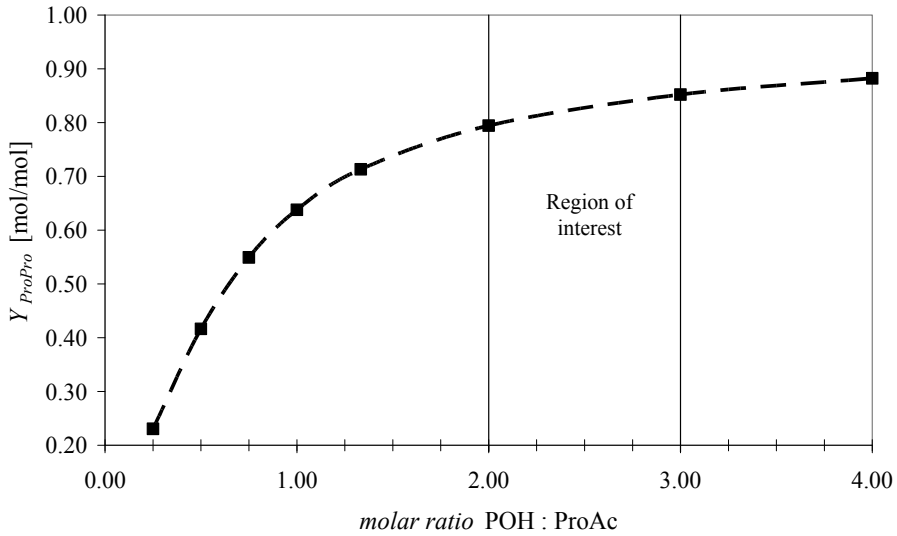

Figure 4.47: Yield of propyl-propionate versus molar ratio POH : ProAc at $T = 353.15$ K. POH: 1-propanol, ProAc: propionic acid. $Y_{ProPro} = \left(n^{eq}_{ProPro} - n^{in}_{ProPro}\right) / n^{in}_{PAc}$

4.3.4.1.2. Step 1b: Need of solvent

In this study, the use of solvents has not been investigated since all reactants are liquid and miscible within the operation window. However we foresee addition of non-reactive solvents to create the second liquid phase with only water, thereby, decreasing the activity of the products and moving reaction towards the product.

4.3.4.1.3. Step 2: Determine process demands

In this case study, the focus is on the batch operation of the process. The main objective is to obtain as high a conversion of the acid to the ester product as possible. More precisely, a molar process yield should be higher than 0.9. The process yield is defined as the ratio between moles of ester produced to the initial moles of the acid. The time of a batch operation is limited to 12 hours and the pressure is maintained at 1 atm.

4.3.4.1.4. Step 3: Selection of separation techniques

Since the continuous removal of product and/or products is likely enhance the conversion of the reactants; therefore in this step, techniques for downstream separation of the reactor effluents are identified through the procedure outlined in section 3.2.1.4 for step 3 of the methodology (see Figure 4.48).

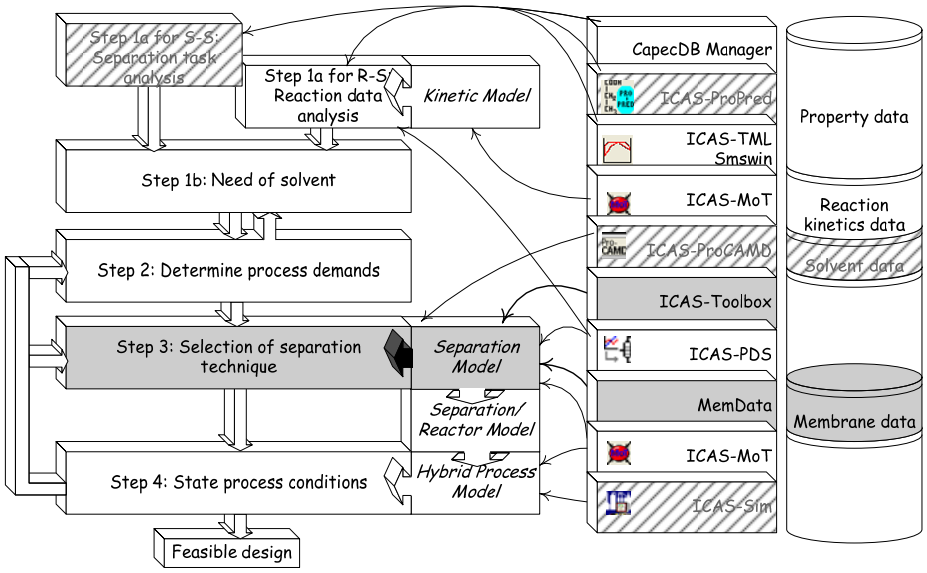

Figure 4.48: Work flow along with used tools at step 3 in the case study of synthesis of n-propyl propionate

R3.1. Identify compound(s) to remove from reaction medium

Since the reaction is equilibrium controlled, the addition of the reactant in excess will increase the conversion of the limiting reactant, while, removal of the product(s) will push the equilibrium towards the product(s) and simultaneously increase the overall

conversion. Two options have been considered: (1) remove the main product ester and (2) remove water. When the removing the ester, it has to be kept in mind the formation of heterogeneous azeotropes between alcohol, water and ester. Second option, to remove water, is advantageous since it is present in all binary and ternary azeotropes (see Table 4.28). By removing water from that quaternary mixture, the potential difficulties in downstream separation is eliminated as the remaining compounds in the ternary mixture do not form azeotropes with each other.

R3.2. Feasibility of distillation

In next step, the relative volatility of components are calculated. The mixture of 1-propanol, propionic acid, n-propyl propionate and water at chemical equilibrium has been used as a feed to a 2-phase (VLE) flash calculation. The list of compounds ranked according to their boiling points and corresponding relative volatilities is given in Table 4.31. None of the reaction products are either on the top or bottom of this list and so the use of simple distillation to increase the reaction product yield is not possible. It is important, however, to highlight the significant differences in the relative volatilities between products (water and ester), which point out possibility of the use of reactive distillation to separate them. Alternatively, the compounds 1-propanol, water and n-propyl propionate form a heterogeneous azeotrope, which is likely to form in the top of the column. Despite these disadvantages Buchaly et al. (2007) reported feasibility of using distillation to the same reactive system obtaining very high conversion of propionic acid.

Table 4.31. Relative volatility of compounds in the post reaction mixture computed at boiling point

Compound		$\alpha_{i,ProAC}$	$\alpha_{i,ProAC}$	$\alpha_{i,ProAC}$
1-propanol (T_b = 370.35 K)		6.13	6.32	6.36
water (T_b = 373.15 K)		14.44	17.32	17.05
n-propyl propionate (T_b = 395.65 K)		4.72	4.75	5.39
propionic acid (T_b = 414.25 K)		1.00	1.00	1.00
Feed composition to flash	1-propanol	0.18	0.39	0.53
	propionic acid	0.18	0.07	0.03
	n-propyl propionate	0.32	0.27	0.22
	water	0.32	0.27	0.22

R3.3. Feasibility of membrane-based separation

Many membrane-based separation processes offer selective removal of a specific compound, for example, pervaporation and vapour permeation are widely used for dehydration of organic mixtures (Koszorz et al., 2004). Comparison of driving force curves for different membrane processes for separation of a binary mixture of 1-propanol and water is presented on Figure 4.49. Since reaction proceeds in liquid phase, pervaporation is favourable compared to vapour permeation because it does not need phase change for the input to the membrane separation unit.

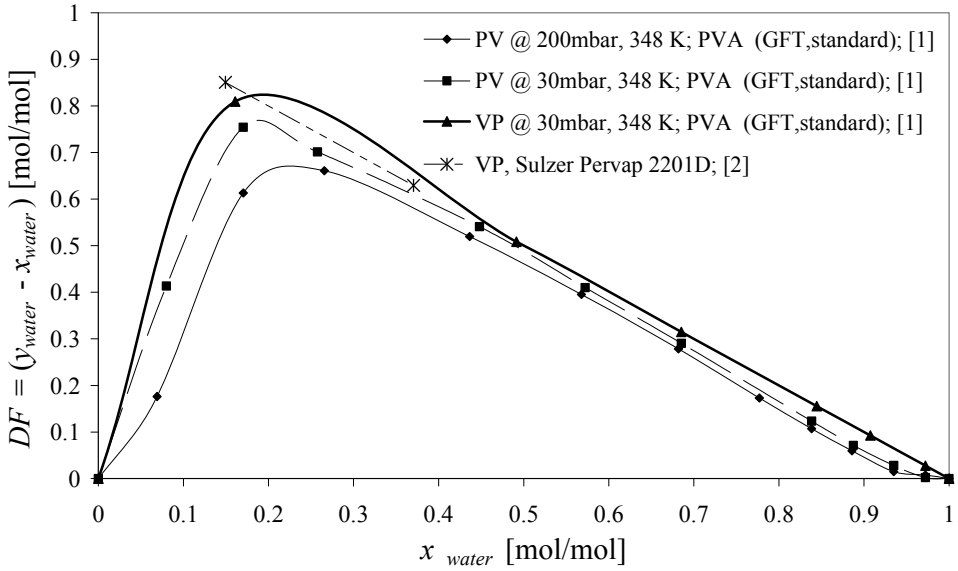

Figure 4.49: Driving force diagrams for membrane-based separation of binary mixture 1-propanol - water. VP - vapour permeation, PV – pervaporation, PVA – poly(vinyl alcohol) membrane, [1] – Will and Lichtenthaler, 1992, [2] – Kreis, 2007.

R3.4. Solvent selection

As it was already explained above (see section 4.3.4.1.2), addition of solvent is not investigated in this work.

R3.5. Separation technique selection

High selectivity towards water and a relatively large driving force available for pervaporation makes it a favourable candidate for further investigation.

4.3.4.1.5. Step 4: Establish process conditions

In this step, hybrid process schemes and their corresponding simulation models are developed (see Figure 4.50). The specific model is simulated at various conditions. Based on a superstructure (see Figure 3.5) the configuration as shown in Figure 4.51, where *Process 1* is a reactor and *Process 2* is a membrane-based separator for selective removal of water, is obtained. Since Amberlyst 46 is a heterogeneous

catalyst, the packed bad reactor with an additional tank to maintain a specific hold-up in the processing system is required. In order to utilize the Amberlyst 46 catalyst, a liquid feed to the reaction zone is required.

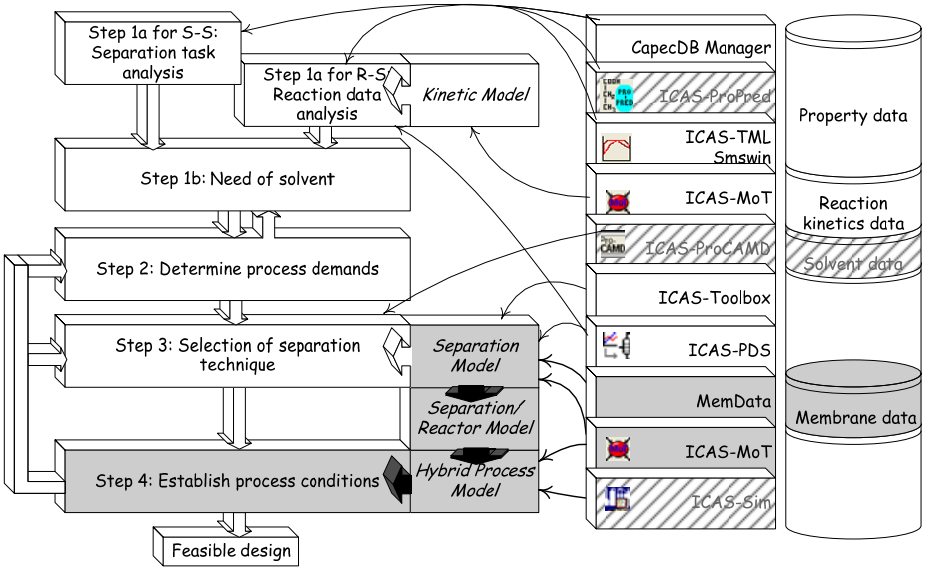

Figure 4.50 : Work flow along with used tools at step 4 in the case study of synthesis of n-propyl propionate

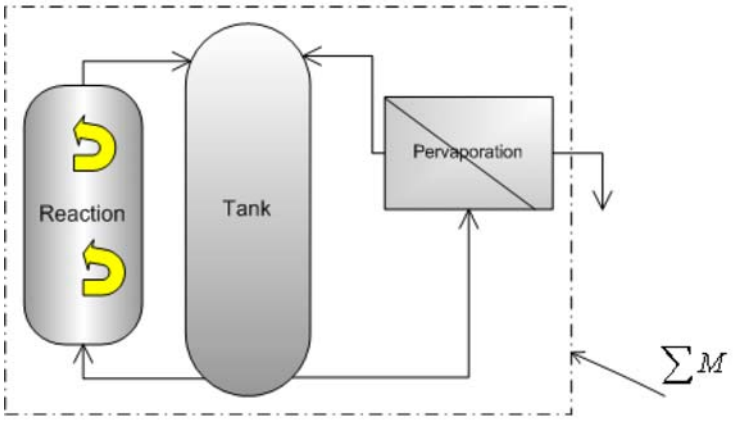

Figure 4.51: Conceptual process configurations: membrane assisted hybrid batch reaction scheme.

However, in this study the focus is on the membrane assisted batch reaction where a membrane is used in the pervaporation operation. From the general model (see section 3.2.1.5) a dynamic process model is generated based on the following assumptions:

A1. Reaction occur only with the use of catalyst,

A2. Reaction occur only in the liquid phase,

A3. Existence of a constant trans-membrane component flux,

A4. Short resident times in reaction (≤15 s) and separation (≤1 s) zones

A5. Constant flow rate around pervaporation and reaction zones.

The generated dynamic process model for the process system represented by Figure 4.51, using generic hybrid model (Eqs. 3.13, 3.15 - 3.32) with following decisions variables follow $\xi^{1}=1$, $\xi^{2}=1$, $\xi^{1in}=0$, $\xi^{2in}=0$, $\xi^{1\alpha}=0$, $\xi^{1\beta}=0$, $\xi^{2\alpha}=1$, $\xi^{2\beta}=0$, $\xi^{R}=1$, $\xi^{R\beta}=0$, $\xi^{(homog)}=0$, $\xi^{(heterog)}=1$ is obtained:

$$\frac{dn_i}{dt} = -a\sigma_i^{2\alpha} x_i^{1\alpha} F_{TOT}^{1\alpha} + \sum_{k=1}^{NKR} \nu_{i,k}^{1\alpha} r_k^{1\alpha(heterog)} \tag{4.38}$$

$$F_i^{1\alpha} = a x_i^{1\alpha} F_{TOT}^{1\alpha} \tag{4.39}$$

$$F_i^{2\alpha} = a\sigma_i^{2\alpha} x_i^{1\alpha} F_{TOT}^{1\alpha} \tag{4.40}$$

$$F_i^{2\beta} = a\sigma_i^{2\beta} x_i^{1\alpha} F_{TOT}^{1\alpha} \tag{4.41}$$

$$F_i^{1\alpha R} = F_i^{1\alpha} \tag{4.42}$$

$$F_i^{1\beta R} = F_i^{1\beta} \tag{4.43}$$

$$F_i^{2\alpha P} = F_i^{2\alpha} \tag{4.44}$$

$$F_i^{2\beta R} = F_i^{2\beta} \tag{4.45}$$

$$r_h^{1\alpha(heterog)} = k_p^{(heterog)} m_{cat} L \prod_{i=1}^{NRK} \left(a_i^{1\alpha}\right)^{\upsilon_{i,h}^{1\alpha}} \tag{4.46}$$

$$a_i^{1\alpha} = x_i^{1\alpha} \gamma_i^{1\alpha} \tag{4.47}$$

$$x_i^{1\alpha} = \frac{n_i}{\sum_{i=1}^{NC} n_i} \tag{4.48}$$

$$a = if\ (t \geq t_{switch})\ than\ (1)\ else\ (0) \tag{4.49}$$

From the definition of separation factor, the separation factor $\sigma_i^{2\alpha}$ is:

$$\sigma_i^{2\alpha} = \frac{F_i^{2\alpha}}{x_i^{1\alpha} F_{TOT}^{1\alpha}} \tag{4.50}$$

The above equations can be rearranged to obtain the following compact form of the model.

Component mass balance:

$$\frac{dn_i}{dt} = -a \cdot F_i^{2\alpha} + \nu_{i,h}^{1\alpha} r_h^{1\alpha(heterog)} \tag{4.51}$$

Constitutive equations:

$$r_h^{1\alpha(heterog)} = k_f \left(a_{POH}^{1\alpha} a_{PAc}^{1\alpha} - \frac{1}{K_{eq}} a_{ProPro}^{1\alpha} a_{H2O}^{1\alpha} \right) m_{CAT} L \tag{4.52}$$

$$k_f = k_0 e^{\left(\frac{-E}{RT}\right)} \tag{4.53}$$

$$K_{eq} = K_{0,eq} e^{\left(\frac{-E_{eq}}{RT}\right)} \tag{4.54}$$

$$a_i^{1\alpha} = x_i^{1\alpha} \gamma_i^{1\alpha} \tag{4.55}$$

$$x_i^{1\alpha} = \frac{n_i}{\sum_{i=1}^{NC} n_i} \tag{4.56}$$

Additionally if condition (Eq. 4.57) is added since hybrid operation is not required at the beginning.

$$a = if\ (t \geq t_{switch})\ than\ (1)\ else\ (0) \tag{4.57}$$

As indicated by Eq. (4.52) the kinetic model is based on the activities of each compound in the reacting system and therefore a model to calculate them is necessary. Duarte et al. (2006) used for this purpose, the Modified UNIFAC (Dortmund) model. In this paper, however, the Modified UNIFAC (Lyngby) model (Larsen et al., 1987) has been used. Therefore, the kinetic parameters have been recalculated using the Modified UNIFAC (Lyngby) model parameters (given in Table 4.32). The following values have been obtained for the kinetic model: $k_0 = 7.872 \cdot 10^9$ [mol·eq^{-1}·s^{-1}], $E = 63080$ [J·mol^{-1}], $K_{0,eq} = 3.511$, $E_{eq} = -4631.4$ [J·mol^{-1}]. This specific model consists of 16 equations (Eq. 4.51-4.57) and 37 variables. The degree of freedom is equal to 21 (not counting the model equations and variables for the calculation of the activities).

Table 4.32 Used parameters of modified UNIFAC (Lyngby) (Larsen et al., 1987)

	CH_2	OH	H_2O	CCOO	COOH	CH_2 (alc)
			A_{ij}			
CH_2	0	972.8	1857	329.1001	664.1001	0
OH	637.5	0	155.6	169.1	61.78	637.5
H_2O	410.7	-47.15	0	218	8.621	410.7
CCOO	44.43	266.8999	245	0	557.8999	44.43
COOH	171.5	-92.21	86.44	-224.6	0	171.5
CH_2 (alc)	0	972.8	1857	329.1	664.1	0
			B_{ij}			
CH_2	0	0.2687	-3.322	-0.1518	1.317	0
OH	-5.832	0	0.3761	0.1902	0	-5.832
H_2O	2.868	-0.4947	0	-0.4269	-1.709	2.868
CCOO	-0.9718	-1.054	-0.0717	0	1.377	-0.9718
COOH	-1.463	0	0.9941	-0.7234	0	-1.463
CH_2 (alc)	0	0.2687	-3.322	-0.1518	1.317	0
			C_{ij}			
CH_2	0	8.773	-9	-1.824	-4.904	0
OH	-0.8703	0	-9	4.625	0	-0.8703
H_2O	9	8.65	0	-6.092	6.413	9
CCOO	0.5518	3.586	2.754	0	0	0.5518
COOH	0.6759	0	-12.74	0	0	0.6759
CH_2 (alc)	0	8.773	-9	-1.824	-4.904	0

The process efficiency is defined here in terms of process yield with respect to n-propyl propionate, as given by Eq. (4.58):

$$Y_{ProPro}^{t} = \frac{\left(n_{ProPro}^{t} - n_{ProPro}^{in}\right)}{n_{PAc}^{in}} \tag{4.58}$$

Since a high conversion of acid is desirable, the introduction of excess of 1-propanol will shift the reaction towards higher ester concentrations. When the batch reactor is combined with the pervaporation unit, it is important to observe the influence of the amount of catalyst as well as the switching time from batch reaction into integrated mode. An increase in the ratio of catalyst mass (m_{cat}) and mass of reaction mixture (m_{mix}) increases the yield in the given processing time (for example 12 h of operation). It is also important to note that the switching time from batch reaction to the combined operation within the first two hours of the operating time of the process does not influence significantly the process yield (see Figure 4.52).

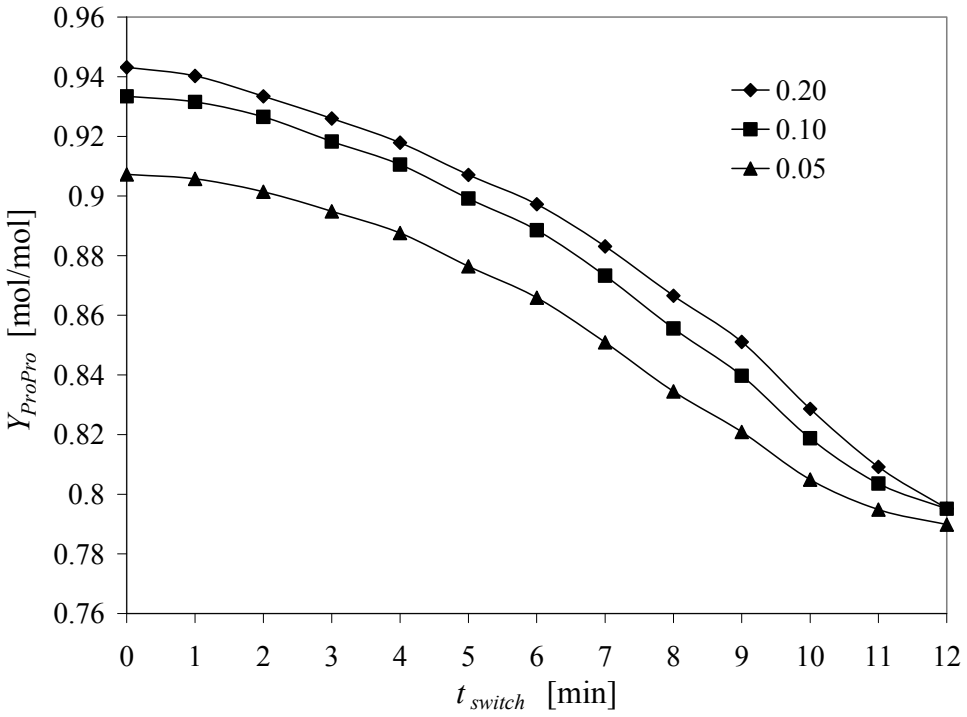

Figure 4.52: Yield of n-propyl propionate versus switching time and mass ratio of catalyst and reaction mixture; POH : ProAc = 2:1, T = 353.15 K, m_{mix} = 1393 g, $F_{\mathrm{ProAc}}^{2\alpha} = F_{\mathrm{ProOH}}^{2\alpha} = F_{\mathrm{ProPro}}^{2\alpha} = 0$ mol/s, $F_{\mathrm{H2O}}^{2\alpha} = 0.13$ mol/s (POH: 1-propanol, ProAc: propionic acid, ProPro: n-propyl propionate)

4.3.4.2. Stage 2: Implementation

The main purpose of performing experiments is to verify the feasibility of the

developed design for the production of the n-propyl propionate in a membrane assisted batch reaction (Figure 4.51). The first step is to establish through experiments the constituent models for reaction kinetic and the membrane separation for temperatures between 343 K and 353 K. For experiments establishing the membrane separation model, the following quaternary mixture has been used: 75 mol% of 1-propanol, 10 mol% of propionic acid, 10 mol% of n-propyl propionate and 5 mol% of water. Reaction kinetic model has been established through two experiments with different mass ratio of catalyst to reaction mixture, 0.22 and 0.14 where the initial molar reactant ratio was 2:1 (1-propanol : propionic acid). The membrane assisted batch reaction experiments were designed to verify the influence of selected operational variables on the overall process performance. These variables are the initial molar ratio of reactant (alcohol to acid), the mass ratio of catalyst to reaction mixture (m_{cat}/m_{mix}), and the switching time from batch reaction to the membrane assisted batch reaction mode as well as the process temperature. The experiment design for membrane assisted batch reaction is illustrated in Figure 4.53, where the performed experiments are highlighted by numbers. The operational variables corresponding to each experiment are listed in Table 4.33.

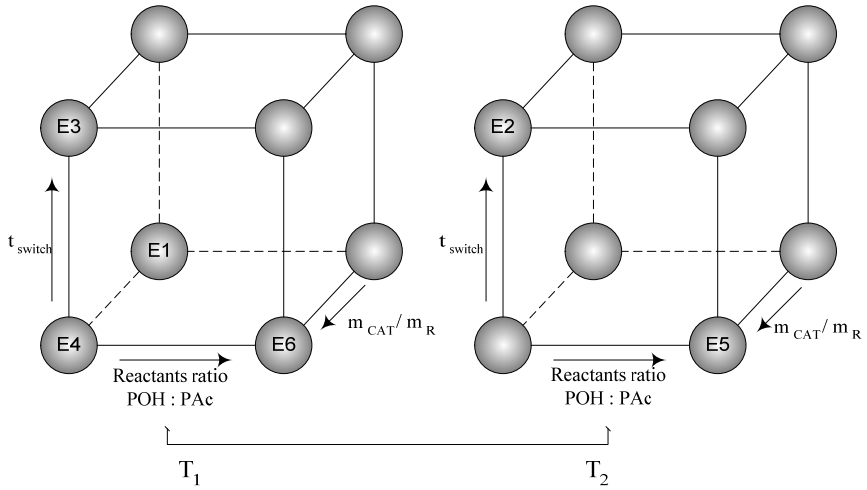

Figure 4.53: The 2^4 factorial design of experiments

Table 4.33: Proposed experiments (see Figure 4.53)

Exp No	E6	E5	E4	E3	E2	E1
T_R , T_M [K]	333	353	343	343	353	343
$m_{cat}/m_{mix\ (initial)}$ [g/g]	0.23	0.23	0.23	0.23	0.23	0.12
POH : ProAc [mol:mol]	3:1	3:1	2:1	2:1	2:1	2:1
Switching time [min]	60	60	60	135	135	60

4.3.4.2.1. Experimental set up

Based on proposed design on Figure 4.51 the multipurpose lab-scale plant at the Chair of Fluid Separation Processes at the University of Dortmund has been built (see Figure 4.55) where all the experiments were performed. The multipurpose lab-scale plant has been designed and constructed in order to perform following process operations:

(1) Heterogeneously catalysed batch reaction (operation around packed bed reactor (PBR) and tank (B1), see Figure 4.54-A),

(2) Membrane-based separation (operation around pervaporation unit (M1) and tank (B1), see Figure 4.54-B),

(3) Membrane assisted batch reaction (operation around pervaporation unit (M1), tank (B1) and pack bed reactor (PBR) see Figure 4.51).

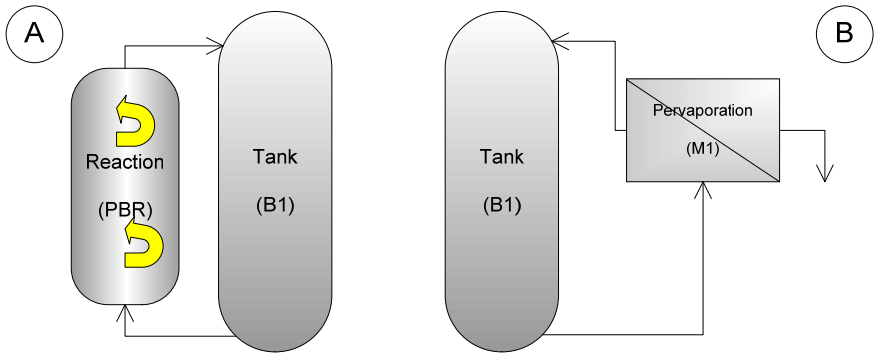

Figure 4.54: Experimental set-up configurations: A. heterogeneously catalysed batch reaction, B. membrane-based separation.

For the pervaporation experiments, a flat membrane PERVAP® 2201-D from Sulzer Chemtech with an active layer of polyvinyl alcohol (PVA) and a support layer of poly(acrylonitrile) (PAN) were used. The investigated membrane is a composite, asymmetric, and acid resistant membrane. It was placed in the flat test cell (M1) whose sizing parameters are as follows:

- membrane width: 60 mm
- membrane surface area: 161.4 cm^2
- gap between membrane and feed side's of module plate: 0.5 mm

The tank (B1, Figure 4.55) has a maximum volume of 1.7 dm^3. The packed-bed reactor (PBR) is constructed in such a way that various amounts of catalyst can be introduced (varying from 130 to 300 g). The inside diameter of the PBR is 50 mm. The pre-heater (W1) and tank (B1) have oil jackets with thermostats to control the temperature. The membrane module temperature can be controlled via a heating band. All equipments are appropriately insulated to assure isothermal conditions.

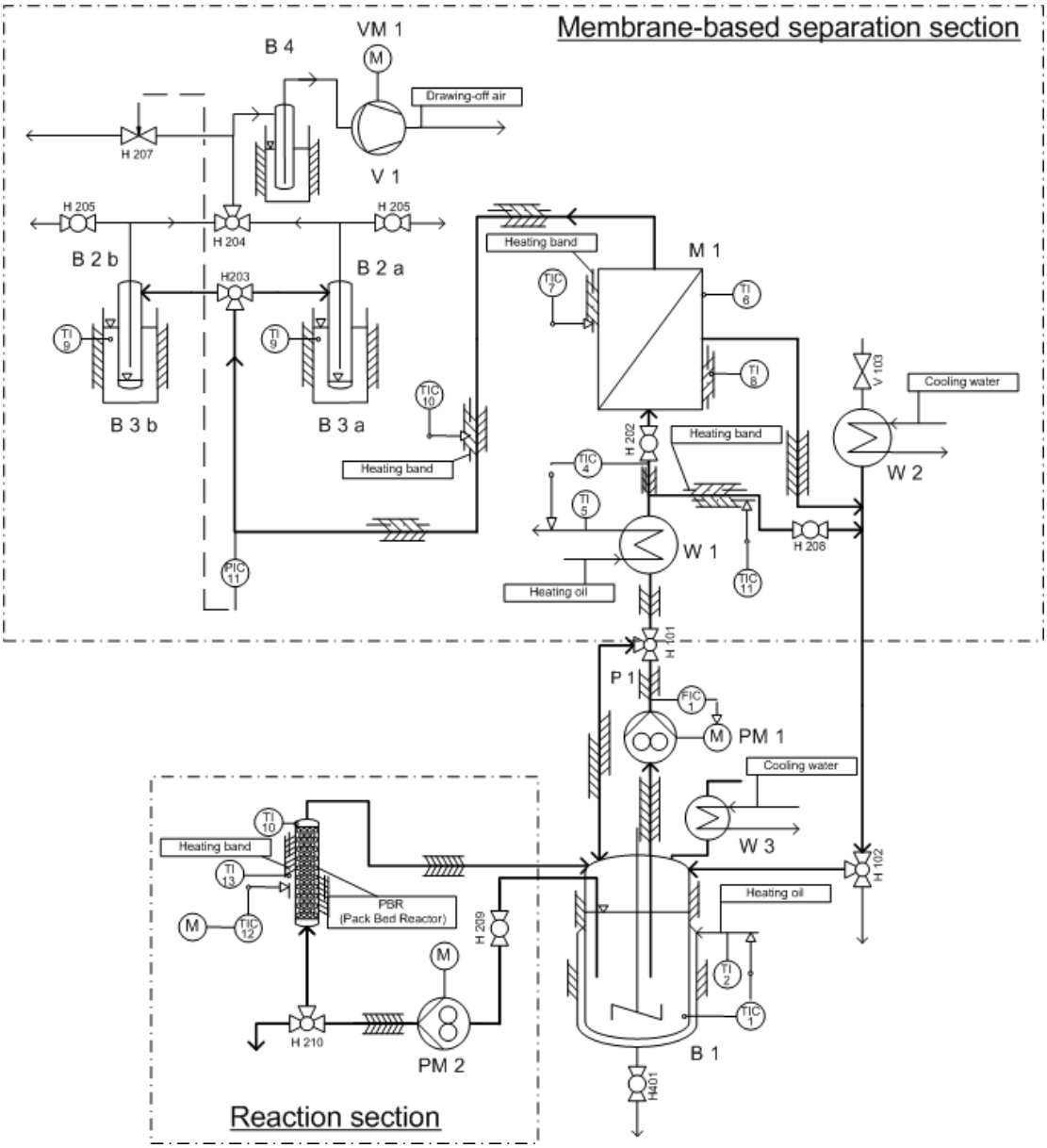

Figure 4.55 : Piping and Instrumentation Diagram (P&ID) of the multipurpose lab-scale membrane reactor. B1-tank, B2a, B2b-cooling trap for permeate, B3a, B3b-cooling vessels, B4-cooling trap for vacuum pump, H----valves, M-manual control, M1-membrane module, PM1, PM2-gear pump, TI-temperature indicator, TIC-temperature controller, V-ventilation, VM-vacuum pump, W1, W2, W3-Liebig condenser.

4.3.4.2.2. Experimental operational procedures

Since all performed experiments were batch operation, the dynamics of the reaction and separation systems have been studied. The procedures described below have been

applied to all experiments presented in this work. It is important to point out that after each experiment the experimental system has been cooled down step-by-step to 313.15°K and then cleaned with a mixture which originally contained 80 w% of POH and 20 w% of H2O. In order to guarantee that the catalyst does not change its characteristic the mixture used to clean is left in the packed-bed reactor until the next experiment. With respect to the membrane module, the vacuum pump VM1 was working permanently in order to avoid membrane destructions. All samples have been stored in a refrigerator until analysis.

4.3.4.2.3. Membrane-based separation (pervaporation)

Start-up

The liquid mixture to be separated is fed into the tank B1, pumped around the pre-heater W1 and heated step by step to obtain the desired experimental conditions. When a constant desired temperature is achieved, the liquid is pumped through the membrane module M1 (open H202 and close H208). Although membrane module was preheated, the temperature of the feed decreased. With continuous heating, it was possible to maintain the desired constant temperature. Measurements were started after the stationary temperatures in tank B1, pre-heater W1 and membrane M1 were attained.

Measurements

At time zero, positions for valves (H203 and H204) of the cooling trap were changed. After changing valves position, a sample was taken from the tank B1. Depending on the amount of the most favourable permeating compound (water), samples have been taken at intervals of 30, 60 and 90 minutes to ensure a sufficient amount of permeate in the cooling traps. At the end of the experiment, positions of valves of the cooling trap (H203 and H204) are changed to another cooling trap and a feed sample from B1 was taken in order to obtain average concentration of the feed (concentration in the feed changed due to compound removal). Next step was to shut-down the experimental set-up.

4.3.4.2.4. Heterogeneously catalysed batch reaction

Start-up

The desired amount of reactant 1-propanol was placed in the tank B1, pumped around the PBR reactor and heated to the desired temperature. When the liquid reached the desired temperature with an offset of 3 K in the outlet of the packed-bed reactor (PBR), the gear pump PM2 was stopped. Reactant propionic acid was now added to tank B1. The batch reaction experiment started after the mixture in the tank B1 achieved the desired temperature.

Measurements

The first sample is taken when the valve H209 was opened and pump PM2 was turned on. Depending on the progress of the reaction, the samples have been taken in

an interval of 2, 5, 10, 15, 30 and 60 minutes. Progress of the reaction was judged based on the batch reaction simulation performed with experimental initial conditions. Experiment was stopped with offset of 2 hours since reaction should reach the chemical equilibrium according to the performed simulation.

4.3.4.2.5. Membrane assisted batch reaction

Start-up is exactly the same as in the batch reaction procedure. Simultaneously to start of the reaction heating of the membrane unit started. The membrane reactor experiment started, when the feed is passed to the membrane module. Samples from the packed-bed reactor (PBR) were taken in 2, 5, 10, 15, 30, 60 and 120 minutes depending on the progress of the reaction. Permeate samples were taken in intervals of 30, 60, 120 and 240 minutes depending on the water concentration in the feed.

4.3.4.2.6. Analytical methods used for samples analysis

Gas chromatography

All samples which contained organic compounds were analysed with gas chromatography having a flame ionization detector (GC-FID) and equipped with an auto sampler where acetonitrile was used as an internal standard. Helium was utilised as a carrier gas. The component calibration curves were approximated by a set of piecewise linear functions. In order to assure correctness of the used component calibration curves during the analysis of samples taken in experiment, the test sample with known concentrations were introduced after analysis of 5 samples. If a test samples gave an inadequate result, a new calibration was performed. Since it was only possible to obtain mass fraction of organic compounds, the water concentration was calculated by the summation condition.

Karl Fischer titration

Karl Fischer (KF) Titrator model DL31 from Mettler Toledo was used for quantifying the water content in all reaction samples. With this analytical method it is possible to determine the water content of an unknown sample (for example sample taken during experiment) accurately from 100 ppm. HYDRANAL®-Water Standard 10 was used for the volumetric titre determination of Karl-Fischer reagents (1 g = 10.04 mg water). Water content determined by KF was used to crosscheck the GC-FID results.

4.3.4.2.7. Data reconciliation

The mass fraction of organic compounds obtained through GC analyses and water mass fraction obtained through KF titration need to satisfy summation condition of components mass fraction, Eq. (4.59). However, due to experimental errors this condition is not always satisfied and therefore, the solution of a data reconciliation problem is necessary.

$$\sum_{i=1}^{NC} w_i = 1 \tag{4.59}$$

The formulation of data reconciliation problem, Eq. (4.60), is posed with use of weighted least square where measured weight fractions of components were varied within their experimental error limits in order to minimize their error.

$$\begin{aligned} \text{Obj} &= \min \sum_{i=1}^{n} \frac{\left(\overline{w}_i^{\text{exp}} - w_i^{\text{reconciled}}\right)^2}{\sigma_{\text{i}}^2} \\ s.t. \quad & \sum_{i=1}^{n} w_i^{\text{reconciled}} - 1 = 0 \\ & w_i^{\text{reconciled}} - \left(\overline{w}_i^{\text{exp}} + \sigma_i\right) \le 0 \\ & \overline{w}_i^{\text{exp}} - \sigma_i - w_i^{\text{reconciled}} \ge 0 \end{aligned} \tag{4.60}$$

The uncertainty of weight fraction of 1-propanol, propionic acid and n-propyl propionate is calculated based on propagation of independent errors. Precisely, in this case uncertainty depends on error of GC analysis, errors related to preparation of sample and uncertainty of calibration and it is given by Eq. (4.61).

$$\sigma_i = w_i \left(\left(\frac{\sigma_{\text{A}_\text{i}}}{\overline{A}_{i/ACN}} \right)^2 + \left(\frac{\varepsilon_{\text{scale}}}{m_{\text{ACN}}} \right)^2 + \left(\frac{\varepsilon_{\text{scale}}}{m_{\text{Sample}}} \right)^2 + \left(\Delta s_{\max} \right)^2 \right)^{\frac{1}{2}} \tag{4.61}$$

for i = 1-propanol, propionic acid, n-propyl propionate

Error of sample preparation for GC analysis is equal to 0.0002 g which is a limitation of analytical scale ($\varepsilon_{\text{scale}}$). Since each sample is analysed by GC three times the standard deviation of pick area for each sample is calculated according to Eq. (4.62).

$$\sigma_{A_i} = \sqrt{\frac{\sum_{n=1}^{3} \left(A_{n,\,i/ACN} - \overline{A}_{i/ACN} \right)^2}{n-1}} \tag{4.62}$$

where $A_{n,\,i/ACN} = \dfrac{A_{\text{n, i}}}{A_{\text{n, ACN}}}$, $A_{n,i}$ is a pick area corresponding to a component present in the original mixture at n-th injection of sample to the GC, $A_{n,ACN}$ is a pick area of internal standard.

The uncertainty of water content in the sample measured directly by KF depends on accuracy of each measurement which is set to 0.0002 g/g ($\Delta\varepsilon_{\text{analysis}}$). The error of water weight fraction measurement through KF titration is calculated according to Eq. (4.63):

$$\sigma_{\mathrm{H2O}} = \overline{w}_{\mathrm{H2O}} \left(\left(\frac{\sigma_{\mathrm{w_{H2O}}}}{\frac{1}{NoA}\sum_{n=1}^{NoA} w_{n,\mathrm{H2O}}} \right)^2 + \sum_{n=1}^{NoA} \left(\frac{\Delta\varepsilon_{\mathrm{analysis}}}{w_{n,\mathrm{H2O}}} \right)^2 \right)^{\frac{1}{2}} \tag{4.63}$$

where:

$$\sigma_{w_{H2O}} = \sqrt{\frac{\sum_{n=1}^{NoA} \left(w_{n,\,H2O} - \overline{w}_{H2O} \right)^2}{NoA - 1}} \tag{4.64}$$

4.3.4.3. Stage 3: Validation

The process conditions, such as, the ratio of the mass of catalyst to the mass of the reactants, the reactants ratio, the operating temperature as well as the switching time have significant influence on the overall process performance, and therefore, these have been further investigated. Validation results in terms of experimental observations as well as simulations corresponding to the experimental measurements are presented. All simulations results have been obtained through the ICAS-MoT modelling tool (Sales & Gani, 2003).

4.3.4.3.1. Heterogeneously catalysed batch reaction

The reaction kinetic data has been verified with the aid of two experiments of heterogeneously catalysed batch reaction (see Figure 4.54-A). The simulation of the heterogeneously catalysed batch reaction utilised the model which is presented in details in Appendix (section 6.4.4.1, page 220). The transient concentrations profiles presented in Figure 4.56 (symbols indicate measured data) represent batch reaction experiment performed at average temperature of 353.35 K. It can be noted from Figure 4.56 that the concentration of substrates (1-propanol and propionic acid) are decreasing over time while the concentration of products (n-propyl propionate and water) are increasing, that is, as reaction takes place. The lines shown in Figure 4.56 represent a simulation result which is in good agreement with experimental points (with accuracy of within 1 %). The measured system was considered to be at chemical equilibrium when the concentrations of reactants and products did not change significantly after 150 minutes. Another comparison of experimental measurements with simulated results is presented in Figure 4.57 for another set of the operational variables. The good match between experimental measurements and simulated results validate the activity-based kinetic model.

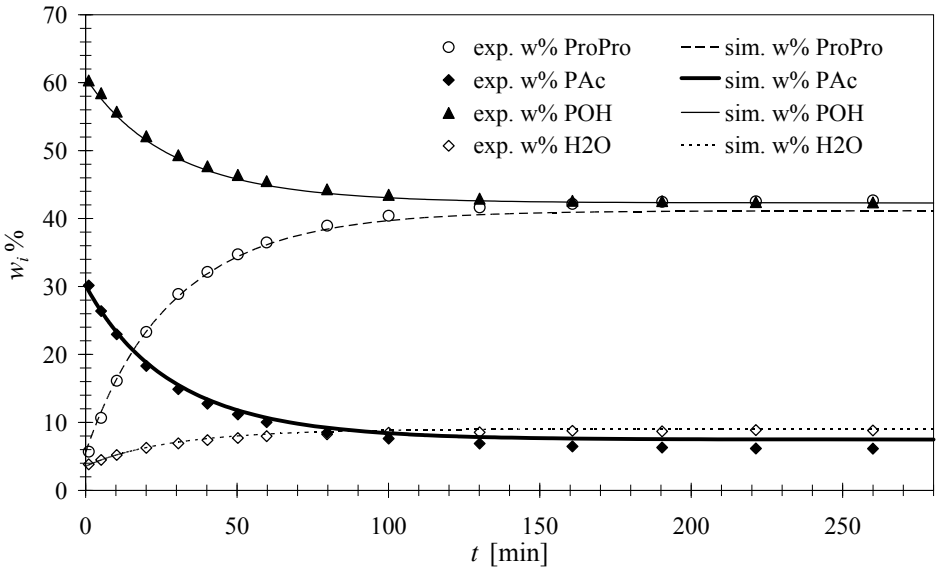

Figure 4.56: Batch reaction experiment, $T = 353.35$ K, $m_{cat}/m_{mix} = 0.22$, POH:ProAc = 2:1, $m_{mix} = 1328.9$ g (ProPro: n-propyl propionate; ProAc: propionic acid; POH: 1-propanol)

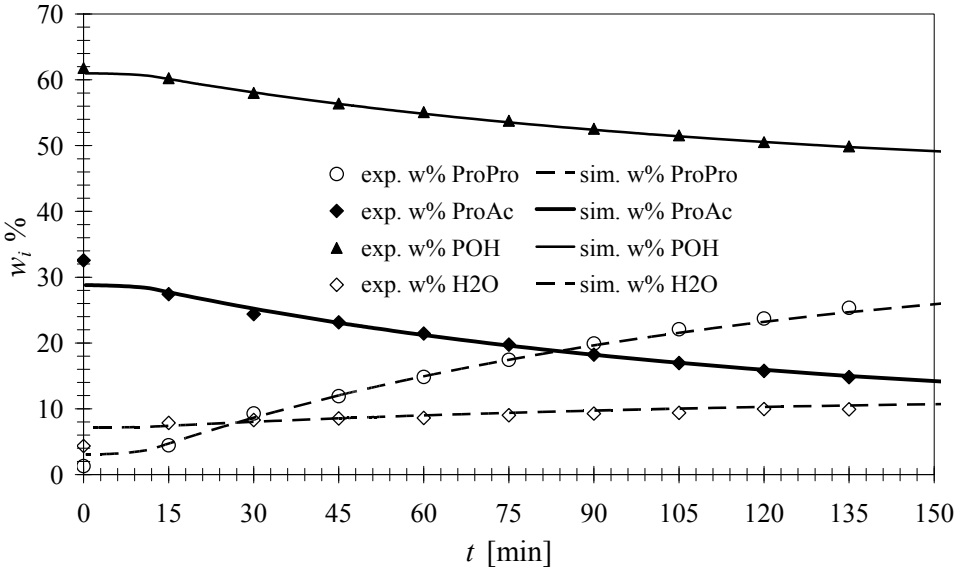

Figure 4.57: Batch reaction experiment, $T = 341.15$ K, $m_{cat}/m_{mix} = 0.14$, POH:ProAc = 2:1, $m_{mix} = 950$ g (ProPro: n-propyl propionate; ProAc: propionic acid; POH: 1-propanol)

4.3.4.3.2. Membrane-based separation: pervaporation

In section 4.3.4.1.5 the constant removal of only one component, water, has been

simulated. For better prediction and comparison of the membrane assisted batch reaction simulation with experimental data, more detailed pervaporation model is required. The trans-membrane component flux in pervaporation process has been modelled with the semi-empirical Meyer-Blumenroth model (Lipnizki & Trägårdh, 2001). This model is based on the solution-diffusion model and includes the effect of coupling of components present in the mixture. The one-dimensional component flux through the membrane (J_i) is proportional to the driving force across the membrane which is expressed by the difference in activities between feed side (a_i^F) and permeate side (a_i^P), and proportional to the ratio of component permeability (P_i) through the membrane and average component activity coefficient across the membrane ($\overline{\gamma}_{M,i}$) (see Eq. 4.65).

$$J_i = \frac{P_i}{\overline{\gamma}_{M,i}}\left(a_i^F - a_i^P\right) \tag{4.65}$$

The temperature dependence of component permeability has a form of Arrhenius-type equation:

$$P_i = P_i^0 \exp\left(-\frac{E_i}{R}\left(\frac{1}{T_M} - \frac{1}{T_R}\right)\right) \tag{4.66}$$

where T_M is a temperature at the membrane and T_R is the reference temperature (333.15 K). The average activity coefficient across the membrane is calculated according to Eq. (4.67).

$$\overline{\gamma}_{M,i} = \sqrt{\gamma_{M,i}^F \gamma_{M,i}^P} \tag{4.67}$$

The activity coefficients at membrane ($\gamma_{M,i}^F$, $\gamma_{M,i}^P$) are correlated by the relationship which includes effect of coupling by means of empirical coupling coefficients (B_{ij}) related to component activities in the feed (a_j^F) and permeate (a_j^P):

$$\gamma_{M,i}^F = \exp\left(B_i^\circ\left(1 - \sum_{j=1}^{NC} B_{ij} a_j^F\right)\right) \tag{4.68}$$

$$\gamma_{M,i}^P = \exp\left(B_i^\circ\left(1 - \sum_{j=1}^{NC} B_{ij} a_j^P\right)\right) \tag{4.69}$$

The activity on the feed side (a_i^F) depends on the composition and is calculated using Modified UNIFAC (Lyngby). The activity on permeate side due to low pressure (5-20 mbar) is assumed to follow the ideal gas. That is:

$$a_i^P = \frac{P^P y_i}{P^\circ} \tag{4.70}$$

Detailed analysis of this model, used for calculation of transmembrane fluxes is given in Appendix (section 6.4.4.2, page 221). Model parameters presented in Table 4.34

were obtained in earlier experiments (Kreis, 2007). However, before performing the membrane reactor experiments a set of pervaporation experiments were conducted in order to verify the applicability of the proposed pervaporation model. The experimental flux has been calculated using Eq. (4.71) and the feed composition by Eq. (4.72).

$$J_i^{\exp} = \frac{m_{permeate} \cdot w_i^{P,\exp}}{A_m \cdot \Delta t} \tag{4.71}$$

$$\overline{w}_i^{F,\exp} = \frac{w_i^{F,initial} + w_i^{F,final}}{2} \tag{4.72}$$

From results presented in Table 4.35 and Table 4.36 it is clear that PERVAP® 2201D membrane is highly selective towards water because the permeate consists of more than 99% water. Only traces of organic compounds were found in permeate. The flux of water was found to increase 4 times when temperature was increased by 25 K.

Table 4.34. Membrane model parameters (Kreis, 2007)

	B_{ij}				$B_i°$	P_i	E_i
	ProAc	POH	ProPro	H2O			
propionic acid	1	0	0	0	0	0	0
1-propanol	0	1	0	0	0	0	0
n-propyl propionate	0	0	1	0	0	0	0
water	-0.2500	-0.1500	-0.5356	1.0000	5.7590	82.5	0.0691

Table 4.35. Pervaporation experiment at T = 346.15 K, P_P = 10 mbar

Compounds	$\overline{w}_i^{F,\exp}$ [g/g]	$w_i^{P,exp}$ [g/g]	J_i^{exp} [g/(m^2·min)]	J_i^{calc} [g/(m^2·min)]
propionic acid	0.0890	0.0007	0.0399	0.0000
1-propanol	0.7400	0.0054	0.0006	0.0000
n-propyl propionate	0.0931	0.0001	0.0011	0.0000
water	0.0778	0.9939	7.4397	7.5080

Table 4.36. Pervaporation experiment at T = 326.15 K, P_P = 8 mbar

Compounds	$\overline{w}_i^{F,\exp}$ [g/g]	$w_i^{P,exp}$ [g/g]	J_i^{exp} [g/(m^2·min)]	J_i^{calc} [g/(m^2·min)]
propionic acid	0.0885	0.0005	0.0091	0.0000
1-propanol	0.7305	0.0049	0.0014	0.0000
n-propyl propionate	0.0909	0.0001	0.0007	0.0000
water	0.0901	0.9945	1.8436	1.8775

4.3.4.3.3. Membrane assisted batch reaction

In this section the dynamic process model (presented in subsection 4.3.4.1.5) with semi-empirical Meyer-Blumenroth model for calculation of component flux (given in subsection 6.4.4.2) is used. The detailed analysis of whole model used in this section is given in Appendix (section 6.4.4.3). Six membrane assisted batch reaction experiments were performed in order to verify the applicability of used process model in the range of variations of process operational variables. A summary of all experiments is presented in Table 4.37 where the product yield (measured) is calculated through Eq. (4.73).

$$Y_{exp,\mathrm{ProPro}} = \frac{\left(\frac{m_{PAc}^{in}}{M_{wPAc}}\right) - \left(m_{total}^{in} - m_{total,Permeate}^{t}\right)\left(\frac{w_{PAc}^{in}}{M_{wPAc}}\right)}{\left(\frac{m_{PAc}^{in}}{M_{wPAc}}\right)} \tag{4.73}$$

The objective of the membrane assisted batch reaction process is to remove one of the products from the reacting mixture and therefore move reaction equilibrium towards a higher product yield. The heterogeneously catalyzed batch reaction is allowed to progress until a switching time, which is the time when the membrane assisted batch reaction process starts and it is pointed by the perpendicular dashed line on all plots (Figures 4.58-4.63). As highlighted in Figures 4.59-4.64 when the hybrid process is operated at temperature above 345 K, the water fraction decreases immediately after switching time, indicating that separation is faster than reaction and leads to the higher product yield. The same is observed for all membrane assisted batch reaction operations indicate thereby, a higher conversion of reactants into the desired ester. From experiments it is clear that increase of process temperature increases the product yield (E6 and E5 increase 3%, E3 and E2 increase 2%). When comparing E4 and E3 the switching time has little influence on yield.

The experimentally measured data, in general, matched reasonably well with the corresponding simulation results (see Figures 4.58-4.64). This confirms that the model validated earlier in separate experiments (e.g. heterogeneously catalysed batch reaction and pervaporation) does not need further improvements. Therefore, it may be concluded that the model used in this work for the hybrid process can be used for process design and analysis.

Table 4.37. Experimental conditions and result for membrane reactor operation

Exp No	E6	E5	E4	E3	E2	E1
T_R (av) [K]	336.21	354.11	346.24	344.85	351.87	346.83
T_M (av) [K]	334.11	353.09	343.19	343.48	349.36	347.65
$m_{r(initial)}$ [g]	1420.65	1192.36	1187.56	1257.76	1323.13	890.83
$m_{cat}/m_{mix\ (initial)}$ [g/g]	0.21	0.23	0.23	0.23	0.24	0.12
POH : ProAc [mol:mol]	3:1	3:1	2:1	2:1	2.2:1	2:1
Y_{ProPro}(exp) [mol/mol]	0.884	-	0.866	0.856	0.879	0.886
@ t [min]	541.02	-	507.70	495.93	497.95	525.02
Y_{ProPro} (exp) [mol/mol]	-	0.913	-	0.877	0.897	-
@ t [min]	-	572.17	-	615.05	600.72	-
Y_{ProPro} (exp) [mol/mol]	0.898	0.929	-	-	-	0.913
@ t (end) [min]	720.08	721.73	-	-	-	720.55
t_{switch} [min]	61.37	61.37	60.00	134.95	135.50	75.80

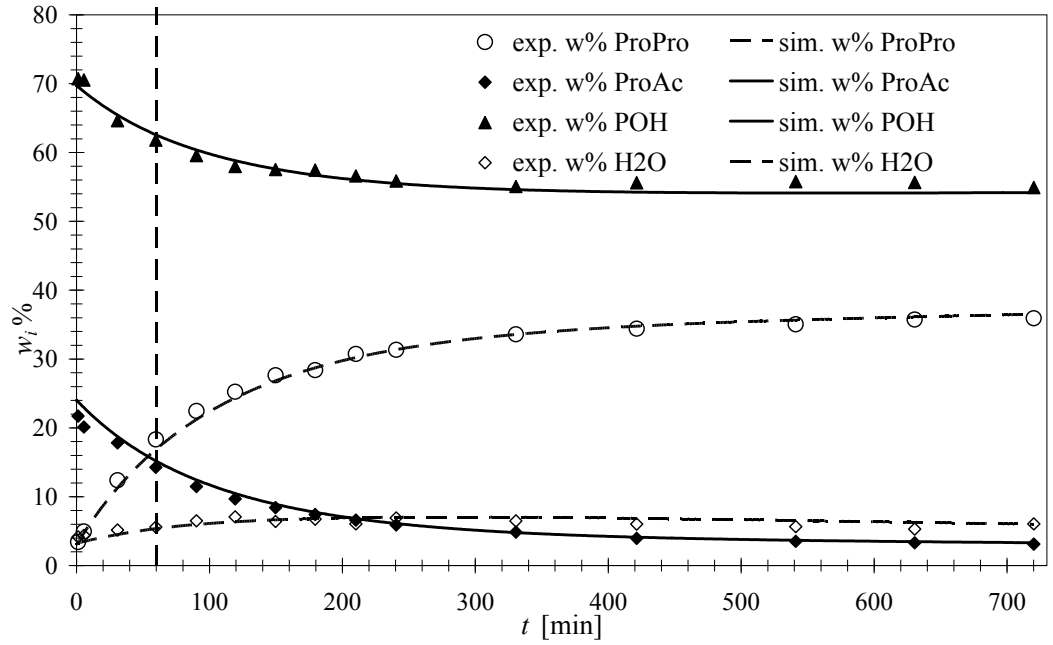

Figure 4.58: Membrane assisted batch reaction. $T_R = 336.21$ K, $T_M = 334.11$ K, $m_{cat}/m_{mix} = 0.21$, POH:ProAc = 3:1, $t_{switch} = 61.37$ min; (E6); (ProPro: n-propyl propionate; ProAc: propionic acid; POH: 1-propanol)

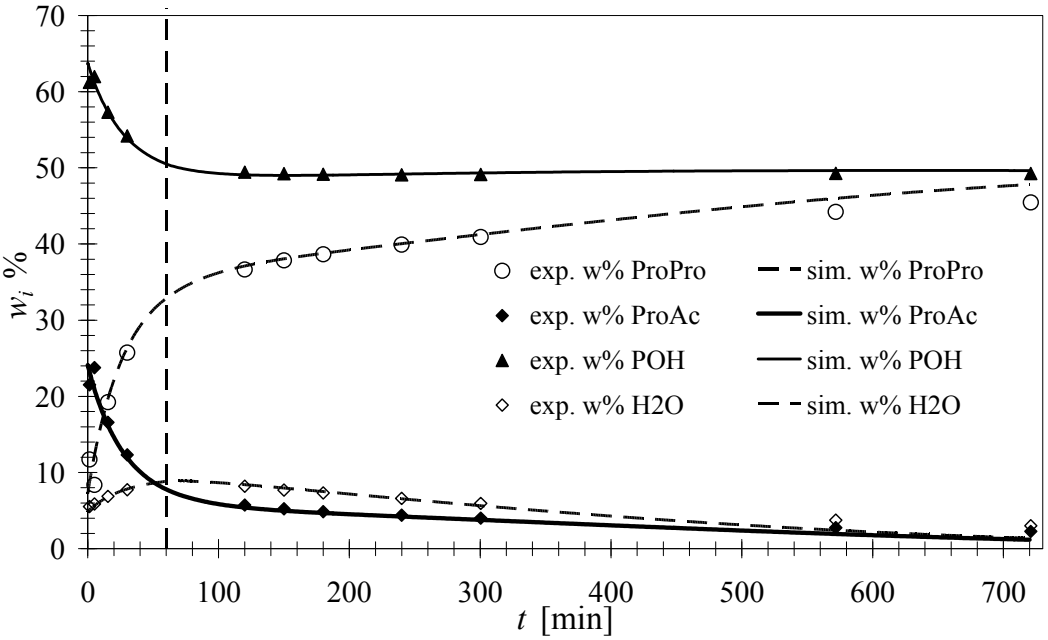

Figure 4.59: Membrane assisted batch reaction. $T_R = 354.11$ K, $T_M = 353.09$ K, $m_{cat}/m_{mix} = 0.23$, POH:ProAc = 3:1, $t_{switch} = 61.37$min; (E5); (ProPro: n-propyl propionate; ProAc: propionic acid; POH: 1-propanol)

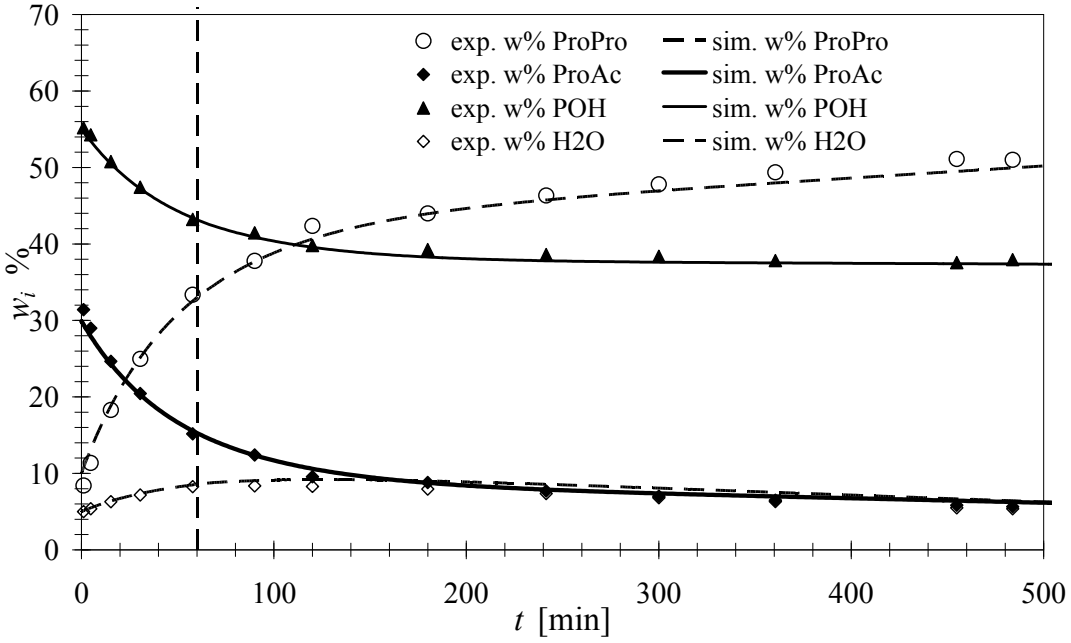

Figure 4.60: Membrane assisted batch reaction. T_R = 346.24 K, T_M = 343.19 K, m_{cat}/m_{mix} = 0.23, POH:ProAc = 2:1, t_{switch} = 60.00 min; (E4); (ProPro: n-propyl propionate; ProAc: propionic acid; POH: 1-propanol)

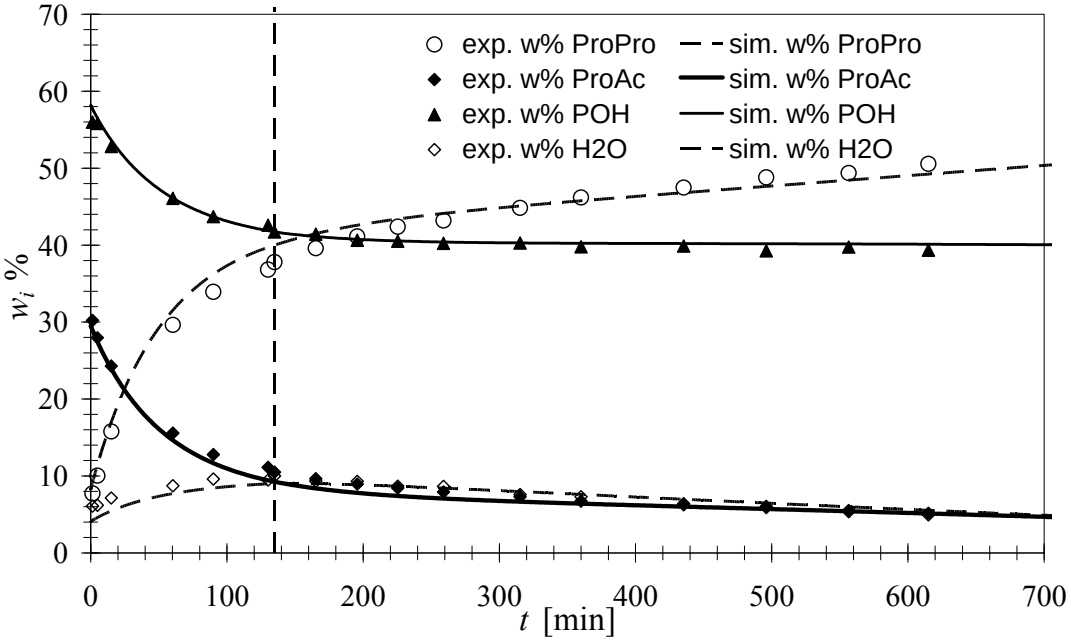

Figure 4.61: Membrane assisted batch reaction. T_R = 344.85 K, T_M = 343.48 K, m_{cat}/m_{mix} = 0.23, POH:ProAc = 2.2:1, t_{switch} = 134.95 min; (E3); (ProPro: n-propyl propionate; ProAc: propionic acid; POH: 1-propanol)

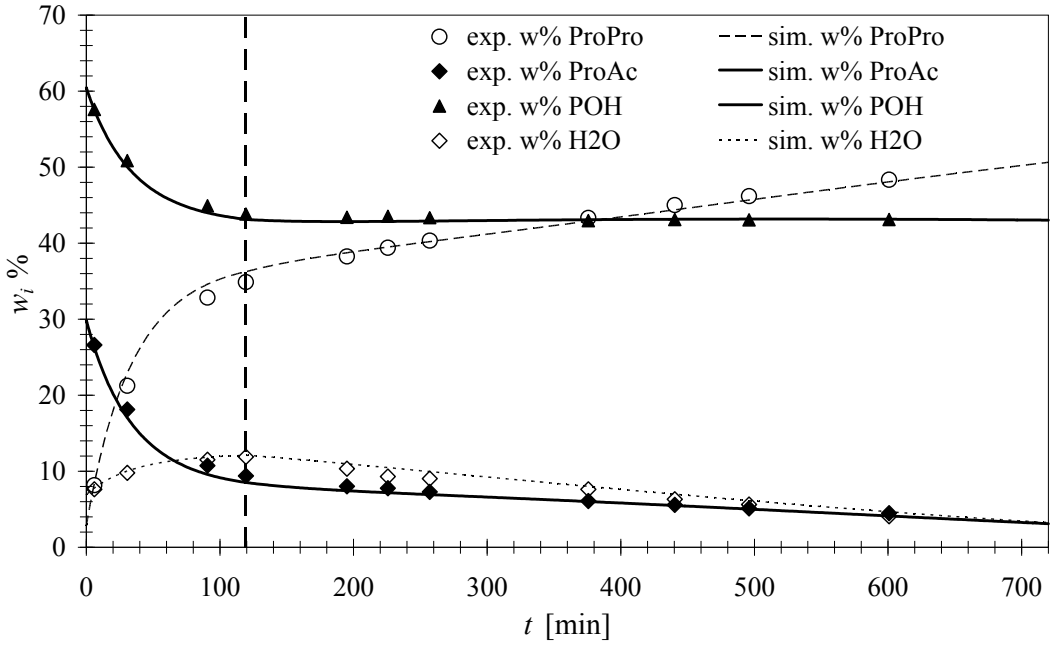

Figure 4.62: Membrane assisted batch reaction. T_R = 351.87 K, T_M = 349.36 K, m_{cat}/m_{mix} = 0.24 , POH:ProAc = 2.2:1, t_{switch} = 135.5 min; (E2); (ProPro: n-propyl propionate; ProAc: propionic acid; POH: 1-propanol)

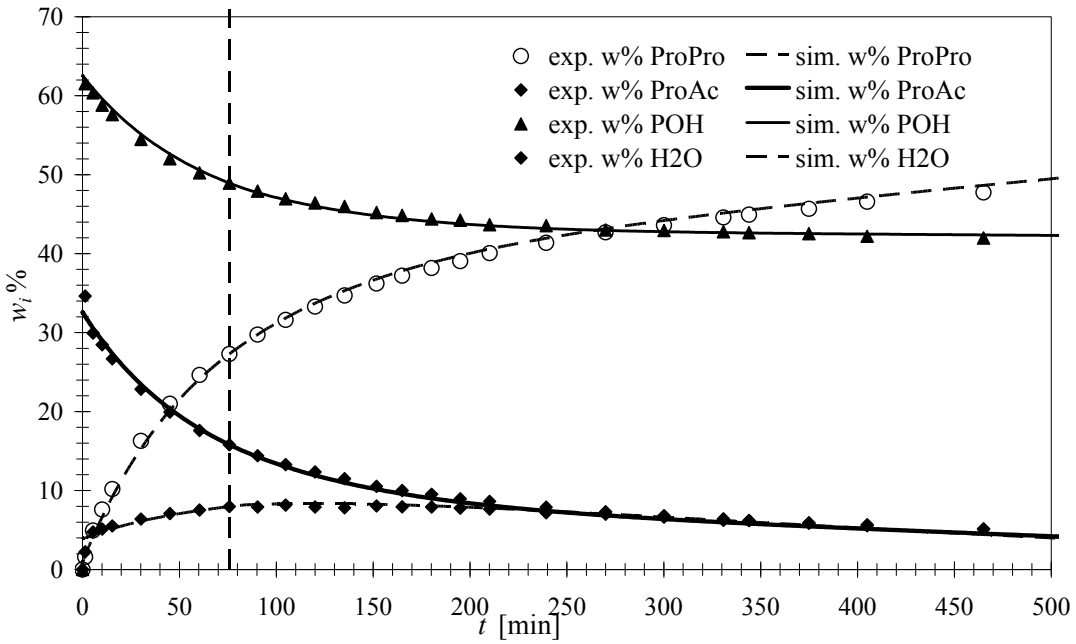

Figure 4.63: Membrane assisted batch reaction. T_R = 346.83 K, T_M = 347.65 K, m_{cat}/m_{mix} = 0.12, POH:ProAc = 2:1, t_{switch} = 75.80 min; (E1); (ProPro: n-propyl propionate; ProAc: propionic acid; POH: 1-propanol)

The process yield obtained in the membrane assisted batch reaction (hybrid process) is much higher than for heterogeneously catalysed batch reaction obtained in the same process time of 720 min (see Table 4.38). The best result has been obtained in E5 (Figure 4.59) where fraction of propionic acid is 3 w% after 12h.

Table 4.38. Comparison of process yield obtained in simulation for batch reaction and membrane reactor

Exp No	E6	E5	E4	E3	E2	E1
Yield P_{AC} (reaction) [mol/mol]	83.9%	78.7%	73.2%	76.4%	75.0%	79.1%
Yield P_{AC} (Membrane assisted batch reaction) [mol/mol]	87.4%	95.6%	85.0%	85.3%	90.2%	93.5%
Difference	3.5%	16.9%	11.8%	9.0%	15.2%	14.5%

*process time 720min

5. Conclusions

"The important thing is not to stop questioning. Curiosity has its own reason for existing"

(Albert Einstein)

5.1. Achievements

In this work the framework for hybrid process design and analysis has been developed. The framework has been presented along with computer-aided techniques which are assisting in the systematic investigation of hybrid/integrated process systems, e.g. reaction-separation and separation-separation systems. Advantages of this framework are the following:

- Step-by-step analysis of the reactive mixture and mixture which needs to be separated. The user of the framework is guided from the analysis of the mixture and to define process limitations, to generate feasible separation techniques and to obtain feasible process configuration(s).
- Various separation techniques are compared using the driving force approach. The advantage of the driving force approach is an easy visualization of the effectiveness of the separation technique along with its separation boundaries like azeotrope.
- Generation of feasible combinations of separation techniques based on the driving force approach. Identification of the bottleneck of the separation technique and sequence of the separation techniques are done by use of the derivative of the driving force.
- The built-in superstructure of the hybrid process along with the generic model. Based on the analysis and decisions taken in steps 2 and 3, and from the generic model, the specific process configurations are generated by fixing specific decision variable.
- Use of already available computer-aided tools such as ICAS-MoT, ICAS-ProPred, ICAS-ProCAMD, ICAS-TML, ICAS-PDS, ICAS-PDS and the CAPEC database manager.
- Use of MemData database (developed in this PhD-project) for fast screening for availability of membrane-based separation techniques reported to separate

specific mixtures.

The application of the developed framework has been highlighted through five case studies: one separation problem and four problems involving reaction-separation. In all case studies focus was on the incorporation of membrane-based separation techniques into combined hybrid processes which are good options when selective removal of compounds from investigated mixture is looked for.

In the first case study (section 4.2.1, page 85) the two hybrid separation-separation operations have been identified for the separation of the binary mixture of water and acetic acid. It has been shown that the most promising alternative is distillation followed by pervaporation (DFP). However, in this case a high selectivity membrane module is required ($\alpha = 50$). The feasible membrane which fulfils the requirement of high selectivity is the doped polyaniline membrane reported by Huang (1998). It was also found that even for the low selective membrane modules ($\alpha = 2.25$) the second design alternative (distillation with side pervaporation module) will give improvements in comparison to the base case.

The second case study deals with the enzymatic esterification of cetyl-oleate (section 4.3.1, page 99). In this case study the hybrid combination of reactor and pervaporation has been proposed and investigated. The proposed design gave yield of 0.93 within 5.5 h of operation. It was found out that increasing the loading of enzyme over 35 w% does not significantly influence the process yield. The hybrid operation should start within the first hour of operation. A feasible membrane that would meet this design is the commercially available polyvinyl alcohol membrane PERVAP 1005 from GFT.

The interesterification of the phosphatidylcholine has been investigated in the third case study (section 4.3.2, page 111). The two reactions, namely hydrolysis and esterification, take place in the same reaction volume. In this case the hybrid combination of reactor and pervaporation has been investigated for fixed initial conditions and different removal of the water from the reaction medium. N-hexane was found to be the most promising as a solvent that could be added for further increase in the product yield. As the membrane, the cellulose acetate membrane is recommended with membrane area of 0.064 m^2 when the volume of reaction medium is equal to 1 dm^3.

In the fourth case study (section 4.3.3, page 125) the production of ethyl lactate in a batch operation has been investigated. It is important to point out that in this case, the influence of addition of the catalyst Amberlyst XN-1010 on the membrane assisted batch reaction is not that significant when compared with the batch reaction operation. With 3.2 w% loading of catalyst the difference in the process yield between membrane assisted batch reaction configurations with 20 w% loading of catalyst is not higher than 3 %. The membrane assisted batch reaction should be operated with molar ratio of reactant 1:1 at 363.15 K with the catalyst loading of 3.2 w%, with the membrane area of 0.08 m^2 when the GFT-1005 membrane is used.

In the last case study (section 4.3.4, page 142) the full 3 stage framework was applied to the problem of synthesis of n-propyl propionate from propionic acid and 1-propanol. It is important to point out that after systematic analysis of the problem (stage 1) the proposed design has been implemented (stage 2) in collaboration with the group of Prof. Andrzej Górak, at University of Dortmund and validated (stage 3). The experiments confirmed the feasibility of the membrane assisted batch reaction giving significant improvement in the product (n-propyl propionate) yield by overcoming limitations of kinetically controlled reaction by removing by-product, water. Selective removal of water was obtained because of use of polyvinyl alcohol membrane PERVAP® 2201D from Sulzer. The best result has been obtained in the membrane assisted batch reaction configuration operated at 354 K, with initial reactant ratio 3:1 and $m_{cat}/m_{mix\ (initial)}$ equal to 0.23. During that operation the weight fraction of propionic acid after 12 h was 3 % which corresponds to the molar yield of 0.93.

For all above mentioned case studies several models have been developed and used, namely: batch reaction models and membrane assisted batch reaction models. The membrane-based separation has been usually modelled with short-cut models (summarized in section 2.4.1.3, page 25). In the last case study component fluxes through the pervaporation membrane have been modelled with the Meyer-Blumenroth model (see section 6.4.4.2, page 221). All these models along with activity coefficient models (Modified UNFAC Lyngby and Modified UNFAC Dortmund) have been implemented in ICAS-MoT. All model equations are provided in the appendices along with their analysis (section 6.2, page 181 and section 6.4, page 192). Moreover, in the appendix 6.1 the full description of algorithm for the reactive flash calculations is provided, which gives a good understanding of the reactive flash calculations performed in the presented reactive-separation case studies in sections 4.3.3 (Synthesis of ethyl lactate) and 4.3.4 (Synthesis of n-propyl-propionate).

In this work the structure of the membrane database covering the pervaporation and gas separation processes has been developed and implemented in the Microsoft Access. The objective for the development of the membrane database was to gather many kinds of the available information in the open literature about membrane-based separation techniques and provide this information to the user with the computer-aided tool for easy retrieval of information. In this way, experimental data, correlations and models can be simply reuse for various purposes, e.g. process and membrane design.

5.2. Recommendation for future work

The main drawback of using the developed framework is availability of the separation characteristic data and models describing the separation techniques as well as reactions. Therefore, when solving any problem it has to be kept in mind that a design will be as good as the provided input data. Other disadvantage is the need of manual generation of the specific hybrid process configuration from the superstructure. Based

on these disadvantages, the recommendations for the future work related to the developed framework are discussed below.

The framework has been used with various reaction kinetic models and pervaporation models. The framework can be expanded to other applications by incorporation of other separation models, for example, models for ultrafiltration, nanofiltration, and extraction. The framework can be also expanded to take into account reactions taking place in the vapour phase.

The developed framework significantly narrows down the search space from many possible process alternatives to just few so that the most promising hybrid processes can be further investigated in detail. However, incorporation of optimization techniques could be used at this stage to obtain the final optimal design. This would require the formulation and solution of a mixed integer nonlinear programming problem, which has not been considered in this work.

The driving force approach used to compare various separation techniques and combining them into hybrid operations using the derivative of the driving force could be automated and implemented in the software. In this way, the user would only provide information about the separation characteristics of any separation technique to compute driving force and the program would generate feasible hybrid process configurations.

Another area of future work could focus on further development of the MemData database. The data gathered in the MemData could be made accessible to many users through a network. Besides the incorporation of new data, more detailed specification of already defined processes (pervaporation, gas separation) and incorporation of other membrane-based separation processes are essential. Moreover, the MemData database could be integrated with another software environment so that users will have an easy access through one “window” to all the important data. Note that all compounds present in the MemData are identified through the CAS-number, therefore, data integrity with data gathered in other databases, like the CAPEC database, is already assured.

6. Appendixes

6.1. Appendix 1: Reactive flash calculation

The computational algorithm for reactive flash calculations with ideal solution approach is given in details in that section which based on algorithm presented by (Pérez-Cisneros et al., 1997).

The reactive flash calculations follow the algorithm shown in Figure 6.1. For given temperature, pressure and feed composition (step 1) the initial guesses for liquid phase composition (x_i), vapour phase composition (y_i) and phase fraction (θ^l, θ^v) have to be provided. Initial values of Langrage multipliers $\underline{\lambda}$ are estimated by certain reorganization of Eq. (2.12). Afterwards in step 3 the equation (6.1) is solved. The solution is tracked by solving the equation (6.5); when Q is decreasing it is sure that step ($\Delta\lambda$) is right if not correction action is performed. Detailed procedure is presented on Figure 6.2.

$$\underline{\Delta} = -\underline{g} \cdot \underline{H}^{-1} \tag{6.1}$$

where:

$$\underline{H} = \begin{bmatrix} \theta^V \sum_{k=1}^{NC} A_{11}A_{11}y_1 + \theta^L \sum_{k=1}^{NC} A_{11}A_{11}x_1 & \cdots & \theta^V \sum_{k=1}^{NC} A_{ik}A_{1k}y_k + \theta^L \sum_{k=1}^{NC} A_{ik}A_{1k}x_k \\ \vdots & \ddots & \vdots \\ \theta^V \sum_{k=1}^{NC} A_{i1}A_{j1}y_1 + \theta^L \sum_{k=1}^{NC} A_{i1}A_{j1}x_1 & \cdots & \theta^V \sum_{k=1}^{NC} A_{ik}A_{jk}y_k + \theta^L \sum_{k=1}^{NC} A_{ik}A_{jk}x_k \end{bmatrix} \tag{6.2}$$

$$\underline{g} = \begin{bmatrix} n_{TOT}^V \sum_{k=1}^{NC} A_{1k}y_k + n_{TOT}^L \sum_{k=1}^{NC} A_{1k}x_k - b_1 \\ \vdots \\ n_{TOT}^V \sum_{k=1}^{NC} A_{jk}y_k + n_{TOT}^L \sum_{k=1}^{NC} A_{jk}x_k - b_1 \end{bmatrix} \tag{6.3}$$

$$\underline{\Delta} = \begin{bmatrix} \Delta\lambda_1 \\ \vdots \\ \Delta\lambda_k \end{bmatrix} \tag{6.4}$$

$$Q = n_{TOT}^V \sum_{k=1}^{NC} y_k - 1 + n_{TOT}^L \sum_{k=1}^{NC} x_k - 1 \tag{6.5}$$

Obtained $\underline{\lambda}$ from previous step (step 3) at the constant phase distribution (θ^V, θ^L) are used in the following part where the phase distribution (θ^l, θ^v) is allowed to change. Afterwards, equation of type (6.1) is solved, however in that step individual matrix (Hessian) and vectors ($\underline{g}, \underline{\Delta}$) have form of (6.6), (6.7) and (6.8), respectively. Based on the value of the corresponding residual (Δ) the existence of adequate phase is considered, if it is found that the phases does not exist the set of equations (6.6-6.8) have to be modified in the way that disappeared phase is not taken into account in following calculation. Detailed solution procedure is shown on Figure 6.3. Results of step 4 $\theta^V, \theta^L, x_k, y_k$ (see Figure 6.1) are obtained under assumption that system is ideal; that fugacity and activity coefficients are constant. Because of that in step 5 non ideal models are used in order to update composition. The solution proceeds with successive substitution as shown on Figure 6.1.

$$\underline{H} = \begin{bmatrix} \theta^V \sum_{k=1}^{NC} A_{ik}A_{jk}y_k + \theta^L \sum_{k=1}^{NC} A_{ik}A_{jk}x_k & \cdots & \cdots & \sum_{k=1}^{NC} A_{ij}y_k & \sum_{k=1}^{NC} A_{ij}x_k \\ \vdots & \vdots & \vdots & \vdots & \vdots \\ \vdots & \vdots & \vdots & \sum_{k=1}^{NC} A_{ij}y_k & \sum_{k=1}^{NC} A_{ij}x_k \\ \sum_{k=1}^{NC} A_{ij}y_k & \cdots & \sum_{k=1}^{NC} A_{ij}y_k & 0 & 0 \\ \sum_{k=1}^{NC} A_{ij}x_k & \cdots & \sum_{k=1}^{NC} A_{ij}x_k & 0 & 0 \end{bmatrix} \quad (6.6)$$

$$\underline{g} = \begin{bmatrix} n_{TOT}^V \sum_{k=1}^{NC} A_{1k}y_k + n_{TOT}^L \sum_{k=1}^{NC} A_{1k}x_k - b_1 \\ \vdots \\ n_{TOT}^V \sum_{k=1}^{NC} A_{jk}y_k + n_{TOT}^L \sum_{k=1}^{NC} A_{jk}x_k - b_1 \\ \sum_{k=1}^{NC} y_k - 1 \\ \sum_{k=1}^{NC} x_k - 1 \end{bmatrix} \quad (6.7)$$

$$\underline{\Delta} = \begin{bmatrix} \Delta\lambda_1 \\ \vdots \\ \Delta\lambda_k \\ \Delta n_{TOT}^V \\ \Delta n_{TOT}^L \end{bmatrix} \quad (6.8)$$

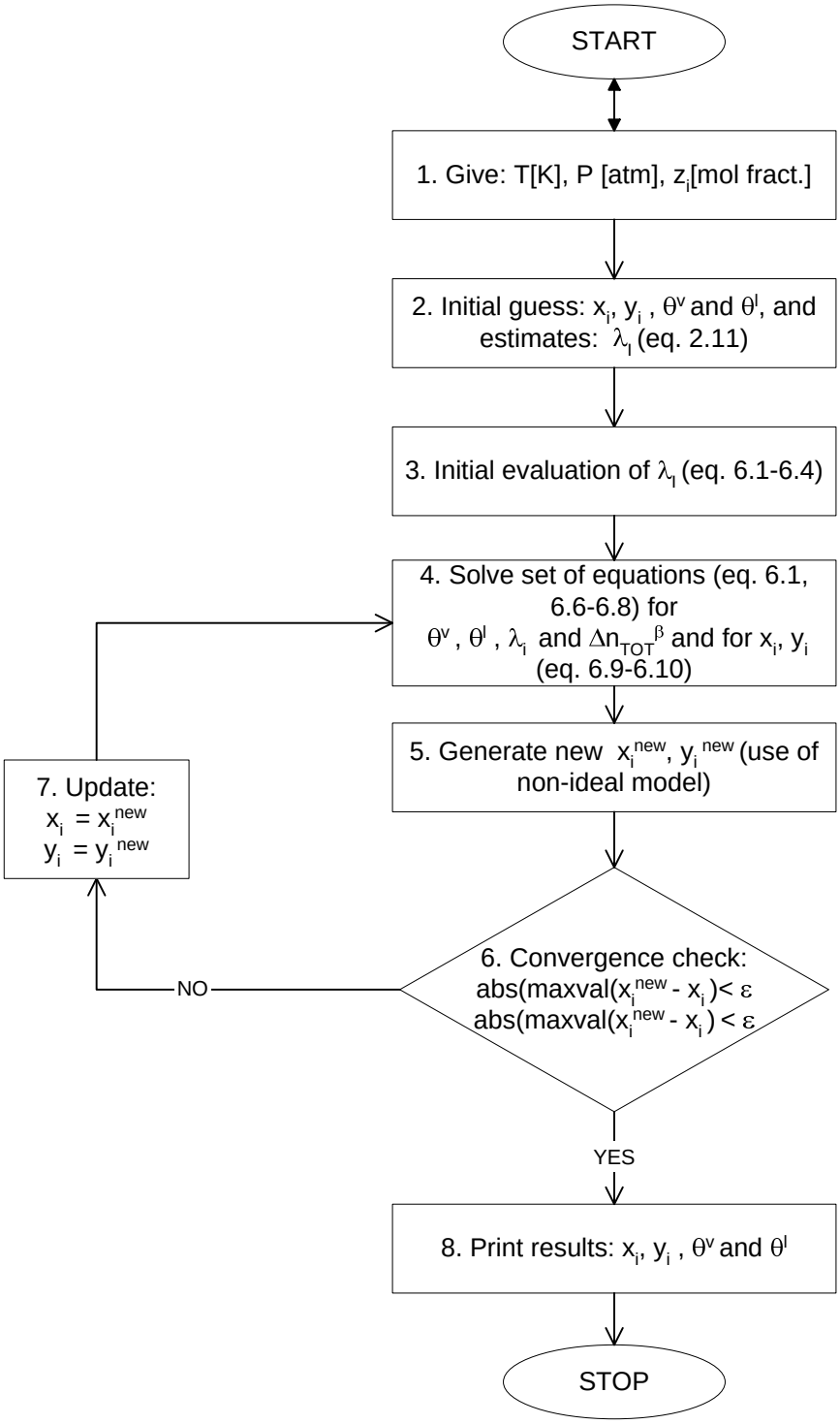

Figure 6.1: Main algorithm of solution procedure

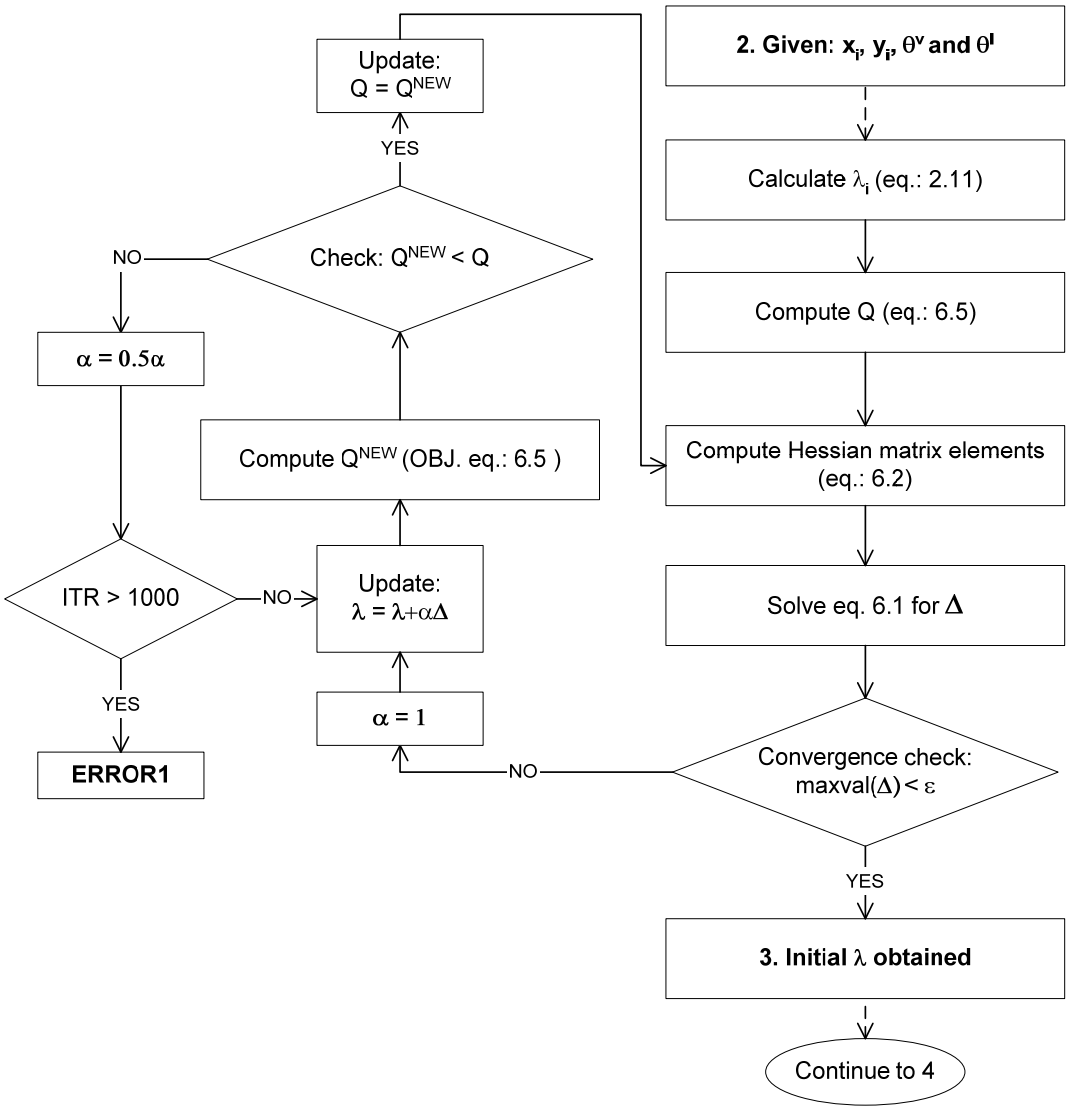

Figure 6.2: Algorithm for calculation of $\underline{\lambda}$ (Step 3 of the main algorithm, see Figure 6.1)

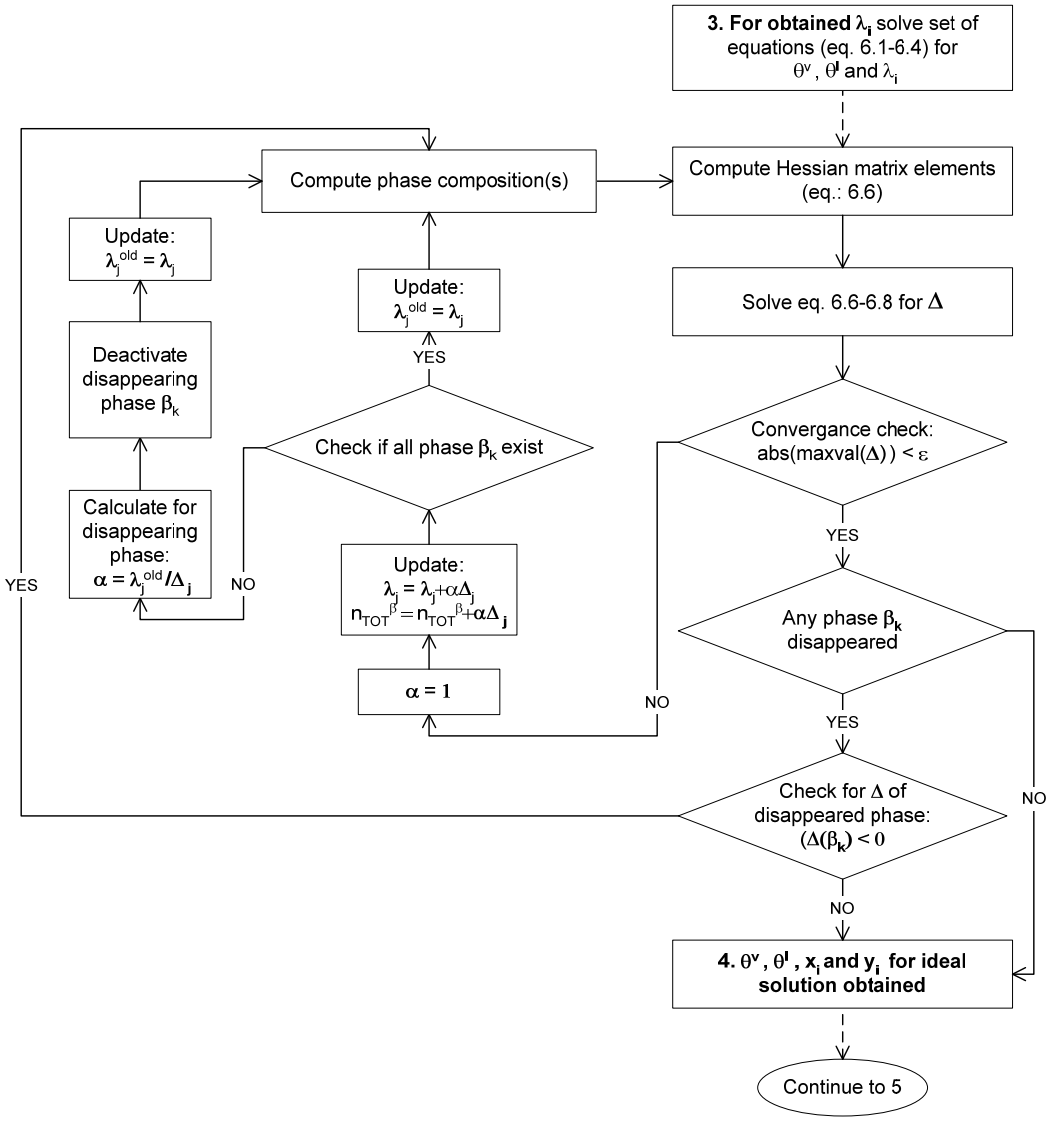

Figure 6.3: Algorithm for calculation of θ^v, θ^l, x_i and y_i (Step 4 of the main algorithm, see Figure 6.1)

6.2. Appendix 2: Activity coefficient models

6.2.1. Modified UNIFAC (Lyngby)

In this subsection a detailed analysis of Modified UNIFAC (version Lyngby) is presented. *NC* stands for number of compounds in the mixture and *NoG* stands for number of groups used to describe the compounds in the mixture. Therefore used subscripts are taking following values: $i, j \in NC \rightarrow \{1..NC\}$, $k, m, p, d \in NoG \rightarrow \{1..NoG\}$. For given number of moles of compounds and

temperature the activity coefficients are calculated utilizing following equations:

$$x_i = \frac{n_i}{\sum_{j=1}^{NC} n_j} \tag{6.9}$$

$$n_k^{group} = \sum_{j=1}^{NoG} \upsilon_{k,j} n_j \tag{6.10}$$

$$n_{k,i}^{group} = \upsilon_{k,i} n_i \tag{6.11}$$

$$r_i = \sum_{k=1}^{NoG} \upsilon_{k,j} R_k \tag{6.12}$$

$$\omega_i = \frac{x_i \left(r_i\right)^{\frac{2}{3}}}{\sum_{p=1}^{NC} x_p \left(r_p\right)^{\frac{2}{3}}} \tag{6.13}$$

$$\ln \gamma_i^c = \ln\left(\frac{\omega_i}{x_i}\right) + 1 - \frac{\omega_i}{x_i} \tag{6.14}$$

$$a_{k,d} = a_{k,d,1} + a_{k,d,2}\left(T - T_0\right) + a_{k,d,3}\left(T \ln\frac{T_0}{T} + T - T_0\right) \tag{6.15}$$

$$\tau_{k,d} = \exp\left(\frac{-a_{k,d}}{T}\right) \tag{6.16}$$

$$\theta_k = \frac{\frac{z}{2} n_k^{group} Q_k}{\sum_{m}^{NoG} \frac{z}{2} n_m^{group} Q_m} \tag{6.17}$$

$$\ln \Gamma_k = \frac{z}{2} Q_k \left[-\left\{ \ln\left(\sum_{m=1}^{NoG} \theta_m \tau_{mk} \right) \right\} + 1 - \sum_{p=1}^{NoG} \frac{\theta_p \tau_{kp}}{\sum_{d=1}^{NoG} \theta_d \tau_{dp}} \right] \tag{6.18}$$

$$\theta_{k,i} = \frac{\frac{z}{2} n_{k,i}^{group} Q_k}{\sum_{m=1}^{NoG} \frac{z}{2} n_{m,i}^{group} Q_m} \tag{6.19}$$

$$\ln \Gamma_{k,i} = \frac{z}{2} Q_k \left[-\left\{ \ln\left(\sum_{m=1}^{NoG} \theta_{m,i} \tau_{m,k} \right) \right\} + 1 - \sum_{p=1}^{NoG} \frac{\theta_p \tau_{kp}}{\sum_{d=1}^{NoG} \theta_d \tau_{dp}} \right] \tag{6.20}$$

$$\ln \gamma_i^R = \sum_{k=1}^{NoG} \upsilon_{k,j} \left(\ln \Gamma_k - \ln \Gamma_{k,i} \right) \tag{6.21}$$

$$\ln \gamma_i = \ln \gamma_i^c + \ln \gamma_i^r \tag{6.22}$$

Table 6.1: List of variables in Modified UNIFAC (Lyngby)

Algebraic variables		Number
Molar fraction	x_i	NC
Total number of groups *k* in mixture	n_k^{group}	NoG
Total number of groups *k* around component *i* in mixture	$n_{k,i}^{group}$	$NoG \cdot NC$
Molecular volume parameter for component *i*	r_i	NC
Modified volume fraction of component *i* in mixture	ω_i	NC
Combinatorial part of activity coefficient	γ_i^c	NC
Interaction parameter for *k*-*d* interaction	$a_{k,d}$	$NoG \cdot NoG$
Boltzmann factor	$\tau_{k,d}$	$NoG \cdot NoG$
Surface area fraction, for *k* in mixture	θ_k	NoG
Residual group activity coefficient for group *k*	Γ_k	NoG
Surface area fraction, local for *k* around *i*	$\theta_{k,i}$	$NoG \cdot NC$
Residual group activity coefficient, in component *i*	$\Gamma_{k,i}$	$NoG \cdot NC$
Residual part of activity coefficient	γ_i^R	NC
Activity coefficient	γ_i	NC
Parameters		**Number**
Number of moles	n_i	NC
Temperature	T	1
Number of groups *k* in component *j*	$\upsilon_{k,j}$	$NoG \cdot NC$
Volume parameter of component *k*	R_k	NoG
Interaction parameters for *k*-*d* interaction	$a_{k,d,1}$, $a_{k,d,2}$, $a_{k,d,3}$	$3 \cdot NoG$
Surface area parameter, for group *k*	Q_k	NoG
Known variables		**Number**
Reference temperature	T_0	1
Lattice coordination number	z	1
Total number of variables: $7 \cdot NC + 4 \cdot NC \cdot NoG + 8 \cdot NoG + 2 \cdot NoG \cdot NoG + 3$		

Table 6.2: List of equations in Modified UNIFAC (Lyngby)

	Equations	Number of equations
Molar fraction	(6.9)	*NC*
Number of groups *k* in the mixture	(6.10)	*NoG*
Number of groups around component *i*	(6.11)	$NoG \cdot NC$
Molecular volume parameter	(6.12)	*NC*
Modified volume fraction of component *i* in mixture	(6.13)	*NC*
Combinatorial part of activity coefficient	(6.14)	*NC*
Temperature dependence of the interaction parameters for *i-j* interactions	(6.15)	$NoG \cdot NoG$
Boltzmann factors	(6.16)	$NoG \cdot NoG$
Surface area fraction	(6.17)	*NoG*
Residual group activity coefficient for group *k*	(6.18)	*NoG*
Summation of structural parameters (surface area parameter) of group *k* around component *i*	(6.19)	$NoG \cdot NC$
Residual group activity coefficient in pure component *i*	(6.20)	$NoG \cdot NC$
Residual part of activity coefficient	(6.21)	*NC*
Activity coefficient	(6.22)	*NC*
Total number of equations: $6 \cdot NC + 3 \cdot NoG \cdot NC + 2 \cdot NoG \cdot NoG + 3 \cdot NoG$		

The degree of freedom is equal to:

$$DOF = NC + 1 \cdot NC \cdot NoG + 5 \cdot NoG + 3 \tag{6.23}$$

6.2.2. Modified UNIFAC (Dortmund)

In this subsection the detailed analysis of the Modified UNIFAC (Dortmund) is presented. *NC* stands for number of compounds in the mixture and *NoG* stands for number of groups used to describe the compounds in the mixture. Therefore used subscripts are taking following values: $i, j \in NC \rightarrow \{1...NC\}$, $k, m, p, d \in NoG \rightarrow \{1...NoG\}$. For given number of moles of compounds and temperature the activity coefficients of compounds are calculated utilizing following equations (6.24-6.41).

$$x_i = \frac{n_i}{\sum_{j=1}^{NC} n_j} \tag{6.24}$$

$$x_{k,i}^{group} = \frac{\upsilon_{k,i}}{\sum_{p=1}^{NoG} \upsilon_{p,i}} \tag{6.25}$$

$$r_i = \sum_{k=1}^{NoG} \upsilon_{k,j} R_k \tag{6.26}$$

$$\upsilon_{P,i} = \frac{\left(r_i\right)^{\frac{3}{4}}}{\sum_{j=1}^{NC} x_j \left(r_j\right)^{\frac{3}{4}}} \tag{6.27}$$

$$\upsilon_{I,i} = \frac{r_i}{\sum_{j=1}^{NC} x_j r_j} \tag{6.28}$$

$$q_i = \sum_{k=1}^{NoG} \upsilon_{k,i} Q_k \tag{6.29}$$

$$\psi_i = \frac{q_i}{\sum_{j=1}^{NC} x_j q_j} \tag{6.30}$$

$$\ln \gamma_i^c = 1 - \upsilon_{P,i} + \ln\left(\upsilon_{P,i}\right) - 5q_i \left(1 - \frac{\upsilon_{I,i}}{\psi_i} + \ln\left(\frac{\upsilon_{I,i}}{\psi_i}\right)\right) \tag{6.31}$$

$$a_{k,d} = a_{k,d,1} + b_{k,d} T + c_{k,d} T^2 \tag{6.32}$$

$$\tau_{k,d} = \exp\left(\frac{-a_{k,d}}{T}\right) \tag{6.33}$$

$$Z_i = \sum_{k=1}^{NoG} \upsilon_{k,i} x_i \tag{6.34}$$

$$X_k = \frac{\sum_{i=1}^{NC} \upsilon_{k,i} x_i}{\sum_{i=1}^{NC} Z_i} \tag{6.35}$$

$$\theta_k = \frac{X_k Q_k}{\sum_{m}^{NoG} X_m Q_m} \tag{6.36}$$

$$\ln \Gamma_k = Q_k \left[-\left\{ \ln\left(\sum_{m=1}^{NoG} \theta_m \tau_{m,k} \right) \right\} + 1 - \sum_{p=1}^{NoG} \frac{\theta_p \tau_{k,p}}{\sum_{d=1}^{NoG} \theta_d \tau_{d,p}} \right] \tag{6.37}$$

$$\theta_{k,i} = \frac{x_{k,i}^{group} Q_k}{\sum_{m=1}^{NoG} x_{m,i}^{group} Q_m} \tag{6.38}$$

$$\ln \Gamma_{k,i} = Q_k \left[-\left\{ \ln\left(\sum_{m=1}^{NoG} \theta_{m,i} \tau_{m,k} \right) \right\} + 1 - \sum_{p=1}^{NoG} \frac{\theta_p \tau_{kp}}{\sum_{d=1}^{NoG} \theta_d \tau_{dp}} \right] \tag{6.39}$$

$$\ln \gamma_i^R = \sum_{k=1}^{NoG} \upsilon_{k,j} \left(\ln \Gamma_k - \ln \Gamma_{k,i} \right) \tag{6.40}$$

$$\ln \gamma_i = \ln \gamma_i^c + \ln \gamma_i^r \tag{6.41}$$

Table 6.3: List of variables in Mod. UNIFAC (Dortmund)

Algebraic variables		Number
Molar fraction	x_i	NC
Fraction of groups *k*	$x_{k,i}^{group}$	$NoG \cdot NC$
Molecular volume parameter for component *i*	r_i	NC
Modified volume fraction of component *i* in mixture	$\upsilon_{P,i}$	NC
Volume fraction of component *i* in mixture	$\upsilon_{I,i}$	NC
Relative van der Waals surface area of component *i*	q_i	NC
Surface area fraction of component *i* in mixture	ψ_i	NC
Combinatorial part of activity coefficient	γ_i^c	NC
Interaction parameter for *k*-*d* interaction	$a_{k,d}$	$NoG \cdot NoG$
Boltzmann factor	$\tau_{k,d}$	$NoG \cdot NoG$
Number of groups in component *i*	Z_i	NC
Surface area fraction of group *k* in mixture	X_k	NoG
Surface area fraction, for *i* in mixture	θ_k	NoG
Residual group activity coefficient for group *k*	Γ_k	NoG
Surface area fraction, local for *k* around *i*	$\theta_{k,i}$	$NoG \cdot NC$
Residual group activity coefficient, in pure component *i*	$\Gamma_{k,i}$	$NoG \cdot NC$
Residual part of activity coefficient	γ_i^R	NC
Activity coefficient	γ_i	NC
Parameters		**Number**
Number of moles	n_i	NC
Temperature	T	1
Number of groups *k* in component *j*	$\upsilon_{k,j}$	$NoG \cdot NC$
Volume parameter of *k*	R_k	NoG
Interaction parameter for *k*-*d* interaction	$a_{k,d,1}$, $b_{k,d}$,	$3 \cdot NoG$

	$c_{k,d}$	
Relative van der Waals surface area parameter of subgroup *k*	Q_k	NoG
Total number of variables: $11 \cdot NC + 4 \cdot NC \cdot NoG + 8 \cdot NoG + 2 \cdot NoG \cdot NoG + 1$		

Table 6.4: List of equations in Mod. UNIFAC (Dortmund)

	Equations	Number of equations
Molar fraction	(6.24)	NC
Fraction of group *k* around component *i*	(6.25)	$NoG \cdot NC$
Molecular volume parameter	(6.26)	NC
Modified volume fraction of component *i* in mixture	(6.27)	NC
Volume fraction of component *i* in mixture	(6.28)	NC
Relative van der Waals surface area of component *i*	(6.29)	NC
Auxiliary property of component *i*	(6.30)	NC
Activity coefficient, combinatorial part	(6.31)	NC
Temperature dependence of the interaction parameters for *i-j* interactions	(6.32)	$NoG \cdot NoG$
Boltzmann factors	(6.33)	$NoG \cdot NoG$
Number of groups in component *i*	(6.34)	NC
Surface area fraction of group *k* in mixture	(6.35)	NoG
Surface area fraction, for group *k* interaction	(6.36)	NoG
Residual group activity coefficient for group *k*	(6.37)	NoG
Surface area fraction of group *k* around component *i*	(6.38)	$NoG \cdot NC$
Residual group activity coefficient in pure component *i*	(6.39)	$NoG \cdot NC$
Activity coefficient, residual part	(6.40)	NC
Activity coefficient	(6.41)	NC
Total number of equations: $10 \cdot NC + 3 \cdot NoG \cdot NC + 2 \cdot NoG \cdot NoG + 3 \cdot NoG$		

$$DOF = NC + NC \cdot NoG + 5 \cdot NoG + 1 \tag{6.42}$$

6.3. Appendix 3: MemData

Detailed list of entities in MemData is given below along with list of related attribute. Entities 1.2, 1.3, 1.3.1, 1.3.2, 1.3.3, 1.3.4, 1.3.5, 1.3.6, 1.4, 1.5, 1.7, 1.8, 2.1, 2.2, 2.3, 2.4, 3.1, 3.2, 3.3 besides all attributes listed below in MemData implementation consists attribute assigning unique auto number to each record in table of entity (e.g. id.NameOfEntity). Moreover each table of entity has attribute txtMiscellaneous in which miscellaneous information related to specific record can be provided. In brackets the name of the attribute representing the specific entity in database is given.

1. Fundamental entities:

1.1. Compounds
- CAS number (txtCAS_number)
- Chemical formula (txtChemicalFormula)
- Chemical name of compound (txtChemicalComponentName)

1.2. Polymer (active layer, support)
- CAS number (txtCAS number)
- Chemical name of component (txtComponentName)
- Abbreviation of chemical component (txtComponentAbreviation)
- IUPAC name (txt.IUPAC_Name)
- Chemical formula (txtComponentFormula)
- Density, ρ (numDensity)
- Crystalinity (numCrystalinity)
- Draw ratio, λ (numDrawRatio)
- Melting temperature, Tm (numTm)
- Glass transition temperature, Tg (numTg)
- CAS number of monomer 1 (idCASnumber-Monomer1)
- CAS number of monomer 2 (idCASnumber-Monomer2)
- CAS number of monomer 3 (idCASnumber-Monomer3)
- CAS number of monomer 4 (idCASnumber-Monomer4)

1.2.1. Monomer
- CAS number (CAS number)
- IUPAC name (txtIUPAC)
- Common name of monomer (txt Common name)
- Chemical formula of monomer (txtChemicalFormula)

1.3. Producer
- Producer name (txtProducerName)
- Country of origin (txtCountry)
- Address (txtAdress)
- Web address (txtWebAdress)

1.4. Membrane process
- Name of the membrane process (txtMembraneProcessName)

1.5. Reference tile
- Title (txtTitle)
- Name of the source (txtSourceName)
- Name of journal (txtJournal)
- Journal of volume (txtVolume-Journal)
- Name of publisher (txtPublisher)
- Date (numData)
- Link to reference placed in C:\MemData\Reference\ (txtReferenceLink)
- Number of the first page (txtPageNumber)

1.6. Authors
- First name (txtFirstName)
- Last name (txtLastName)
- Email (txtEmail)
- Institution/company (txtInstitution/Company)
- Address (txtAdress)

- Web address (txtWebAdress)

1.7. Inorganic compound
- Name of chemical compound (txtCompoundCommonName)
- Chemical formula (txtChemicalFormula)
- CAS number (txtCASnumber)

2. Collection entities:

2.1. Membrane information
- Membrane name (txtMembraneName)
- Producer name selected from table 1.7 (txtProducer/supplierName)
- Membrane type selected from table 2.1.1 (txtMembraneType)
- Active layer: Chemical compound selected from table 1.2 (txtAL_Compound)
- Active layer: Thickness (numAL_Thickness)
- Active layer: Porous (txtAL_Porous)
- Active layer: Nonporous (txtAL_Nonporous)
- Active layer: Porosity (numAL_Porosity)
- Active layer: Pore size (numAL_PoreSize)
- Active layer: Pore tortuosity (numAL_Tortuosity)
- Support: Chemical compound: Polymer (txtSupportCompoundPolymer)
- Support: Chemical compound: Inorganic (txtSupportCompoundInorganic)
- Support: Thickness (numSupportThicknes)
- Philicity selected from table 2.1.2 (txt*philic)
- Reference title selected from table 1.5 (txtReference)

2.1.1. Membrane type
– Name of type of the membrane (txtMembraneType)

2.1.2. Philicity
- Philicity of membrane (txtPhlicity)

2.2. Module
- Module name (txtModuleName)
- Type of module (txtTypeOfModule)
- Link to specific hollow fibber module record in table 1.3.1.1 (numHollowFiber)
- Link to specific plate and frame module record in table 1.3.1.2 (numPlateAndFrame)
- Link to specific spiral wound module record in table 1.3.1.3 (num SpiralWound)
- Link to specific tubular module record in table 1.3.1.4 (numTubular)
- Link to specific capillary module record in table 1.3.1.5 (numCapilary)
- Link to specific membrane reactor record in table 1.3.1.6 (numMembraneReactor)
- Producer (txtProducer)
- Total membrane area (numAreaTotal)
- Effective membrane area (numAreaEffective)

- Minimum flow rate (numMinFlowRate)
- Maximum flow rate (numMaxFlowRate)
- Minimum operating pressure (numMinPressure)
- Maximum operating pressure (numMaxPressure)
- Minimum operating temperature (numMinTemperature)
- Maximum operating temperature (numMaxTemperature)
- Holdup on the permeate side (numHoldupPermeateSide)
- Holdup on the feed side (numHoldupFeedSide)

2.2.1. Type of module

- Name of type of the membrane module (txtNameOfTypeOfModule)

2.2.1.1. Hollow fibber module

- Noumber of fibbers (numNumberOfFibers)
- Length of fibbers (numLengthOfFibers)
- Inner radius of fibbers (numInnerRadius)
- Outer radius of fibbers (numOuterRadius

2.2.1.2. Plate-and-frame module

- Number of sheets in the module (numNumberOfSheets)
- Length of membrane (numLength)
- Width of membrane (numWidth)
- Radius of membrane (numRadius)
- Area of membrane sheet (numArea)
- Channel height on the permeate side (numChannelHightPermeateSide)
- Channel height on the feed side (numChannelHightFeedSide)

2.2.1.3. Spiral wound module

- Channel height on the permeate side (numChannelHightPermeateSide)
- Channel height on the feed side (numChannelHightFeedSide

2.2.1.4. Tubular module

- Length of fibers (numLengthOfFibers)
- Inner radius (numInnerRadius)
- Outer radius (numOuterRadius)

2.2.1.5. Capillary module

- Number of capilars (numNumberOfCapilars)
- Length of capilars (numLengthofCapilars)
- Inner radius (numInnerRadius)
- Outer radius (numOuterradius)

2.2.1.6. Membrane reactor

- Reactor volume (numReactorVolume)
- Reactor hight (numReactorHight)

- Reactor radius (numReactorRadius)

2.3. Experimental set up
- Membrane selected from table 2.1 (txtMembrane)
- Module selected from table 1.3 (txtModule)
- Type of process, selected from table 1.4 (txtProcess)
- Title of reference, selected from table 1.5 (txtReference)
- Number of component present in the mixture (numNoOfComponents)

2.4. Experimental conditions
- Temperature of feed (numTemperatureFeed)
- Pressure at the feed side (numPressureFeed)
- Temperature at the permeate side (numTemperaturePermeate)
- Pressure at the permeate side (numTemperaturePermeate)
- Temperature at the retentate side (numTemperatureRetenate)
- Pressure at the retentate side (numTemperatureRetenate)

2.5. Reference-Author relation
- Title of reference, selected from table 1.5 (txtReference)
- Author/co-author, selected from table 1.6 (txtAuthor)
- Position of co-author between all author of reference (numPlace)

3. End entities

3.1. Flux experimental data
- Related experimental conditions, selected from table 2.3 (idExperimentConditionFlux)
- Ordinal number of data series (numDataSeries)
- Ordinal number of data point (numDataPoint)
- Chemical name of component (txtComponent
- Molar fraction in the feed (num_x)
- Flux (numJmol/m2/h)

3.2. Model
- Reference (txtReference)
- Modelled membrane (txtMembrane)
- Type of process (txtProcess)
- Used module (txtModule)
- Type of model: Short-cut model (txtS-C_Model), Solution-Diffusion model (txtS-D_Model) or Mayer-Blumenroth model (numM-B_Model)
- Feed: low limit of pressure (numLowLimitPressureFeed)
- Feed: upper limit of pressure (numUpperLimitPressureFeed)
- Feed: low limit of temperature (numLowLimitTemperatureFeed)
- Feed: upper limit of temperature (numUpperLimitTemperatureFeed)
- Permeate: low limit of pressure (numLowLimitPressurePermeate)
- Permeate: upper limit of pressure (numUpperLimitPressurePermeate)
- Permeate: low limit of temperature (numLowLimitTemperaturePermeate)
- Permeate: upper limit of temperature (numUpperLimitTemperaturePermeate)

- Retantate: low limit of pressure (numLowLimitPressureRetantate)
- Retantate: upper limit of pressure (numUpperLimitPressureRetantate)
- Retantate: low limit of temperature (numLowLimitTemperatureRetantate)
- Retantate: upper limit of temperature (numUpperLimitTemperatureRetantate)
- Text file with model equations (txtFile)
- ICAS-MoT file with model

3.2.1. Short-cut model
- Identification number of model (numModel)
- Compound for which model parameters are given (txtCompound)
- Composition limits of component *i* (numLowLimit_x, numUpperLimit_x)
- Model parameters Q_i^0 (numS-C_Qi0), E_i (numS-C_Ei) and T^0 (numS-C_T0)

3.2.2. Sorption-diffusion model
- Identification number of model (numModel)
- Compound for which model parameters are given (txtCompound)
- Composition limits of component *i* (numLowLimit_x, numUpperLimit_x)
- Model parameters P_i^0 (numS-D_Pi0), l_M (numS-D_lm), E_i (numS-D_Ei) and T^0 (numS-D_T0)

3.2.3. Mayer-Blumenroth model
- Identification number of model (numModel)
- Compound for which model parameters are given (txtCompound)
- Composition limits of component *i* (numLowLimit_x, numUpperLimit_x)
- Model parameters $\bar{D}_i^T\left(T^0\right)$ (numM-B_Pi0), E_i (numM-B_Ei), T^0 (numM-B_T0), B_i° (numM-B_Bi0) and B_{ij} parameters for mixture with maximum five components (numM-B_Bi0, numM-B_Bi1, numM-B_Bi2, numM-B_Bi3, numM-B_Bi4)

3.3. Permeability of pure compounds
- Membrane (txtMembrane)
- Permeated compound (txtPermeant)
- Temperature at which permeability was measured (numTemperature)
- Permeability at specified temperature (numPermeability)
- Diffusivity at specified temperature (numDiffusivity)
- Solubility at specified temperature (numSolubility)
- Tempearture range for which temperature dependence is specified (txtTemperatureRange)
- Temperature dependence in terms of P_0,(numPermeability_0) E_P (numEp), E_D (numEd) and E_S (numEs)

6.4. Appendix 4: Supplements to the case studies

In this section models used in all case studies are presented along with their analysis.

In order to solve a model the degree of freedom has to be equal to zero, therefore values of all parameters and known variables need to be provided. Moreover, initial variables for differential variables need to be provided.

6.4.1. Supplement to the case study of synthesis of cetyl oleate

6.4.1.1. Model for batch reactor for enzymatic esterification of cetyl oleate

Model described below was used to simulate the batch reaction in section 4.3.1.1 (page 99). The model was derived from superstructure (see Figure 3.5) and model equations (3.13, 3.15-3.32) for *NC* = 4, *NRKh* = 1, *NRK* = 0 and by specifying decision variables: $\xi^{1}=1$, $\xi^{2}=0$, $\xi^{1in}=0$, $\xi^{2in}=0$, $\xi^{1\alpha}=0$, $\xi^{1\beta}=0$, $\xi^{2\alpha}=0$, $\xi^{2\beta}=0$, $\xi^{R}=1$, $\xi^{\beta}=0$, $\xi^{homog}=0$, $\xi^{heterog}=1$. Therefore the mass balance is expressed by Eq. 6.43. Eqs. (3.15-3.32) are cancelled since only one process is considered.

$$\frac{dn_i}{dt}=\nu_i\, r^{1\alpha(heterog)} \tag{6.43}$$

Constitutive equations:

Reaction rate expression in synthesis of cetyl oleate is expressed by Eq. (6.76):

$$r^{1\alpha(heterog)}=\frac{\left(-r_{Ac}\right)^{f}_{\max}\left(-r_{Ac}\right)^{r}_{\max}\left(C_{Al}C_{Ac}-\frac{C_{Es}C_{W}}{K_{eq}}\right)}{\left(\begin{array}{l}\left(-r_{Ac}\right)^{r}_{\max}K_{i_{Ac}}K_{m_{Al}}\left(1+\frac{C_{Al}}{K'_{i_{Al}}}+\frac{C_{Es}}{K'_{i_{Es}}}\right)+\left(-r_{Ac}\right)^{r}_{\max}K_{m_{Al}}C_{Ac}\left(1+\frac{C_{Ac}}{K'_{i_{Ac}}}+\frac{C_{Es}}{K''_{i_{Es}}}\right)+\\ \left(-r_{Ac}\right)^{r}_{\max}K_{m_{Ac}}C_{Al}\left(1+\frac{C_{Al}}{K'_{i_{Al}}}+\frac{C_{Es}}{K'_{i_{Es}}}\right)+\left(-r_{Ac}\right)^{f}_{\max}K_{m_{W}}\frac{C_{Es}}{K_{eq}}+\left(-r_{Ac}\right)^{f}_{\max}K_{m_{Es}}\frac{C_{W}}{K_{eq}}+\\ \left(-r_{Ac}\right)^{r}_{\max}C_{Al}C_{Ac}+\left(-r_{Ac}\right)^{f}_{\max}K_{m_{W}}\frac{C_{Al}C_{Es}}{K_{eq}K_{i_{Al}}}+\left(-r_{Ac}\right)^{f}_{\max}\frac{C_{Es}C_{W}}{K_{eq}}+\\ \left(-r_{Ac}\right)^{r}_{\max}K_{m_{Ac}}\frac{C_{Al}C_{W}}{K_{i_{W}}}+\left(-r_{Ac}\right)^{r}_{\max}\frac{C_{Al}C_{Ac}C_{Es}}{K_{i_{Es}}}+\left(-r_{Ac}\right)^{f}_{\max}\frac{C_{Ac}C_{Es}C_{W}}{K_{i_{Al}}K_{eq}}\end{array}\right)}\cdot V\cdot m_{enz} \tag{6.44}$$

Where: Al-cetyl alcohol, Ac-oleic acid, Es-cetyl oleate, W-water.

Two variables present in Eq. (6.44) ($\left(-r_{Ac}\right)^{r}_{\max}$,$\left(-r_{Ac}\right)^{f}_{\max}$) characterize the maximum

reaction rate for esterification and hydrolysis reaction and they are expressed by Eq. (6.45-6.46).

$$\left(-r_{Ac}\right)_{\max}^{r} = \left(k\right)^{r} C_{Es} C_{W} \tag{6.45}$$

$$\left(-r_{Ac}\right)_{\max}^{f} = \left(k\right)^{f} \left(C_{Ac}\right)^{in} \left(C_{Al}\right)^{in} \tag{6.46}$$

The effect of temperature on the *K* constants in Eq. (6.47) is expressed by Van't Hoff type equation:

$$K = \exp\left(\frac{-\Delta H^{\circ}}{RT} + \frac{-\Delta S^{\circ}}{R}\right) \tag{6.47}$$

Dependency of the reaction rate constant is expressed by Arrhenius type equation:

$$k = k_{\circ} \exp\left(\frac{-E_a}{RT}\right) \tag{6.48}$$

The list of all values of parameters corresponding to Eqs. (6.47-6.48) is given in Table 6.5 and Table 6.6. The component molar densities are function of temperature (Eq. 6.49). Mass of the added enzyme (m_{enz}) is calculated as a weight fraction (*wf*) of initial mass of reacting mixture (Eq. 6.54). Reaction volume (*V*) is calculated based on ideal mixing rule (Eq. 6.50).

$$\rho_i = \left(\frac{A_i}{B_i}\right)^{\left(1+\left(1-T/C_i\right)^{D_i}\right)} \tag{6.49}$$

$$V = \sum_{i=1}^{4} \frac{n_i}{\rho_i} \tag{6.50}$$

$$V^0 = \sum_{i=1}^{4} \frac{n_i^0}{\rho_i} \tag{6.51}$$

$$C_i = \frac{n_i}{V} \tag{6.52}$$

$$\left(C_i\right)^{in} = \frac{n_i^0}{V_0} \tag{6.53}$$

$$m_{enz} = wf \cdot \sum_{i=1}^{4} n_i^0 MW_i \tag{6.54}$$

Condition about activity of water in the reaction is introduced by Eq. (6.55).

$$b = if\left(a_W > 0.11\right) than\left(b = 1\right) else\left(b = 0\right) \tag{6.55}$$

$$a_i = \gamma_i x_i \tag{6.56}$$

where $$x_i = \frac{n_i}{\sum_{i=1}^{4} n_i} \quad (6.57)$$

In order to solve this model 61 parameters and known variables, additionally 4 initial conditions need to be provided. Note that 4 activity coefficients γ_i are calculated by subroutine. All model variables and model equations are reported and described in Table 6.7 and Table 6.8 respectively.

Table 6.5: Thermodynamic constants for Michaelis-Menten constants and inhibition constants

Parameter (no. of all parameters 26)	$-\Delta H^{\circ}\left[\frac{Kcal}{mol}\right]$	$-\Delta S^{\circ}\left[\frac{cal}{mol \cdot K}\right]$
$K_{m_{Ac}}$	15.57	40.61
$K_{m_{Al}}$	15.04	39.11
$K_{m_{Es}}$	26.69	57.92
$K_{m_{W}}$	18.78	41.19
$K_{i_{Ac}}$	42.91	110.28
$K_{i_{Al}}$	18.37	43.08
$K_{i_{Es}}$	13.90	28.38
$K_{i_{W}}$	12.00	26.78
$K'_{i_{Ac}}$	25.64	60.21
$K'_{i_{Al}}$	46.23	121.74
$K'_{i_{Es}}$	32.86	88.50
$K''_{i_{Es}}$	11.96	24.78
K_{eq}	32.24	99.23

Table 6.6: Pre-exponential factor and activation energy

Parameter (o. of all parameters 4)	$k_{\circ}\left[\frac{l}{mol \cdot g_{cat} \cdot min}\right]$	$-E_a\left[\frac{cal}{mol}\right]$
$(k)^f$	6.91.10 13	23860
$(k)^r$	1.14.10 13	23840

Table 6.7: Variables in model for enzymatic esterification of batch reaction model

Differential variables		Number
Molar hold-up	n_i	4
Algebraic variables		**Number**
Reaction rate	$r^{1\alpha(heterog)}$	1
Maximum reaction rates	$\left(-r_{Ac}\right)^{r}_{\max}, \left(-r_{Ac}\right)^{f}_{\max}$	2
Reaction rate constants	see first column in Table 6.5 and Table 6.6	15
Components activity	a_i	4
Molar density	ρ_i	4
Molar fraction	x_i	4
Reaction volume	V	1
Concentration	C_i	4
Initial moles of compounds, volume and concentration	$\left(C_i\right)^{in}$, V^0	5
Mass of enzyme	m_{enz}	1
Conditional parameters	b	1
Algebraic variable calculated by subroutine		**Number**
Activity coefficient	γ_i (calculated using Modified UNIFAC Lyngby, all parameters for that model reported in section 6.4.1.3, page 202)	4
Parameters		**Number**
Process parameters	T	1
Weight fraction of enzyme	wf	1
Initial moles of compounds	n_i^0	4
Known variables		**Number**
Thermodynamic constants	see 2nd and 3rd column in Table 6.5	26
Max reaction rates constants	See 2nd and 3rd column in Table 6.6	4
Density constants	A_i, B_i, C_i, D_i	16
Stoichiometric coefficients	υ_i	4
Molecular weight	MW_i	4
Ideal gas constant	R	1
Total number of variables: 111		

Table 6.8: Equations in enzymatic membrane assisting batch reaction model

	Equations	Number of equations
Mass balance	(6.43)	4
Reaction kinetics	(6.44)	1
Temperature dependences	(6.47-6.48)	15
Maximum reaction rate	(6.45-6.46)	2
Temperature dependence of density	(6.49)	4
Reaction volume	(6.50)	1
Concentration	(6.52)	4
Initial volume and concentrations	(6.51, 6.53)	5
Mass of added enzyme	(6.54)	1
Activity of compound	(6.56) plus subroutine for γ_i	8
Molar fraction	(6.57)	4
"If" condition	(6.55)	1
Total number of equations: 50		
DOF: 61		

6.4.1.2. Model used in the case study of synthesis of cetyl oleate

Model described below was used to simulate the membrane assisted batch reaction in section 4.3.1.5 (page 106). The model was derived from the superstructure (see Figure 3.5) and model equations (3.13, 3.15-3.32) for *NC* = 4, *NKRh* = 1, *NRK* = 0 and by specifying decision variables: $\xi^{1}=1$, $\xi^{2}=1$, $\xi^{1\alpha}=0$, $\xi^{1\beta}=0$, $\xi^{2\alpha}=1$, $\xi^{2\beta}=0$, $\xi^{1in}=0$, $\xi^{2in}=0$, $\xi^{R}=1$, $\xi^{\beta}=0$, $\xi^{(homog)}=0$, $\xi^{(heterog)}=1$. Therefore the component mass balance is:

$$\frac{dn_i}{dt} = -\sigma_i^{2\alpha} x_i^{1\alpha} a \cdot F_{TOT}^{1\alpha} + \nu_{i,h}^{1\alpha} r_h^{1\alpha(heterog)} \tag{6.58}$$

Other streams in the hybrid process are related as follows:

$$F_i^{1\alpha P} = 0 \tag{6.59}$$

$$F_i^{1\beta P} = 0 \tag{6.60}$$

$$F_i^{1\alpha R} = F_i^{1\alpha} \tag{6.61}$$

$$F_i^{1\beta R} = F_i^{1\beta} \tag{6.62}$$

$$F_i^{2\alpha P} = F_i^{2\alpha} \tag{6.63}$$

$$F_i^{2\beta P} = 0 \tag{6.64}$$

$$F_i^{2\alpha R} = 0 \tag{6.65}$$

$$F_i^{2\beta R} = F_i^{2\beta} \tag{6.66}$$

$$F_i^{1\alpha} = a x_i^{1\alpha} F_{TOT}^{1\alpha} \tag{6.67}$$

$$F_i^{1\beta} = 0 \tag{6.68}$$

$$F_i^{2\alpha} = a\sigma_i^{2\alpha} x_i^{1\alpha} F_{TOT}^{1\alpha} \tag{6.69}$$

$$F_i^{2\beta} = a\sigma_i^{2\beta} x_i^{1\alpha} F_{TOT}^{1\alpha} \tag{6.70}$$

$$x_i^{1\alpha} = \frac{n_i}{\sum_{i=1}^{NC} n_i} \tag{6.71}$$

$$a = if\ (t \geq t_{switch})\ than\ (1)\ else\ (0) \tag{6.72}$$

From the definition of separation factor:

$$\sigma_i^{2\alpha} = \frac{F_i^{2\alpha}}{F_{TOT}^{1\alpha}} \tag{6.73}$$

and from definition of component flux, the rate of component removal from the system ($F_i^{2\alpha}$) is equal to component flux (J_i) multiplied by membrane area (A_m) the specific mass balance is written as follow:

$$\frac{dn_i}{dt} = -a \cdot J_i A_m + \nu_i^{1\alpha} r^{1\alpha(heterog)} \tag{6.74}$$

Including additionally, operational parameters *b* in Eq. 6.74 the following mass balance is obtained:

$$\frac{dn_i}{dt} = a \cdot b \cdot \left(-J_i A_m\right) + \nu_i r^{1\alpha(heterog)} \tag{6.75}$$

Parameter *b* is equal to 1 when activity of water is grater than 0.11, otherwise is zero. Note that since reaction kinetics are expressed by different type of equation than Eqs. (3.30-3.31) different equation representing $r^{1\alpha(heterog)}$ is used (see below).

Constitutive equations:

$$r^{1\alpha(heterog)} = \frac{\left(-r_{Ac}\right)^{f}_{\max}\left(-r_{Ac}\right)^{r}_{\max}\left(C_{Al}C_{Ac} - \frac{C_{Es}C_{W}}{K_{eq}}\right)}{\left(\begin{array}{l}\left(-r_{Ac}\right)^{r}_{\max} K_{i_{Ac}} K_{m_{Al}}\left(1+\frac{C_{Al}}{K'_{i_{Al}}}+\frac{C_{Es}}{K'_{i_{Es}}}\right)+\left(-r_{Ac}\right)^{r}_{\max} K_{m_{Al}} C_{Ac}\left(1+\frac{C_{Ac}}{K'_{i_{Ac}}}+\frac{C_{Es}}{K''_{i_{Es}}}\right)+\\ \left(-r_{Ac}\right)^{r}_{\max} K_{m_{Ac}} C_{Al}\left(1+\frac{C_{Al}}{K'_{i_{Al}}}+\frac{C_{Es}}{K'_{i_{Es}}}\right)+\left(-r_{Ac}\right)^{f}_{\max} K_{m_{W}}\frac{C_{Es}}{K_{eq}}+\left(-r_{Ac}\right)^{f}_{\max} K_{m_{Es}}\frac{C_{W}}{K_{eq}}+\\ \left(-r_{Ac}\right)^{r}_{\max} C_{Al}C_{Ac}+\left(-r_{Ac}\right)^{f}_{\max} K_{m_{W}}\frac{C_{Al}C_{Es}}{K_{eq}K_{i_{Al}}}+\left(-r_{Ac}\right)^{f}_{\max}\frac{C_{Es}C_{W}}{K_{eq}}+\\ \left(-r_{Ac}\right)^{r}_{\max} K_{m_{Ac}}\frac{C_{Al}C_{W}}{K_{i_{W}}}+\left(-r_{Ac}\right)^{r}_{\max}\frac{C_{Al}C_{Ac}C_{Es}}{K_{i_{Es}}}+\left(-r_{Ac}\right)^{f}_{\max}\frac{C_{Ac}C_{Es}C_{W}}{K_{i_{Al}}K_{eq}}\end{array}\right)} \cdot V \cdot m_{enz}$$

(6.76)

$$\left(-r_{Ac}\right)^{r}_{\max} = \left(k\right)^{r} C_{Es}C_{W} \tag{6.77}$$

$$\left(-r_{Ac}\right)^{f}_{\max} = \left(k\right)^{f}\left(C_{Ac}\right)^{in}\left(C_{Al}\right)^{in} \tag{6.78}$$

$$K = \exp\left(\frac{-\Delta H^{\circ}}{RT}+\frac{-\Delta S^{\circ}}{R}\right) \tag{6.79}$$

$$k = k_{\circ}\exp\left(\frac{-E_{a}}{RT}\right) \tag{6.80}$$

$$\rho_{i} = \left(\frac{A_{i}}{B_{i}}\right)^{\left(1+\left(1-T/C_{i}\right)^{D_{i}}\right)} \tag{6.81}$$

$$V = \sum_{i=1}^{4}\frac{n_{i}}{\rho_{i}} \tag{6.82}$$

$$V^{0} = \sum_{i=1}^{4}\frac{n_{i}^{0}}{\rho_{i}} \tag{6.83}$$

$$C_{i} = \frac{n_{i}}{V} \tag{6.84}$$

$$\left(C_{i}\right)^{in} = \frac{n_{i}^{0}}{V_{0}} \tag{6.85}$$

$$m_{enz} = wf \cdot \sum_{i=1}^{4} n_{i}^{0} MW_{i} \tag{6.86}$$

The rate of component removal has been described with Eq. (6.87).

$$J_{i} = P_{i}\, x_{i} \tag{6.87}$$

where

$$x_i = \frac{n_i}{\sum_{i=1}^{4} n_i} \tag{6.88}$$

Additionally, the process variable switching time t_{switch} is introduced as "if condition" given by Eq. (6.89). Condition about activity of water in the reaction is introduced by Eq. (6.90).

$$a = if\left(t \geq t_{switch}\right) than\left(a = 1\right) else\left(a = 0\right) \tag{6.89}$$

$$b = if\left(a_W > 0.11\right) than\left(b = 1\right) else\left(b = 0\right) \tag{6.90}$$

$$a_i = \gamma_i x_i \tag{6.91}$$

In order to solve this model 67 parameters and known variables, additionally 4 initial conditions need to be provided. All model variables and model equations are reported in Table 6.9 and Table 6.10.

Table 6.9: Variables in model for enzymatic membrane assisted batch reaction model

Differential variables		Number
Molar hold-up	n_i	4
Algebraic (unknown) variables		**Number**
Reaction rate	$r^{1\alpha(heterog)}$	1
Maximum reaction rates	$(-r_{Ac})^{r}_{\max}$, $(-r_{Ac})^{f}_{\max}$	2
Reaction rate constants	see first column in Table 6.5 and Table 6.6, page 195	15
Components activity	a_i	4
Molar density	ρ_i	4
Molar fraction	x_i	4
Reaction volume	V	1
Concentration	C_i	4
Initial moles of compounds, volume and concentration	$(C_i)^{in}$, V^0	5
Mass of enzyme	m_{enz}	1
Conditional parameters	a, b	2
Component flux	J_i	4
Algebraic variable calculated by external subroutine		**Number**
Activity coefficient	γ_i (calculated using Modified UNIFAC Lyngby, all parameters for that model reported in section 6.4.1.3, page 202)	4
Parameters		**Number**
Process parameters	T	1
Weight fraction of enzyme	wf	1
Initial moles of compounds	n_i^0	4
Switching time	t_{switch}	1
Known variables		**Number**
Thermodynamic constants	see 2nd and 3rd column in Table 6.5, page 195	26
Max reaction rates constants	See 2nd and 3rd column in Table 6.6, page 195	4
Density constants	A_i, B_i, C_i, D_i	16
Permeability	P_i	4
Membrane area	A_m	1
Stoichiometric coefficients	υ_i	4
Molecular weight	MW_i	4
Ideal gas constant	R	1
Total number of variables: 122		

Table 6.10: Equations in enzymatic membrane assisting batch reaction model

	Equations	Number of equations
Mass balance	(6.75)	4
Reaction kinetics	(6.76)	1
Temperature dependences	(6.79-6.80)	15
Maximum reaction rate	(6.77-6.78)	2
Temperature dependence of density	(6.81)	4
Reaction volume	(6.82)	1
Concentration	(6.84)	4
Initial volume and concentrations	(6.83, 6.85)	5
Mass of enzyme	(6.86)	1
Component flux	(6.87)	4
Activity of compounds	(6.91) plus subroutine for γ_i	8
Molar fraction	(6.88)	4
"If" conditions	(6.89-6.90)	2
Total number of equations: 55		
DOF: 67		

6.4.1.3. UNIFAC parameters used in the case study of synthesis of cetyl oleate

Table 6.11: Modified UNIFAC (Lyngby) groups representation for cetyl oleate, water, oleic acid and 1-hexadecanol

	Representation	Sub group	Main group
Cetyl oleate	2	'CH3'	'CH2'
	28	'CH2'	'CH2'
	1	'CH=CH'	'C=C'
	1	'CH2COO'	'CCOO'
Water	1	'H2O'	'H2O'
Oleic acid	1	'CH3'	'CH2'
	14	'CH2'	'CH2'
	1	'CH=CH'	'C=C'
	1	'COOH'	'COOH'
1-hexadecanol	1	'CH3'	'CH2'
	14	'CH2'	'CH2'
	1	'OH'	'OH'
	1	'CH2'alc'	'CH2'alc'

Table 6.12: R_i and Q_i for Modified UNIFAC (Lyngby). Groups present in mixture of cetyl oleate, water, oleic acid and 1-hexadecanol.

	R_i	Qi
CH3	0.9011	0.848
CH2	0.6744	0.54
CH=CH	1.1168	0.86
CH2COO	1.6764	1.42
H2O	0.92	1.4
COOH	1.3013	1.224
OH	1	1.2
CH2 alc	0.6744	0.54

Table 6.13: Values of parameters for Modified UNIFAC (Lyngby) used in the case study of synthesis of cetyl oleate

	CH2	C=C	OH	H2O	CCOO	COOH	CH2 alc
				A_{ij}			
CH2	0	76.46	972.8	1857	-329.1001	664.1001	0
C=C	-46.45	0	633.5	1049	-24.65	186	-46.45
OH	637.5	794.7	0	155.6	169.1	61.78	637.5
H2O	410.7	564.3999	-47.15	0	218	8.621	410.7
CCOO	44.43	200.3	266.899	245	0	557.8999	44.43
COOH	171.5	227.3	-92.21	86.44	-224.6	0	171.5
CH2alc	0	76.46	972.8	1857	329.1	664.1	0
				B_{ij}			
CH2	0	-0.1834	0.2687	-3.322	-0.1518	1.317	0
C=C	-0.1817	0	0	-3.305	0	0	-0.1817
OH	-5.832	0	0	0.3761	0.1902	0	-5.832
H2O	2.868	0	-0.4947	0	-0.4269	-1.709	2.868
CCOO	-0.9718	0	-1.054	-0.0717	0	1.377	-0.9718
COOH	-1.463	0	0	0.9941	0.7234	0	-1.463
CH2alc	0	-0.1834	0.2687	-3.322	0.1518	1.317	0
				C_{ij}			
CH2	0	-0.3659	8.773	-9	-1.824	-4.904	0
C=C	-0.4888	0	0	0	0	0	-0.4888
OH	-0.8703	0	0	-9	4.625	0	-0.8703
H2O	9	0	8.65	0	-6.092	6.413	9
CCOO	0.5518	0	3.586	2.754	0	0	0.5518
COOH	0.6759	0	0	-12.74	0	0	0.6759
CH2alc	0	-0.3659	8.773	-9	1.824	-4.904	0

6.4.2. Supplement to the case study of interesterification of phosphatidylcholine

6.4.2.1. Model for enzymatic interesterification in the batch operation

Model presented in this section has been used to validate the experimental results published by Egger et al. (1997). The batch reactor model was derived from superstructure (see Figure 3.5) for *NC* = 7, *NRKh* = 2, *NRK* = 0 and by specifying decision variables: $\xi^1 = 1$, $\xi^2 = 0$, $\xi^{1in} = 0$, $\xi^{2in} = 0$, $\xi^{1\alpha} = 0$, $\xi^{1\beta} = 0$, $\xi^{2\alpha} = 0$, $\xi^{2\beta} = 0$, $\xi^R = 1$, $\xi^\beta = 0$, $\xi^{homog} = 0$, $\xi^{heterog} = 1$. Therefore the mass balance is expressed by Eq. (6.92). Note that reaction rate expressed in Eq. (3.13) as $r_h^{1\alpha(heterog)}$ is substituted by r_j . Eqs. (3.15-3.32) are cancelled since only one process is considered. The component mass balance in the batch reactor is as follows:

$$\frac{dn_i}{dt} = \upsilon_{1,i} \cdot r_1 + \upsilon_{2,i} \cdot r_2 \tag{6.92}$$

Following reaction rate expressions were adapted from article published by Teusink et al., (2000) and represent reversible Michaelis-Menten kinetics for two noncompeting substrate-product couples. Reaction rate expression for enzymatic hydrolysis given by Eq. (4.22), (see page 111):

$$r_1 = r_{\max} \frac{\dfrac{C_1 C_2}{K_{m1} K_{m2}} \left(1 - \dfrac{C_3 C_4}{C_1 C_2} \dfrac{1}{K_{eq,1}} \right)}{\left(1 + \dfrac{C_1}{K_{m1}} + \dfrac{C_3}{K_{m3}} \right) \left(1 + \dfrac{C_2}{K_{m2}} + \dfrac{C_4}{K_{m4}} \right)} \cdot m_{enz} \tag{6.93}$$

Reaction rate expression for enzymatic esterification given by Eq. (4.23) (see page111):

$$r_2 = r_{\max,2} \frac{\dfrac{C_3 C_5}{K_{m3} K_{m5}} \left(1 - \dfrac{C_6 C_2}{C_3 C_5} \dfrac{1}{K_{eq,2}} \right)}{\left(1 + \dfrac{C_3}{K_{m3}} + \dfrac{C_2}{K_{m2}} \right) \left(1 + \dfrac{C_6}{K_{m6}} + \dfrac{C_5}{K_{m5}} \right)} \cdot m_{enz} \tag{6.94}$$

Where apparent equilibrium constants are defined by Eqs. (6.95-6.96).

$$K_{eq,2} = -0.000159 \cdot C_2 + 0.017 \tag{6.95}$$

$$K_{eq,1} = \frac{1}{K_{eq,2}} \tag{6.96}$$

Volume is defined by Eq. (6.97) and it is expressed in dm^3.

$$V = \sum_{i=1}^{6} \frac{n_i \cdot Mw_i}{\rho_i \cdot 1000} \tag{6.97}$$

$$C_i = \frac{n_i}{V} \tag{6.98}$$

where (1) 1,2-dihexadecanoyl-glycero-3-phosphocholine, (2) water, (3) 1-hexadecanoyl-glycero-3-phosphocholine, (4) palmitic acid, (5) oleic acid, (6) 1-hexadeca-2-octadeca-9,12-dienoyl-glycero-2-phosphocholine and (0) toluene (solvent).

Table 6.14: Values of Michaelis-Menten parameters present in Eqs. 6.93-6.94

		Hydrolysis (Eq. 6.93)		Esterification (Eq. 6.94)	
r_{max} [mmol·mg^{-1}·h^{-1}]		$8.25 \cdot 10^{-4}$		$1.04 \cdot 10^{-4}$	
K_{m1}	K_{m2}	K_{m3}	K_{m4}	K_{m5}	K_{m6}
4.9	4.9	4.9	4.9	4.9	4.9

Table 6.15: List of variables in model of the batch reactor for enzymatic interesterification of phosphatidylcholine

Differential variables		Number
Molar hold-up	n_i	7
Algebraic (unknown) variables		**Number**
Reaction rate	r_1 , r_2	2
Apparent equilibrium constants	$K_{eq,1}$, K_{m2}	2
Reaction volume	V	1
Components concentrations	C_i	7
Parameters		**Number**
Reaction rate constants	K_{m1} , K_{m2} , K_{m3} , K_{m4} , K_{m5} , K_{m6}	6
Process parameters	m_{enz} [μg]	1
Known variables		**Number**
Stoichiometric coefficients	υ_i	14
Component molar densities	ρ_i	7
Molecular weight	Mw_i	7
Total number of variables: 54		

Table 6.16: List of equations in model of the batch reactor for enzymatic interesterification of phosphatidylcholine

	Equations	Number of equations
Mass balance	(6.92)	7
Reaction kinetics	(6.93-6.94)	2
Equilibrium constants	(6.95- 6.96)	2
Volume	(6.97)	1
Concentration	(6.98)	7
Total number of equations: 19		
DOF: 35		

Egger et al. (1999) reported results for two kinds of experiments. First set consider only esterification reaction of lysophosphatidylcholine with oleic acid to phosphatidylcholine which are compared with simulation (lines) on Figures 6.4-6.7. Second kinds of experiments considered simultaneous hydrolysis and esterification. However, in that case a cumulative data for both phosphatidylcholine, e.g. original and modified phosphatidylcholine were compared on Figures 6.8-6-10 since only these results were available.

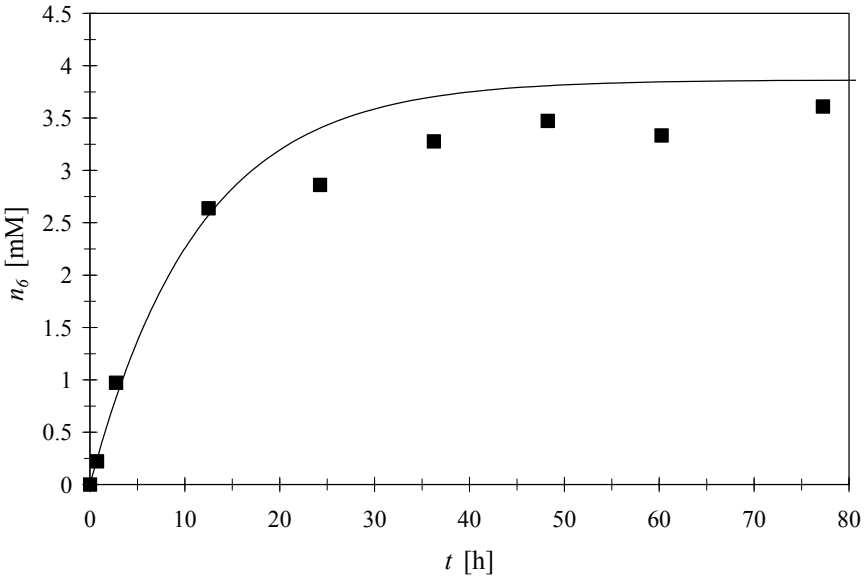

Figure 6.4: Comparison of experimental points from Egger et al. (1997) and simulations. m_{enz} = 50mg, n_1 = 0 mmol, n_2 = 17.8 mmol, n_3 = 10.0 mmol, n_4 = 0 mmol, n_5 = 800 mmol, n_6 = 0.00 mmol, n_7 = 8185 mmol

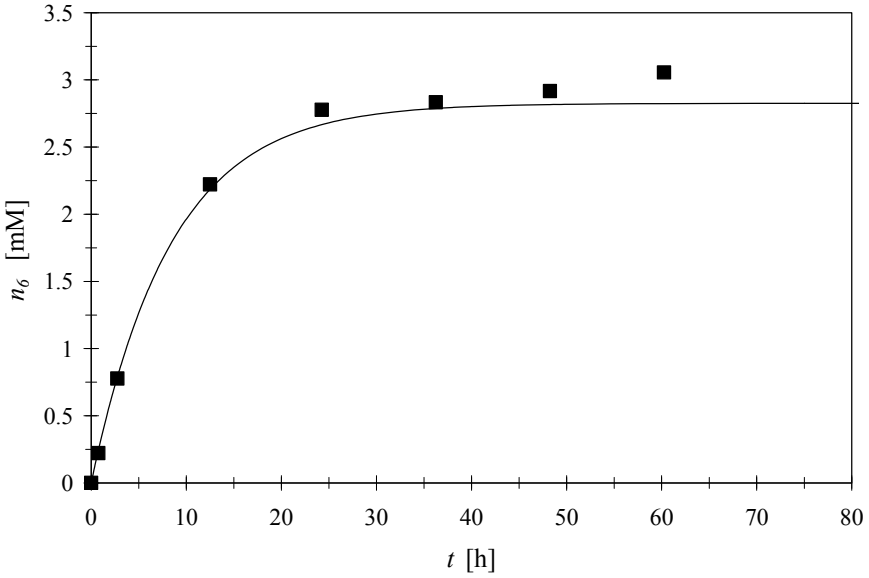

Figure 6.5: Comparison of experimental points from Egger et al. (1997) and simulations. m_{enz} = 50mg, n_1 = 0 mmol, n_2 = 26.0 mmol, n_3 = 10.0 mmol, n_4 = 0 mmol, n_5 = 800 mmol, n_6 = 0.00 mmol, n_7 = 8185 mmol

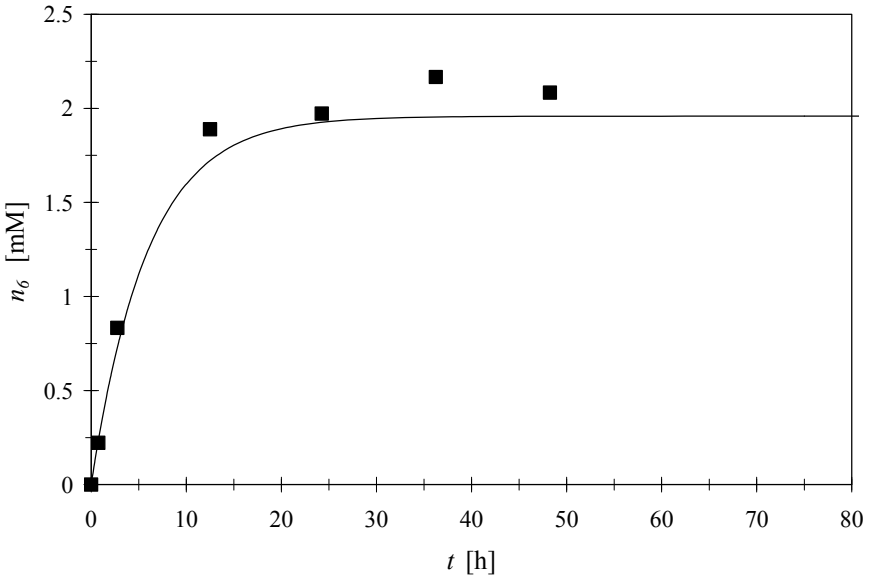

Figure 6.6: Comparison of experimental points from Egger et al. (1997) and simulations. m_{enz} = 50mg, n_1 = 0 mmol, n_2 = 36.0 mmol, n_3 = 10.0 mmol, n_4 = 0 mmol, n_5 = 800 mmol, n_6 = 0.00 mmol, n_7 = 8185 mmol

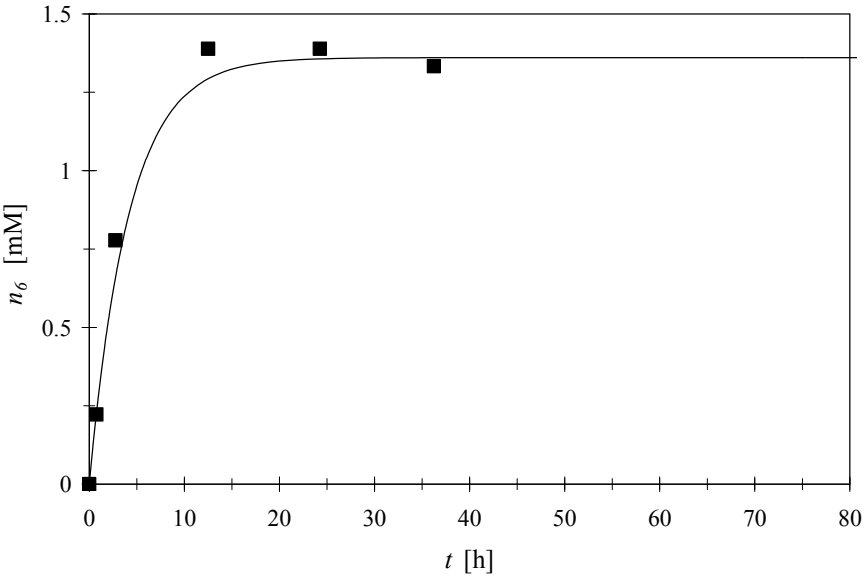

Figure 6.7: Comparison of experimental points from Egger et al. (1997) and simulations. m_{enz} = 50mg, n_1 = 0 mmol, n_2 = 46.0 mmol, n_3 = 10.0 mmol, n_4 = 0 mmol, n_5 = 800 mmol, n_6 = 0.00 mmol, n_7 = 8185 mmol

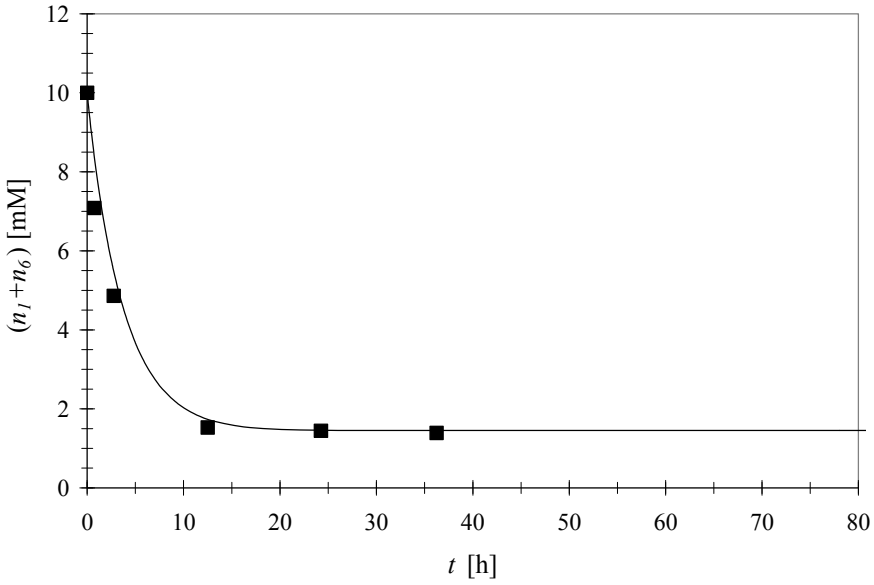

Figure 6.8: Comparison of experimental points from Egger et al. (1997) and simulations. n_1 = 10.0 mmol, n_2 = 46.3 mmol, n_3 = 0.02 mmol, n_4 = 0.02 mmol, n_5 = 800 mmol, n_6 = 0.00 mmol, n_7 = 8186 mmol

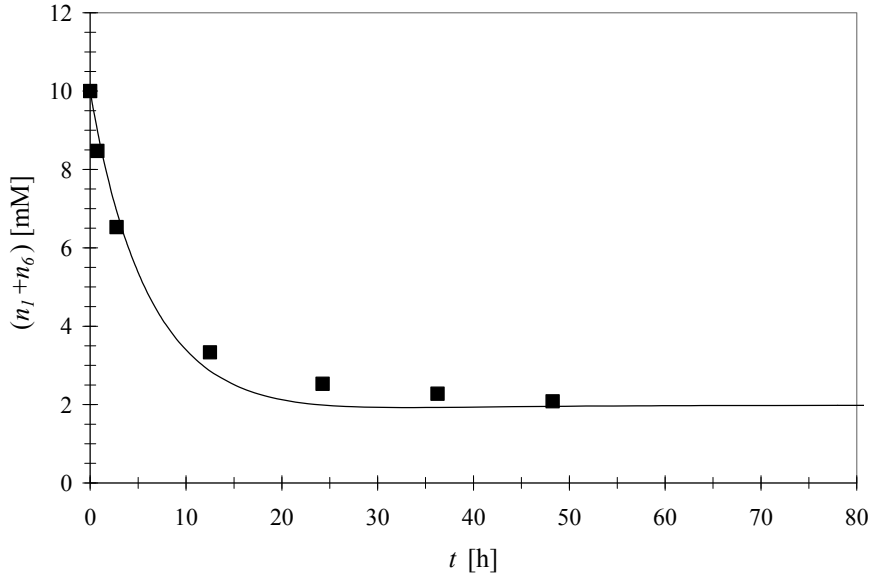

Figure 6.9: Comparison of experimental points from Egger et al. (1997) and simulations. n_1 = 10.0 mmol, n_2 = 36.62 mmol, n_3 = 0.02 mmol, n_4 = 0.02 mmol, n_5 = 800 mmol, n_6 = 0.00 mmol, n_7 = 8186 mmol

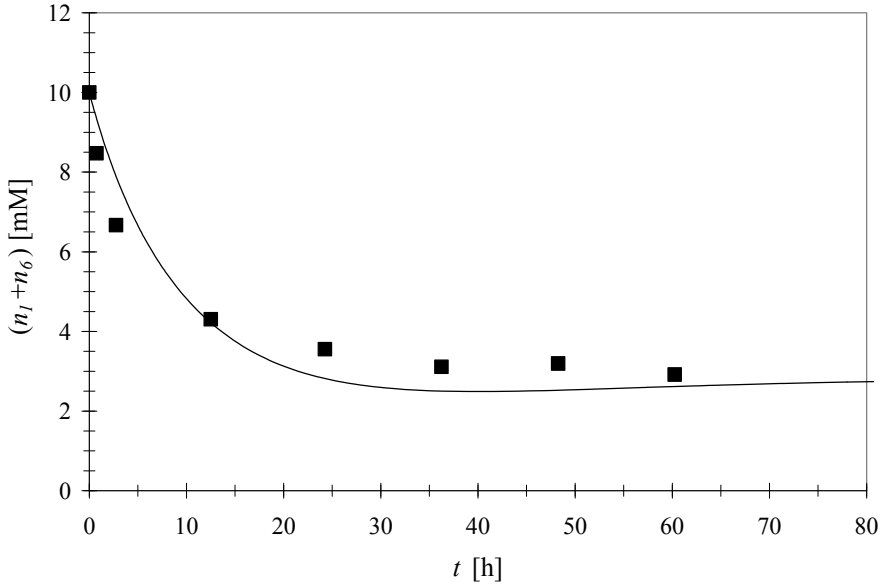

Figure 6.10: Comparison of experimental points from Egger et al. (1997) and simulations. n_1 = 10.0 mmol, n_2 = 26.06 mmol, n_3 = 0.01 mmol, n_4 = 0.01 mmol, n_5 = 800 mmol, n_6 = 0.00 mmol, n_7 = 8186 mmol

6.4.2.2. Model for membrane assisted batch reaction

Model described below was used to simulate the membrane assisted batch reaction in section 4.3.2.5 (page 122). The model was derived from the superstructure (see Figure 3.5) and model equations (3.13, 3.21-3.20) for $NC = 7$, $NRKh = 2$, $NRK = 0$ and by specifying the decision variables: $\xi^{1} = 1$, $\xi^{2} = 1$, $\xi^{1\alpha} = 0$, $\xi^{1\beta} = 0$, $\xi^{2\alpha} = 1$, $\xi^{2\beta} = 0$, $\xi^{1in} = 0$, $\xi^{2in} = 0$, $\xi^{R} = 1$, $\xi^{\beta} = 0$, $\xi^{(homog)} = 0$, $\xi^{(heterog)} = 1$. Therefore the mass balance is:

$$\frac{dn_i}{dt} = -a\sigma_i^{2\alpha} F_{TOT}^{1\alpha} + \nu_{1,i}^{1\alpha} r_1^{1\alpha} + \nu_{2,i}^{1\alpha} r_2^{1\alpha} \tag{6.99}$$

From the definition of separation factor given by Eq. 6.73 and from definition of component flux, the rate of component removal from the system ($F_i^{2\alpha}$) is equal to component flux (J_i) multiplied by membrane area (A_m) the specific mass balance is written as follow:

$$\frac{dn_i}{dt} = a \cdot \left(-J_i A_m\right) + \nu_{1,i} r_1 + \nu_{2,i} r_2 \tag{6.100}$$

Constitutive equations:

$$r_1 = r_{\max} \frac{\frac{C_1 C_2}{K_{m1} K_{m2}} \left(1 - \frac{C_3 C_4}{C_1 C_2} \frac{1}{K_{eq,1}}\right)}{\left(1 + \frac{C_1}{K_{m1}} + \frac{C_3}{K_{m3}}\right)\left(1 + \frac{C_2}{K_{m2}} + \frac{C_4}{K_{m4}}\right)} \cdot m_{enz} \tag{6.101}$$

$$r_2 = r_{\max,2} \frac{\frac{C_3 C_5}{K_{m3} K_{m5}} \left(1 - \frac{C_6 C_2}{C_3 C_5} \frac{1}{K_{eq,2}}\right)}{\left(1 + \frac{C_3}{K_{m3}} + \frac{C_2}{K_{m2}}\right)\left(1 + \frac{C_6}{K_{m6}} + \frac{C_5}{K_{m5}}\right)} \cdot m_{enz} \tag{6.102}$$

$$K_{eq,2} = -0.000159 \cdot C_2 + 0.017 \tag{6.103}$$

$$K_{eq,1} = \frac{1}{K_{eq,2}} \tag{6.104}$$

$$V = \sum_{i=1}^{6} \frac{n_i \cdot Mw_i}{\rho_i \cdot 1000} \tag{6.105}$$

$$C_i = \frac{n_i}{V} \tag{6.106}$$

$$a = if\left(t \geq t_{switch}\right) than\left(a = 1\right) else\left(a = 0\right) \tag{6.107}$$

Subscripts: 0-solvent, 1-phosphatidylcholine 1, 2-water, 3-lysophatidylcholine, 4-free

fatty acid, 5-oleic acid, 6-phosphatidylcholine 2.

Depending on the scenario different relation to calculate component fluxes have been used. In the first calculations constant fluxes of compounds through the membrane are used. In the case when n-hexane was used the data published by Kang et al. (2004) have been fitted to the Eq. (6.108).

$$J_i = P_i \left(a_i^F - a_i^P \right) \tag{6.108}$$

$$a_i^F = \gamma_i x_i \tag{6.109}$$

$$a_i^P = \frac{P^P y_i}{P} \tag{6.110}$$

$$x_i = \frac{n_i}{\sum_{j=1}^{7} n_j} \tag{6.111}$$

Table 6.17: List of variables in the model of membrane assisted batch reaction for enzymatic interesterification of phosphatidylcholine when n-hexane was used as the solvent

Differential variables		Number
Molar hold-up	n_i	7
Algebraic (unknown) variables		**Number**
Reaction rate	r_1 , r_2	2
Apparent equilibrium constants	$K_{eq,1}$, K_{m2}	2
Reaction volume	V	1
Components concentrations	C_i	7
Component flux	J_i	7
Activities	a_i^F , a_i^P	14
Mol fraction	x_i	7
Condition variable	a	1
Algebraic variable calculated by external subroutine		**Number**
Activity coefficient	γ_i	7
Parameters		**Number**
Reaction rate constants	K_{m1}, K_{m2}, K_{m3}, K_{m4}, K_{m5}, K_{m6}	6
Component permeability	P_i	7
Permeate composition	y_i	7
Permeate pressure	P^P	1
Time switch	t_{switch}	1
Process parameters	m_{enz} [μg]	1
Known variables		**Number**
Stoichiometric coefficients	$\upsilon_{1,i}$, $\upsilon_{1,i}$	14
Component molar densities	ρ_i	7
Pressure	P	1
Molecular weight	Mw_i	7
Total number of variables: 107		

Table 6.18: List of equations in the model of membrane assisted batch reaction for enzymatic interesterification of phosphatidylcholine when n-hexane was used as the solvent

	Equations	Number of equations
Mass balance	(6.100)	7
Reaction kinetics	(6.101-6.102)	2
Equilibrium constants	(6.103-6.104)	2
Volume	(6.105)	1
Concentration	(6.106)	7
Condition	(6.107)	1
Flux	(6.108)	7
Activities	(6.109-6.110) plus subroutine for γ_i	21
Mol fraction	(6.111)	7
Total number of equations: 55		
DOF: 52		

6.4.3. Production of ethyl lactate

6.4.3.1. Model for heterogeneously catalyzed synthesis of ethyl lactate in batch reactor

Following model of the batch reactor was used to simulate heterogeneously catalysed batch reaction in section 4.3.3.1 (page 126). The model was derived from superstructure (see Figure 3.5) and model equations (3.13, 3.15-3.32) for *NC* = 4, *NRKh* = 1, *NRK* = 0 and by specifying the decision variables: $\xi^{1}=1$, $\xi^{2}=0$, $\xi^{1in}=0$, $\xi^{2in}=0$, $\xi^{1\alpha}=0$, $\xi^{1\beta}=0$, $\xi^{2\alpha}=0$, $\xi^{2\beta}=0$, $\xi^{R}=1$, $\xi^{\beta}=0$, $\xi^{homog}=0$, $\xi^{heterog}=1$.

Mass balance:

$$\frac{dn_1}{dt} = \nu_i \, r_1^{1\alpha(heterog)} \tag{6.112}$$

Constitutive equations:

$$r_1^{1\alpha(heterog)} = \frac{k_1\left(C_0C_1 - \frac{1}{K_{eq}}C_2C_3\right)}{C_1 + K_1C_2C_3}\frac{m_{CAT}}{1000} \tag{6.113}$$

Where 0: lactic acid, 1: ethanol, 2:ethyl lactate, 3: water.

$$k_1 = k_0 e^{\left(\frac{-E_1}{RT}\right)} \tag{6.114}$$

$$K = K_0 e^{\left(\frac{-E}{RT}\right)} \tag{6.115}$$

$$K_1 = K_{1,0} e^{\left(\frac{-E_{1,0}}{RT}\right)} \tag{6.116}$$

$$w_i = \frac{n_i Mw_i}{\sum_{j=1}^{4} n_j Mw_j} \tag{6.117}$$

$$\rho_i = \frac{A_i}{B_i^{1+\left(1-\frac{T}{C_i}\right)^{D_i}}} \tag{6.118}$$

$$d_i = \rho_i Mw_i \tag{6.119}$$

$$V = \frac{\sum_{i=1}^{4} n_i Mw_i}{\sum_{i=1}^{4} d_i w_i} \tag{6.120}$$

$$C_i = \frac{n_i}{V} \tag{6.121}$$

$$Yield = \frac{n_0(t=0) - n_0}{n_0(t=0)} \tag{6.122}$$

Table 6.19: Reaction constants for temperature dependence

E [J/mol]	E_1 [J/mol]	$E_{1,0}$ [J/mol]	K_0 [-]	k_0 [dm^3/kg$_{CAT}$/min]	$K_{1,0}$ [dm^3/mol]
-4441.88	30593.51	-33927.4	0.65082	12759.4	$3.11 \cdot 10^{-6}$

Table 6.20: Variables in the model of batch reactor for heterogeneously catalysed synthesis of ethyl lactate

Differential variables		Number
Molar hold-up	n_i	4
Auxiliary variables		**Number**
Reaction rate	$r_1^{1\alpha}$	1
Reaction rate constants	k_1 , K , K_1	3
Weight fraction	w_i	4
Molar density	ρ_i	4
Mass density	d_i	4
Reaction volume	V	1
Components concentration	C_i	4
Yield	$Yield$	1
Parameters		**Number**
Process parameters	T , m_{CAT}	2
Known variables		**Number**
Reaction related constants	k_0 , K_0 , $K_{1,0}$, E_1 , E , $E_{1,0}$	6
Stoichiometric coefficients	υ_i	4
Molar liquid density constants	A_i , B_i , C_i , D_i	16
Molecular weight	Mw_i	4
Constants	R	1
Total number of variables: 59 (total number of parameters and known variables 33)		

Table 6.21: Equations in the model of batch reactor for heterogeneously catalysed synthesis of ethyl lactate

	Equations	Number of equations
Mass balance	(6.112)	4
Reaction kinetics	(6.113)	1
Temperature dependences	(6.114-6.116)	3
Density and volume	(6.118-6.120)	9
Concentration	(6.121)	4
Weight fraction	(6.117)	4
Yield	(6.122)	1
Total number of equations: 26		

Degree of freedom of that model is equal to 33, therefore in order to solve all parameters and known variables needs to be specified. Additional four initial conditions with respect to number of moles of compounds present in the system need to be given.

6.4.3.2. Model for membrane assisted batch reaction

Model described below was used to simulate the membrane assisted batch reaction in section 4.3.3.5 (page 135). The model was derived from superstructure (see Figure 3.5) and model equations (3.13, 3.15-3.32) for *NC* = 4, *NRKh* = 1, *NRK* = 0 and by specifying decision variables: $\xi^{1}=1$, $\xi^{2}=1$, $\xi^{1\alpha}=0$, $\xi^{1\beta}=0$, $\xi^{2\alpha}=1$, $\xi^{2\beta}=0$, $\xi^{1in}=0$, $\xi^{2in}=0$, $\xi^{R}=1$, $\xi^{\beta}=0$, $\xi^{(homog)}=0$, $\xi^{(heterog)}=1$. Therefore the mass balance is:

$$\frac{dn_i}{dt} = -a\sigma_i^{2\alpha} F_{TOT}^{1\alpha} + \nu_i^{1\alpha} r^{1\alpha} \tag{6.123}$$

From the definition of separation factor given by Eq. 6.73 and from definition of component flux, the rate of component removal from the system ($F_i^{2\alpha}$) is equal to component flux (J_i) multiplied by membrane area (A_m) the specific mass balance is written as follow:

$$\frac{dn_i}{dt} = a \cdot \left(-J_i\, A_m\right) + \nu\, r_1^{1\alpha(heterog)} \tag{6.124}$$

Constitutive equations:

$$r_1^{1\alpha(heterog)} = \frac{k_1\left(C_0C_1 - \frac{1}{K_{eq}}C_2C_3\right)}{C_1 + K_1C_2C_3}\frac{m_{CAT}}{1000} \tag{6.125}$$

Where 0: lactic acid, 1: ethanol, 2:ethyl lactate, 3: water.

$$k_1 = k_0 e^{\left(\frac{-E_1}{RT}\right)} \tag{6.126}$$

$$K = K_0 e^{\left(\frac{-E}{RT}\right)} \tag{6.127}$$

$$K_1 = K_{1,0} e^{\left(\frac{-E_{1,0}}{RT}\right)} \tag{6.128}$$

$$w_i = \frac{n_i Mw_i}{\sum_{j=1}^{4} n_j Mw_j} \tag{6.129}$$

$$\rho_i = \frac{A_i}{B_i^{1+\left(1-\frac{T}{C_i}\right)^{D_i}}} \tag{6.130}$$

$$d_i = \rho_i Mw_i \tag{6.131}$$

$$V = \frac{\sum_{i=1}^{4} n_i Mw_i}{\sum_{i=1}^{4} d_i w_i} \tag{6.132}$$

$$C_i = \frac{n_i}{V} \tag{6.133}$$

$$Yield = \frac{n_0(t=0) - n_0}{n_0(t=0)} \tag{6.134}$$

Component flux is calculated using correlation reported by Benedict et al. (2006) for the quaternary mixture of lactic acid, ethanol, ethyl lactate and water. Membrane GFT-1005 has high selectivity; therefore it is assumed that only water permeates. Correlation expressed by Eq. (6.135) is valid for temperature 368.15 K and pressure on the permeate side of 0.44 kPa.

$$J_3 = \alpha_3 C_3^{\beta_3} \frac{1000}{60 \cdot Mw_3} \tag{6.135}$$

$$J_i = 0 \quad i \in \{0,1,2\} \tag{6.136}$$

Where $\alpha_3 = 0.508$, $\beta_3 = 1.1242$.

$$a = if\left(t \geq t_{switch}\right) than\left(a=1\right) else\left(a=0\right) \tag{6.137}$$

Additionally, mass of collected permeate has been calculated according Eq. 6.138in order to compare simulation results with experimental data reported by Benedict et al. (2006).

$$\frac{dP}{dt} = \sum_{i=1}^{4} J_i A_m Mw_i \tag{6.138}$$

Volume of collected permeate

$$\rho_i^{permeate} = \frac{A_i}{B_i^{1+\left(1-\frac{T_{permeate}}{C_i}\right)^{D_i}}} \tag{6.139}$$

$$d_i^{permeate} = \rho_i^{permeate} Mw_i \tag{6.140}$$

$$V_{permeate} = \frac{P}{\sum_{i=1}^{4} d_i^{permeate} w_i^P} \tag{6.141}$$

$$w_i^P = \frac{J_i Mw_i}{\sum_{j=1}^{4} J_j Mw_i} \tag{6.142}$$

Table 6.22: Variables in the model of membrane assisted batch reaction for heterogeneously catalysed synthesis of ethyl lactate

Differential variables		Number
Molar hold-up	n_i	4
Mass of collected permeate	P	1
Algebraic (unknown) variables		**Number**
Reaction rate	$r_1^{1\alpha(heterog)}$	1
Reaction rate constants	k_1 , K , K_1	3
Weight fraction	w_i	4
Molar density	ρ_i , $\rho_i^{permeate}$	8
Mass density	d_i , $d_i^{permeate}$	8
Reaction volume	V	1
Components concentration	C_i	4
Yield	$Yield$	1
Component flux	J_i	4
Permeate volume	V_{perm}	1
Weight fraction of permeate	w_i^P	4
Hybrid operation (a=1), batch reaction (a=0)	a	1
Parameters		**Number**
Process parameters	T , $T_{permeate}$, m_{CAT} , A_m	4
Initial moles of lactic acid	$n_0(t=0)$	1
Switching time	t_{switch}	1
Known variables		**Number**
Reaction related constants	k_0 , K_0 , $K_{1,0}$, E_1 , E , $E_{1,0}$	6
Stoichiometric coefficients	υ_i	4
Molar liquid density constants	A_i , B_i , C_i , D_i	16
Molecular weight	Mw_i	4
Flux constants	α_3 , β_3	2
Constants	R	1
Total number of variables: 84		

Table 6.23: Equations in the model of membrane assisted batch reaction for heterogeneously catalysed synthesis of ethyl lactate

	Equations	Number of equations
Mass balance	(6.124)	4
Collected permeate	(6.138)	1
Reaction kinetics	(6.125)	1
Temperature dependences	(6.126-6.128)	3
Density and volume	(6.130-6.132)	9
Concentration	(6.133)	4
Weight fraction	(6.129)	4
Yield	(6.134)	1
Component flux	(6.135-6.136)	4
Condition	(6.137)	1
Volume of collected permeate	(6.141)	1
Weight fraction of compound in permeate	(6.142)	4
Density of permeate	(6.139-6.140)	8
Total number of equations: 45		
DOF: 39		

6.4.3.3. UNIFAC parameters used in the case study of synthesis of ethyl lactate

Table 6.24: R_i and Q_i parameters of the UNIFAC groups

	R_i	Q_i
Lactic acid	3.6493	3.5000
Ethanol	2.5755	2.5880
Ethyl lactate	4.9255	4.5440
Water	0.9200	1.4000

Table 6.25. Representation of compounds in terms of the UNIFAC groups

	CH3	CH2	CH	OH	H2O	CH2COO	COOH
Main group	1	1	1	5	7	11	20
Lactic acid	1	0	1	1	0	0	1
Ethanol	1	1	0	1	0	0	0
Ethyl lactate	2	0	1	1	0	1	0
Water	0	0	0	0	1	0	0

Table 6.26. Values of UNIFAC parameters for groups present in the reacting mixture

	CH3	OH	H2O	CH2COO	COOH
CH3	0	986.5	1318	232.1	663.5
OH	156.4	0	353.5	101.1	199
H2O	300	-229.1	0	72.87	-14.09
CH2COO	114.8	245.4	200.8	0	660.2
COOH	315.3	-151	-66.17	-256.3	0

6.4.4. Production of n-propyl propionate

In this appendix all model equations and model analysis for each of the simulated processes in section 4.3.4.3 is presented. Since, all experiments have been performed under isothermal conditions and the interest here is on productivity only the mass balance is reported. In all models the component activity coefficients in liquid phase are calculated using Modified UNIFAC (Lyngby) (Fredenslund et al., 1977) which is used as a submodel.

6.4.4.1. Model for heterogeneously catalysed batch reaction

The following model was used to simulate a heterogeneously catalysed batch reaction in section 4.3.4.3.1. The schematic configuration of process modelled in this subsection is presented in Figure 4.54-A. The model was derived from superstructure (see Figure 3.5) and model equations (3.13, 3.15-3.32) for $NC = 4$, $NRKh = 1$, $NRK = 0$ and by specifying the decision variables: $\xi^{1} = 1$, $\xi^{2} = 0$, $\xi^{1in} = 0$, $\xi^{2in} = 0$, $\xi^{1\alpha} = 0$, $\xi^{1\beta} = 0$, $\xi^{2\alpha} = 0$, $\xi^{2\beta} = 0$, $\xi^{R} = 1$, $\xi^{R\beta} = 0$, $\xi^{(homog)} = 0$, $\xi^{(heterog)} = 1$, $t_{switch} = 0$. Since only *Process 1* is considered the $F_{TOT}^{1\alpha}$ is zero. The specific reaction kinetic presented in section 4.3.4.1 has been introduced.

Mass balance:

$$\frac{dn_i}{dt} = \nu_{i,h}^{1\alpha} r_h^{1\alpha(heterog)} \tag{6.143}$$

Constitutive equations:

$$r_h^{1\alpha(heterog)} = k_f \left(a_1 a_2 - \frac{1}{K_{eq}} a_3 a_4 \right) m_{CAT} L \tag{6.144}$$

Where 1: propionic acid, 2: propanol, 3: propyl propionate, 4: water.

$$k_f = k_0 e^{\left(\frac{-E}{RT}\right)} \tag{6.145}$$

$$K_{eq} = K_{0,eq} e^{\left(\frac{-E_{eq}}{RT}\right)} \tag{6.146}$$

$$a_i = x_i \gamma_i \tag{6.147}$$

$$x_i = \frac{n_i}{\sum_{i=1}^{4} n_i} \tag{6.148}$$

Table 6.27: Variables in model for heterogeneously catalysed batch reaction

Differential variables		Number
Molar hold-up	n_i	4
Algebraic (unknown) variables		**Number**
Reaction rate	$r_h^{1\alpha(heterog)}$	1
Reaction rate constants	k_f , K_{eq}	2
Components activity	a_i	4
Molar fraction	x_i	4
Activity coefficient	γ_i (calculated using Mod. UNIFAC Lyngby)	4
Parameters		**Number**
Process parameters	T , m_{CAT} , L	3
Known variables		**Number**
Reaction related constants	k_0 , $K_{0,eq}$, E , E_{eq}	4
Stoichiometric coefficients	$\upsilon_i^{1\alpha}$	4
Constants	R	1
Total number of variables: 31		

Table 6.28: Equations in model for heterogeneously catalysed batch reaction

	Equations	Number of equations
Mass balance	(6.143)	4
Reaction kinetics	(6.144)	1
Temperature dependences	(6.145 - 6.146)	2
Activity	(6.147) plus subroutine for γ_i	8
Molar fraction	(6.148)	4
Total number of equations: 19		
DOF: 12		

6.4.4.2. Model for membrane-based separation: pervaporation

Model for calculating component fluxes through the membrane in a pervaporation presented in this section was used in section 4.3.4.3.2. The schematic configuration of the experimental set up of this process is given in Figure 4.54-B. Note that this model only calculates the permeability and so it is not generated from the generic model. In this model it is assumed that feed flow rate to pervaporation unit does not influence the component flux J_i and in permeate only water is present.

$$J_i = \frac{P_i}{\overline{\gamma}_{M,i}}\left(a_i^F - a_i^P\right) \qquad (6.149)$$

$$P_i = P_i^0 \exp\left(-\frac{E_i}{R}\left(\frac{1}{T_M}-\frac{1}{T_R}\right)\right) \tag{6.150}$$

$$\overline{\gamma}_{M,i} = \sqrt{\gamma_{M,i}^F \gamma_{M,i}^P} \tag{6.151}$$

$$\gamma_{M,i}^F = \exp\left(B_i^\circ\left(1-\sum_{j=1}^{NC} B_{ij} a_j^F\right)\right) \tag{6.152}$$

$$\gamma_{M,i}^P = \exp\left(B_i^\circ\left(1-\sum_{j=1}^{NC} B_{ij} a_j^P\right)\right) \tag{6.153}$$

$$a_i^P = \frac{P^P y_i}{P^\circ} \tag{6.154}$$

$$a_i^F = x_i^F \gamma_i^F \tag{6.155}$$

Table 6.29: Variables in model for membrane-based separation: pervaporation

Algebraic (unknown) variables		Number
Component flux	J_i	4
Permeability	P_i	4
Components activity	a_i^F , a_i^P	8
Average activity across membrane	$\overline{\gamma}_{M,i}$	4
Activity coefficient at membrane	$\gamma_{M,i}^F$, $\gamma_{M,i}^P$	8
Activity coefficient	γ_i^F (calculated using Mod. UNIFAC Lyngby)	4
Parameters		**Number**
Process parameters	T_M , P^P	2
Parameters	B_i^0 , B_{ij}	20
Permeability constants	P_i^0 , E_i	8
Known variables		**Number**
Component composition	x_i , y_i	8
Constants	R , T_R , P^0	3
Total number of variables: 73		

Table 6.30: Equations in model for membrane-based separation: pervaporation

	Equations	Number of equations
Component flux	(6.149)	4
Temperature dependences	(6.150)	4
Activity coefficient across membrane	(6.151 - 6.153)	12
Activity	(6.154 - 6.155) plus subroutine for γ_i	12
Total number of equations: 32		

Degree of freedom of this model is 41.

6.4.4.3. Model for membrane assisted batch reaction

Model described below was used to simulate a membrane assisted batch reaction in section 4.3.4.3.3. The model was derived from superstructure (see Figure 3.5) and model equations (3.13, 3.15-3.32) for $NC = 4$, $NKRh = 1$, $NRK = 0$ and by specifying the decision variables: $\xi^1 = 1$, $\xi^2 = 1$, $\xi^{1\alpha} = 0$, $\xi^{1\beta} = 0$, $\xi^{2\alpha} = 1$, $\xi^{2\beta} = 0$, $\xi^{1in} = 0$, $\xi^{2in} = 0$, $\xi^R = 1$, $\xi^{R\beta} = 0$, $\xi^{(homog)} = 0$, $\xi^{(heterog)} = 1$. Therefore the mass balance is:

$$\frac{dn_i}{dt} = -\sigma_i^{2\alpha} x_i^{1\alpha} a \cdot F_{TOT}^{1\alpha} + \nu_{i,h}^{1\alpha} r_h^{1\alpha(heterog)} \tag{6.156}$$

Other streams in the hybrid process are related as follows:

$$F_i^{1\alpha P} = 0 \tag{6.157}$$

$$F_i^{1\beta P} = 0 \tag{6.158}$$

$$F_i^{1\alpha R} = F_i^{1\alpha} \tag{6.159}$$

$$F_i^{1\beta R} = F_i^{1\beta} \tag{6.160}$$

$$F_i^{2\alpha P} = F_i^{2\alpha} \tag{6.161}$$

$$F_i^{2\beta P} = 0 \tag{6.162}$$

$$F_i^{2\alpha R} = 0 \tag{6.163}$$

$$F_i^{2\beta R} = F_i^{2\beta} \tag{6.164}$$

$$F_i^{1\alpha} = a x_i^{1\alpha} F_{TOT}^{1\alpha} \tag{6.165}$$

$$F_i^{1\beta} = 0 \tag{6.166}$$

$$F_i^{2\alpha} = a\sigma_i^{2\alpha} x_i^{1\alpha} F_{TOT}^{1\alpha} \tag{6.167}$$

$$F_i^{2\beta} = a\sigma_i^{2\beta} x_i^{1\alpha} F_{TOT}^{1\alpha} \tag{6.168}$$

$$x_i^{1\alpha} = \frac{n_i}{\sum_{i=1}^{NC} n_i} \tag{6.169}$$

$$a = if\ (t \geq t_{switch})\ than\ (1)\ else\ (0) \tag{6.170}$$

From the definition of separation factor, the separation factor $\sigma_i^{2\alpha}$ is:

$$\sigma_i^{2\alpha} = \frac{F_i^{2\alpha}}{F_{TOT}^{1\alpha}} \tag{6.171}$$

The rate of component removal from the system ($F_i^{2\alpha}$) is equal to the component flux (J_i) multiplied by membrane area (A) the specific mass balance around hybrid process is written below (Eq. 6.172). Since flow rate between connected units (e.g. reactor and pervaporation unit) is constant the flow rate equations (Eq. 6.157-6.168) are not included in this simplified model (Eqs. 6.172-6.185).

$$\frac{dn_i}{dt} = -aJ_i A + \nu_{i,h}^{1\alpha} r_h^{1\alpha(heterog)} \tag{6.172}$$

Constitutive equations:

$$r_h^{1\alpha(heterog)} = k_f \left(a_1 a_2 - \frac{1}{K_{eq}} a_3 a_4 \right) m_{CAT} L \tag{6.173}$$

$$k_f = k_0 e^{\left(\frac{-E}{RT}\right)} \tag{6.174}$$

$$K_{eq} = K_{0,eq} e^{\left(\frac{-E_{eq}}{RT}\right)} \tag{6.175}$$

$$a_i = x_i \gamma_i \tag{6.176}$$

$$J_i = \frac{P_i}{\overline{\gamma}_{M,i}} \left(a_i - a_i^P \right) \tag{6.177}$$

$$P_i = P_i^0 \exp\left(-\frac{E_i}{R} \left(\frac{1}{T_M} - \frac{1}{T_R} \right) \right) \tag{6.178}$$

$$\overline{\gamma}_{M,i} = \sqrt{\gamma_{M,i}^F \gamma_{M,i}^P} \tag{6.179}$$

$$\gamma_{M,i}^F = \exp\left(B_i^\circ \left(1 - \sum_{j=1}^{NC} B_{ij} a_j \right) \right) \tag{6.180}$$

$$\gamma_{M,i}^P = \exp\left(B_i^\circ \left(1 - \sum_{j=1}^{NC} B_{ij} a_j^P \right) \right) \tag{6.181}$$

$$a_i^P = \frac{P^P y_i}{P^\circ} \tag{6.182}$$

$$a = if\ (t \geq t_{switch})\ than\ (1)\ else\ (0) \tag{6.183}$$

Knowing that only one (liquid) phase is present in the hybrid process the mole fraction represented by Eq. (6.169) is substituted by Eq. (6.184).

$$x_i^{1\alpha} = \frac{n_i}{\sum_{i=1}^{4} n_i} \tag{6.184}$$

For easier comparison between simulated and experimental data the weight fraction has been defined:

$$w_i = \frac{n_i \cdot Mw_i}{\sum_{i=1}^{4} n_i \cdot Mw_i} \tag{6.185}$$

Table 6.31: Variables in model for membrane assisted batch reaction for synthesis of n-propyl propionate

Differential variables		Number
Molar hold-up	n_i	4
Algebraic (unknown) variables		**Number**
Reaction rate	$r_h^{1\alpha(heterog)}$	1
Reaction rate constants	k_f , K_{eq}	2
Components activity	a_i	4
Molar fraction	x_i	4
Component flux	J_i	4
Permeability	P_i	4
Components activity	a_i^P	4
Average activity across membrane	$\overline{\gamma}_{M,i}$	4
Activity coefficient at membrane	$\gamma_{M,i}^F$, $\gamma_{M,i}^P$	8
Weight fractions	w_i	4
Other	a	1
Variable calculated by external subroutine		**Number**
Activity coefficient	γ_i	4
Parameters		**Number**
Process parameters	T , m_{CAT} , L , P^P	4
Switching time	t_{switch}	1
Known variables		**Number**
Reaction related constants	k_0 , $K_{0,eq}$, E , E_{eq}	4
Stoichiometric coefficients	υ_i	4
Component composition	x_i , y_i ,	8
Permeability constants	P_i^0 , E_i	8
Parameters	B_i° , B_{ij}	20
Molecular weight of components	Mw_i	4
Constants	R , T_R , P^a	3
Total number of variables: 104 (total number of parameters and known var. is 60)		

Table 6.32: List of equations in the model of membrane assisted batch reaction for synthesis of n-propyl propionate

	Equations	Number of equations
Mass balance	(6.172)	4
Reaction kinetics	(6.173)	1
Temperature dependences	(6.174-6.175)	2
Activity	(6.176) plus subroutine for γ_i	8
Molar fraction	(6.184)	4
Component flux	(6.177)	4
Permeate temperature dependences	(6.178)	4
Average activity coefficient across membrane	(6.179 - 6.181)	12
Activity on permeate side	(6.182)	4
Switching condition	(6.183)	1
Weight fraction	(6.185)	4
Total number of equations: 48		

Degree of freedom of this model (Eqs. 6.172-6.185) is equal to 56.

6.4.4.4. Experimental data in tables

In this section all experimental data depicted on figures in section 4.3.4.3 Stage 3: Validation are given in the tabulated form.

Table 6.33: Experiment E1 - Data related to the permeate

No	Sample name	time [min]	w_i (permeate) [%g/g]				m permeate [g]	T [K]	P_{perm} [kPa]
			w_{POH}	w_{ProPro}	w_{Pac}	w_{H2O}			
1	H021 P0	104.80	0.27	0.02	0.08	99.62	5.67	347.15	1.3
2	H023 P0	135.25	0.28	0.03	0.07	99.62	6.45	347.15	1.3
3	H025 P0	164.95	0.10	0.01	0.03	99.86	6.50	347.15	1.3
4	H027 P0	194.95	0.18	0.02	0.04	99.76	6.68	347.15	1.4
5	H029 P0	239.28	0.02	0.00	0.02	99.97	9.29	347.15	1.4
6	H030 P0	269.97	0.10	0.01	0.02	99.86	6.31	348.15	1.3
7	H031 P0	300.08	0.05	0.01	0.01	99.93	5.78	348.15	1.3
8	H033 P0	344.00	0.12	0.02	0.01	99.85	5.64	348.15	3.9
9	H035 P0	404.97	0.11	0.02	0.02	99.85	11.56	347.15	1.4
10	H037 P0	525.02	0.11	0.03	0.01	99.85	15.84	348.15	1.5
11	H040 P0	651.67	0.02	0.00	0.01	99.97	11.13	348.15	0.8
12	H041 P0	720.55	0.09	0.02	0.01	99.88	4.95	348.15	0.8

Table 6.34: Experiment E1 - Data related to the reactor

No	Sample name	time [min]	w_i (permeate) [%g/g]				T [K]
			w_{POH}	w_{ProPro}	w_{Pac}	w_{H2O}	
1	H011 F0	1.33	61.53	1.60	34.63	2.24	356.69
2	H012 F0	5.40	60.36	4.94	29.94	4.76	347.47
3	H013 F0	10.12	58.81	7.60	28.47	5.12	347.41
4	H014 F0	15.38	57.62	10.19	26.68	5.51	347.38
5	H015 F0	30.13	54.48	16.30	22.84	6.38	347.42
6	H016 F0	45.05	52.01	20.98	19.92	7.09	347.20
7	H018 F0	60.40	50.24	24.64	17.59	7.53	347.03
8	H019 F0	75.80	48.93	27.30	15.80	7.97	346.97
9	H020 F0	90.38	47.92	29.75	14.41	7.92	346.69
10	H021 F0	104.80	46.96	31.60	13.29	8.15	346.71
11	H022 F0	120.02	46.44	33.29	12.36	7.91	346.71
12	H023 F0	135.25	45.97	34.70	11.50	7.82	346.68
13	H024 F0	151.70	45.21	36.21	10.53	8.05	346.70
14	H025 F0	164.95	44.84	37.21	10.01	7.93	346.62
15	H026 F0	180.12	44.40	38.17	9.52	7.91	346.95
16	H027 F0	194.95	44.22	39.04	8.95	7.78	347.17
17	H028 F0	210.10	43.67	40.07	8.62	7.65	346.81
18	H029 F0	239.28	43.55	41.37	7.89	7.19	346.71
19	H030 F0	269.97	43.00	42.71	7.30	6.99	346.77
20	H031 F0	300.08	42.94	43.60	6.83	6.64	346.60
21	H032 F0	330.75	42.77	44.59	6.42	6.23	346.43
22	H033 F0	344.00	42.66	44.93	6.20	6.21	346.53
23	H034 F0	374.90	42.53	45.67	5.90	5.90	346.41
24	H035 F0	404.97	42.20	46.58	5.67	5.55	346.77
25	H036 F0	465.00	41.98	47.75	5.11	5.15	346.88
26	H037 F0	525.02	41.89	48.86	4.66	4.59	346.96
27	H038 F0	585.00	41.73	49.79	4.28	4.20	346.16
28	H040 F0	651.67	41.45	50.76	3.93	3.85	346.79
29	H041 F0	720.55	41.65	51.17	3.63	3.55	346.90

Table 6.35: Experiment E2 - Data related to the reactor

No	Sample name	time [min]	w_i (permeate) [%g/g] w_{POH}	w_{ProPro}	w_{Pac}	w_{H2O}	T [K]
1	H045 F	6.00	57.59	8.17	26.62	7.62	351.01
2	H047 F	30.60	50.86	21.24	18.12	9.78	353.11
3	H049 F	90.63	44.92	32.83	10.74	11.51	353.20
4	H050 F	119.43	43.84	34.89	9.39	11.88	353.27
5	H053 F	195.05	43.40	38.26	8.01	10.33	351.23
6	H054 F	225.68	43.54	39.40	7.76	9.30	351.21
7	H055 F	257.03	43.35	40.34	7.28	9.03	351.57
8	H057 F	375.67	42.97	43.33	6.08	7.62	351.86
9	H058 F	440.35	43.11	45.02	5.56	6.31	352.18
10	H059 F	495.95	43.06	46.20	5.12	5.62	352.19
11	H060 F	600.72	43.11	48.35	4.47	4.07	352.03

Table 6.36: Experiment E2 - Data related to the permeate

No	Sample name	time [min]	w_i (permeate) [%g/g] w_{POH}	w_{ProPro}	w_{Pac}	w_{H2O}	m permeate [g]	T [K]	P_{perm} [kPa]
1	H051P	138.00	0.30	0.01	0.05	99.64	1.58	349.15	4.9
2	H052P	165.30	0.05	0.00	0.03	99.92	14.33	349.15	4.3
3	H053P	195.90	0.07	0.00	0.03	99.90	14.18	349.15	3.7
4	H054P	225.83	0.10	0.01	0.03	99.86	14.30	349.15	3.7
5	H055P	257.77	0.07	0.01	0.02	99.91	13.51	349.15	3.7
6	H056P	316.25	0.05	0.00	0.02	99.93	17.01	349.15	4.8
7	H057P	376.67	0.16	0.02	0.02	99.80	20.18	349.15	4.1
8	H058P	442.12	0.22	0.04	0.02	99.72	18.74	349.15	3.1
9	H059P	497.95	0.21	0.03	0.02	99.74	13.50	350.15	2.9
10	H060P	603.07					20.03	349.15	2.4
11	H061P	722.67	0.19	0.04	0.02	99.76	17.15	349.15	2.6

Table 6.37: Experiment E3 - Data related to the reactor

No	Sample name	time [min]	w_i (permeate) [%g/g] w_{POH}	w_{ProPro}	w_{Pac}	w_{H2O}	T [K]
1	H062 F	1.33	55.99	7.72	30.22	6.08	345.33
2	H063 F	4.90	55.81	10.04	27.96	6.18	344.94
3	H064 F	15.12	52.81	15.77	24.27	7.14	344.54
4	H065 F	60.32	46.08	29.63	15.57	8.72	344.58
5	H066 F	90.00	43.70	33.92	12.78	9.59	344.83
6	H067 F	130.18	42.58	36.82	11.13	9.47	345.06
7	H068 F	134.95	41.71	37.80	10.49	10.00	344.96
8	H069 F	165.25	41.43	39.60	9.64	9.34	345.17
9	H070 F	195.70	40.63	41.13	8.95	9.30	345.77
10	H071 F	225.43	40.50	42.39	8.43	8.68	345.76
11	H072 F	259.02	40.25	43.20	7.92	8.64	345.64
12	H073 F	315.22	40.28	44.85	7.29	7.59	345.59
13	H074 F	360.00	39.78	46.19	6.74	7.30	345.87
14	H075 F	435.28	39.88	47.49	6.24	6.39	345.19
15	H076 F	495.93	39.26	48.80	5.89	6.05	345.19
16	H077 F	556.52	39.75	49.38	5.51	5.36	345.04
17	H078 F	615.05	39.34	50.57	5.16	4.93	345.11

Table 6.38: Experiment E3 - Data related to the permeate

No	Sample name	time [min]	w_i (permeate) [%g/g] w_{POH}	w_{ProPro}	w_{Pac}	w_{H2O}	$m_{permeate}$ [g]	T [K]	P_{perm} [kPa]
1	H069 P	165.43	0.11	0.02	0.03	99.85	9.12	343.15	1.8
2	H070 P	195.90	0.14	0.01	0.03	99.82	9.45	343.15	2.4
3	H071 P	240.00	0.08	0.01	0.02	99.89	9.14	343.15	2
4	H072 P	259.33	0.04	0.00	0.01	99.95	10.03	343.15	1.8
5	H073 P	315.50	0.05	0.01	0.01	99.93	15.07	343.15	2
6	H074 P	375.35	0.13	0.02	0.02	99.83	14.80	344.15	1.8
7	H075 P	435.62	0.13	0.02	0.02	99.83	12.87	344.15	1.7
8	H076 P	496.33	0.00	0.00	0.00	100.00	11.34	343.15	1.4
9	H077 P	556.83	0.09	0.01	0.01	99.89	9.93	343.15	1.7
10	H078P	615.42					8.44	343.15	1
11	H079P	721.67					12.83	343.15	1.9

Table 6.39: Experiment E4 - Data related to the reactor

No	Sample name	time [min]	w_i (permeate) [%g/g] w_{POH}	w_{ProPro}	w_{Pac}	w_{H2O}	T [K]
1	H082 F	1.10	55.19	8.41	31.41	4.99	346.38
2	H083 F	4.77	54.27	11.37	28.97	5.38	345.80
3	H084 F	15.23	50.78	18.29	24.65	6.29	345.89
4	H085 F	30.53	47.41	24.96	20.45	7.18	346.07
5	H086 F	57.75	43.21	33.36	15.17	8.25	345.90
6	H087 F	89.98	41.45	37.79	12.41	8.36	344.83
7	H088 F	120.02	39.81	42.34	9.55	8.29	344.74
8	H090 F	179.97	39.26	43.99	8.80	7.95	344.93
9	H091 F	241.50	38.60	46.34	7.70	7.37	344.40
10	H092 F	300.03	38.37	47.80	7.02	6.82	344.92
11	H093 F	360.62	37.82	49.37	6.50	6.32	345.22
12	H094 F	454.85	37.56	51.11	5.83	5.50	345.17
13	H095 F	483.90	37.95	51.01	5.66	5.38	345.13
14	H096 F	507.70	37.66	51.63	5.52	5.19	344.87

Table 6.40: Experiment E4 - Data related to the permeate

No	Sample name	time [min]	w_i (permeate) [%g/g] w_{POH}	w_{ProPro}	w_{Pac}	w_{H2O}	$m_{permeate}$ [g]	T [K]	P_{perm} [kPa]
1	H087 P	90.15	0.13	0.02	0.03	99.82	6.74	344.15	2.2
2	H088 P	120.17	0.15	0.00	0.00	99.85	7.46	343.15	1.4
3	H089P	150.18	0.11	0.02	0.03	99.85	7.63	343.15	1.5
4	H090P	180.32	0.00	0.00	0.00	100.00	7.56	343.15	1.7
5	H091P	240.67	0.00	0.00	0.00	100.00	14.76	343.15	2.3
6	H092P	300.27	0.00	0.00	0.00	100.00	13.05	343.15	2.1
7	H093P	360.87	0.00	0.00	0.00	100.00	12.13	343.15	1.9
8	H094P	455.00	0.00	0.00	0.00	100.00	15.41	343.15	1.2
9	H095P	508.23	0.00	0.00	0.00	100.00	6.38	343.15	1.1

Table 6.41: Experiment E5 - Data related to the reactor

No	Sample name	time [min]	w_i (permeate) [%g/g] w_{POH}	w_{ProPro}	w_{Pac}	w_{H2O}	T [K]
1	H100 F	1.33	61.24	11.72	21.52	5.52	354.46
2	H101 F	5.08	61.99	8.38	23.77	5.87	354.46
3	H102 F	15.43	57.31	19.24	16.58	6.87	354.70
4	H103 F	30.20	54.20	25.74	12.33	7.74	354.74
5	H106 F	120.00	49.43	36.65	5.73	8.20	353.31
6	H107 F	150.00	49.23	37.84	5.23	7.70	353.40
7	H108 F	180.00	49.16	38.66	4.87	7.32	353.50
8	H109 F	239.98	49.09	39.92	4.39	6.59	353.50
9	H110 F	300.45	49.13	40.92	4.01	5.94	353.93
10	H113 F	571.78	49.28	44.23	2.75	3.74	353.79
11	H114 F	720.87	49.26	45.46	2.27	3.01	353.37

Table 6.42: Experiment E5 - Data related to the permeate

No	Sample name	time [min]	w_i (permeate) [%g/g] w_{POH}	w_{ProPro}	w_{Pac}	w_{H2O}	m permeate [g]	T [K]	P_{perm} [kPa]
1	H105P	90.33	0.21	0.00	0.00	99.79	9.30	353.15	1.7
2	H106P	120.17	0.11	0.00	0.00	99.89	9.30	353.15	1.8
3	H107P	150.23	0.06	0.00	0.00	99.94	9.10	352.15	1.7
4	H108P	180.17	0.06	0.00	0.00	99.94	8.26	353.15	1.6
5	H109P	240.33	0.00	0.00	0.00	100.00	15.44	352.15	1.4
6	H110P	300.92	0.27	0.03	0.02	99.69	13.75	352.15	1.3
7	H111P	360.23	0.16	0.02	0.01	99.81	11.60	353.15	1.1
8	H112P	451.88	0.27	0.03	0.01	99.68	14.95	353.15	1.1
9	H113P	572.17					13.59	353.15	0.9
10	H114P	721.73	0.39	0.06	0.01	99.54	14.15	353.15	0.7

Table 6.43: Experiment E6 - Data related to the reactor

No	Sample name	time [min]	w_i (permeate) [%g/g] w_{POH}	w_{ProPro}	w_{Pac}	w_{H2O}	T [K]
1	H118 F	1.18	70.72	3.42	21.70	4.16	336.26
2	H119 F	5.52	70.54	4.96	20.12	4.39	336.15
3	H121 F	30.87	64.63	12.39	17.83	5.15	336.30
4	H122 F	59.65	61.81	18.33	14.26	5.59	336.80
5	H123 F	90.23	59.57	22.45	11.49	6.49	336.32
6	H124 F	119.27	57.98	25.24	9.70	7.08	335.95
7	H125 F	149.75	57.53	27.66	8.41	6.40	336.20
8	H126 F	179.50	57.45	28.39	7.42	6.74	336.27
9	H127 F	210.12	56.60	30.74	6.60	6.05	336.02
10	H128 F	240.47	55.86	31.34	5.89	6.91	336.17
11	H129 F	330.52	55.07	33.60	4.85	6.48	335.99
12	H131 F	421.35	55.61	34.41	3.96	6.02	336.56
13	H132 F	541.02	55.77	35.05	3.52	5.65	336.56
14	H133 F	630.47	55.66	35.74	3.30	5.30	335.97
15	H134 F	720.08	54.92	35.93	3.11	6.04	335.82

Table 6.44: Experiment E6 - Data related to permeate

No	Sample name	time [min]	w_i (permeate) [%g/g] w_{POH}	w_{ProPro}	w_{Pac}	w_{H2O}	$m_{permeate}$ [g]	T [K]	P_{perm} [kPa]
1	H124P	120.03	0.21	0.01	0.03	99.74	4.34	334.15	1
2	H126P	180.05	0.03	0.00	0.01	99.96	5.28	334.15	1
3	H128P	241.32	0.00	0.00	0.00	100.00	5.96	334.15	1.1
4	H129P	330.75	0.00	0.00	0.00	100.00	8.66	334.15	1.3
5	H131P	422.10	0.00	0.00	0.00	100.00	8.76	334.15	1
6	H132P	541.97	0.00	0.00	0.00	100.00	10.10	334.15	0.8
7	H134P	721.55	0.00	0.00	0.00	100.00	13.41	334.15	0.6

Table 6.45: Experimental data for the batch reaction operated at $T = 353.35$ K, $m_{cat}/m_{mix} = 0.22$, POH:ProAc = 2:1, $m_{mix} = 1328.9$ g

No	Sample name	time [min]	w_i (tank) [% g/g]				T [K]
			w_{POH}	w_{ProPro}	w_{Pac}	w_{H2O}	
1	H138	1.05	60.32	5.70	30.16	3.82	353.04
2	H139	5.12	58.44	10.68	26.39	4.48	353.22
3	H140	10.30	55.72	16.12	22.96	5.20	353.28
4	H141	20.03	52.11	23.31	18.32	6.26	353.43
5	H142	30.62	49.32	28.88	14.88	6.92	353.48
6	H143	40.23	47.69	32.15	12.77	7.40	353.48
7	H144	50.30	46.41	34.72	11.17	7.70	353.57
8	H145	59.78	45.51	36.48	10.03	7.97	353.46
9	H146	79.75	44.30	38.95	8.49	8.26	353.26
10	H147	100.07	43.49	40.41	7.61	8.49	353.25
11	H148	130.12	42.92	41.65	6.88	8.55	353.34
12	H149	160.75	42.61	42.16	6.47	8.76	353.44
13	H150	190.37	42.56	42.46	6.30	8.68	353.28
14	H151	221.35	42.43	42.53	6.16	8.88	352.85
15	H152	259.98	42.37	42.67	6.14	8.82	352.91

7. Nomenclature

a_i – activity [-],

A_{ij}, B_{ij}, C_{ij} – interaction parameters for *i-j* interaction for modified UNIFAC (Lyngby). In model presented in section 6.2.1 these parameters are represented by $a_{k,d,1}$, $a_{k,d,2}$ and $a_{k,d,3}$ respectively.

A_i – component pick area,

A_{jk} – invariant element of the formula matrix (*k*-component, *j*-chemical element,

A_m – membrane area [m^2],

A_p – surface area, m^2

$b_{M,i}$ – mobility of component *i* in membrane *M* [m^2·mol/J/s]

C_p – heat capacity [J/mol·K],

D – Fick's diffusion coefficient [cm^2/s],

DFP – distillation followed by membrane-based separation,

DSP – distillation with side membrane-based separation,

D^T – thermodynamic diffusion coefficient [cm^2/s],

E – activation energy in Arrhenius-type temperature dependence [J/mol]

F – component molar flow, mol/s

f – fugacity,

FD – driving force [mol/mol],

G – Gibbs free energy [J],

H – enthalpy [J],

h – specific enthalpy [J/mol],

h – specific enthalpy, J/mol

J_i – component flux [mol/s/m^2],

k – reaction rate constant [mol/s],

k_0 – independent of temperature reaction rate constant 4.52 [mol/s],

K_{eq} – reaction equilibrium constant [-],

k_f – reaction rate constant in Eq. 4.52 [mol/s/eq],

L – concentration of active sides in Eq 4.52 0.95 eq/kg,

l – thickness of polymer film [μm],

L_p – hydraulic permeability

m – weight [g],

m_{CAT} – mass of catalyst [g],

M_w – molecular mass [g/mol],

NF – nanofiltration,

NC – number of components [-],

$No\ FM$ – number of the stage from which the feed to membrane is withdraw,

NoA – number of analyses [-],

NRK – number of homogenous reactions [-],

$NRKh$ – number of heterogeneous reactions [-],

P – permeability in eq. 3.58 [cm3 (273.15K;1.013.105Pa).cm/cm^3/s/Pa]

P – pressure [Pa],

P_i – phenomological permeability [mol/m/s],

PV – pervaporation,

Q – heat duty, MJ

Q°_i – permeance constant in Eq. 2.35,

Q_1 – energy addition to *Process 1* [J/s],

Q_2 – energy addition to *Process 2* [J/s],

Q_i – permeance in Eq. 2.34,

Q_k – area parameter,

Q_k – van der Waals area,

r – reaction rate [mol/s/eq],

R – universal gas constant, 8.3144 [J·K^{-1}·mol^{-1}],

r – pore size [nm],

r – reaction rate, mol/s/dm^3

RCPE – reaction coupled with pervaporation,

R_k – volume parameter,

RS – reaction-solvent index,

S – solubility [cm^2 (273.15K;1.013.105Pa)/cm^3/Pa]

t – time [min],

t	–	time, s
T_d	–	denaturation temperature, K
T_g	–	glass transition temperature [K],
T_R	–	in Eq. 6.150 reference temperature in membrane model, 333.15 K
V	–	reaction volume, dm^3
V_k	–	van der Waals volume,
V_0	–	initial volume of a semi-batch reactor,
$V_{permeate}$	–	volume of permeate,
VP	–	vapour permeation,
w	–	weight fraction [g/g],
x	–	molar fraction of compound *i* in the liquid phase [mol/mol],
y	–	molar fraction of compound *i* in the vapour phase [mol/mol],
Y	–	yield of process [mol/mol],
v	–	stoichiometric coefficient,
α_i	–	relative volatility of compound *i* [mol/mol],
ε	–	measurement error,
σ	–	standard deviation,
μ	–	chemical potential [J/mol],
ξ	–	decision variable [-],
λ	–	Lagrange multiplier [-],
θ	–	phase fraction [mol/mol],
ε	–	porosity [-],
θ	–	score value in section R3.4.,
σ	–	separation factors [mol/mol],
τ	–	tortuosity [-],
ξ^{β}	–	existence of second phase in *Process 1* [-],
ξ^{l}	–	existence of *Process 1* [-],
$\xi^{l\alpha}$	–	existence of bottom outlet from *Process 1* [-],
$\xi^{l\beta}$	–	existence of top outlet from *Process 1* [-],

$\nu^{1\alpha}_{i,k}$ – stoichiometric coefficient of compound *i* in reaction *k* [-],

ξ^{1in} – existence of fresh inlet to *Process 1* [-],

ξ^{2} – existence of *Process 2* [-],

$\xi^{2\alpha}$ – existence of bottom outlet from *Process 2* [-],

$\xi^{2\beta}$ – existence of top outlet from *Process 2* [-],

ξ^{2in} – existence of fresh inlet to *Process 2* [-],

σ_{Ai} – standard deviation in Eq. (4.62),

γ_i – activity coefficient,

σ_i – relative error related to the measurement of concentration of compound *i* in Eq. 4.61,

ρ_p – density of polymer [g/cm^3],

ξ^{R} – existence of reaction(s) in *Process 1* [-],

Δs_{max} – maximum of calibration error, in Eq. (4.61),

Δt – time of measurement [min],

Subscripts and superscripts

Cond – condenser

exp – experimental,

eq – equilibrium,

F – feed,

i – compound,

j – stream in Eq. 3.33

k – reaction,

mix – mixture,

P – permeate,

P – product stream

R – recycle stream,

Reb – reboiler,

RF – reactive flash,

α – bottom stream in superstructure (see Figure 3.5),

β – top stream in superstructure (see Figure 3.5),

V	–	vapour phase,
L	–	liquid phase,
M	–	membrane,
c	–	combinatorial part,
r	–	residual part,
heterog	–	heterogeneous reaction,
homog	–	homogeneous reaction,
vap	–	vaporization,
TOT	–	total flow rate

8. References

Acros (2007) www.acros.com

Adlercreutz, P.; Lyberg, Ann-Marie, Adlercreutz, D., (2003). Enzymatic fatty acid exchange in glycero-phospholipids, *Journal Title European Journal of Lipid Science and Technology* , 105, 10, 638-645.

Bek-Pedersen, E., Gani, R., (2004). Design and synthesis of distillation systems using driving –force-based approach, *Chemical Engineering and Processing, 43, 251-262.*

Benedict, D. J., Parulekar, S. J., Shih-Perng Tsai (2003). Esterification of lactic acid and ethanol with/without pervaporation, *Industrial and Engineering Chemistry Research*, 42, 2282-2291.

Brandrup, J., Immergut, E.H., Grulke, E.A., (editors) (1999). Polymer handbook, fourth edition , *John Wiley & Sons, Inc.*

Buchaly, K., Kreis, P., Górak, (2007). A., Hybrid separation processes—Combination of reactive distillation with membrane separation, *Chemical Engineering and Processing*, 46, 790–799

Cai, B.; Zhou, Y.; Hu, J.; Zhu, L.; Wu, C.; Gao, C., (2003). Solvent treatment of CTA hollow fiber membrane and its pervaporation performance for organic/organic mixture, Desalination, 151, 117-121.

Colombo, A., Battilana, P., Ragaini, V., Bianchi, C. L. Carvoli, G., (1999). Liquid-Liquid Equilibria of the Ternary Systems Water + Acetic Acid + Ethyl Acetate and Water + Acetic Acid + Isophorone (3,5,5-Trimethyl-2-cyclohexen-1-one), *Journal of Chemical & Engineering Data*, 44, 1, 35-39

Constantinou, L., Bagherpourj, K., Gani, R., Klein, J. A., Wu, D. T., (1996). Computer aided product design: problem formulations, methodology and applications, *Computers and Chemical Engineering*, 20, 6/7, 685-702.

d'Anterroches, L. (2005). Process flow sheet generation and design through a group contribution approach, PhD thesis, Technical University of Denmark.

Delgado, P., Sanz, M. T., Beltrán, S. (2007). Kinetic study for esterification of lactic acid with ethanol and hydrolysis of ethyl lactate using an ion-exchange resin catalyst, *Chemical Engineering Journal*, 126, 111-118

Delgado, P., Sanz, M. T., Beltrán, S. (2007). Isobaric vapour-liquid equilibria for the quaternary reactive system: ethanol + water + ethyl lactate + lactic acid at 101.33 kPa, *Fluid Phase Equilibria*, 255, 17-23

Douglas, J.M., (1988). Conceptual Design of Chemical Processes, McGraw-Hill, New York.

Duarte, C., Buchaly, C., Kreis, P., Loureiro, J.M. (2006). Esterification of propionic acid with n-propanol: catalytic and non-catalytic kinetic study, *Inżynieria Chemiczna i Procesowa*, 27.

Egger, D., Wehtje, E., Adlercreutz, P., (1997). Characterization and optimization of phospholipase A2 catalyzed synthesis of phosphatidylcholine, *Biochimica et Biophysica Acta*, 1343, 76-84.

Engin, A., Haluk, H., Gurkan, K. (2003). Production of lactic acid esters catalyzed by heteropoly acid supported over ion-exchange resins, *Green Chemistry*, 5, 460-466

Ferreira, F. C., Han, S., Boam, A., Zhang, S., Livingstone, A.G., (2002). Membrane aromatic recovery system (MARS): lab bench to industrial pilot scale, *Desalination*, 148, 267-273.

Fogler H. S. (2006). Elements of Chemical Reaction Engineering, 4th edition, *Pearson Education*.

Folić, M., Adjiman, C. S., Pistikopoulos, E. N., (2004). The design of solvents for optimal reaction rates, European Symposium on Computer-Aided Process Engineering – 14.

Fredenslund, A., Gmehling, J., Michelsen, M. L., Rasmussen, P., Prausnitz, J. M. (1977). Computerized Design of Multicomponent Distillation Columns Using the UNIFAC Group Contribution Method for Calculation of Activity Coefficients, Ind. Eng. Chem. Proc. Des. Dev.; 16, 4, 450 – 462.

Fredenslund, A., Gmehling, J., Michelsen, M. L., Rasmussen, P., Prausnitz, J. M. (1977). Computerized design of multicomponent distillation columns using the UNIFAC group contribution method for calculation of activity coefficients, *Industrial and Engineering Chemistry Process Design and Development*, 16, 450-462.

Gani, R., Hytoft, G., Jaksland, C., Jensen, A. K. (1997). An integrated computer aided system for integrated design of chemical processes, Computers chemical Engineering, 21, 1135-1146.

Gani, R., Jim´enez-Gonz´alez, C., Constable, D.J.C. (2005). Method for selection of solvents for promotion of organic reactions, Computers and Chemical Engineering, 29, 1661–1676.

Gani, R. (2001). ICAS Documentations, CAPEC Internal Report, Technical University of Denmark, Lyngby, Denmark

Gmehling et al. (1977). Vapour-liquid equilibrium data collection

Gmehling, J., Li, J., Schiller, M., (1993). A Modified UNIFAC Model. 2. Present Parameter Matrix and Results for Different Thermodynamic Properties, *Ind. Eng. Chem. Res.*, 32, 178-193.

Günther, R., Hapke, J., (1996). Design of membrane separation plants using a module

data base, *Desalination*, 104, 119-128.

Halling, P. J., Valivety, R. H., Johnston, G. A., Suckling, C. J. (1991). Solvent effect on biocatalysis on organic systems: Equilibrium position and rates of lipase catalyzed esterification, *Biotechnology and Bioengineering*, 38, 1137-1143.

Harper, P. M., Gani, R. (2000). A multi-step and multi-level approach for computer aided molecular design, *Computer and Chemical Engineering*, 24, 677-683.

Harper, P., (2000). A multi-phase, multi-level framework for computer aided molecular design, Ph.D. thesis, Technical University of Denmark.

Heintz, A.; Stephan, W.(1994). A generalized solution diffusion model of the pervaporation process through composite membranes Part II. Concentration polarization, coupled diffusion and the influence of the porous support layer, Journal of Membrane Science, 89, 153-169.

Ho, W. S. W., Sirkar, K. K. (1992). Membrane handbook. Published by Van Nostrand Reinhold, ISBN: 0-442-23747-2

Hostrup, M., (2002). Integrated approach to computer aided process synthesis, PhD thesis, Technical University of Denmark.

Huang, Shu-Chuan, Ball, I. J. Kaner, R. B.(1998). Polyaniline membranes for pervaporation of carboxylic acids and water, *Macromolecules*, 31, 5456-5464

Jaksland, C. (1996). Separation process design and synthesis based on thermodynamic insights, Ph.D. thesis, Department of Chemical Engineering, Technical University of Denmark.

Kang, I. J., Rezac, M. E., Pfromm, P. H., (2004). Membrane permeation based sensing for dissolved water in organic micro-aqueous media, Journal of Membrane Science, 239, 2, 213-217.

Kolár, P., Shen, J. W., Tsuboi, A., Ishikawa T. (2002). Solvent selection for pharmaceuticals, *Fluid Phase Equilibria* 194–197, 771–782.

Koszorz, Z., Nemestothy, N., Ziobrowski, Z., Belafi-Bako, K., Krupiczka, R. (2004). Influence of pervaporation process parameters on enzymatic catalyst deactivation, *Desalination*, 162, 307-313.

Kreis, P., (2005). Prozessanalyse hybrider Trennverahren, Ph-D thesis, University of Dortmund, Shaker Verlag, Aachen 2005.

Kreis, P., (2005). Prozessanalyse hybrider Trennverfahren, Ph-D thesis, D290 (Diss. Universität), Shaker Verlag Aachen.

Personal communication with Dr Peter Kreis.

Kwon, S. J., Song, K. M., Hong, W. H., Rhee, J. S., (1994). Removal of water produced from lipase-catalyzed esterification in organic solvent by pervaporation, *Biotechnology and Bioengineering*, 46, 393-395.

Larsen, B. L., Rasmussen, P., Fredenslund, A. (1987). A modified UNIFAC group-

contribution model for prediction of phase equilibria and heats of mixing, *Industrial & Engineering Chemistry Research*, 26, 2274-2286.

Lipnizki, F., Trägårdh, G. (2001). Modelling of pervaporation: Models to analyze and predict the mass transport in pervaporation, *Separation and Purification Methods*, 30, 49-125.

Lipnizki, F., Olsson, J., Trägårdh, G. (2002). Scale-up of pervaporation for the recovery of natural aroma compounds in the food industry. Part 1: simulation and performance, Journal of Food Engineering, 54, 183-195.

Lipnizki, F., Field, R.W.,. Ten, P-K (1999). Pervaporation-based hybrid process: a review of process design, applications and economics, *Journal of Membrane Science*, 153, 183-210.

Marrero, J., Gani, R., (2001). Group-contribution based estimation of pure component properties, *Fluid Phase Equilibria* 183–184, 183–208

Marrero, J., Gani, R., (2001). Group-contribution based estimation of pure component properties, *Fluid Phase Equilibria* 183–184, 183–208

Marx, S., Everson, R. C., Neomagus, H. W. J. P., (2005). Organic-organic separation by pervaporation. II. Separation of methanol from tame by an α-alumina supported Nay-Zeolite membrane, *Separation Science and Technology*, 40, 1047–1065.

Matouq, M., Tagawa T., Goto S. (1994). Combined process for production of methyl tert-buthyl ether from tert-buthyl alcohol and methanol, *Journal of Chemical Engineering of Japan*, 27, 302-306.

Matouq, M., Tagawa, T., Gotp, S., (1994). Combined process for production of methyl tert-butyl ether from tert-butyl alcohol and methanol, *Journal of Chemical Engineering of Japan*, 27, 302-306.

McDonald, C. M.; Floudas, C. A. (1995). Global optimization for the phase and chemical equilibrium problem: application to the NRTL equation, *Computers & Chemical Engineering* , 19, 11, 1111-1139

Michelsen, M. L. (1989). Calculation of multiphase ideal solution chemical equilibrium, *Fluid Phase Equilibria*, 53, 78-80.

Minarro, I., Abad, C., Braco, L., (1994). Characterization of acylating and deacylating activities of an extracellular phospholipase A2 in a water-restricted environment, Biochemistry, 33, 4652-4660.

Mitkowski, P.T., Jonsson, G., Gani, R. (2007). Model-based hybrid reaction-separation process design, ESCAPE17, *Computer-Aided Chemical Engineering*, 24, 395-400.

Mitkowski, P.T., Jonsson, G., Gani, R. (2007). Computer aided design and analysis of hybrid processes, *Chemical and Process Engineering*, 28, 769-781.

Montgomery, D. C. (2001). Design and analysis of experiments, 5th edition, *John*

Wiley & Sons Inc.

Mulder, M., (2003). Basic principles of membrane technology, *Kluwer Academic Publisher*, second edition.

Muller, P., (1994). Glossary of terms used in physical organic chemistry, *Pure and Applied Chemistry*, 66, 5, 1077-1184.

Nair, D., Scarpello, J. T., Vankelecom, I. F. J., Freitas Dos Santos, L. M., White, L. S., Kloetzing, R. J., Welton, T., Livingston, A. G., (2002). Increased catalytic productivity for nanofiltration-coupled Heck reactions using highly stable catalyst systems, *Green Chemistry*, 4, 319–324.

Nielsen, T.L., Gani, R. (2001). A computer aided system for correlation and prediction of phase equilibrium data, *Fluid Phase Equilibria*, 185, 13–20

Nielsen, T.L., Abildskov, J., Harper, P.M., Papaeconomou, I., Gani, R. (2001). The CAPEC Database, *Journal of Chemical Engineering Data*, 46, 1041-1044.

Ohshima, T., Kogami, Y., Miyata, T., Uragami, T. (2005). Pervaporation characteristics of cross-linked poly(dimethylsiloxane) membranes for removal of various volatile organic compounds from water, *Journal of Membrane Science*, 260, 156–163.

Panek, D., Konieczny, K. (2006).Pervaporation of toluene and toluene/acetone/ethyl acetate aqueous mixtures through dense composite polydimethylsiloxane membranes, *Desalination*, 200, 367–373.

Parulekar, S.J. (2007). Analysis of pervaporation-aided esterification of organic acids, *Industrial and Engineering Chemistry Research*, 46, 8490-8504

Peeva, L. G., Gibbins, E., Luthra, S. S., White, L. S., Stateva, R. P., Livingston, A. G., (2004). Effect of concentration polarization and osmotic pressure on flux in organic solvent nanofiltration, *Journal of Membrane Science*, 236, 121-136.

Pérez-Cisneros, E.S.P.; Gani, R.; Michelsen, M.L. (1997). Reactive separation systems--I. Computation of physical and chemical equilibrium, *Chemical Engineering Science*, 52, 527-543.

Place, A. R., Roby, D. D., (1986). Assimilation and deposition of dietary fatty alcohols in Leach's storm petrel, Oceanodroma leucorhoa, *The Journal of Experimental Zoology*, 240:149-161.

Rautenbach, R., Albrecht, R., (1989). Membrane processes, Translated by Valerie Cottrell, John Wiley & Sons.

Sales-Cruz, M., Gani, R., (2003). Dynamic Model Development, *Computer-Aided Chemical Engineering Eds. S.P. Asprey and S. Macchietto*, 16, 229-237.

Salis, A., Solinas, V., Monduzzi, M., (2003). Wax esters synthesis from heavy fraction of sheep milk fat and cetyl alcohol by immobilised lipases, *Journal of Molecular Catalysis B: Enzymatic*, 21, 4-6, 167-174

Sanz, M. T., Gmehling, J. (2006). Study of the dehydration of isopropanol by a pervaporation-based hybrid process, *Chemical Engineering and Technology,* 29, 473-480.

Satyanarayana, K. C., Gani, R., (2007). ICAS Documentations, Internal Report PEC07-32, CAPEC, Department of Chemical Engineering, DTU, Lyngby, Denmark.

Scarpello, J.T., Nair, D., Freitas dos Santos, L.M., White, L.S., Livingstone, A.G., (2002). The separation of homogeneous organometalic catalysts using solvent resistant nanofiltration, *Journal of Membrane Science*, 203, 71-85.

Schmidt-Traub, H., Górak, A. (2006). Integrated reaction and separation operations. Modelling and experimental operations. Springer-Verlag Berlin Heidelberg.

Silva, P., Han, S., Livingston, A. G., (2005). Solvent transport in organic solvent nanofiltration membranes, *Journal of Membrane Science*, 262, 49-50.

Smith, W.R., Missen, R.W., (1982). Chemical reaction equilibrium analysis: theory and algorithms, John Wiley.

Sommer, S., Melin, T., (2005). Influence of operation parameters on the separation of mixtures by pervaporation and vapor permeation with inorganic membranes. Part 2: Purely organic systems, *Chemical Engineering Science*, 60, 16, 4525-4533.

Staudt-Bickel, C., Lichtenthaler, R.N., (1996). Integration of pervaporation of the removal of water in production process of methylisobutylketone, *Journal of Membrane Science*, 111, 135-141.

Teusink, B., Passarge, J., Reijenga, C. A., Esgalhado, E., van der Weijden, C. C., Schepper, M., Walsh, M. C., Bakker, B. M., van Dam, K., Westerhoff, H. V., Snoep, J. L. (2000). Can yeast glycolysis be understood in terms of in vitro kinetics of the constituent enzymes? Testing biochemistry, *European Journal of Biochemistry*, 267, 5313-5329

The Dow Chemical Company Sales Specification, UCAR n-propyl propionate (2006).

Ung, S. Doherty, M. F., (1995). Vapor-liquid phase equilibrium in systems with multiple chemical reactions, *Chemical Engineering Science*, 50, 1, 23-48.

Van Baelen, D., Van der Bruggen, B., Van den Dungen, K., Degreve, J., Vandecasteele, C., (2005). Pervaporation of water–alcohol mixtures and acetic acid–water mixtures, *Chemical Engineering Science*, 60, 1583-1590.

Van Krevelen, D.W., (1990). Properties of polymers. Their correlation with chemical structure; their numerical estimation and prediction from additive group contributions, third edition, Elsevier.

Vikbjerg, A. F., Mu, H., Xu, X., (2005). Lipase-catalyzed acyl exchange of soybean phosphatidylcholine in n-hexane: A critical evaluation of both acyl

incorporation and product recovery, *Biotechnology Progress*, 21, 397-404.

Vu, D. T., Asthana, N. S., Kolah, A. K., Miller, D. J. (2006). Vapor-Liquid Equilibria in the systems ethyl-lactate+ethanol and ethyl lactate+water, *Journal of Chemical Engineering Data*, 51, 1220-1225.

White, L. S., Nitsch A. R., (2000). Solvent recovery from lube oil filtrates with a polyimide membrane, *Journal of Membrane Science*, 179, 267–274.

Whu, J. A., Baltzis, B. C., Sirkar, K. K., (1999). Modelling of nanofiltration – assisted organic synthesis, *Journal of Membrane Science*, 163, 319-331.

Whu, J.A., Baltzis, B.C., Sirkar, K.K. (1999). Modelling of nanofiltration - assisted organic synthesis, *Journal of Membrane Science*, 163, 319–331.

Wijmans, J. G., Baker, R. W., (1995). The solution-diffusion model: a review, Journal of Membrane Science107, 1-21.

Wisconsin Biorefining Development Initiative, 2004. http://www.wisbiorefine.org/prod/lac.pdf

Zhang, Y., Ma, L., Yang, J. (2004). Kinetics of esterification of lactic acid with ethanol catalyzed by cation-exchange resins, *Reactive and Functional Polymers*, 61, 101-114.

Fangbin Zhou (2005). Novel pervaporation for separating acetic acid and water mixtures using hollow fibber membranes, PhD thesis, School of Chemical and Biomolecular Engineering, Georgia Institute of Technology.

Seader, J.D., Henley, E.J., (1998). Separation process principles, John Wiley & Sons Ltd.

Frost and Sullivan (2006). U.S. membrane separation systems market, *Research and Markets*, available on: http://www.researchandmarkets.com/reports/358839/ .

Baker, R.W. (2004). Membrane technology and applications, second edition, John Wiley & Sons Ltd.

9. Index

"What you get by achieving your goal is not as important as what you become by achieving your goal."

(Anonym)